ฤทธิ์ของสารไซยานิดิน-3-รูติโนไซด์ต่อการเกิดไกลเคชั่นของโปรตีน การเกิดความเสียหายของสารพันธุกรรม และความผิดปกติของหลอดเลือดที่เหนี่ยวนำด้วยสารเมทิลไกลออกซอล

นางสาวถาวรีย์ ถิละเวช

วิทยานิพนธ์นี้เป็นส่วนหนึ่งของการศึกษาตามหลักสูตรปริญญาวิทยาศาสตรดุษฎีบัณฑิต
สาขาวิชาชีวเวชศาสตร์ (สหสาขาวิชา)
บัณฑิตวิทยาลัย จุฬาลงกรณ์มหาวิทยาลัย
ปีการศึกษา 2558

EFFECTS OF CYANIDIN-3-RUTINOSIDE ON METHYLGLYOXAL-INDUCED PROTEIN GLYCATION, OXIDATIVE DNA DAMAGE AND VASCULAR ABNORMALITIES

Miss Thavaree Thilavech

A Dissertation Submitted in Partial Fulfillment of the Requirements
for the Degree of Doctor of Philosophy Program in Biomedical Sciences
(Interdisciplinary Program)
Graduate School
Chulalongkorn University
Academic Year 2015

Thesis Title	EFFECTS OF CYANIDIN-3-RUTINOSIDE ON METHYLGLYOXAL-INDUCED PROTEIN GLYCATION, OXIDATIVE DNA DAMAGE AND VASCULAR ABNORMALITIES
By	Miss Thavaree Thilavech
Field of Study	Biomedical Sciences
Thesis Advisor	Associate Professor Sirichai Adisakwattana, Ph.D.
Thesis Co-Advisor	Sathaporn Ngamukote, Ph.D.
	Mahinda Abeywardena, Ph.D.

Accepted by the Graduate School, Chulalongkorn University in Partial Fulfillment of the Requirements for the Doctoral Degree

.....Dean of the Graduate School
(Associate Professor Sunait Chutintaranond, Ph.D.)

THESIS COMMITTEE

.....Chairman
(Assistant Professor Amornpun Sereemaspun, M.D., Ph.D.)

.....Thesis Advisor
(Associate Professor Sirichai Adisakwattana, Ph.D.)

.....Thesis Co-Advisor
(Sathaporn Ngamukote, Ph.D.)

.....Thesis Co-Advisor
(Mahinda Abeywardena, Ph.D.)

.....Examiner
(Kittana Makynen, Ph.D.)

.....Examiner
(Associate Professor Wilai Anomasiri, Ph.D.)

.....External Examiner
(Associate Professor Supatra Srichairat)

ถาวรีย์ ถิละเวช : ฤทธิ์ของสารไซยานิดิน-3-รูติโนไซด์ต่อการเกิดไกลเคชั่นของโปรตีน การเกิดความเสียหายของสารพันธุกรรม และความผิดปกติของหลอดเลือดที่เหนี่ยวนำด้วยสารเมทิลไกลออกซอล (EFFECTS OF CYANIDIN-3-RUTINOSIDE ON METHYLGLYOXAL-INDUCED PROTEIN GLYCATION, OXIDATIVE DNA DAMAGE AND VASCULAR ABNORMALITIES) อ.ที่ปรึกษาวิทยานิพนธ์หลัก: รศ. ดร. สิริชัย อดิศักดิ์วัฒนา, อ.ที่ปรึกษาวิทยานิพนธ์ร่วม: อ. ดร. สถาพร งามอุโฆษ, ดร.มาฮินดา อเบย์วาเดนา, 214 หน้า.

ไกลเคชั่นของโปรตีนคือปฏิกิริยาแบบไม่อาศัยเอนไซม์ระหว่างน้ำตาลรีดิวซ์หรือสารประกอบไดคาร์บอนิล (เช่น เมทิลไกลออกซอล) กับโปรตีนทำให้เกิดผลิตภัณฑ์สุดท้ายของปฏิกิริยาไกลเคชั่น เกี่ยวข้องกับการเกิดความผิดปกติของหลอดเลือดซึ่งเป็นภาวะแทรกซ้อนในโรคเบาหวาน สารไซด์ยานิดิน-3-รูติโนไซด์เป็นสารกลุ่มแอนโทไซด์ยานิน พบได้ในผักและผลไม้ มีรายงานการศึกษามากมายเกี่ยวกับฤทธิ์ทางยาของสารไซด์ยานิดิน-3-รูติโนไซด์กับผลต่อสุขภาพ วัตถุประสงค์ของการศึกษาครั้งนี้เพื่อศึกษาฤทธิ์ของสารไซด์ยานิดิน-3-รูติโนไซด์ต่อการต้านการเกิดไกลเคชั่นและการป้องกันความผิดปกติของหลอดเลือดในหลอดทดลองและสัตว์ทดลอง ผลการศึกษาพบว่าสารไซด์ยานิดิน-3-รูติโนไซด์ที่ความเข้มข้น 0.125 ถึง 1 มิลลิโมลาร์ สามารถยับยั้งการเกิดผลิตภัณฑ์สุดท้ายของปฏิกิริยาไกลเคชั่น ลดการเกิดฟรุกโตซามีนและโปรตีนคาร์บอนิล ป้องกันการสูญเสียของหมู่ไทออลในโมเลกุลของโปรตีน และลดการเกิดโครงสร้างเบต้าอะไมลอยด์ในอัลบูมินจากซีรัมของวัวที่เหนี่ยวนำด้วยน้ำตาลไรโบส ฟรุกโทส กลูโคส กาแลคโทส หรือเมทิลไกลออกซอล โดยพบว่าสารไซด์ยานิดิน-3-รูติโนไซด์สามารถจับกับเมทิลไกลออกซอลโดยตรง ร่วมกับการดักจับสารอะนุมูลอิสระซูเปอร์ออกไซด์และไฮดรอกซิลซึ่งเหนี่ยวนำให้เกิดการทำลายสารพันธุกรรมดีเอ็นเอจากปฏิกิริยาออกซิเดชั่นที่เกิดขึ้นระหว่างปฏิกิริยาของเมทิลไกลออกซอลและกรดอะมิโนไลซีน นอกจากนี้ยังพบว่าสารไซด์ยานิดิน-3-รูติโนไซด์ (ที่ความเข้มข้น 3 ไมโครโมลาร์) สามารถป้องกันการหดและขยายตัวที่ผิดปกติของหลอดเลือดหลอดเลือดเอออร์ตาส่วนอกและหลอดเลือดมีเซนเทอริก อาร์เทอรีจากการเหนี่ยวนำด้วยเมทิลไกลออกซอล การศึกษาในสัตว์ทดลองพบว่าการให้สารไซด์ยานิดิน-3-รูติโนไซด์ปริมาณ 30 และ 100 มิลลิกรัม/น้ำหนักตัว (กิโลกรัม)/วัน สามารถลดระดับเมทิลไกลออกซอลในพลาสมา ในหนูกลุ่มที่ได้รับเมทิลไกลออกซอล (60-120 มิลลิกรัม/วัน) เป็นเวลา 8 สัปดาห์ และลดความผิดปกติของของหลอดเลือดควบคู่ไปกับการเพิ่มการแสดงออกของเอนไซม์เอนโดทีเลียมไนตริกออกไซด์ซินเทส และลดการสะสมของผลิตภัณฑ์สุดท้ายของปฏิกิริยาไกลเคชั่นในหลอดเลือด จากผลการทดลองข้างต้นสารไซด์ยานิดิน-3-รูติโนไซด์อาจนำมาใช้สำหรับป้องกันการเกิดภาวะแซรกซ้อนของโรคเบาหวานที่เกิดจากการเหนี่ยวนำด้วยสารเมทิลไกลออกซอลได้

สาขาวิชา ชีวเวชศาสตร์ ลายมือชื่อนิสิต .....

ปีการศึกษา 2558 ลายมือชื่อ อ.ที่ปรึกษาหลัก .....

ลายมือชื่อ อ.ที่ปรึกษาร่วม .....

ลายมือชื่อ อ.ที่ปรึกษาร่วม .....

5487768520 : MAJOR BIOMEDICAL SCIENCES
KEYWORDS: CYANIDIN-3-RUTINOSIDE, METHYLGLYOXAL, ADVANCED GLYCATION END PRODUCTS, OXIDATIVE DNA DAMAGE, VASCULAR ABNORMALITY

THAVAREE THILAVECH: EFFECTS OF CYANIDIN-3-RUTINOSIDE ON METHYLGLYOXAL-INDUCED PROTEIN GLYCATION, OXIDATIVE DNA DAMAGE AND VASCULAR ABNORMALITIES. ADVISOR: ASSOC. PROF. SIRICHAI ADISAKWATTANA, Ph.D., CO-ADVISOR: SATHAPORN NGAMUKOTE, Ph.D., MAHINDA ABEYWARDENA, Ph.D., 214 pp.

Protein glycation is a non-enzymatic reaction between reducing sugars or dicarbonyl compounds (such as methylglyoxal) with protein causing the formation of advanced glycation end products (AGEs) linked to the development of diabetic vascular complications. Cyanidin-3-rutinoside (C3R), a natural anthocyanin present in fruits and vegetables, possesses various pharmacological activities. The objectives of the present study were to investigate the anti-glycation and cardioprotective effect of C3R in *in vitro* and in animal model. The results showed that C3R (0.125-1 mM) markedly inhibited fluorescent and non-fluorescent AGEs formation, fructosamine formation, protein carbonyl formation, protein thiol groups depletion and β-amyloid cross structure formation in bovine serum albumin (BSA) induced by ribose, fructose, glucose, galactose or methylglyoxal. C3R directly trapped methylglyoxal and scavenged superoxide anion and hydroxyl radicals-induced oxidative DNA fragmentation during methylglyoxal/lysine reaction. Moreover, C3R (3 μM) prevented methylglyoxal-induced vascular abnormalities in isolated rat thoracic aorta and mesenteric arterial bed by normalizing vascular functions (contraction and relaxation). In feeding studies, C3R treatment (30 and 100 mg/kg/day) decreased the accumulation of plasma methylglyoxal after 8 weeks of feeding period with methylglyoxal (60-120 mg/day). In addition, C3R also attenuated methylglyoxal-impaired vascular functions through normalizing contraction and relaxation as well as upregulating endothelial nitric oxide synthase (eNOS) mRNA and decreasing AGEs accumulation in aortic tissue. The present study demonstrated that C3R could be a potential compound for preventing methylglyoxal-mediated diabetic vascular complications.

Field of Study: Biomedical Sciences
Academic Year: 2015

Student's Signature .....
Advisor's Signature .....
Co-Advisor's Signature .....
Co-Advisor's Signature .....

ACKNOWLEDGEMENTS

I am indebted to my thesis advisor, Associate Professor Dr. Sirichai Adisakwattana for his guidance of my Ph.D study and research, and for his patience, advices, and motivation. His valuable comments and suggestions helped me all time of research and writing of thesis dissertation.

I owe deep gratitude to my co-advisor, Dr. Mahinda Abeywardena for an opportunity to be a member in Pre-clinical research group at CSIRO Food and Nutrition Flagship, Adelaide, Australia. My placement in his laboratory was an extremely valuable experience to fulfill my knowledge and technical skills in animal studies.

I would like to thanks my co-advisor, Dr. Sathaporn Ngamukote for helping, supporting and encouragement all the time of research.

I am also grateful to my committee members, Assistant Professor Dr. Amornpun Sereemaspun, Associate Professor Dr. Wilai Anomasiri, Associate Professor Dr. Supatra Srichairat and Dr.Kittana Mäkynen for their suggestions and dissertation correction.

I would like to express my deepest sincere gratitude to my family, Mr. Niyom Thilavech and Mr. Tanapol Thilavech for their unconditional love and support. This thesis is dedicated to the memory of mother, Mrs. Maneerat Thilavech, who passed away before the competition of this effort.

I wish to thank all those who have helped me with my research in Adisakwattana's research group at Department of Nutrition and Dietetic, Faculty of Allied Health Sciences, Chulalongkorn University.

These acknowledgements would not be complete without mentioning my research lab colleagues at CSIRO Food and Nutrition Flagships: Dr. Damien Belobrajdic, Dr. Ross Hamilton, Mrs. Sharon Burnard, Mrs. Julie Dallimore, Mr. Michael Adams, Ms. Darien Sander and Mrs. Michelle Vuaran for their kind help and support.

Moreover, I wish to thank the RGJ-PhD program (PHD/0027/2554) by the Thailand Research Fund (TRF) and Chulalongkorn University, and the 90th Anniversary of Chulalongkorn University Fund for financial supporting.

CONTENTS

Page

Page

LIST OF TABLES

Page

TABLE OF FIGURES

CHAPTER I

INTRODUCTION

1.1 Background and significance of the present study

Protein glycation is a non-enzymatic reaction between carbonyl group of reducing sugar and free amino group of proteins. The glycation process initiates the formation of unstable Schiff's base, which then undergoes rearrangement resulting in a more stable ketoamine compound, known as the amadori products such as fructosamine and hemoglobinA_{1c} (Ulrich and Cerami, 2001, Leslie and Cohen, 2009). Glycoxydation, Schiff's base oxidation and free-radical generation further promote the formation of reactive dicarbonyl molecules which cause the modification of proteins by cross-linking and reducing disulfides of target proteins to form irreversible advanced glycation end products (AGEs) (Goldin *et al.*, 2006, Wu *et al.*, 2011). AGEs contribute the formation of cross-links in proteins that permanently alters cellular structures and actions mediated via activation of the receptor for AGEs (RAGE) (Wu et al., 2011). As present in poorly managed diabetics, chronic hyperglycemia in diabetic patients accelerates the formation and accumulation of AGEs. AGEs have been considered to be a significant contributor of age-related diseases (Khazaei *et al.*, 2010), hypertension, atherosclerosis, and diabetic vascular complications (Rosolova *et al.*, 2008)

In early stages of the glycation with monosaccharides, specifically reducing sugars, induce protein glycation, the rate of progression depending on the type and concentration (Syrovy, 1994). Apart from monosaccharides, scientific evidence indicates that a dicarbonyl molecule, methylglyoxal that formed during propagation stages of glycation, glycolysis, and polyol pathway is a reactive precursor to produce

AGEs (Ramasamy *et al.*, 2006, Riboulet-Chavey *et al.*, 2006). The elevation of serum and tissue concentration of methylglyoxal has been found in pathological conditions, especially diabetes (Wang *et al.*, 2007, Vander Jagt, 2008). Methylglyoxal have been showed to modify the amino groups of lysine, resulting in the formation of AGEs and the production of free radical, including superoxide and hydroxyl radicals (Suji and Sivakami, 2007). It is supposed to be a causative factor mediated an oxidative modification and subsequent damage on cellular components including proteins (Seneviratne *et al.*, 2011) and DNA (Kang *et al.*, 2006, Suji and Sivakami, 2007). Free radicals mediated oxidative DNA damage has been hypothesized to play critical roles in diverse process mutagenesis, carcinogenesis and physiological aging (Sagripanti and Kraemer, 1989).

Higher concentrations of methylglyoxal have been shown to be associated with vascular abnormalities in diabetic patients (Wang *et al.*, 2005, Matafome *et al.*, 2013) and correlated with the degree of hypertension in spontaneous hypertensive rats (SHR) (Huang *et al.*, 1997, Anuradha and Balakrishnan, 1999, Tran *et al.*, 2009). Similarly to SHR, long-term methylglyoxal treatment in isolated mesenteric artery has also been reported to promote endothelial dysfunction by decreasing nitric oxide (NO) production via the down regulation of endothelial nitric oxide synthase (eNOS) expression, leading to impair vascular functions (vasoconstriction and vasodilation) (Wang *et al.*, 2004, Mukohda *et al.*, 2012, Mukohda *et al.*, 2013). The methylglyoxal-derived AGEs triggers RAGE interaction cascades the signaling to stimulate NADPH oxidase and increases ROS production, attributes to activation of transcription factor NF-κB that play a crucial role in inflammatory injury and vascular damage (Goldin et al., 2006). Methylglyoxal could affect inflammation responses in endothelial cell in addition to impaired vascular reactivity which occurs as early event in atherosclerosis, hypertension and vascular complication in diabetic patients (O'Keefe *et al.*, 2009).

Thus, the possible way to reduce the risks of diabetic complications is to inhibit methylglyoxal accumulation and AGEs formation (Wu et al., 2011). Anti-glycating agents such as aminoguanidine as received the most interest from a clinical trials perspective due to its inhibitory effect on AGEs formation (Ihm *et al.*, 1999). However, previous studies have indicated some deleterious properties of aminoguanidine in patient with diabetic nephropathy (Freedman *et al.*, 1999, Bolton *et al.*, 2004). Therefore, much effort has been extended in search of effective phytochemical compounds from dietary fruits, plants and herbal medicines on inhibition of AGEs formation (Ardestani and Yazdanparast, 2007, Zafra-Stone *et al.*, 2007, Tupe and Agte, 2010).

One of interesting compounds is anthocyanin pigments which are responsible for red, purple or blue color of many fruits and vegetables. They belong to a parent class of flavonoids which have been identified as antioxidant, anti-carcinogen and anti-inflammation (Nijveldt *et al.*, 2001). In addition, the anthocyanins also showed the beneficial health effect by lowering the risk of cardiovascular disease as well (Galvano *et al.*, 2007, de Pascual-Teresa *et al.*, 2010). Numerous previous studies have reported that anthocyanin-rich plant extracts potentially inhibit the formation of AGEs in *in vitro* models of glycated albumin and hemoglobin (Beaulieu *et al.*, 2010, Jariyapamornkoon *et al.*, 2013, Sri Harsha *et al.*, 2013). The proposed mechanisms of anthocyanins have been reported as an antioxidant activity and methylglyoxal trapping capacity (Liu *et al.*, 2011, Jariyapamornkoon et al., 2013). Cyanidin-3-rutonoside (C3R), a natural of anthocyanin, is found to have high proportion in dietary source such as blackberry, lychee and capulin. Several lines of evidence indicate C3R being an effective antioxidant (Tulio *et al.*, 2008, Li *et al.*, 2012, Ortiz *et al.*, 2013) and also anti-hyperglycemic by its ability to inhibit intestinal α-glucosidase and pancreatic α-amylase (Akkarachiyasit *et al.*, 2010, Adisakwattana *et*

al., 2011, Lu *et al.*, 2013). The inhibition of C3R on the enzymes that play important role in carbohydrate digestion and absorption could be proposed mechanism to decrease postprandial hyperglycemia. However, no research has been so far accomplished on C3R in relation to its anti-glycation activity. Therefore, it would be interesting to investigate the protective effect of C3R on methylglyoxal-mediated protein glycation, oxidative DNA damage and vascular abnormality *in vitro* and in animal model

1.2 Research questions

1. Does C3R inhibit monosaccharides- or methyglyoxal-mediated protein glycation?

2. Does C3R prevent methylglyoxal-induced oxidative DNA damage?

3. Does C3R prevent methylglyoxal-induced vascular abnormalities?

1.3 Objectives of the present study

1. To investigate the effect of C3R on protein glycation mediated by monosaccharides, including ribose, fructose, glucose and galactose, and reactive dicarbonyls molecule, methylglyoxal*, in vitro*

2. To examine the effect of C3R on methylglyoxal-induced oxidative DNA damage *in vitro*

3. To investigate the effect of C3R on methylglyoxal-mediated vascular abnormalities in isolated vascular preparations (rat aortic tissue and mesenteric artery)

4. To investigate the effect of C3R on alleviating vascular abnormalities in methylglyoxal-treated rats

1.3 Hypotheses of the present study

1. C3R could inhibit ribose-, fructose-, glucose-, galactose- and methylglyoxal-mediated protein glycation by decreasing formation of advanced glycation end products (AGEs) as well as oxidation-dependent protein damage.

2. C3R could prevent methyglyoxal-induced oxidative DNA damage by scavenging of reactive oxygen species production, DNA fragmentation and direct trapping to methylglyoxal.

3. C3R might prevent methylglyoxal-mediated vascular abnormalities in isolated vascular tissues by normalizing vascular functions (contraction and relaxation).

4. Dietary intake of C3R may prevent or delay the pathogenesis of vascular abnormalities in methylglyoxal-treated rats by decreasing methylglyoxal concentration in plasma, AGEs accumulation and endothelial dysfunction, and normalizing vascular functions.

CHAPTER II

LITERATURE REVIEW

2.1 Diabetes

Diabetes is one of the most common chronic diseases associated with the metabolics disorder. Hyperglycemia or high circulating blood glucose is the major characteristic of diabetic patient, resulting from abnormalities in either insulin secretion or insulin function or both. Chronic hyperglycemia plays important roles in the dysfunction and serious damage of several organs particularly kidneys, eyes, nerves, heart and blood vessels (American Diabetes, 2007). The World Health Organization reported the number of people with diabetes has risen from 108 million in 1980 to 422 million in 2014. Diabetes caused 1.5 million deaths in 2012, and high blood glucose caused an additional 2.2 million deaths, by increasing the risk of cardiovascular and other diseases.

The pathogenic processes involved in the development of diabetes are the autoimmune destruction of β-cell of pancreases with consequent insulin deficiency and abnormality that result in resistance to insulin action. The impairment of insulin secretion and insulin action usually occur as combination in the same patient, and it is unclear which abnormality is the primary cause of hyperglycemia. The degree of hyperglycemia depends on the underlying disease process and associates the pathologic and functional change in several target organs in diabetes patient. These may be present for a long period of time without the clinical symptoms before diabetes is diagnosed.

2.1.1 Classification

- **Type 1 diabetes**

Type 1 diabetes or insulin-dependent diabetes accounts for only 5-10% of all diabetes cases. It usually found in childhood or young adulthood, but also develop at any age. Type 1 diabetes is insulin deficiency category resulting from a cellular-mediated autoimmune destruction of the β-cell of the pancreas. This process occurs over many months or years asymptomatic of diabetes. High blood glucose and others symptoms (such as polyuria, polydipsia, weight loss and blurred vision) occur when the function of β-cell have been destroyed more than 90%. The causes of type 1 diabetes are still unclear. It has been found to develop in people with family history of diabetes, but also develop in people with no family history. Genetic disorders and environmental factors might activate the autoimmune response to damage β-cell. Diabetic ketoacidosis is serious condition occur mostly in type 1 diabetes when the level of blood glucose get too high leading to diabetic coma or event death. In addition to acute condition, chronic hyperglycemia in people with type 1 diabetes involves in the increased risk of cardiovascular diseases which are causes of premature mortality. Therefore, blood glucose control within target range is important prevention or amelioration the development of complications. Secondary, insulin replacement is one component of treatment for people with type 1 diabetes.

- **Type 2 diabetes**

Type 2 diabetes or non-insulin-dependent diabetes accounts for only 90-95% of all diabetes cases. Hyperglycemia in type 2 diabetes results from insulin resistance of target organs and usually related to the impairment of insulin secretion. Hyperglycemia itself also causes the adverse in metabolic state as a vicious cycle by impairing insulin production from pancreatic β-cell and exacerbating insulin resistance (Li *et al.*, 2004). Moreover, genetic and environmental factors such as obesity,

sedentary lifestyle, overeating, aging and stress also affect β-cell function and insulin sensitivity of insulin target organs (muscle, liver, adipose tissue and pancreas). Reduced insulin sensitivity of target organs is a major feature in type 2 diabetes (Scheen, 2003). Insulin resistance develops and expands prior to disease onset. The elevation of postprandial blood glucose in patient with early stage of type 2 diabetes is slowly raised as a result of increased insulin resistance and decreased early-phase insulin secretion. The progression of impairment of pancreatic β-cell function greatly affects the long-term control of blood glucose and permanently elevate blood glucose (Kohei, 2010). The risk of cardiovascular disorders is increased in individuals with marginal blood glucose elevation. Therefore, the early intervention to control blood glucose in normal range is an important factor to prevent the onset of diabetes and control the progression of complications.

- **Gestational diabetes**

Gestational diabetes is the hyperglycemia condition that first recognized during pregnancy involving in the increasing risk of adverse pregnancy outcomes. Gestational diabetes is approximately 7% of all pregnancies. Fetal macrosomia, neonatal hypoglycemia, jaundice, polycythemia and hypocalcemia may found in any severity of gestational diabetes. Severe hyperglycemia in pregnancy associated with the risk of intrauterine fetal death during the last 4-8 weeks of gestation and the maternal hypertensive disorder. The high risk factors of gestational diabetes include obesity, glycosuria, unrecognized glucose intolerance personal history of gestational diabetes or family history of diabetes. Woman with gestation diabetes are increased in the risk of the development of diabetes (usually type 2) after pregnancy whereas offspring are increased the risk of obesity, glucose intolerance and diabetes in late adolescence and young adulthood. Insulin therapy or only diet modification is used for treatment to control maternal blood glucose (Association, 2003).

2.1.2 Role of hyperglycemia on diabetic complications

Chronic hyperglycemia induces the direct and indirect effects on vascular health which is central to the high prevalence of morbidity and mortality in both type 1 and type 2 diabetes (Kitabchi *et al.*, 2009). The hyperglycemia-mediated vascular complications are divided into macrovascular complications (coronary artery disease, atherosclerosis, and stroke) and microvascular complications (diabetic retinopathy, nephropathy and neuropathy) (Metascreen Writing *et al.*, 2006, Rosolova et al., 2008).

The general feature of diabetic patient is hyperglycemia that induced tissue damage and subsequently develops the complications in diabetes. The diabetic tissue damage by hyperglycemia is modified by genetic determination and independent accelerating factors such as hypertension (Giacco and Brownlee, 2010). Hyperglycemia-induced cellular damage associates with the overproduction superoxide anion by electron transport chain in mitochondria. Under physiological situation, the electron donor NADH and $FADH_2$ are generated during glucose metabolism through glycolysis and tricarboxylic acid (TCA) cycle, then transfers electron to protein complexes in mitochondria electron transport chain for ATP generation. In diabetic cell with high glucose, there are more glucose being metabolited in glycolysis and TCA cycle, and generates more electron donor into mitochondria respiratory chain (Brownlee, 2005, Giacco and Brownlee, 2010). When the clinical threshold of voltage gradient across the mitochondria membrane is reached, the electron transfer is blocked and donates electron to oxygen molecule, thereby generating superoxide anion. Excessive superoxide anion production in vascular endothelial cell inhibits aldehyde-3-phoaphate dehydrogenase (GAPDH) activity that catalyze the conversion of glyceraldehyde-3-phosphate to 1,3-bis-phosphateglycerate in glycolysis pathway (Kanwar and Kowluru, 2009). The inhibition

of GAPDH activity cause an increase of all glycolytic intermediate that are upstream of GAPDH including glucose, glucose-6-phosphate, fructose-6-phosphate and glyceraldehyde-3-phosphatecause which are precursors for the damaging pathways including polyol pathway, protein kinase C activation, hexosamine pathway and advanced glycation end products (AGEs) via protein glycation as shown in figure 1.

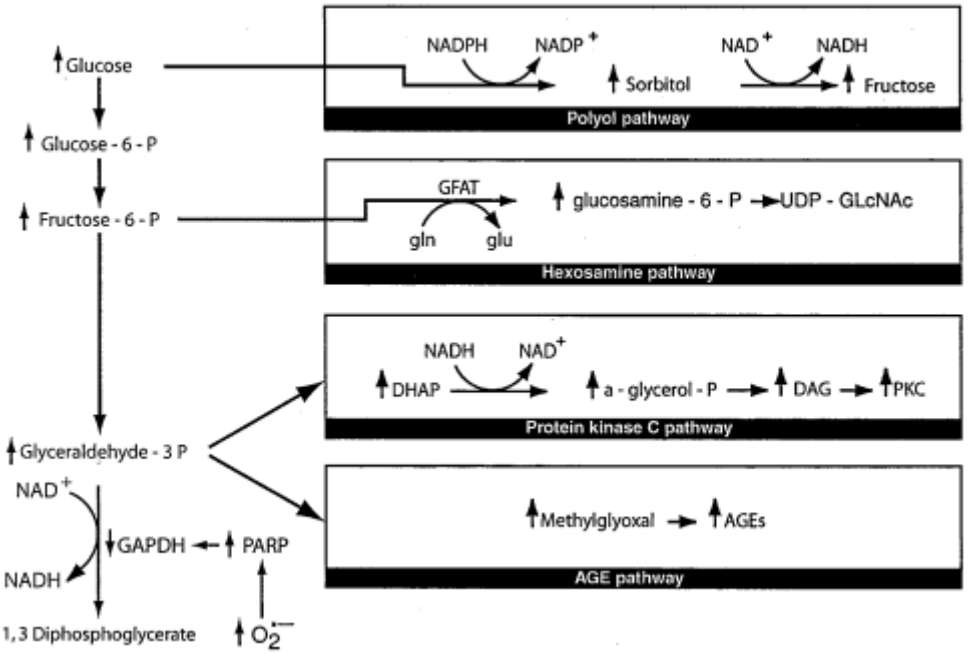

Figure 1 The cellular mechanism of hyperglycemic damage (Brownlee, 2005)

- **Polyol pathway**

The polyol pathway plays a role in the reduction of toxic aldehydes such as glucose in the cell to inactive alcohol using aldose reductase as key enzyme. Glucose is reduced to sorbitol, and then converted to fructose. In hyperglycemia condition, the impairment of aldose reductase function reduces the metabolism of glucose into sorbitol that is consequently oxidized to fructose. Intracellular

antioxidant cofactor NADPH is also used as cofactor in polyol pathway that increases susceptibility to intracellular oxidative stress (Brownlee, 2005).

- **Protein kinase C (PKC) activation**

Intracellular hyperglycemia increases secondary messenger molecule diacylglycerol to activate protein kinase-C-α, -β and –δ isoform. The activation of PKC in endothelial cell causes vascular abnormalities by reducing the production of vasodilator nitric oxide and increasing the production of vasoconstrictor endothelin-1. Moreover, hyperglycemia-activated PCK also involves in vascular permeability angiogenesis, capillary occlusion, pro-inflammatory gene expression and oxidative stress via NADPH oxidase activation (Galvano et al., 2007).

- **Hexosamine pathway**

The metabolic rate of glucose increases when hyperglycemia condition is present inside the cell. In addition to metabolism via glycosis pathway, some of fructose-6-phosphate, an intermediate in glycolysis, also converts to glucosamine-6 phosphate and finally to UDP *N*-acetyl glucosamine by using glutamine: fructose-6 phosphate aminotransferase (GFAT). *N*-acetyl glucosamine binds to serine and threonine on transcription factors resulting in the modification of transcription factors-regulated gene expression, and the development of diabetic complications (Bunn and Higgins, 1981).

- **Advanced glycation end product (AGEs) formation**

AGEs are product from non-enzymatic reactions between carbonyl containing compounds such as glucose and free amino groups of biomolecules, particularly protein, called protein glycation reaction. There are three major mechanisms of AGEs to damage cells. The first mechanism is the modification of intracellular protein,

especially protein involved in the regulation of gene expression. The second mechanism is the modification of extracellular matrix molecules when AGEs diffuses out of the cells resulting in the alteration of cellular signaling activated by matrix and caused cellular dysfunction. The third mechanism is the modification of circulating protein such as albumin. The modified protein can binds and activates AGEs receptor on cell membrane to generate inflammatory cytokines and growth factors which cause vascular damage (Jariyapamornkoon et al., 2013).

2.2 Protein Glycation

Diabetes is chronic disease marked by hyperglycemia resulting in the accumulation of AGEs via non-enzymatic glycation that chemically modifies biological protein then causing the wide variety of tissue pathologies (McCance *et al.*, 1993, Brownlee, 2005). The study of protein glycation and AGEs formation has become of great interest due to the suspected effects of glycation on the pathogenesis of diabetic complications. This interest is illustrated in figure 2 by the increasing number of publications that have appeared on this topic over the last decade.

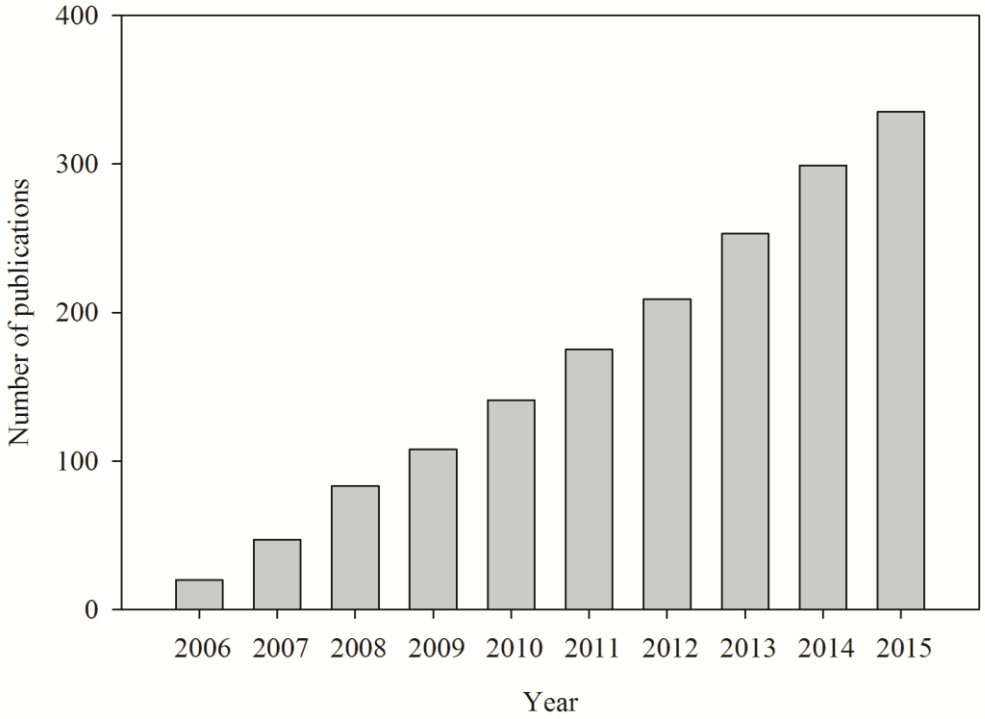

Figure 2 Number of publications that have appeared over the last decade that are related to the topic of advanced glycation end products (AGEs) and diabetic complications.

A complex process of protein glycation is initiated by non-enzymatic interaction between free amino groups of amino acid, peptide or protein and carbonyl group of reducing sugars such as ribose, glucose, fructose and galactose causing the formation of irreversible product called AGEs. The major targets on protein molecule in glycation process include side chain groups of amino acid lysine (amino group), arginine (guanidine group) and cysteine (thiol group) (Smith and Thornalley, 1992, Westwood and Thornalley, 1995)

2.2.1 Endogenous source of AGEs

AGEs endogenously produces via glycation process that includes initiation stage, propagation stage and advanced stage (Wu et al., 2011).

In initiation stage, a complex process of protein glycation is initiated by non-enzymatic interaction between free amino groups of protein and carbonyl group of reducing sugar, such as glucose and fructose, leading to the formation of reversible structure called Schiff's bases (figure 3). This structure can further rearrange, through the formation of more stable ketoamine termed Amadori products, such as fructosamine and HemoglobinA1c (Wu et al., 2011). The reaction is reversible up to the point of Amadori product formation. HemoglobinA1c is the Amadori product of glucose and hemoglobin in red blood cell and is used as marker for monitoring long-term glycemic control in diabetic patient (Ansari and Dash, 2013). Amadori product fructosamine is an alternative marker of glycemic control (Juraschek *et al.*, 2012). It is a glycated product of non-enzymatic reaction between albumin in blood circulation and glucose or fructose (Armbruster, 1987).

In propagation stage, Amadori products undergo further degradation, dehydration, rearrangement and oxidation which lead to release some reactive oxygen species (ROS) and generation of reactive carbonyl intermediates, including 3-deoxyglucosone, glyoxal and methylglyoxal. The overproduction of ROS also involves in the reactive carbonyl intermediates formation through several oxidative metabolisms such as Schiff base oxidation via Namiki pathway (figure 4), glyoxidation or the Wolff pathway (figure 5).

In the late stage, Amadori products as well as reactive dicarbonyl compounds again modify with free amino, guanidine and thiol groups of protein leading to cosrrlink and formation of AGEs. Reactive carbonyl intermediates is more reactive AGEs precursor than the parent sugar. Therefore, reactive dicarbonyl compounds-derived AGEs formation play an important role in the pathogenesis of diabetic complications including diabetic retinopathy, nephropathy, neuropathy, coronary artery disease and stroke (Wu et al., 2011, Semchyshyn and Lushchak, 2012).

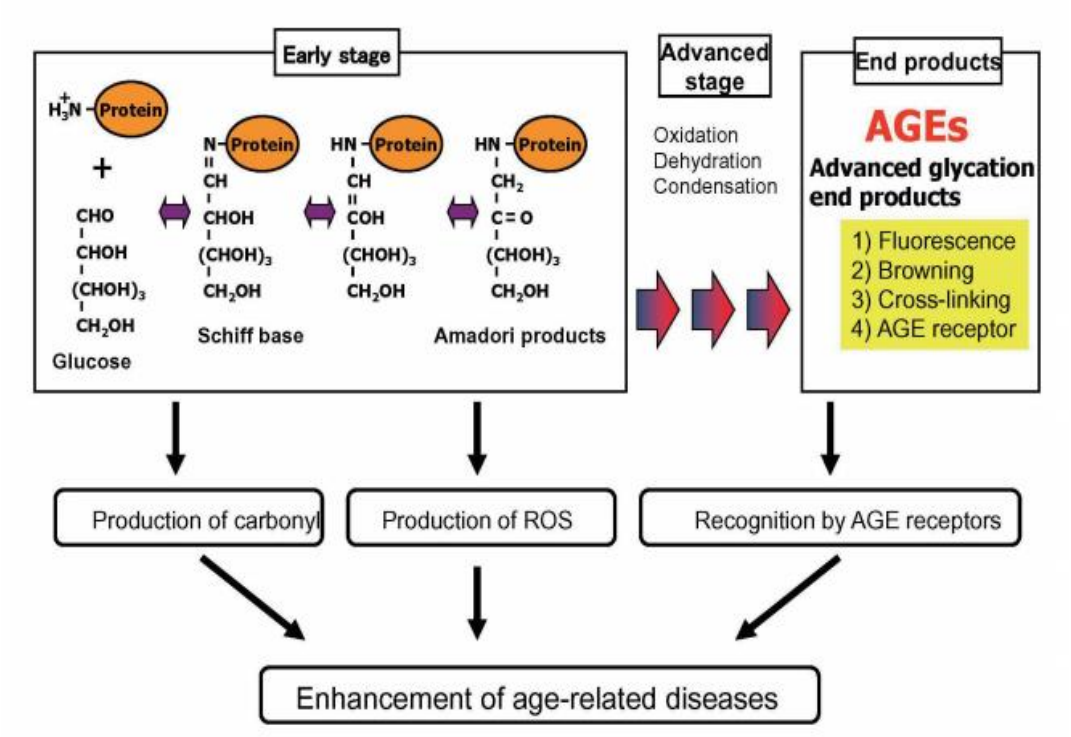

Figure 3 Glycation process

(Nagai *et al.*, 2012)

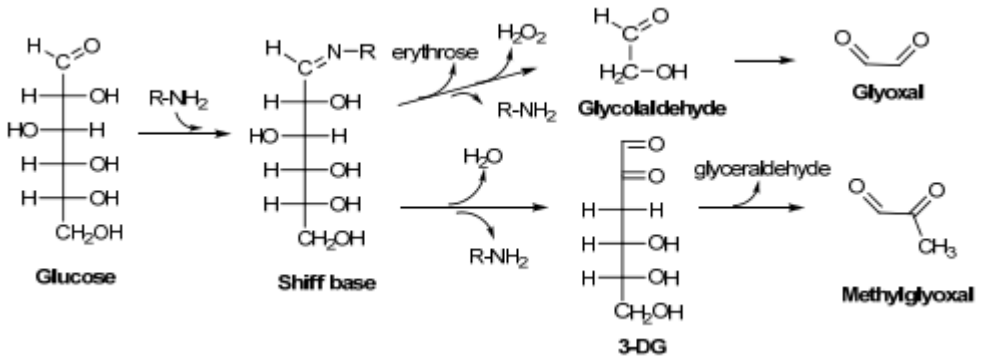

Figure 4 Reactive carbonyl species formation during the fragmentation of Schiff base via Namiki pathway

(Semchyshyn and Lushchak, 2012).

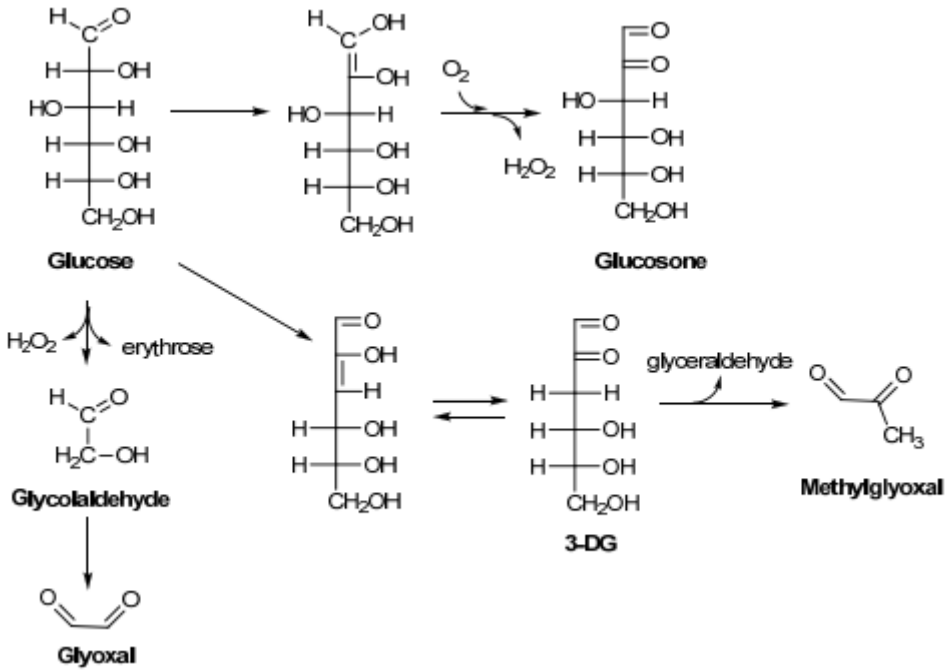

Figure 5 Oxidative degration of glucose or Wolff pathway leads to generate reactive carbonyl species
(Semchyshyn and Lushchak, 2012).

2.2.2 Exogenous source of AGEs

The formation of AGEs also derived from exogenous sources such as smoking and food. Cigarette smoke has been reported to derive AGEs in lens crystalline and arterial wall of coronary artery (Singh *et al.*, 2001). However, mechanism of AGEs formation and AGEs type are still unclear. In addition to smoking, heat treatment of food causes non-enzymatic browning, called Millard reaction. The AGEs crosslink formation in food is resistance to enzymatic degradation. Thus, the oral administration of food-containing AGEs is poorly absorbed from gastrointestinal tract (Uribarri *et al.*, 2010). There has been increased evidence that dietary AGEs associate with the development of chronic degenerative diseases of aging such as Alzheimer's disease, cardiovascular diseases and diabetic complications. In animal models and humans, the restriction of dietary AGEs consumption improved wound healing,

insulin resistance and cardiovascular diseases and increase the lifespan in animal models (Luevano-Contreras and Chapman-Novakofski, 2010). However, the mechanisms of food-containing AGEs consumption are still unclear because of the confounding factors in dietary based studies (Clarke *et al.*, 2016).

Table 1 The advanced glycation end product (AGEs) content of foods, beverages and fruits, based on carboxymethyllysine content
(Uribarri et al., 2010)

Food	AGE Content (kU/100g)
Fat	
Olive, ripe, large (5 g)	1,670
Oil, corn	2,400
Cashews, roasted	9,807
Oil, olive	11,900
Margarine, tub	17,520
Butter, whipped	26,480
Protein	
Salmon, smoked	572
Egg, fried	2,749
Pork, roast	3,544
Sausage, beef and pork links, pan fried	5,426
Beef, roast	6,071
Chicken, breast, roasted	6,639
Carbohydrate	
Sugar, white	0
Syrup, caramel	0
Honey	7
Rice, white	9
Bread, 100% whole wheat	53
Potato, sweet, roasted	72

Chips, potato	2,883
Fruits	**AGE Content (kU/100g)**
Banana	9
Cantaloupe	20
Apple	45
Raisin	120
Vegetables	**AGE Content (kU/100g)**
Tomato	23
Cucumber	31
Celery	43
Eggplant	256
Dairy products	**AGE Content (kU/100g)**
Milk, fat-free	1
Yogurt	3
Milk, whole	5
Milk, soy	31
Cheese, cheddar	5,523
Beverages	**AGE Content (kU/100g)**
Juice, cranberry	2
Coffee, with milk and sugar	2
Tea, Lipton Tea bag	2
Coca Cola, classic	3
Juice, orange	6
Wine, pinot grigio	33

2.3 Advanced glycation end products (AGEs)

2.3.1 Types of AGEs

AGEs are a group of variety of structurally compounds that results from protein glycation mediated by reducing sugars and dicarbonyl compounds. Consequently, heterocyclic crosslinking and fragmentation of intermolecular or intramolecular occur in the protein molecule causing protein dysfunction and irreversible damage. The damaging proteins are resistance to enzymatic digestion and accumulate in tissues (Bierhaus *et al.*, 1998). According to chemical structure, AGEs may be characterized by crosslinking structure and fluorescence property into 2 types: 1) crosslinking and fluorescence AGEs such as pentosidine, crossline, 2-(2-furoyl)-4(5)-(2-furanyl)-1*H*-imidazole (FFI), fluorolink, glyoxal-lysine dimer (GOLD), methylglyoxal-lysine dimer (MOLD) and vesperlysine A, B and C (figure 6), and 2) non-crosslinking and non-fluorescence AGEs such as N^{ε}-(carboxymethyl) lysine (N^{ε}-CML), N^{ε}-(carboxyethyl) lysine (N^{ε}-CEL), pyrraline and argpyrimidine (figure 7) (Wu et al., 2011).

Pentosidine is fluorescent AGEs that can be formed during the reaction between lysine or arginine amino acid residual and several precursors such as glucose, ribose and 3-deoxy glucosone. Pentosidine and N^{ε}-CML have been found to accumulate in skin and lens in diabetic models (Dyer *et al.*, 1993). In addition, Amadori product modify protein causes the generation of N^{ε}-CML, N^{ε}-CEL, MOLD and GOLD as well as unidentified compounds (Wu et al., 2011).

N^{ε}-CML, N^{ε}-CEL, GOLD and MOLD are used as the major biomarkers of glycation in tissue protein. The elevation of N^{ε}-CEL and MOLD had found in lens proteins and skin collagen with ageing that consistent with an increase N^{ε}-CML and N^{ε}-CEL in skin collagen and plasma proteins in uremia in diabetic model. The level of

GOLD and MOLD concentration present in tissue is higher than the concentration of fluorescent crosslink, pentosidine (Degenhardt *et al.*, 1998).

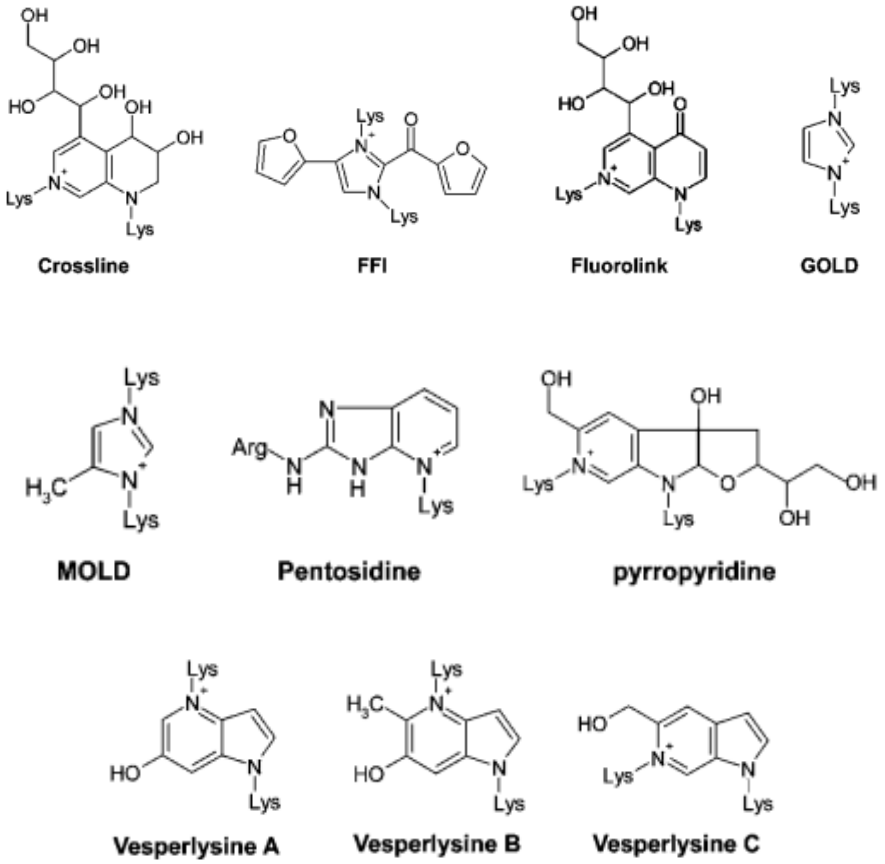

Figure 6 Chemical structures of fluorescent and crosslink AGEs (Wu et al., 2011)

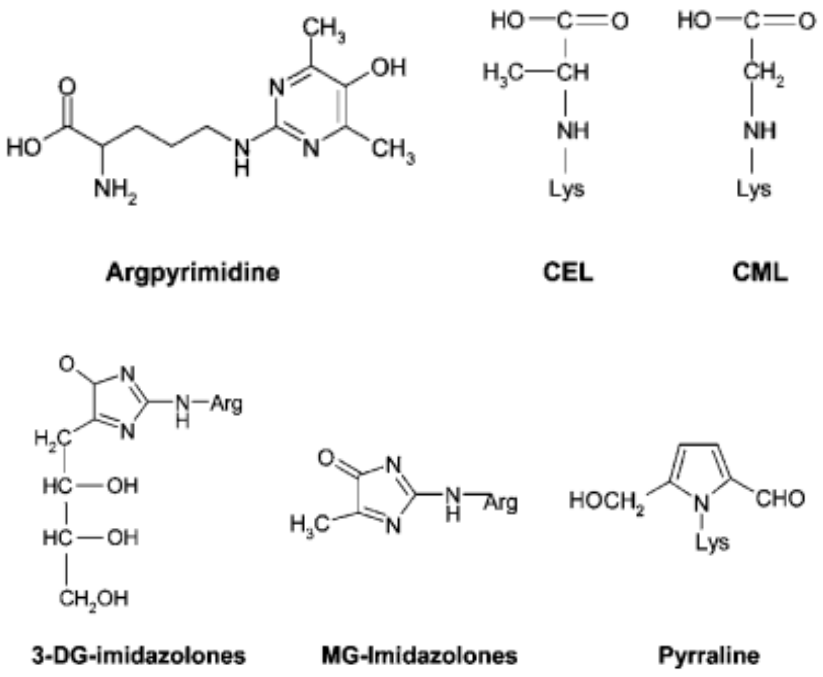

Figure 7 Chemical structures of non-fluorescent and non-crosslinking AGEs (Wu et al., 2011)

2.3.2 Roles of AGEs in several pathologies

The different rate of glycation would accelerate the production rate of glycated products, leading to increase a risk of complications related to diabetes (Bunn and Higgins, 1981). In the experimental studies, glycation with D-ribose triggers misfolding and forms globular amyloids-like aggregations in albumin that induces the apoptosis of neuroblast cell (Wei *et al.*, 2009, Wei *et al.*, 2012). Moreover, rats fed a high galactose, which is one-tenth stability of the ring structure of glucose, had more extensive nonenzymatic glycosylation of lens crystallins than normal and diabetic rats.

Clinical and experimental evidences reported that the level of AGEs is significant higher in diabetes models, accelerated by hyperglycemia (Kilhovd *et al.*, 1999, Turk *et al.*, 1999). The glycation of protein modifies their physiological

functions by disrupting conformation, altering enzymatic activity and reducing degradation capacity. The accumulation of AGEs in tissues and organs is a major factor, involving in the pathogenesis of diabetic complications and other health disorders. AGEs-involved in the development of pathologies in diabetic complications are the overproduction of ROS and the activation of chronic inflammatory process through the receptor for AGEs (RAGE) (McCance et al., 1993, Stitt, 2001). The modification of circulating protein generates AGEs which binds to RAGE. The binding stimulates the translocation of transcription factor NF-kB to trigger intracellular signaling, gene expression and release of inflammatory mediators and reactive oxygen species (ROS) production including superoxide anions and hydroxyl radicals (McCance et al., 1993, Kang, 2003, Harman, 2009). The overproduction of ROS leads to protein oxidation contributing to oxidative stress. The loss of free sulfhydryl group (thiol group) and the increased content of protein carbonyls in protein reflect oxidative protein damage (Dalle-Donne *et al.*, 2003, Balu *et al.*, 2005, Aćimović *et al.*, 2009). Furthermore, glycation cause protein conformation change as shown by increasing the aggregation of cross-linked protein in the form of β-amyloid cross structure (Khazaei et al., 2010). Protein aggregation is mostly found in various degenerative disorders such as Alzheimer's disease and ageing (Bouma *et al.*, 2003). AGEs has also been revealed to affect transcription factors that regulates insulin gene expression. As the results, AGEs decreased expression and nuclear tranlocation of insulin gene activator pancreatic and duodenal box-1 (PDX-1) and reduced phosphorelation of insulin gene inhibitor forkhead transcription factor (FoxO1), resulting in a dereased insulin content in pancreatic islet cell line HIT-T15 (Puddu *et al.*, 2010).

In diabetic patient, chronic hyperglycemia plays crucial roles in the development of microvascular and macrovascular complication, including

retinopathy, nephropathy, neuropathy, atherosclerosis and stroke which are associated with higher level of AGEs (Ahmed, 2005, Wada and Yagihashi, 2005). The AGEs-activated proinflammatory process plays a role in an increasing vascular endothelial damage and vascular remodeling. The previous studies showed that AGEs relates to the formation and progression of atherosclerotic lesions (Basta *et al.*, 2004) by promoting the overproduction of ROS, then triggers the expression of adhesion molecules (vascular cell adhesion molecule 1 (VCAM1) and intercellular adhesion molecule 1 (ICAM–1)) on endothelial cell membrane. The adhesion molecules expression is an important marker of endothelial dysfunction by increasing vascular permeability and white blood cell infiltration in to vascular wall (Tan *et al.,* 2002). Moreover, AGEs-crosslink formation with structural molecule in vascular wall collagen results in arterial stiffening with loss of elasticity of vessels. These processes accelerate initiation and progression of atherosclerosis (Dyer *et al.,* 1993, Ulrich and Cerami 2001). In addition, the glycation of lens crystallines also contributes the pathogenesis of diabetic retinopathy via the glycation of Na^{+}-K^{+} ATPase enzyme leading conformation change and its activity impairment. The dysfunction of Na^{+}-K^{+} ATPase enzyme alters intracellular ion concentration and subsequent water movement via osmosis could result in the cataract formation (Stevens, 1998, Ulrich and Cerami, 2001).

2.4 AGEs precursors

2.4.1 Reducing sugars

It is well known that the *in vitro* glycation rate is a function of the anomerization of the sugar. The rate of glycation reaction of various monosaccharides varied over a 300-fold range and strongly correlates with the number of open form of sugar that exists in the solution. Aldose sugars react more

rapidly than ketose sugars, as would be expected in that aldehyde carbonyl groups are relatively more electrophilic than ketone carbonyl groups. Moreover, the interaction of monosaccharides with protein can be affected by the presence of charged groups on the sugar. Ribose has been revealed as the most active glycation inducer among the reducing monosaccharides. The reactivity of the sugar increases as follows: e.g., glucose < mannose < galactose < xylose < fructose < arabinose < ribose (Syrovy, 1994).

In aqueous solution, sugars exist as an intramolecular hemiacetal in which the free hydroxyl group at C-5 form bond with the aldehydic C-1, rendering the latter asymmetric and giving rise to stereoisomers. The aldofuranose ring of ribose is puckered conformations which is unstable, and then vulnerable to react with amino groups of protein. This may be one reason why furanoses are more reactive in glycation than pyranoses. In contrast, the six-membered aldopyranose ring, such as glucose, is much more stable ring structure rather than other stereoisomers because of the equatorial orientation of its hydroxyl groups. This stable ring structure greatly retards the rate of glucose condensation with proteins. Thus, the relatively high stability of its ring structure allows high concentrations of glucose and proteins to coexist in various tissues with a minimal risk of irreversible covalent modification. Conversely, if organisms contained a comparatively high concentration of a metabolic fuel having a relatively unstable ring structure, it is likely that extensive covalent modification of proteins would occur along with potential impairment of function.

2.4.2 Dicarbonyl compounds (α-oxoaldehyde)

The formation of dicarbonyl compounds, namely the reactive carbonyl species (RCSs), is considered the critical event in glycation process. Dicarbonyl

compounds including glyoxal, methylglyoxal and 3-deoxyglucosone are generated as intermediates in glycation process during Amadori product rearrangement and glyoxidation. They are precursor of AGEs with far more reactive than parent compounds, reducing sugars and play a key role in the cytotoxicity of AGEs and susceptible to diabetic complications (Wu et al., 2011).

Glyoxal and glycolaldehyde modify protein during glycation under physiological conditions leading to protein cross-linking and N^{ε}-(carboxymethyl)lysine (N^{ε}-CML) formation. The N^{ε}- CML formation mediated glyoxal and glycoaldehyde occur through an intramolecular Cannizzaro reaction without oxidation (Glomb and Monnier, 1995). The major modification site by glyoxal in protein molecule is arginine residuals that have been demonstrated in glycated ribonuclease (RNase) (Cotham *et al.*, 2004). In addition, glyoxal-lysine dimer (GOLD) also forms during the reaction of glyoxal with protein.

3-deoxyglucosone is a potent AGEs precursor contributing to AGEs formation. 3-deoxyglucosone rapidly reacts with lysine or arginine residuals in protein molecule to generate pyrraline, pentosidine and other compounds (Wu et al., 2011). The elevation of 3-deoxyglucosone-medified protein has found in diabetic kidney versus control rat (Kusunoki *et al.*, 2003).

Under physiological condition, the irreversible reaction of methylglyoxal with guanidine group on arginine residual causes the formation of immidazolone adducts, while the reaction with animo group on lysine residual in protein lead to form N^{ε}-(carboxyethyl)lysine (N^{ε}-CEL) and methylglyoxal-lysine dimer (MOLD) (Degenhardt et al., 1998). It has been indicated that methylglyoxal showed the highest potent to induce the glycation of lysozyme than glyoxal, 3-deoxyglucosone and glucose (Millar *et al.*, 2002).

2.5 Methylglyoxal

Methylglyoxal, also called pyruvaldehyde or 2-oxopropanal, belongs to reactive carbonyl intermediates that contain two carbonyl groups in the molecule (figure 8). In addition to sugars, methylglyoxal are known as potent precursor to form AGEs under physiological condition at physiological concentrations of methylglyoxal (Lo *et al.*, 1994). The accumulation of AGEs in tissue associates with the progression of ageing and diabetic complication.

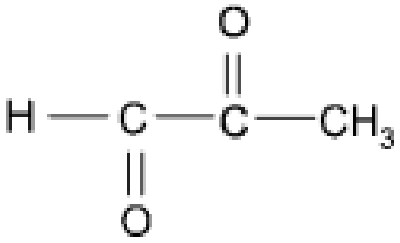

Figure 8 Chemical structure of methylglyoxal

(Wu et al., 2011)

A number of proteins have been revealed to modify methylglyoxal including bovine serum albumin, collagen, lysozyme and ribonuclease. According to the higher concentration of methylglyoxal in the plasma, it suggests that methylglyoxal may a common AGEs precursor of AGEs formation *in vivo* (Xue *et al.*, 2011). Methylgyoxal has been reported to primarily react with arginine residues to form AGEs adducts such as N^{δ}-(5-methyl-4-imidazolon-2-yl)-L-ornithine (5-methylimidazolone) and N^{δ}-(5-hydro-5-methyl-4-imidazolon-2-yl)-L-ornithine (MG-H1). N^{δ}-(5-hydroxy-4,6-dimethylpyrimidine-2-yl)-L-ornithine (argpyrimidine) has been identified as a major fluorescent product in methylglyoxal-modified arginine residual. Argpyrimidine accumulation has been demonstrated in the human serum and cornea (Shamsi *et al.*, 1998). The reaction of methylglyoxal with lysine residues generates an N^{ε}-carboxyethyllysine (CEL) amd imidazolysine as AGEs adducts (Shamsi et al., 1998).

The rapid reaction of methylglyoxal with sulfhydryl group of cysteine residual has been revealed using Nα-acethyl-cysteine results in the formation of hemithioacetal adduct as product (figure 9). Methylglyoxal-derived AGEs formation accumulates in tissues with aging and its related diseases.

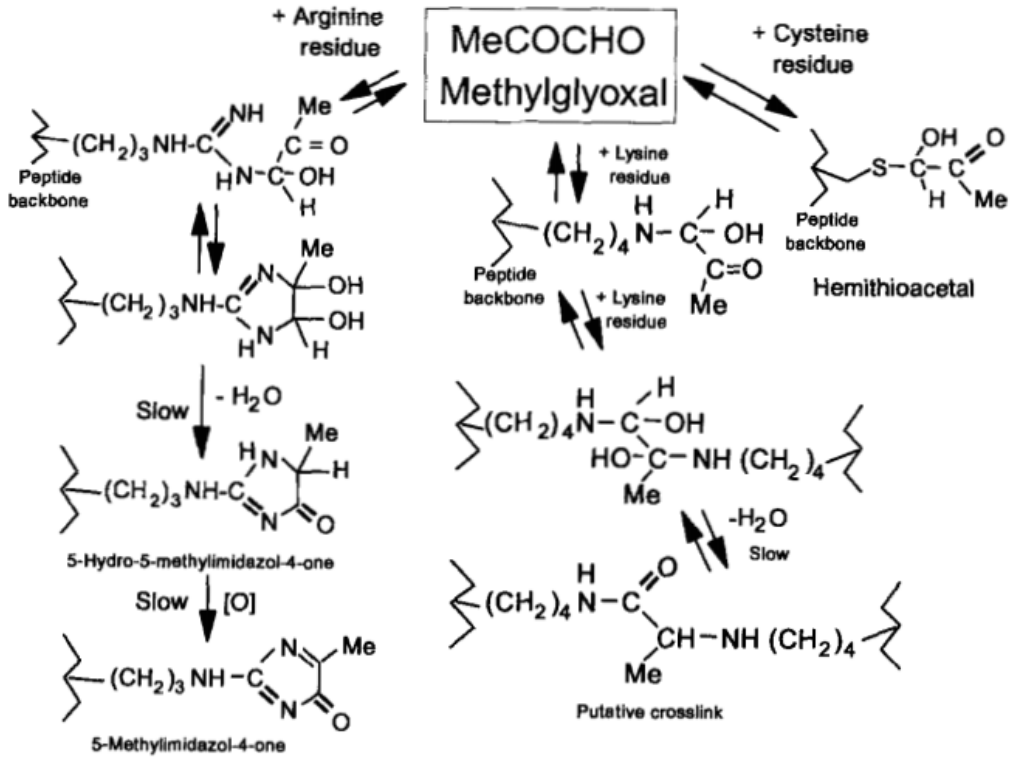

Figure 9 Mechanism of methylglyoxal modify arginine, lysine and cysteine residuals (Lo et al., 1994)

2.5.1 Endogenous source of methylglyoxal

Under physiological condition, methylglyoxal is formed endogenously as intermediate in several metabolic pathways both in mammals and microorganism (figure 10). For example, the metabolism of acetone is catalyzed by acetolmonooxygenase (AMO); the metabolism of aminoacetone is catalyzed by semicarbazide-sensitive amine oxidase (SSAO). In addition, it can be derived from the

catabolism of ketone bodies and threonine. Nevertheless, the most important source of methylglyoxal is glycolysis pathway through enzymatic elimination of phosphate from glyceraldehydes-3-phosphate (G-3-P) and dihydroxyacetone phosphate (DHAP) (Lee *et al.*, 1998, Kalapos, 1999). In non-enzymatic glycation process, methylglyoxal is formed via the amadori product rearrangement, schiff base oxidation and glyoxidation as well (Ramasamy et al., 2006, Wu et al., 2011).

In carbohydrate metabolism, methylglyoxal is generated as an intermediate during the non-enzymatic protein glycation mediated by reducing sugars in hyperglycemia condition (Wu et al., 2011). Under physiological system, methylglyoxal is mainly produced as a by-product in glycolysis pathway through non-enzymatic elimination of from metabolism dihydroxyacetone phosphate (DHAP) and glyceraldehyde-3-phosphate (G-3-P) by 40-67% and 33-60%, respectively (Phillips and Thornalley, 1993). Methylglyoxal can also be produced by enzymatic pathway such as triose phosphate isomerase that catalysts the conversion of DHAP and G-3-P. Moreover, methylglyoxal synthase also produces methylglyoxal by catalyzing the conversion of DHAP to methyglyoxal (Phillips and Thornalley, 1993). In addition to glycolysis pathway, methylglyoxal is also produced in pentose phosphate shunt, glyoxidation and sorbitol pathway. The formation of methylglyoxal via non-enzymatic pathway was estimated approximately 0.1 mmol/L/day (Richard, 1991).

Minor endogenous sources of methylglyoxal are generated during protein and lipid metabolism. In protein metabolism, semicarbazide-sensitive amine oxidase (SSAO) enzyme catalyzes amino acetone to methylglyoxal and hydrogen peroxide (Kalapos, 1999). Aminoacetone is an intermediate in metabolism of amino acid threonine and glycine. An increase of SSAO activity has been reported under diabetic condition (Mitch *et al.*, 1999). In lipid metabolism, methyglyoxal are generated from non-enzymatic and enzymatic metabolism of acetoacetate or acetone

intermediates, respectively. In enzymatic reactions, the conversion of acetone to methylglyoxal is catalyzed by acetone monooxygenase that converts acetone to acetol and acetol monooxygenase that converts acetol to methyglyoxal with NADPH as a cofactor (Kalapos, 1999).

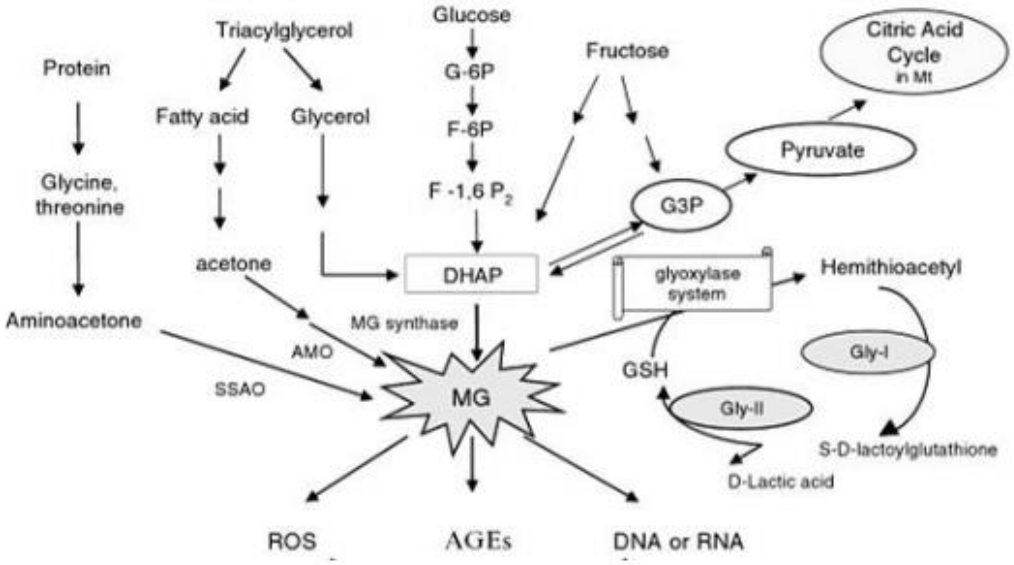

Figure 10 The endogenous sources of methylglyoxal from carbohydrate, protein and lipid metabolism.

SSAO: semicarbazide-sensitive amine oxidase, AMO: acetol monooxygenase, G-6P: glucose-6-phosphate, F-6P: fructose-6-phosphate, F-1,6P: fructose-1,6-phosphate, DHAP: dihydrogenacetone phoaphate, G3P: glyceraldehyde-3-phosphate, GSH: glutathione, Gly-I: glyoxalase I, Gyl-II: glyoxalse II: ROS: reactiveoxygen species, AGEs: advanced glycation end products (AGEs) (Kalapos, 1999).

2.5.2 Exogenous source of methylglyoxal

Methylglyoxal also found in natural products of both animal and plant origin and therefore exogenous exposure occurs through consumption of all foods. Very high levels of methylglyoxal have been reported in manuka honey that contains

high levels of antioxidants (Marceau and Yaylayan, 2009). In fact, the major exogenous sources of methylglyoxal are processed alimentary products which are strongly affected by the cooking process. The commercial beverages, cheese, coffee or milk contain extremely high methylglyoxal levels (Gensberger *et al.*, 2012).

Table 2 Methylglyoxal content in foods and beverages
(Uribarri et al., 2010)

Food	Total MG (nmol/100 g)
Fat	
Olive oil, fresh	7,700
Margarine	10,790
Protein	
Tuna, solid white packed in water	4,060
Salmon, pan fried in olive oil	9,090
Egg, fried	13,670
Chicken, grilled	14,440
Cheese, American	16,790
Carbohydrate	
Bread, white	3,630
Bread, wheat	4,840
Dairy products	**Total MG nmol/100 g**
Milk, whole	620
Yogurt	830
Beverages	**Total MG nmol/100 g**
Coca Cola Classic	13
Pepsi, regular	325

2.5.3 Methylglyoxal detoxification system

Several enzymatic systems are responsible for methylglyoxal detoxification in the body including glyoxalase, aldose reductase, betaine aldehyde dehydrogenase and 2-oxoaldehyde dehydrogenase (Vander Jagt and Hunsaker, 2003).

- **Glyoxalase system**

Methylglyoxal levels are ultimately controlled by glyoxalase system as the major pathway in the cytosol of all mammalian cells. Glyoxalase system that consists of two enzymes: gloxalase-I (GLO1) and gloxalase-II (GLO2) that catalyze the conversion of methylglyoxal to a non-toxic substance S-D-lactoylglutathione and D-lactate, respectively (figure 2.10). D-lactate is further metabolized to pyruvate. Glutathione, the strong vital antioxidant system, is a cofactor in glyoxalase system. Therefore, a depletion of GSH in oxidative stress status that mostly found in diabetic condition leads to decrease GLO1 activity (Park *et al.*, 2003), resulting in higher level of methylglyoxal.

- **Aldose reductase**

Methylglyoxal is also metabolite by aldose reductase with NADPH dependent. The product distribution is glutathione-dependent that non-enzymatically reacts with methylglyoxal to form hemithioacetal. Methylglyoxal is converted into acetol through reduction of the aldehyde group in the absence of glutathione whereas hemithioacetal is converted into D-lactaldehyde through reduction of the ketone group in the presence of glutathione. Then, acetol and D-lactaldehyde are catalyzed to L-1,2-propanediol and D-propanediol, respectively. However, distribution of aldose reductase in human tissue is restricted with low expression in liver (Vander Jagt and Hunsaker, 2003).

- **Aldehyde dehydrogenase**

Aldehyde dehyprogenase including Betaine aldehyde dehydrogenase and 2-oxoaldehyde dehydrogenase can catalyst the conversion of methylglyoxal into pyruvate. 2-oxoaldehyde dehydrogenase has higher efficiency then Betaine aldehyde dehydrogenase. The reaction is required NAD and NADPH for its activity (Vander Jagt and Hunsaker, 2003).

2.5.4 Methylglyoxal and diabetic complications

In fact, many researchers reported the elevation of methylglyoxal level has been observed in hyperglycemia associated with diabetes. The serum concentration of methylglyoxal increased by 5-6 folds in patients with type 1 diabetes and by 2-3 folds in patients with type 2 diabetes (Park et al., 2003). In glycation process, methylglyoxal is a potent AGEs precursor which is effective substrate of protein crosslink. Therefore, the higher level of methylglyoxal in diabetes causes greater AGEs formation and accumulation. Elevated methylglyoxal levels and associated AGEs adducts in the kidney, lens and blood vessels have been associated with complications commonly found in patients with diabetes. The recent study shows that methylglyoxal has been implicated in diabetes related vascular disorders and endothelial inflammation (Mukohda *et al.*, 2012). Methylglyoxal-protein interaction also produces hydroxyl radicals and superoxide anion that damage cell components particularly DNA (Kang, 2003). In human, the overproduction of ROS involves in the development of cancer and cardiovascular disease (Wu et al., 2011)

- **Roles of methylglyoxal in diabetic vascular complications**

In hyperglycemia condition, increased methylglyoxal level has been linked to the development of diabetes and its vascular complications by increasing endothelial damage and vascular remodeling at the macrovascular and

microvascular levels where inflammation plays a role. The progression of diabetic vascular complication results in cardiovascular disease (CVD), chronic renal failure, retinal damage, neuropathy and poor wound healing. The promotion of methylglyoxal on diabetic complication probably derives mostly from the endogenous production in hyperglycemia condition. To understand the role of methylglyoxal in hyperglycemia-induced vascular damage several studies focused on cellular pathways by direct stimulation culture endothelial or other vascular cells (Wu and Juurlink, 2002, Dhar *et al.*, 2010, Su *et al.*, 2013). The overall results show that methylglyoxal has cytotoxic properties, genotoxicity and apoptosis. methylglyoxal- and AGEs-modified dietary proteins are poorly absorbed, passed to blood flow, and excreted in urine. However, the dietary methylglyoxal has been considered as a key role in diabetic complication (Singh *et al.*, 2014). The study showed that glucose, a monosaccharide, increased methylglyoxal levels in plasma and impaired vessel function after one single feeing (Beisswenger *et al.*, 2001). Methylglyoxal-modified protein was correlated with LDL cholesterol serum level which is an important factor in atherosclerosis progression (Matafome *et al.*, 2012). The potential vascular targets of excessive methylglyoxal remain to be understood. Prolonged exposure to methylglyoxal causes vascular ATP-sensitive K^+ channel disruption. The overexpression of GLO1, the enzyme that is important for methylglyoxal degradation, reduced the development of pathophysiological complication in the model of lesions of retinal neuroglia and vessels (Bener *et al.*, 2011).

The elevation of methylglyoxal serum levels were observed in diabetic patients and spontaneous hypertensive rats (SHR) (Wang et al., 2005, Crisostomo *et al.*, 2013), associated with vascular disorder (Rabbani *et al.*, 2011). The elevation of methylglyoxal in SHR correlated with the degree of hypertension (Huang et al., 1997,

Anuradha and Balakrishnan, 1999, Tran et al., 2009, Babacanoglu *et al.*, 2013). The scientific evidence indicated that the long-term methylglyoxal treatment in isolated mesenteric artery caused endothelial dysfunction by decreasing nitric oxide (NO) production and endothelial nitric oxide synthase (eNOS) expression, undergo impaired vascular functions (vasoconstriction and vasodilation) (Mukohda et al., 2012, Mukohda et al., 2013). The effects of methylglyoxal accumulation in arterial wall of SHR on vascular functions were similar to the *in vitro* studies (Wang et al., 2005, Mukohda *et al.*, 2012). Methylglyoxal activate NADPH oxidase subunit 1 (NOX1)-derived superoxide anion production has been proposed as an underling mechanism of vascular abnormalities and subsequent apoptosis in endothelial cell and smooth muscle (figure 11) (Mukohda et al., 2012). Related to diabetic vascular complications, methylglyoxal is able to attack free amino group of protein to form irreversible AGEs and play a role as a ROS inducer. AGEs contributes to the formation of cross-link of extracellular matrix molecules, permanently altering cellular structure and engages the receptor for AGEs (RAGE), altering cellular function (Wu et al., 2011). The AGEs-RAGE interaction cascades the signaling to stimulate NADPH oxidase and increases ROS production, attributes to activation of transcription factor NF-κB that play a crucial role in inflammatory response (figure 12) (Goldin et al., 2006). Methylglyoxal could affect inflammation responses in endothelial cell in addition to impaired vascular reactivity which occurs as early event in atherosclerosis, hypertension and vascular complication in diabetic patients (O'Keefe et al., 2009).

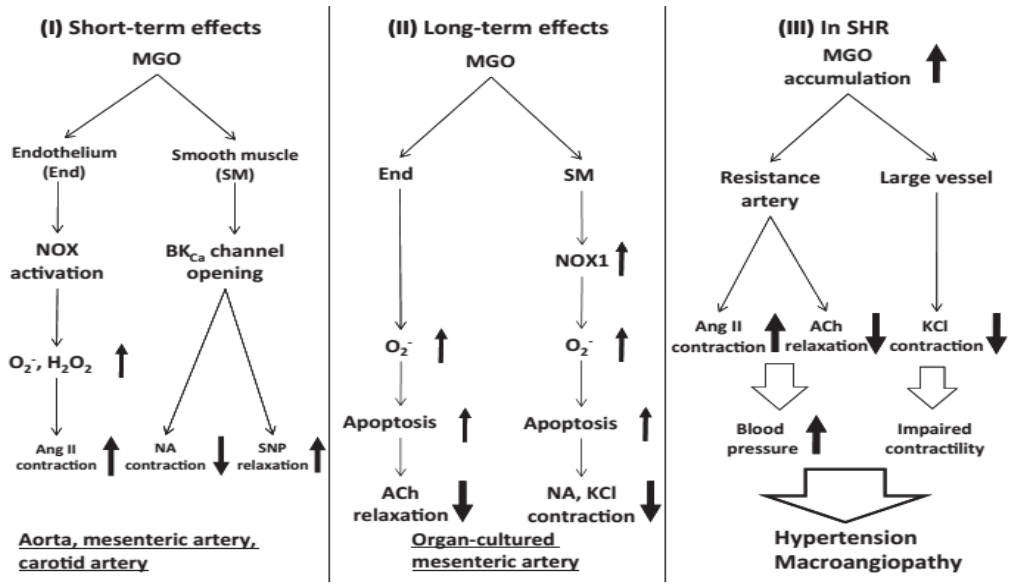

Figure 11 The effect of methylglyoxal on vascular reactivity

(Mukohda et al., 2012)

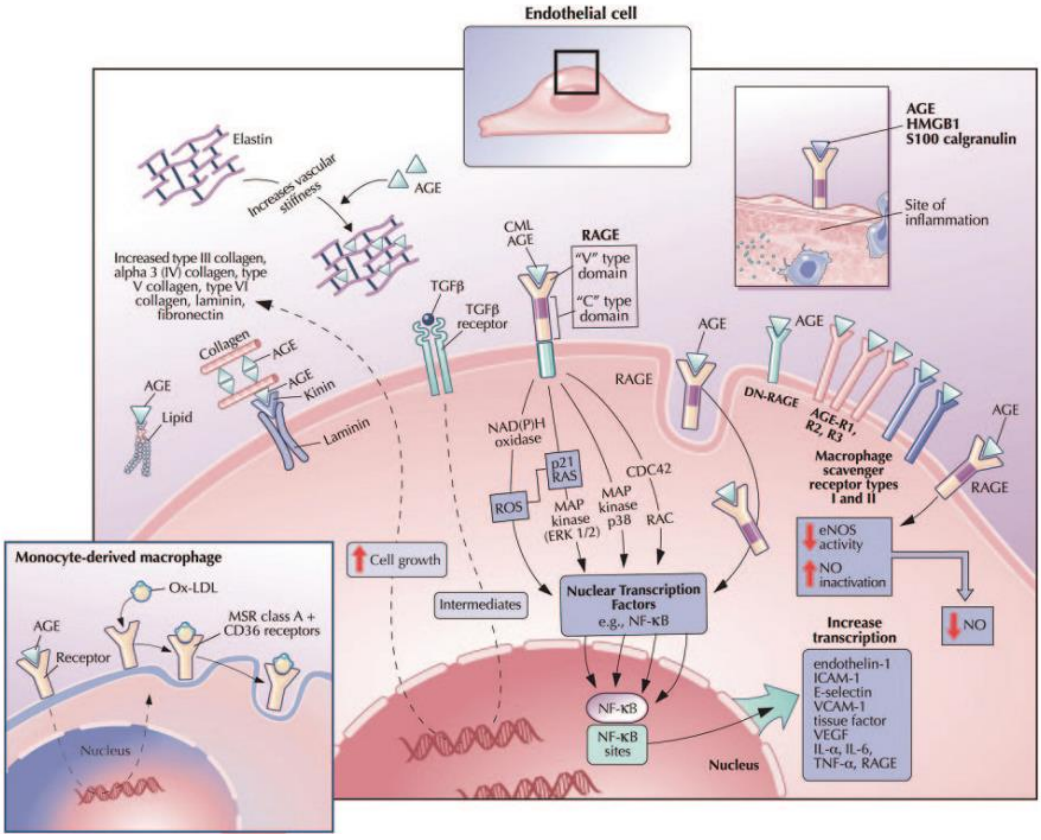

Figure 12 The extracellular and intracellular effects of AGEs

(Goldin et al., 2006)

2.6 Anti-glycation agents

2.6.1 Proposed mechanisms for anti-glycation

Anti-glycation agents are considering for the inhibition of protein glycation to delay or prevent the development of diabetic vascular complications. Nowadays, the specific anti-glycation compounds are not yet available. Anti-glycation may acts as any of the proposed biochemical mechanism as shown in figure 13 to inhibit AGEs formation (Dhar and Desai, 2012).

1. Compounds that have the ability of bind with amino group of proteins can prevent the binding of carbonyl group of reducing sugar to protein leading to inhibit protein glycation (Dhar and Desai, 2012). For example, aspirin has been reported to inhibit protein glycation in lens proteins presumably through the capping of free amino groups in lysine residuals (Swamy and Abraham, 1989). In recently, eugenol, a member of the phenylpropanoids class of chemical compounds, also showed anti-glycation ability in bovine serum albumin by strongly binding with exposed lysine residuals (Singh *et al.*, 2016).

2. Compounds that bind to carbonyl groups of reducing sugars can prevent the reaction between sugars and protein molecular, resulting in the inhibition of protein glycation. For instance, aminoguanidine has an potent ability to bind with carbonyl group of glucose and inhibit AGEs formation on β_2-microglobulin (Hou *et al.*, 1998).

3. Compounds that can acts as antioxidant to scavenge free radicals that are generated during glycation process and accelerate the damaging effect. The supplement with vitamin E and vitamin C inhibited non-enzymatic glycation in diabetic rats and protect the damaging effect on kidney (Qian *et al.*, 2000).

4. Compounds that can trap the carbonyl groups of reactive dicarbonyl compounds including glyoxal, 3-deoxyglucosone and methylglyoxal. Reactive dicarbonyl compounds are generated during propagation stage of protein glycation. They are potent AGEs precursor by using carbonyls groups in the molecule to bind with protein (Wu et al., 2011). Metformin has been reported as an anti-glycation agent by binding to dicabonyl compounds methyglyoxal and 3-deoxyglucosone (Beisswenger and Ruggiero-Lopez, 2003).

5. Compounds that can quench Amadori products that formed during initiation stage of protein glycation and then inhibit the further step of the process. Aminoguanidine also acts in this manner to inhibit protein glycation (Dhar and Desai, 2012).

6. Compounds that can break the final product AGEs and decrease the accumulation of AGEs in tissues. Phenacylthiazolium bromide, metformin and alagebrium has been reported to break AGEs cross-links (Coughlan *et al.*, 2007)

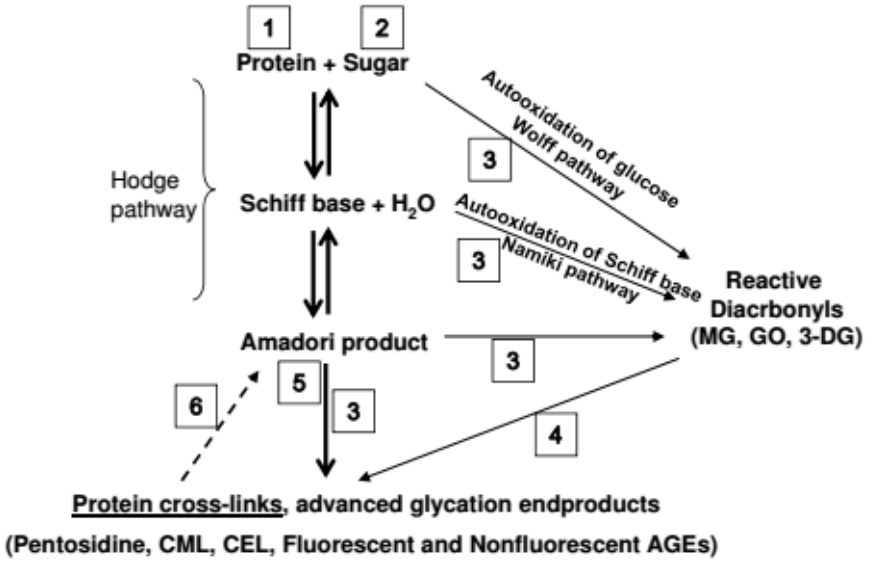

Figure 13 The proposed mechanisms for anti-glycation agent (Dhar and Desai, 2012).

2.6.2 Aminoguanidine

Aminoguanidine, the first pharmaceutical AGEs inhibitor to be tested in clinical trial, is a derivative of nucleophilic hydrazine that binds irreversibly to reactive dicarbonyl intermediate in propagation stage of protein glycation including 3-deoxyglucosone and methyglyoxal, resulting in prevents AGEs formation and protein cross-linking (figure 14) (Brownlee *et al.*, 1986, Thornalley *et al.*, 2000). Treatment of aminoguanidine in type 1 and type 2 diabetic animals associated with the inhibition of diabetic nephropathy, retinopathy neuropath and vascular complications (Thornalley, 2003). Aminoguanidine displayed potency to prevent the progression of diabetic nephropathy by reducing AGEs accumulation in glomerular basement membrane, binding to IgG, decreasing albuminuria and slows mesangial matrix expansion in diabetic rat (Soulis-Liparota *et al.*, 1991). High doses of animoguanidine are required in severe hyperglycemia condition in animal study. However, it has short half-life in plasma. Apart from the reaction with dicarbonyl compounds, aminoguanidine also reacts to deplete vitamin B6 and pyridoxal (Nagai *et al.*, 2012). The early clinical trials with aminoguanidine showed great promise as an AGEs inhibitor. However, studies in people with diabetic nephropathy were terminated following safety and efficacy concerns of aminoguanidine (Freedman *et al.*, 1999, Bolton et al., 2004)

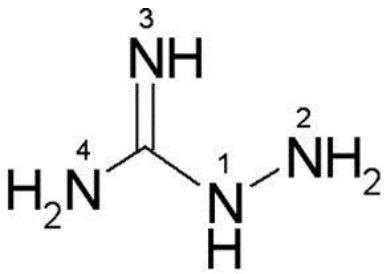

Figure 14 Chemical structure of aminoguanidine
(Kazachkov *et al.*, 2007).

2.6.3 Alternative medicines

The current scientific evidence have been searched for antiglycation agent from several phytochemical compounds that can delay or prevent glycation process (Adisakwattana *et al.*, 2012, da Silva Morrone *et al.*, 2013, Sri Harsha et al., 2013). The mechanisms of phytochemical compounds have recently been proposed as Amadori products inhibitor, AGEs inhibitor, reactive dicarbonyl compounds scavenger, free-radicals scavenger and chelating transition metal ion scavenger (Wu et al., 2011). It has been reported that polyphenols and flavonoids showed the high antioxidant activities by reacting against ROS and thus interrupting the propagation of new free radical species. The ROS scavenging activities may cause from double bonds presented in the phenolic ring and the hydroxyl side chains.

- **Anthocyanin**

Anthocyanins, an effective phytochemical substance, are one class of flavonoids. The beneficial health effects of anthocyanin are being antioxidant, anti-inflammatory, anti-carcinogenic as well as lowing the risk of cardiovascular (Bowen-Forbes *et al.*, 2010, Wallace, 2011). Data from animal studies have shown that anthocyanins promote vascular health. Relatively low-dose anthocyanin interventions with patients clinically diagnosed with vascular diseases have been associated with significant reductions in ischemia, blood pressure, lipid levels and inflammatory status (Wallace, 2011). In high fructose-fed rat, anthocyanin treatment prevented the progression of hypertension, cardiac hypertrophy and the production of ROS by decreasing the expression of NADPH oxidase (Al-Awwadi *et al.*, 2005). Many studies have founded that the plants that contain anthocyanin have an ability to eliminate AGEs which are triggered by ROS. According to the experimental data, high content of anthocyanin in plants is associated with the high antiglycation activity

(Hanamura *et al.*, 2005, Yao and Brownlee, 2010, Jariyapamornkoon et al., 2013). It can be concluded that antioxidant activity is a strategy to inhibit protein glycation. In fact, recently study reported the inhibitory effect of anthocyanin containing plant on protein glycation by trapping reactive carbonyl intermediates such as methylglyoxal (Liu et al., 2011).

2.7 Cyanidin-3-O-rutinoside (C3R)

2.7.1 General property of C3R

C3R (cyanidin-3-O-rhamnosylglucoside, cyanidin-3-O-rhamnoglucoside or Keracyanin) is a glycoside of flavylium (2-phenylbenzopyrylium) salts base on anthocyanidins, cyanidin. As shown in figure 15. The sugar moiety is disaccharide rutinose at R3 hydroxyl group position on aromatic C ring. C3R has hydroxyl group at R5 and R7 position on aromatic A ring and R3' and R4' on aromatic B ring. The chemical formula is $C_{27}H_{31}O_{15}Cl$. The molecular weight is 631 g/mol.

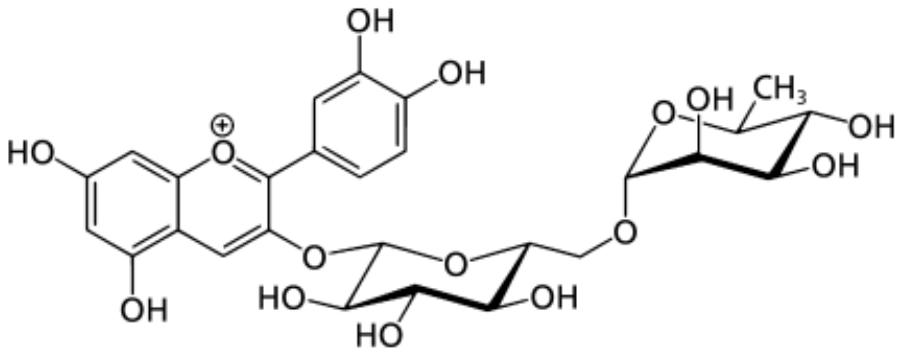

Figure 15 Chemical structure of cyanidin-3-rutinoside (Adisakwattana et al., 2011).

C3R is responsible for red, purple and blue colors in fruits, flowers and vegetables. It predominates in dietary sources, comprising 19%–70% of total anthocyanin in fruits and grain such as açaí berry (Gouvêa *et al.*, 2012), mulberry (Hassimotto *et al.*, 2008), blackberry (Jung *et al.*, 2014), blackcurrant (Edirisinghe *et*

al., 2011, Diaconeasa *et al.*, 2015), raspberry (Jung et al., 2014), pigmented rice (Deng *et al.*, 2013) and litchi (Li et al., 2012).

Table 3 C3R content in fruits and vegetables.

Source	C3R concentration	Unit	References
Acai, freeze-dried	58.73	mg/100 gram	(Gouvêa et al., 2012)
Litchi, nine varieties	1.29-19.11	mg/100 gram	(Li et al., 2012)
Buckwheat Sprouts, dry	1.36-65.5	mg/100 gram	(Watanabe, 2007)
Blackcurrant, juice	50.6	mg/100 mL	(Diaconeasa et al., 2015)

2.7.2 Bioavailability of C3R

In general, glycoside conjugated in anthocyanin can be deglycosylated by endogenous β-glycosidase (lactase phloridzin hydrolase) or by gut microflora enzynes, and further absorped by passive disfussion. Hassimoto *et al*. reported that C3R was deglycosylated in *in vitro* fermentation by incubated with feces (Hassimotto et al., 2008). However, the oral administration of C3R can pass through the intestinal mucosa and distributed to blood circulation as intact glycoside that can be detected in plasma of animal and human (Matsumoto *et al.*, 2001, Hassimotto et al., 2008). C3R binds to sodium glucose cotransporter SGLT1 for intestinal absorption. In addition, because of high hydrophilicity and neutral pH ionization, C3R can make passive diffusion across intestinal membrane as well. The maximum concentration of C3R in plasma has been reached after administration for 15-30 min in rats (Matsumoto et al., 2001, Hassimotto et al., 2008) and after 90 min in human (Matsumoto et al., 2001). Apart from plasma, C3R was also presented in kidney and gastrointestinal tract including stomach and small and large intestines (Hassimotto et al., 2008). Only 0.11% of cyanidin glycoside was absorbed after administration for 8

hours and increased the antioxidant capacity in rat plasma (Hassimotto et al., 2008). C3R was excreted in to urine after 2 hours as the intact form, the level of urinary excretion in human was low (Matsumoto et al., 2001).

2.7.3 Beneficial health effects of C3R

- **Antioxidant and anti-inflammatory activity**

Several evidence indicated the antioxidant activity of C3R by scavenging superoxide anion, hydroxyl radicals, peroxyl and peroxynitrite *in vitro* (Feng *et al.*, 2007, Tulio et al., 2008, Li et al., 2012, Ortiz et al., 2013). Treatment of C3R decreased intracellular ROS and DNA damage and also increased the cellular ferric reducing antioxidant power in hydrogen peroxide-induced RAW264.7 cell toxicity. C3R also inhibited lipopolysaccharide-induced prostaglandin E_2 production in macrophage that correlated with downregulation of inducible nitric oxide synthase (iNOS), cycoxygenase-2 (COX-2) and NF-κB (Seeram *et al.*, 2001, Jung *et al.*, 2014). In animal study, treatment of cherry juice-containing C3R showed ability to increase antoxidant action through increased superoxide dismutase (liver and blood) and glutathione peroxidase (liver) activity and decreased lipid peroxidation concentration. Cherry juice has been identified as a potent anti-inflammatory agent by inhibiting cyclooxygenase 2 (liver) (Saric *et al.*, 2009).

- **Anti-carcinogenic activity**

The effect of C3R on the induction of apoptosis in leukemic cell HL-60 has previously reported via ROS-dependent activation of MAPK signaling pathwy without toxicity effect on normal human peripheral blood mononuclear cells (Feng et al., 2007). C3R also showed a potent to inhibit the migration and invasion of highly metastatic human lung cancer cell line. In the level of transcription, treatment of

C3R inhibited the activation of c-Jun and NF-κB, while, C3R decreased matrix matalloprotinase-2 (MMP-2) and urokinase-plasminogen activator (u-PA) and increased the expression of tissue inhibitor of MMP-2 and plasminogen activator inhibitor (PAI) in the level of translation (Feng et al., 2007)

- **Anti-diabetic activity**

Anti-hyperglycemic activity has been reported by discovering the inhibitory effects of C3R on α-glucosidase (Adisakwattana *et al.*, 2004, He and Lu, 2013). The IC_{50} value of C3R to inhibit α-glucosidase *in vitro* is 2,323 ± 14.8 μM in maltase and 250.2 ± 8.1 in sucrose. Oral administration of C3R at 100 and 300 mg/kg significantly decreased postpandrial blood glucose in maltose and sucrose tolerance tests (Adisakwattana et al., 2011). The interaction of glycoside in C3R molecule to α-glucosidase reduced the hydrophobic surface of α-glucosidase and caused the enzyme conformational change (He and Lu, 2013). Moreover, C3R also inhibited pancreatic α-amylase with IC50 value of 24.45±0.03 μM. In oral ingestion study, C3R at concentration 100 and 300 mg/kg significantly decreased plasma glucose after 60 min starch loading (Akkarachiyasit *et al.*, 2011). α-glucosidase and pancreatic α-amylase play an important role in carbohydrate digestion and absorption. Thus, it could be an important mechanism to decrease postprandial hyperglycemia in diabetic patient

- **Cardioprotective activity**

C3R from black currant juice extract has been revealed to activate eNOS activity via phosphorylate-AKt and phosphorylate-eNOS *in vitro* in human umbilical vein endothelial cell (Edirisinghe et al., 2011). In rat thoracic aorta, the black currant concentrate-containing C3R (37.6% of total anthocyanin) have shown to induce

vascular relaxation via H_1-receptors on the endothelium and escalate nitric oxide production (Nakamura *et al.*, 2002).

CHAPTER III

MATERIALS AND METHODS

3.1 Materials

❖ Chemicals	Company
Rutin, 97+%	ACROS organics (Thermo Fisher Scientific, Geel Belgium)
Zinc power	Ajex finechem (Taren Point, Australia)
Hydrochloric acid (HCl)	Merck (Darmstadt, Germany)
Mercury red	ACROS organics (Thermo Fisher Scientific, Geel Belgium)
Diethyl ether	Merck (Darmstadt, Germany)
Methanol (analysis grade; MeOH)	Merck (Darmstadt, Germany)
Bovine serum albumin (BSA) fraction V	Fisher (Loughborough, LE, UK)
D(+)Ribose	Sigma-Aldrich CO. (St. Louis, MO, USA)
D(+)fructose	Fisher (Loughborough, LE, UK)
D(+)Glucose	Ajex finechem (Taren Point, Australia)
D(+)galactose	Ajex finechem (Taren Point, Australia)
40% Methylglyoxal solution	Sigma-Aldrich CO. (St. Louis, MO, USA)
5,5'-dithiobis (2-nitrobenzoic acid) (DTNB)	Sigma-Aldrich CO. (St. Louis, MO, USA)
Thioflavin T	Sigma-Aldrich CO. (St. Louis, MO, USA)
Nitrobluetetrazolium (NTB)	Sigma-Aldrich CO. (St. Louis, MO, USA)

❖ Chemicals	Company
Ethyl acetate	Fisher (Loughborough, LE, UK)
Ethanol (EtOH)	Merck (Darmstadt, Germany)
1-deoxy-1-morpholino-D-fructose (DMF)	Sigma-Aldrich CO. (St. Louis, MO, USA)
L-cysteine	Sigma-Aldrich CO. (St. Louis, MO, USA)
Aminoguanidine hydrochloride (AG)	Sigma-Aldrich CO. (St. Louis, MO, USA)
2,4-dinitrophenylhydrazine (DNPH)	Ajex finechem (Taren Point, Australia)
Trichloroacetic acid (TCA)	Merck (Darmstadt, Germany)
Guanidine hydrochloride	Merck (Darmstadt, Germany)
Sodium chloride (NaCl)	Ajex finechem (Taren Point, Australia)
Monosodium phosphate (NaH_2PO_4)	Qrec chemical co, Ltd. (New Zealand)
Disodium phosphate (Na_2HPO_4)	Ajex finechem (Taren Point, Australia)
Sodium azide (NaN_3)	Merck (Darmstadt, Germany)
Dimethyl sulfoxide (DMSO)	Merck (Darmstadt, Germany)
Amplicilin sodium salt	AppliChem Inc. (St. Louis, MO, USA)
L-lysine hydrochloric acid	HiMedia Laboratories (Mumbai, India)
Agarose	ISC BioExpress (Kaysville, Utah, USA)
Tris (hydrodroxymethyl) amiomethane	Bio-rad Laboratories (Hercules, CA, USA)
Boric acid (ACS reagent)	Research organics, Inc. (Clevelnd, OH, USA)
Ethylenediaminetetraacetic acid (EDTA)	Sigma-Aldrich CO. (St. Louis, MO, USA)

❖ Chemicals	Company
Cupric Sulfate, 5-hydrate	J.T.Baker® Chemical (Center Valley, PA, USA)
LB Broth	Bio Basic, Int. (Markham, ON, Canada)
Agar A	Bio Basic, Int. (Markham, ON, Canada)
Cytochrome *c*	Affymetrix (Santa Clara, CA, USA)
Thiobarbituric acid (TBA)	Sigma-Aldrich CO. (St. Louis, MO, USA)
2-deoxy-D-ribose	Sigma-Aldrich CO. (St. Louis, MO, USA)
Methanol (gradient grade for liquid chromatography; MeOH)	Merck (Darmstadt, Germany)
o-phynylenediamine (*o*-PD)	Sigma-Aldrich CO. (St. Louis, MO, USA)
5-Methylquinoxaline (5-MQ)	Sigma-Aldrich CO. (St. Louis, MO, USA)
Perchloric acid	Sigma-Aldrich CO. (St. Louis, MO, USA)
Dulbecco's modified eagle's medium, high glucose	Sigma-Aldrich CO. (St. Louis, MO, USA)
Sodium bicarbonate, molecular grade	Sigma-Aldrich CO. (St. Louis, MO, USA)
Penicillin-streptomycin (10,000u/mL)	Gibco, Thermo Scientific, Inc. (Waltham, MA, USA)
Phosphate buffer saline (PBS)	Gibco, Thermo Scientific, Inc. (Waltham, MA, USA)
HEPES sodium salt	Sigma-Aldrich CO. (St. Louis, MO, USA)
Noradrenaline bitartrate (NA)	Sigma-Aldrich CO. (St. Louis, MO, USA)

❖ Chemicals	Company
Acetylcholine chloride (Ach)	Sigma-Aldrich CO. (St. Louis, MO, USA)
Sodium nitroprusside (SNP)	Sigma-Aldrich CO. (St. Louis, MO, USA)
N^{ω}-Nitro-L-arginine	Sigma-Aldrich CO. (St. Louis, MO, USA)
Potassium chloride (KCl)	Ajex finechem (Taren Point, Australia)
Potassium phosphate monobasic (KH_2PO_4)	Ajex finechem (Taren Point, Australia)
Magnesium sulfate heptahydrate ($MgSO_4 \cdot 7H_2O$)	Ajex finechem (Taren Point, Australia)
Ascorbic acid	Sigma-Aldrich CO. (St. Louis, MO, USA)
Calcium chloride solution ($CaCl_2$)	
Heparin Sodium (porcine mucous)	Hospira, Inc. (Lake Forest, IL, USA)
Cell lysis buffer	CST Cell Signaling Technology (Danvers, MA, USA)
Bradford reagent	Bio-rad Laboratories (Hercules, CA, USA)

❖ <u>Laboratory equipment</u>	<u>Company</u>
Spectrofluorometer	Perkin Elmer (Waltham, MA, USA)
Spectrophotometer	Perkin Elmer (Waltham, MA, USA)
High-performance liquid chromatography (HPLC)	Shimadzu Corporation (Kyoto, Japan)

❖ Laboratory equipment	Company
pH meter	Thermo Scientific, Inc. (Waltham, MA, USA)
Laboratory refrigerator	Sanden intercool (Thailand)
Orbital shaker	Labnet international Unc. (Edison, NJ, USA)
Heating water bath	Memmert GmbH + Co. KG (Schwabach, Germany)
Orbital shaker incubator	Labnet International, Inc. (Edison, NJ, USA)
Hot plate	IKA-Works, Staufen im Breisgau, Germany
Vortex mixer	Gemmy industrial corp. (Taipei, Taiwan)
Autoclave	Amegax Instruments, Inc. (Concord, CA, USA)
Modular tissue bath system	EMKA Technologies (Boulevard du Général Martial Valin, Paris, France
Perfusion system for mesenteric beds	EMKA Technologies (Boulevard du Général Martial Valin, Paris, France
CFX384 Tough™ Real-time PCR detection system	Bio-rad Laboratories (Hercules, CA, USA)

❖ Laboratory equipment	Company
Biosafety Cabinet (class II)	Esco Micro Pte. Ltd (Singapore)
Gel electrophoresis chamber	CS Cleaver Scientific Ltd. (Warwickshire, United kingdom)
Electrophoresis power supply	Bio-rad Laboratories (Hercules, CA, USA)
Gel imaging system	Bio-rad Laboratories (Hercules, CA, USA)
CO2 incubator	Skadi Europe B.V. (Netherlands)
C1000 Touch™ Thermal cycler	Bio-rad Laboratories (Hercules, CA, USA)
Mini-Beadbeater-24	BioSpec Products, Inc. (Barlesville, OK, USA)
EpMotion 5070 Liquid Handling Robot	Eppendrof (Hamburg, Germany)
MP100 device	BIOPAC System, inc

❖ <u>Miscellaneous</u>	<u>Company</u>
N^{ε}-(carboxymethyl) lysine (N^{ε}-CML) ELISA kit	Cell Biolabs, Inc. (San Diego, CA, USA)
Plasmid Miniprep Kit (DNA extraction)	QIAGEN Inc. (Valencia, CA, USA)
Urea nitrogen reagent kit	Beckman coulter (Brea, CA, USA)
Creatinine reagent kit	Beckman coulter (Brea, CA, USA)

❖ Miscellaneous	Company
Alanine aminotransferase (ALT) reagent kit	Beckman coulter (Brea, CA, USA)
Column chromatography bead Diaion® HP-20	Sigma-Aldrich CO. (St. Louis, MO, USA)
Fibrous tissue RNA extraction kit	QIAGEN Inc. (Valencia, CA, USA)
SsoAdvanced Universal SYBR Green Supermix	Bio-rad Laboratories (Hercules, CA, USA)
iScript Reverse Transcription Supermix for RT-qPCR	Bio-rad Laboratories (Hercules, CA, USA)
Experion RNA Analysis Kits	Bio-rad Laboratories (Hercules, CA, USA)
HPLC C18 column	GL Sciences Inc. (hinjuku-Ku, TK, Japan)
Surgery equipment	

3.2 Methods

3.2.1 Synthesis of cyanidin-3-rutinoside (C3R)

C3R was obtained by chemical synthesis according to previous study by converting flavonols quercetin-3-*O*-rutinoside (Rutin) (Elhabiri *et al.*, 1995).

- **Preparation of zinc amalgam**

Zinc powder (10.5 g) was weighted and added 30 mL of 1 M HCl. After 5 min, HCl solution was removed. The zinc powder was washed with 20 mL distilled water 2 times and kept in distilled water. The color solution was prepared by dissolving 0.347 g Mercury red in 1 mL concentrated HCl. Color solution was quickly added to zinc powder in distilled water with stirring for 10 min. Then, the zinc amalgam was filtered through NO.1 filter paper and washed with 50 mL distilled water for 5 times. The water was then removed by suction pump and by diethyl ether. The dried zinc amalgam powder was kept at room temperature and protected from light.

- **Synthesis of C3R**

Rutin (1 g) was dissolved in 16 mL 3% MeOH-HCl, and 1.58 g zinc amalgam was slowly added into solution with stirring. Rutin (yellow color) was reduced to give C3R (dark red color). After 10 min, the solution was filtered with NO.1 filter paper to remove zinc amalgam. The C3R solution was purified by column chromatography with Diaion® HP-20 as stationary phase and MeOH as mobile phase. The dark red C3R fraction was collected. To concentrate C3R fraction, MeOH was gently evaporated by using rotary evaporator until 10 mL of C3R fraction remaining. It was slowly dropped into 50% (v/v) 1%MeOH-HCl in diethyl ether to crystallization. The dryness C3R was obtained after repeatly evaporated solution. The C3R was kept at -20^{o}C and protected from light. The yield is 60%.

3.2.2 Determination of inhibitory effect of C3R on ribose, fructose, glucose, galactose or methylglyoxal-induced protein glycation *in vitro*

Glycation of bovine serum albumin

The glycated BSA formation was prepared according to the previous method (Meeprom *et al.*, 2013). The reaction setting was divided into for 2 groups: blank and test to determine the inhibitory effect of AGEs formation. The reaction mixtures were set up in 0.1 M phosphate buffer saline (PBS), pH 7.4 for 1 mL final volume by adding difference volumes of chemicals as shown in table 4. The final concentration of BSA was 10 mg/mL, methylglyoxal was 1 mM and ribose was 0.1 M while fructose, glucose and galactose were 0.5 M. AG with final concentration 1 mM was used as positive control. The treatment C3R (final concentration 0.125, 0.25, 0.5 and 1 mM) was dissolved in dimethylsulfoxide (DMSO) and added to the solution to give a final concentration of 4% DMSO. All samples were incubated at 37°C for 7 and 14 days. To determine the inhibitory effect, the samples in each period were detected the formation AGEs, fructosamine, protein oxidation and protein aggregation

Table 4 Chemicals were presented in glycation of bovine serum albumin (BSA)

Experimental groups	PBS (µL)	0.22 M Ribose/ 1.1 M Fructose/ 1.1 M Glucose/ 1.1 M Galactose/ 0.22 mM MG	20 mg/mL BSA (µL)	25 mM AG (µL)	3.125-25 mM C3R (µL)	100% DMSO (µL)
Blank						
● Blank	1000	-	-	-	-	-
● Negative	500	460	-	-	-	40
● Positive	500	460	-	40	-	-
● Treatment	500	460	-	-	40	-
Test						
● Blank	500	-	500	-	-	-
● Negative	-	460	500	-	-	40
● Positive	-	460	-	40	-	-
● Treatment	-	460	-	-	40	-

PBS: Phosphate buffer saline, MG: Methylglyoxal, AG: Aminoguanidine hydrochloride, C3R: Cyanidid-3-rutinoside, DMSO: Dimetyl sulfoxide

Determination of fluorescent AGEs formation

The glycated BSA from each incubation period was quantified the formation of fluorescent AGEs according to a previous report (Meeprom et al., 2013). Glycated samples (50 µL) from blank and test groups were placed into 96-wells plates and measured by using spectrofluorometer at excitation and emission wavelengths 355 and 460 nm, respectively. The percentage of inhibition was calculated by following equation below:

$$\text{Inhibition of fluorescent AGEs (\%)} = [((FC - FCB) - (FS - FSB))/(FC - FCB)] \times 100$$

Where FC and FCB were the fluorescent intensity of control with monosaccharides or methylglyoxal and blank of control without monosaccharides or methylglyoxal, FS and FSB were the fluorescent intensity of sample with monosacchardeor methylglyoxal and blank of sample without monosaccharides or methylglyoxal

Determination of non-fluorescent AGE, N^{ε}-(carboxymethyl) lysine (N^{ε}-CML) formation

N^{ε}-CML, a major non-fluorescent AGE structure, was determined by using enzyme linked immunosorbant assay (ELISA) kit according to the manufacturer's manual (OxiSelect™ N^{ε}-(carboxymethyl)lysine (CML) ELISA Kit, Cell Biolabs , CA, USA). The glycated samples from test group 100 µL (1,000-fold dilution in reduced BSA) were placed into 96 well plates and incubated at 37°C for 2 hours. The solution was discarded and then washed each well with 250 µL 1xPBS for twice. Assay dilutant (200 µL) was added in the plate then incubated at room temperature for 2 hours on orbital shaker. After discarded and washed each well with 1x wash buffer (250 µL) for 3 times, 100 µL of diluted anti-CML antibody (1:1000 anti-CML antibody in assay dilutant) was added and incubated for 1 hour at room temperature on orbital shaker. The solution was discarded and the wells were washed each well with 250 µL wash

buffer for 3 times. 100 µL diluted anti-HRP conjugated antibody (1:100 anti- HRP conjugated antibody in assay dilutant) was added and then incubated at room temperature on orbital shaker for 1 hour. The wells were discarded and washed again by using 250 µL wash buffer for 5 times and 100 µL of substrate solution (warmed at room temperature) was placed to each wells for 20 min (time can be different depend on N^{ε}-CML concentration) on orbital shaker. The reaction was stopped by adding 100 µL stop solution. The absorbance was immediately measured at 450 nm with spectrophotometer. The concentration of N^{ε}-CML was calculated from the standard curve of N^{ε}-CML-BSA (0-12.5 ng/mL).

Determination of fructosamine content

The level of fructosamine was analyzed by nitrobluetetrazolium (NBT) assay (Johnson *et al.*, 1983). The glycated BSA from test (10 µL) was placed in 96 well plates and incubated with 0.5 mM NBT in 0.1 M carbonate buffer (90 µL), pH 10.3 at 37°C. The absorbance was measured at 590 nm at 10 and 15 min and subtracted by the absorbance of sample blank (10 µL glycated BSA with 90 µL 0.1 M carbonate buffer) at each time point. The concentration of fructosamine was calculated by using the different absorption at 10 and 15 min time points compared with the standard 1-deoxy-1-morpholino-fructose (1-DMF) curve (concentration range 0-5 mM).

Determination of protein carbonyl content

Protein carbonyl content is a marker of oxidative protein damage which was analyzed according to a previous method with slight modifications (Levine *et al.*, 1990). The glycated BSA (100 µL) from test group was placed in microcentrifuge tube and incubated with 0.4 mL of 10 mM 2,4 dinitrophenylhydrazine (DNPH) in 2.5 M HCl or with 0.4 mL of 2.5 M HCl as sample blank at 25°C in dark and mixed every 15 min. After 60 min of incubation, protein were precipitated by adding 0.5 mL of 20% (w/v)

trichloroacetic acid (TCA) for 5 min on ice, and then centrifuged at 10,000 g for 10 min at 4°C. The supernatant was removed and 1 mL of 1:1 (v/v) ethanol/ethyl acetate mixture was added to wash protein pellet for twice. Finally, the protein pellet was dissolved in 0.25 mL of 6 M guanidine hydrochloride and separated 110 µL for carbonyl content detection by spectrophotometer at 370 nm. The protein representing in carbonyl group was measured in sample blank by spectrophotometer at 280 nm. The carbonyl content of each sample was subtracted with the absorbance of sample blank and calculated based on the extinction coefficient for DNPH (ε = 22 000 M^{-1} cm^{-1}). The results were expressed as nmol carbonyl/mg protein.

Determination of protein thiol groups

The free thiol group was determined according to Ellman's assay with slight modification (Ellman, 1959). The glycated BSA from test group (10 µL) was placed in 96 well plates and incubated with 90 µL of 25 mM 5,5 -dithiobis-(2-nitrobenzoic acid) (DTNB) in, pH 7.4 for 0.1 M PBS 15 min at room temperature. The sample blank was prepared by incubating glycated BSA with 0.1 M PBS. The absorbance was measured using spectrophotometer at 412 nm. The free thiol concentration was calculated for the standard curve of l-cysteine (concentration range 0-10 nM) and the result was expression as µmol/mg protein.

Determination of protein aggregation

Thioflavin T was used to determine protein aggregation during glycation precess by measuring the level of β-amyloid cross structure according to a previous method with minor modifications (Tupe and Agte, 2010). The test group of glycated BSA (50 µL) was placed in 96 well plates and incubated with 64 µM thioflavin T (50 µL) in 0.1 M PBS for 60 min at 25 °C. The fluorescence intensity was measured at

excitation 435 nm and emission 485 nm and subtracted with the fluorescence intensity of sample blank (50 µL glycated BSA with 50 µL 64 µM thioflavin T).

Determination of methylglyoxal-trapping ability

Methylglyoxal is a reactive precursor to induce protein glycation. The ability to directly trap methylglyoxal was assessed using high performance liquid chromatography (HPLC) according to previously report (Peng *et al.*, 2008). The reactions were in 0.1 M phosphate buffer saline (PBS), pH 7.4 for 0.8 mL final volume by adding difference volumes of chemicals as shown in table 5 C3R was incubated with methylglyoxal at various molar ratios including 0.25:1, 0.5:1, 1:1, 2:1, 4:1 and 16:1 in 0.1 M PBS, pH 7.4. AG was used as positive control to incubate with methylglyoxal at 1:1 molar ratio. The reaction mixtures were incubated at 37°C for 1 and 24 hours. After incubation period, 100 µL of 20 mM *o*-phenylenediamine (*o*-PD) was added to stop the reaction by converting the remaining methylglyoxal into 2-methylquinoxaline (2-MQ), and then added 100 µL of the internal standard (0.06% (v/v) 5-methylquinoxaline (5-MQ) in methanol). All samples were filtered with 0.45 µm nylon syringe filter and transferred to HPLC vial for injection. The quantification of methylglyoxal was based on the determination of its derivative compound (2-MQ). An Inersil-ODS3V C_{18} column (150×4.6 mm i.d.; 5-µm particle size) was used along with a LC-10AD pump, SPD-10A UV-Vis detector and LC-Solution software (Shimadzu Corp., Kyoto, Japan). The absorbance was recorded at 315 nm and the injection volume was 10 µL. An isocratic program was performed with 50% HPLC grade water and 50% methanol (v/v) with a constant flow rate set at 1 mL/min. The total running time was 14 min. The percentage of methylglyoxal reduction was calculated using the equation below:

$$\%\text{methylglyoxal (MG) trapping ability} = \frac{\text{Amount of } (\text{MG in control - MG in C3R})}{\text{Amount of MG in control}} \times 10$$

Table 5 Chemicals were presented in the determination of methylglyoxal-trapping ability

Experimental group	Molar ratio Treatment: MG	1.14 mM MG (µL)	32% DMSO (µL)	8 mM AG (µL)	2 mM C3R (µL)	4 mM C3R (µL)	8 mM C3R (µL)	16 mM C3R (µL)	32 mM C3R (µL)	128 mM C3R (µL)	Incubated at 37°C for 1 or 24 hours	20 mM *o*-PD (µL)	0.06% 5-MQ (µL)
Negative	0:1	700	100	-	-	-	-	-	-	-		100	100
Positive (AG)	1:1	700	-	100	-	-	-	-	-	-		100	100
Treatment	0.25:1	700	-	-	100	-	-	-	-	-		100	100
(C3R)	0.5:1	700	-	-	-	100	-	-	-	-		100	100
	1:1	700	-	-	-	-	100	-	-	-		100	100
	2:1	700	-	-	-	-	-	100	-	-		100	100
	4:1	700	-	-	-	-	-	-	100	-		100	100
	16:1	700	-	-	-	-	-	-	-	100		100	100

AG: Aminoguanidine hydrochloride, DMSO: Dimethy sulfoxide, MG: Methylglyoxal, C3R: Cyanidin-3-rutinoside, *o*-PD: *o*-phenylenediamine, 5-MQ: 5-methylquenoxaline

3.2.3 Determination of protective effect cyanidin-3-rutinoside on methylglyoxal-mediated DNA oxidative damage

Analysis of DNA strand breaks

- **Preparation of LB media and LB agar plate for bacterial growth**

LB media was prepared at concentration 25% (w/v) in distilled water, and Agar A (1.5%, w/v) was added to LB media to make LB agar. The solution was mixed and then autoclaved on liquid setting. The solutions were allowed to cool down to 55^{o}C after removing from the autoclave and divided into 2 parts: non-selective (without antibiotic) and selective (containing antibiotic). 100 µL Ampicillin (100 mg/mL) was added to 100 mL selective LB media or LB agar solution. For LB agar, the solution (around 20 mL) was poured 10cm Petri dish. Placed the lid on the plate and allow cooling down. The cooled LB media and LB agar was kept at 4^{o}C and warmed to room temperature before use.

- **Bacterial transformation and bacterial growth**

The transformation of pCU19 plasmid into Escherichia coli (E. coli) bacteria was provided using heat shock reaction. Before staring, all equipment was autoclaved and the work area was sterilized with 70% EtOH. The bacterial competent cell was thawed on ice and 1 ng/µL pCU19 plasmid (1-5 µL) was added to bacterial cells, gently mixed and put on ice. After 30 min, the cell and plasmid were heat shock by placing in a water bath at 42^{o}C for 30 seconds. The mixture was immediately put on ice after removing from bath and 450 µL LB media was added. The reaction was incubated in shacking incubator (225 rpm) at 37^{o}C for 1 hour. The bacteria (200 µL) were dropped on selective LB agar plate and spread the medium around the plate with bacterial spreader. The plates was incubated overnight (around 16 hours) in

shacking incubator (225 rpm) at 37^{o}C. The colonies growth on plate is transformed pCU19 plasmid (containing antibiotic sequence) in bacteria.

- **Plasmid extraction**

pUC19 plasmid DNA was purified from E. coli cultures using a QIAprep® spin miniprep kit according to the manufacturer's manual (Santa Clarita, USA). The transformation plasmid colonies were picked up and streaked on selective LB agar in shacking incubator (225 rpm) at 37^{o}C overnight. The next day, a single colony was picked, inoculated a culture of 5 mL selective LB medium and incubated for 12 hours at 37^{o}C with vigorous shaking. The bacterial cells were harvested by centrifugation at 6800g for 3 min at room temperature. The supernatant was removed and the pelleted bacterial cells was suspended in buffer P1 (250 µL) and transferred to microcentrifuge tube. Buffer P2 (250 µL) was added and mixed by inverting the tube. Then Buffer N3 (350 µL) was added, repeatly mixed by inverting the tube and centrifuged for 10 min at 17,900g. The supernatant (800 µL) was applied to QIAprep spin column and then centrifuged for 1 min at 17,900g. The flow-through was discarded. Buffer PB (0.5 mL) was added to wash the spin column and centrifuged again for 1 min at 17,900g. The spin column was washed with Buffer PE (0.75 mL), centrifuged for 1 min at 17,900g to remove buffer. To remove residual wash buffer, the spin column was centrifuged with full speed for additional 1 min. To elute DNA, Buffer EB (50 µL) was added to the center of each column placed on microcentrifuge tube, stand for 1 min and centrifuged for 1 min to collect the eluted DNA. The concentration of DNA was determined using NanoDrop™ Spectrophotometer.

- **DNA strand break analysis**

The cleavage of plasmid DNA was analyzed according to a previous report (Kang, 2003). Plasmid DNA pUC19 (250 ng) was incubated in 0.1 M phosphate buffer saline (PBS), pH 7.4 for 10 µL final volume by adding difference volumes of chemicals as shown in table 6. The final concentration the chemicals were 50 mM lysine, 50 mM methylglyoxal, and 0.125-1 mM C3R with or without 300 µM Cu^{2+}. The reactions was incubated at 37°C for 3 h. Samples were frozen immediately at -20°C to stop reactions. After 90 min, the plasmid DNA was mixed with DNA loading dye and then resolved by 0.8% agarose gel electrophoresis at 80V in TBE buffer for 60 min. Plasmid DNA fragments were visualized and photographed by a Gel Doc imager (Syngene, UK). The relative amounts of supercoiled (SC) and open circular (OC) DNA was quantified by the intensities of the band obtained using GeneTools software (Syngene, UK) and the percentage of opened circular DNA (% OC) was calculated using the following equation. The results were expressed as relative % OC after subtracting by %OC of control (DNA alone).

$$\% \text{ OC} = \frac{\text{Intensity of OC}}{\text{Intensity of OC+SC}} \times 100$$

Table 6 Chemicals were presented in the analysis of DNA strand break (total volume 10 µL)

Experimental groups	Plasmid (ng)	250 mM Lysine (µL)	250 mM MG (µL)	10% DMSO (µL)	1.25-10 mM C3R (µL)	PBS (uL)
Blank	250	-	-	-	-	Variable
Lysine	250	2	-	1	-	Variable
MG	250	-	2	1	-	Variable
Negative	250	2	2	1	-	Variable
Treatment (C3R)	250	2	2	-	1	variable

Experimental groups	Plasmid (ng)	3 mM $CuSO_4$ (µL)	250 mM Lysine (µL)	250 mM MG (µL)	10% DMSO (µL)	1.25-10 mM C3R (µL)	PBS (uL)
Blank	250	1	-	-	-	-	Variable
Lysine	250	1	2	-	1	-	Variable
MG	250	1	-	2	1	-	Variable
Negative	250	1	2	2	1	-	Variable
Treatment (C3R)	250	1	2	2	-	1	variable

MG: methylglyoxal, DMSO: Dimetyl sulfoxide, C3R: Cyanidin-3-rutinoside, PBS: Phosphate buffer saline

Determination of superoxide anions

The level of superoxide anions was determined by measurement of cytochrome *c* reduction assay according to a previous method (Kang, 2003). The reactions were prepared in 0.1 M phosphate buffer saline (PBS), pH 7.4 for 1 mL final volume by adding difference volumes of chemicals as shown in table 7. The chemicals at final concentration included 10 mM lysine, 10 mM methylglyoxal, 10 μM cytochrome *c* and 0.125-1 mM C3R. The reduction rate of cyctochrome *c* was measured at room temperature using a spectrophotometer at 550 nm at 10 min intervals for 50 min and subtracted with the absorbance of sample blank at each time point. The level of reduced cytochrome *c* was calculated based on the extinction coefficient for cytochrome *c* (ε = 27,700 $M^{-1}cm^{-1}$).

Table 7 Chemicals were presented in the determination of superoxide anion

Experimental groups	40 µM Cytochrome *c* (µL)	40 mM Lysine (µL)	40 mM MG (µL)	4% DMSO (µL)	0.5-4 mM C3R (µL)	PBS (uL)
Blank						
Lysine	-	250	-	250	-	500
MG	-	-	250	250	-	500
Negative	-	250	250	250	-	250
Treatment (C3R)	-	250	250	-	250	250
Test						
Lysine	250	250	-	250	-	250
MG	250	-	250	-	-	250
Negative	250	250	250	250	-	-
Treatment (C3R)	250	250	250	-	250	-

MG: methylglyoxal, DMSO: Dimetyl sulfoxide, C3R: Cyanidin-3-rutinoside, PBS: Phosphate buffer saline

Determination of hydroxyl radicals

Thiobarbituric acid reactive substances (TBARS) assay was used to evaluate the level of hydroxyl radical according to a previously described method (Chan and Wu, 2006). The reaction mixture (0.2 mL total volume) containing 10 mM lysine, 10 mM methylglyoxal, and 20 mM 2-deoxy-d-ribose (DR) was incubated at 37°C with or without C3R (0.125-1 mM) for 3 hours in 0.1 M phosphate buffer saline (PBS), pH 7.4. The difference volumes of chemicals were showed in table 8. After incubation period, 0.2 mL PBS and 0.2 mL TCA (2.8% w/v) was added to the reaction mixture, followed by 0.2 mL thiobarbituric acid (TBA; 1% w/v). The solution was boiled at 100°C for 10 min and then cooled to room temperature. The degradation of 2-deoxy-d-ribose was measured at a wavelength 532 nm using a spectrophotometer and the absorbance of sample blank was used to subtract. Hydroxyl radicals were expressed as the level of TBARS which was quantified by using standard curve of malondialdehyde (concentration range 0-50 μM).

Table 8 Chemicals were presented in the determination of hydroxyl radicals

Experimental groups	80 mM DR (µL)	40 mM Lysine (µL)	40 mM MG (µL)	4% DMSO (µL)	0.5-4 mM C3R (µL)	PBS (uL)	Incubated at 37°C for 3 hours	PBS (uL)	2.8% TCA (uL)	1% TBA (uL)
Blank								200	200	200
● Lysine	-	50	-	50	-	100		200	200	200
● MG	-	-	50	50	-	100		200	200	200
● Negative	-	50	50	50	-	50		200	200	200
● Treatment (C3R)	-	50	50	-	50	50		200	200	200
Test								200	200	200
● Lysine	50	50	-	50	-	50		200	200	200
● MG	50	-	50	50	-	50		200	200	200
● Negative	50	50	50	50	-	-		200	200	200
● Treatment (C3R)	50	50	50	-	50	-		200	200	200

DR: 2-deoxy-D-Ribose, MG: methylglyoxal, DMSO: Dimetyl sulfoxide, C3R: Cyanidin-3-rutinoside, PBS: Phosphate buffer saline, Trichloroacetic acid, TBA: Thiobarbituric acid

3.2.4 Determination of protective effect of cyanidin-3-rutinoside on methylglyoxal-mediated vascular abnormalities in isolated vascular preparations

Animals

Male Wistar-Kyoto (WKY) rats were obtained from Animal Resource Centre (Canning Vale, WA, Australia). Animal were maintained on AIN93M standard diet at 22 ± 2 ^{o}C on 12 h light/12 dark cycle with free access to food and tap water. All animal work was carried out in accordance with the Australian code of practice for the care and use of animals for scientific purposes, 8th edition 2013 (AEC number: 798-03/16).

Aortic ring and mesenteric arterial bed preparation

Rats (250-350g) were anesthetized for all experiments by intraperitoneal injection with single bolus dose of sodium pentobarbital (60 mg/kg). The vascular tissue preparation and isolation was described by previous report (Runnie *et al.*, 2004). The descending thoracic aorta were isolated, cleared of adhering tissue and cut into rings approximately 3 mm in length. Endothelium was removed by gently rubbing the intimal surface of the vessels for a few seconds. Endothelium-intact and –denuded aortic rings were mounted in stainless steel stirrups and placed in 20 mL modular tissue bath (EMKA Technologies, Paris, France) containing physiological Krebs-Henseleit buffer solution, bubbled with carbogen gas (95% O_2.5% CO_2) and maintained at 37^{o}C. The Krebs-Henseleit buffer solution consisted of the following: 113 mM NaCl, 4.8 mM KCl 1.2 mM KH_2PO_4, 1.2 mM $MgSO_4$, 25 mM $NaHCO_3$, 2.5 mM $CaCl_2$, 11.2 mM glucose and 0.57 mM ascorbic acid in ultrapure water. The aortic rings were equilibrated for 60 min under 4 g of resting tension. Before testing, the viability of tissue was assessed by contracting with 20 mM KCl until plateau maximal

contraction (30 min). Then, the aortic rings were washed with Krebs solution and re-equilibrated for 30 min before starting the experiment.

The mesenteric arterial beds were isolated from anesthetized rats and prepared according to previous study (Longhurst *et al.*, 1986). Briefly, the superior mesentery artery was cannulated and flushed with heparin-saline. The intestinal tract was removed from entire mesenteric bed. The preparation was mounted in 50 mL perfusion bath (EMKA Technologies, Paris, France) and continuously perfused with oxygenated Krebs solution. After 30 min of equilibration, the viability of tissue was assessed by cumulative intraluminal injection of KCl (10^{-2} to 10^{-1} M), and then the tissue was continuously perfused with Kreb solution to re-equilibrate for 10 min before starting the experiment. The changed in tension of aortic ring and pressure of mesenteric arterial bed were monitored and analyzed by using iox2 software (EMKA Technologies, Paris, France).

Determination of vasorelaxant effect in rat aorta

After re-equilibration period, cumulative concentration of noradrenaline (9×10^{-11} to 6×10^{-7}) was assessed. noradrenaline was continuously added to the chamber when the maximum contraction response to previous concentration was observed. The percent contraction response to noradrenaline was calculated by using the maximal contraction response to KCl as 100% contraction. Half maximal effective concentration (EC_{50}) of noradrenaline was established and used to induce pre-contraction the rings both endothelial-intact and -denuded rings. When the contraction to noradrenaline EC_{50} reached the maximum and maintained that level, the cumulative dose of C3R (0.1 nM to 30 μM) were separately added to the bath. The further dose of C3R was added when a maximum relaxation response of each concentration was observed, as indicated by plateau response. The viability of tissue

was repeated by adding 20 mM KCl after C3R relaxation response study. DMSO was used as solvent for C3R in this study with final concentration 0.1% in chamber.

The contraction response curve of noradrenaline was assessed to establish noradrenaline EC_{50} in endothelial-intact ring after pre-treatment with endothelial nitric oxide synthase (eNOS) inhibitor, N^{ω}-nitro-L-arginine (NOLA; 10 μM) for 30 min. Noradrenaline EC_{50} at concentration 5 nM was used to induce pre-contraction for the rings pre-treatment with NOLA. The response curve to cumulative concentration of C3R (0.1 nM-30 μM) was measured when the maximal steady contraction to noradrenaline EC_{50} was reached.

Determination of endothelial nitric oxide synthase expression in aortic tissue

The thoracic aorta from WKY rats (300 g) were isolated, cleared of adhering tissue and cut into rings approximately 1.5 cm in length. The EC_{50} of C3R to induce relaxation in isometric tension study was selected for eNOS gene expression study. The preparation aorta was placed in Kreb solution contained C3R for different concentration (3 and 10 μM) and incubation periods (0.5 and 24 hours) in 6-wells plate and DMSO (0.1%) was used as control. The vessel was incubated at 37^{o}C in a 5% atmosphere incubator. After incubation period, aortic tissue was storage in RNA*later*® solution.

- **RNA extraction**

Total RNA was isolated from tissue using RNeasy fibrous tissue mini kit (Qiagen Science Inc, MD, USA). Tissue was removed from RNA*later*® solution and placed in 1.5 mL microcentrifuge tube containing Buffer RLT (300 μL) and three stainless steel bead (2.5 mm mean dianeter). The tissue was immediately disrupted and homogenized using Mini-Beadbeater 30 second for 3 times. RNase-free water (590 μL)

was added to the lysate, and then proteinase K solution (10 µL) was added, mixed thoroughly by pipetting and incubated 55^{o}C. After 10 min, the lysate was centrifuged at 10,000g for 3 min at room temperature. The supernatant was transferred to new microcentrifuged tube and EtOH (450 uL) was added and mixed by pipetting. The samples (700 µL) was transferred to RNase Mini spin column placed in a 2 mL collection tube and centrifuged at 8,000g for 30 second at room temperature. The flow-through was discarded and the remainder of sample was transferred to the same column and repeated the step before. Buffer RW1 (350 µL) was added to the column and then centrifuged at 8,000g for 30 second at room temperature to wash the membrane. The flow-through was discarded and 80 µL DNase I incubation mix (10 µL DNase stock solution and 70 µL Buffer RDD) was directly added to the membrane and stranded for 20 min at room temperature. Buffer RW1 (350 µL) was added to the column after incubation period and centrifuged at 8,000g for 30 second at room temperature. After discard the flow-through, Buffer RPE (500 µL) was added and centrifuged at 8,000g for 30 second at room temperature (repeat this step for 2 times). The flow-through was discarded and centrifuged with highest speed for 1 min at room temperature. The column was carefully removed from collection tube and placed in microcentrifuge tube. RNase-free water (20 µL) was added directly to membrane, stranded for 1 min and then centrifuged at 8,000g for 1 min. this step was repeated for 1 time. The RNA in flow-through was collected. The RNA concentration and qualification was analyzed using by Qubit® fluorometer (Life Technology, USA) and Experion RNA Analysis Kits (Bio-RAD Labolatories Inc., California, USA), respectively.

- **Reverse transcription and PCR reaction**

The 1 µg of total RNA was reverse transcribed to cDNA using iScript cDNA synthesis kit for RT-qPCR (Bio-RAD Labolatories Inc., California, USA) by C1000 thermal

Cycler (Bio-RAD) at a final volume 20 µL. Rat primers (Nitric oxide synthase-NOS3 and 40S ribosomal 60S ribosomal protein L13a-Rpl 13a) were provided by PrimePCR assay (Bio-RAD). RT-PCR was carried out in CFX384 Touch™ Real-Time PCR Detection system (Bio-RAD) using SYRB green detection. A master-mix of the following reaction components was prepared to indicate final concentrations (10 µL): 2.5 ng cDNA template, 1x primers, 1x SsoAdvanced Universal SYRB Green supermix (Bio-RAD). The difference volumes of chemicals were showed in table 9. All samples were carried out in triplicate. The following RT-PCR protocol was employed: activation for 2 min at 95^{o}C, 40 cycles of at 95^{o}C for 5s and 60^{o}C for 30s, followed by malting step with slow heating from 65^{o}C-95^{o}C with a rate of 0.5^{o}C/s. The reference gene ribosomal protein L13a (Rpl13a) data were used to normalize the amount of RNA.

Table 9 Chemicals were presented in the determination of gene expression

Component	Volume (µL)
20x Primer	0.5
2x SsoAdvanced Universal SYRB Green supermix	5
8.3 ng/mL cDNA template	3
Nuclease-free water	1.5

Determination of vasorelaxation response in rat mesenteric arterial bed

The EC_{50} of noradrenaline was established by cumulative intraluminal injection of noradrenaline (10 nM-100 µM). To monitor vasorelaxation effect of C3R, the EC_{50} of noradrenaline was applied for Krebs solution perfusate to induce a partial pressure development state. The cumulative concentration of C3R (1 nM-1 mM) was intraluminally injected and the changed pressure was recorded. The pressure was allowed to re-equilibrate to half maximal contraction before injecting further dose of C3R. The vasorelaxation response to cumulative dose of C3R in mesenteric arterial

bed was repeated in the presence of either NOLA (10 μM) or indomethacin (10 μM) in the perfusat for 30 min before adding noradrenaline at the EC_{50} in Kreb perfusate to induce pre-contraction.

Determination of vascular reactivity of isolated thoracic aorta in acute methylglyoxal treatment

After tissue viability testing with KCl, the rings was washed out with Krebs solution for 30 min, and then incubated in the 0.1% DMSO (control), methylglyoxal (500 μM) or methylglyoxal (500 μM)/C3R (3 μM) for 30 min. The cumulative dose response to N noradrenaline was analyzed after incubation period. All rings were washed out for 60 min and stabilized at resting tension of 4 g. Then, the rings were pre-contracted with half maximal dose of noradrenaline EC_{50}. When reached the maximum contraction (20 min), the relaxation response curves of cumulative application of Ach or SNP was evaluated in endothelial-intact or endothelial-denuded. The relaxation curve to SNP was repeatedly determined in endothelial-intact ring pre-contraction with noradrenaline EC_{50} after washout and stabilized period.

Determination of vascular reactivity of mesenteric arterial bed-perfusated by acute methylglyoxal treatment

After washout period by perfusing Krebs solution for 20 min, tissues were perfusated with Krebs solution containing 0.1% DMSO as control, Krebs solution containing methylglyoxal (500 μM) or methylglyoxal (500 μM)/C3R (3 μM) for 30 min. After washout for 20 min, the cumulative intraluminal injection of noradrenaline (10^{-8} to 10^{-4} M) was determined. The tissue was re-equilibrated for 20 min and then the half maximal dose of noradrenaline was included in Krebs solution perfusate to induce a partial pressure development state. To monitor vasorelaxation response,

cumulative dose of Ach were intraluminally injected. Change in mesenteric pressure was recorded.

3.2.4 The effect of effect of cyanidin-3-rutinoside on alleviating vascular abnormalities in methylglyoxal-treated rats

Animals, diets and experimental design

A total of 24 Wistar-Kyoto (WKY) rats were obtained from Animal Resource Centre (Canning Vale, WA, Australia) at 8 weeks of age. After arrival in the Animal House, they were maintained on AIN93M standard diet at 22 ± 2 ^{o}C on 12 h light/12 dark cycle with free access to food and tap water. The diet composition of AIN93M was shown in table 10. The vehicle was prepared by 1 g white bread spread with 0.5 g peanut butter as control. Methylglyoxal was treated by dropping 125 µL of 40% methylglyoxal (200 mg/rat/day) on control vehicle, while C3R was mixed with peanut butter before spread on the bread. After 2 weeks of acclimatization period, the feeding practice was daily provided for the all animals with control vehicle in the morning. At the age of 12 weeks, the rats were divided into 4 groups and started supplementation: control, methylglyoxal, methylglyoxal with C3R at 30 mg/kg/day and methylglyoxal with C3R at 100 mg/kg/day groups. The rats were fed with the vehicle daily for 3 weeks. Then, the feeding was fed twice a day for 5 weeks. After 8 weeks of feeding period, the animal was anesthetized by intraperitoneal injection of sodium pentobarbital (60 mg/Kg). Animal weight was recorded weekly during study period. Blood and tissues were collected from analysis. A part of descending thoracic aorta was used for isometric tension study. Remain thoracic aorta from isometric tension study was placed in liquid nitrogen and then transferred to -80^{o}C for further experiments. Liver and left kidney was collected, placed in liquid nitrogen and

transferred to -80^{o}C for further experiments. All animal work was carried out in accordance with the Australian code of practice for the care and use of animals for scientific purposes, 8th edition 2013 (AEC number: 796-06/16).

Table 10 Diet composition of AIN93M

Ingredient	Amount (% weight/weight)
Starch	52.95
Caesin	20.0
Sucrose	10.0
Sunflower oil	7.0
Cellulose	5.0
Vitamin mix	1.0
Mineral mix	3.5
L-cystine	0.3
Choline	0.25
Water (4.5L/10 kg diet)	

Blood biochemical analysis

Blood was collected from abdominal aorta using lithium heparin anticoagulant blood collection tube and centrifuged for 3,000g at 4^{o}C. The level of blood glucose, blood urea nitrogen (BUN), creatinine, aspartate aminotransferase (AST), alanine aminotransferase (ALT) were analyzed using commercial kit from Beckman coulter (Brea, CA, USA).

Determination of plasma and tissue methylglyoxal level

Blood was collected from abdominal aorta of anesthetized rats in EDTA anticoagulant blood collecting tube. Plasma was separated by centrifugation at 3,000g for 10 min and kept at -80^{o}C before starting experiment. Liver and left kidney was removed from anesthetized and was frozen in liquid nitrogen. The tissue

samples were homogenized in liquid nitrogen and weighted for 100 mg. The homogenized samples were reconstituted in sodium phosphate in buffer (500 µL), pH 4.5 and sonicated for 5 min. The samples were centrifuged at 12,000g at 4^{o}C for 10 min. The supernatant was collected for methylglyoxal level measurement. The samples (plasma and tissues) were incubated with difference volumes of chemicals (final volume = 0.7 mL) as shown in table 11. The chemicals at final concentration included 0.45N perchloric acid, 10 mM *O*-phenylenediamine (*O*-PD), 0.005% 5-methylquinoxaline (5-MQ). The reaction was stranded at room temperature for 24 hours in dark. After incubation period, all samples were filtered with 0.45 µm PES syringe filter and transferred to HPLC vial for injection. The quantification of methylglyoxal was based on the determination of its derivative compound (2-MQ). An Inersil-ODS3V C_{18} column (150×4.6 mm i.d.; 5-µm particle size) was used along with a LC-10AD pump, SPD-10A UV-Vis detector and LC-Solution software (Shimadzu Corp., Kyoto, Japan). The absorbance was recorded at 315 nm and the injection volume was 10 µL. An isocratic program was performed with 50% HPLC grade water and 50% methanol (v/v) with a constant flow rate set at 1 mL/min. The total running time was 14 min. The level of methylglyoxal was calculated compared to standard curve of methylglyoxal (concentration range 0-20 µM). The results were expressed as µmol/mg protein.

Table 11 Chemicals were presented in the determination of plasma and tissue methylglyoxal level

Plasma or tissue supernatant (µL)	**1.5 N** Perchloric acid **(µL)**	**70 mM** *o*-PD **(µL)**	**0.04%** 5-MQ **(µL)**
300	210	100	90

o-PD: *o*-phenylenediamine, 5-MQ: 5-methylquenoxaline

Determination of non-fluorescent AGE, N-(carboxymethyl) lysine (N^{ε}-CML) formation in aorta

The aorta was weighted for 30 mg and placed in 2 mL microcentrifuge tube containing 1 mL 1X RIPA Buffer (10X RIPA Buffer was diluted to a 1X solution using distilled water). The samples were chopped into small piece and homogenized using homogenizer. The samples were process on ice. The lysate tissues were sonicated for 5 min, and then centrifuged 14,000g for 10 min at 4°C. The supernatant was collected and kept at -20°C for N^{ε}-CML measurement.

N^{ε}-CML was determined by using enzyme linked immunosorbant assay (ELISA) kit according to the manufacturer's manual (OxiSelect™ N^{ε}-(carboxymethyl)lysine (CML) ELISA Kit, Cell Biolabs , CA, USA). The lysate tissues 50 µL were placed into 96 well plates which pre-coated with CML conjugated solution overnight before use. The plate was incubated at room temperature for 10 min on orbital shaker, and then 100 µL of diluted anti-CML antibody (1:1000 anti-CML antibody in assay dilutant) was added and incubated for 1 hour at room temperature on orbital shaker. The solution was discarded and the wells were washed each well with 250 µL wash buffer for 3 times. 100 µL diluted anti-HRP conjugated antibody (1:1000 anti- HRP conjugated antibody in assay dilutant) was added and then incubated at room temperature on orbital shaker for 1 hour. The wells were discarded and washed again by using 250 µL wash buffer for 5 times and 100 µL of substrate solution (warmed at room temperature) was placed to each wells for 20 min (time can be different depend on N^{ε}-CML concentration) on orbital shaker. The reaction was stopped by adding 100 µL stop solution. The absorbance was immediately measured at 450 nm with spectrophotometer. The concentration of N^{ε}-CML was calculated from the standard curve of N^{ε}-CML-BSA (0-12.5 ng/mL). The results were expressed as µg/mg protein.

Determination of vascular function

- **Aortic ring preparation**

The aortic rings were prepared according to previous study (Runnie et al., 2004). Rats (250-350g) were anesthetized for all experiments by intraperitoneal injection with single bolus dose of sodium pentobarbital (60 mg/kg). The descending thoracic aorta were isolated, cleared of adhering tissue and cut into rings approximately 3 mm in length. Endothelium was removed by gently rubbing the intimal surface of the vessels for a few seconds. Endothelium-intact and –denuded aortic rings were mounted in stainless steel stirrups and placed in 20 mL modular tissue bath (EMKA Technologies, Paris, France) containing physiological Krebs-Henseleit buffer solution, bubbled with carbogen gas (95% O_2.5% CO_2) and maintained at 37 °C. The Krebs-Henseleit buffer solution consisted of the following: 113 mM NaCl, 4.8 mM KCl 1.2 mM KH_2PO_4, 1.2 mM $MgSO_4$, 25 mM $NaHCO_3$, 2.5 mM $CaCl_2$, 11.2 mM glucose and 0.57 mM ascorbic acid in ultrapure water. The aortic rings were equilibrated for 60 min under 4 g of resting tension. Before testing, the viability of tissue was assessed by contracting with 20 mM KCl until plateau maximal contraction (30 min). Then, the aortic rings were washed with Krebs solution and re-equilibrated for 30 min before starting the experiment.

The viability of tissue was assessed by testing contraction response to KCl (20 mM). When the maximal contraction to KCl was reached, the rings were washed out with Krebs solution for 30 min, and the cumulative dose response to noradrenaline (9×10^{-11} to 6×10^{-7}) was analyzed. All rings were washed out for 60 min and stabilized at resting tension of 4 g. Then, the rings were pre-contracted with half maximal dose of noradrenaline EC_{50}. When reached the maximum contraction (20 min), the relaxation response curves of cumulative application of Ach or SNP was evaluated in

endothelial-intact or endothelial-denuded. The relaxation curve to SNP was repeatedly determined in endothelial-intact ring pre-contraction with noradrenaline EC_{50} after washout and stabilized period.

- **Mesenteric arterial bed preparation**

The mesenteric arterial beds were isolated from anesthetized rats and prepared according to previous study (Longhurst et al., 1986). Briefly, the superior mesentery artery was cannulated and flushed with heparin-saline. The intestinal tract was removed from entire mesenteric bed. The preparation was mounted in 50 mL perfusion bath (EMKA Technologies, Paris, France) and continuously perfused with oxygenated Krebs solution. After 30 min of equilibration, the viability of tissue was assessed by cumulative intraluminal injection of KCl (10^{-2} to 10^{-1} M), and then the tissue was continuously perfused with Kreb solution to re-equilibrate for 10 min before starting the experiment. The changed in tension of aortic ring and pressure of mesenteric arterial bed were monitored and analyzed by using iox2 software (EMKA Technologies, Paris, France).

After washout period by perfusing Krebs solution for 20 min, the cumulative intraluminal injection of noradrenaline (10^{-8} to 10^{-4} M) was determined. The tissue was re-equilibrated for 20 min and then the half maximal dose of noradrenaline was included in Krebs solution perfusate to induce a partial pressure development state. To monitor vasorelaxation response, cumulative dose of Ach were intraluminally injected. Change in mesenteric pressure was recorded.

<u>Determination of gene expression in aorta</u>

The frozen thoracic aorta was weighted for 30 mg, placed in cold RNA*later*®-ICE frozen tissue solution (300µL) and kept at -20^{o}C for 24 hours before experiment.

Total RNA was isolated from tissue using RNeasy fibrous tissue mini kit (Qiagen Science Inc, MD, USA). Tissue was removed from RNA*later*®-ICE frozen tissue solution and placed in 1.5 mL microcentrifuge tube containing Buffer RLT (300 µL) and three stainless steel bead (2.5 mm mean dianeter). The tissue was immediately disrupted and homogenized using Mini-Beadbeater 30 second for 3 times. RNase-free water (590 µL) was added to the lysate, and then proteinase K solution (10 µL) was added, mixed thoroughly by pipetting and incubated 55^{o}C. After 10 min, the lysate was centrifuged at 10,000g for 3 min at room temperature. The supernatant was transferred to new microcentrifuged tube and ethanol (450 uL) was added and mixed by pipetting. The samples (700 µL) was transferred to RNase Mini spin column placed in a 2 mL collection tube and centrifuged at 8,000g for 30 second at room temperature. The flow-through was discarded and the remainder of sample was transferred to the same column and repeated the step before. Buffer RW1 (350 µL) was added to the column and then centrifuged at 8,000g for 30 second at room temperature to wash the membrane. The flow-through was discarded and 80 µL DNase I incubation mix (10 µL DNase stock solution and 70 µL Buffer RDD) was directly added to the membrane and stranded for 20 min at room temperature. Buffer RW1 (350 µL) was added to the column after incubation period and centrifuged at 8,000g for 30 second at room temperature. After discard the flow-through, Buffer RPE (500 µL) was added and centrifuged at 8,000g for 30 second at room temperature (repeat this step for 2 times). The flow-through was discarded and centrifuged with highest speed for 1 min at room temperature. The column was carefully removed from collection tube and placed in microcentrifuge tube. RNase-free water (20 µL) was added directly to membrane, stranded for 1 min and then centrifuged at 8,000g for 1 min. this step was repeated for 1 time. The RNA in flow-through was collected. The RNA concentration and qualification was analyzed using

by Qubit® fluorometer (Life Technology, USA) and Experion RNA Analysis Kits (Bio-RAD Labolatories Inc., California, USA), respectively.

The 1 µg of total RNA was reverse transcribed to cDNA using iScript cDNA synthesis kit for RT-qPCR (Bio-RAD Labolatories Inc., California, USA) by C1000 thermal Cycler (Bio-RAD) at a final volume 20 µL. Rat primers (Nitric oxide synthase-NOS3 and 40S ribosomal 60S ribosomal protein L13a-Rpl 13a) were provided by PrimePCR assay (Bio-RAD). RT-PCR was carried out in CFX384 Touch™ Real-Time PCR Detection system (Bio-RAD) using SYRB green detection. A master-mix of the following reaction components was prepared to indicate final concentrations (10 µL): 2.5 ng cDNA template, 1x primers, 1x SsoAdvanced Universal SYRB Green supermix kit (Bio-RAD). The difference volumes of chemicals (final volume = 0.7 mL) are shown in table 9. All samples were carried out in triplicate. The following RT-PCR protocol was employed: activation for 2 min at 95^{o}C, 40 cycles of at 95^{o}C for 5s and 60^{o}C for 30s, followed by malting step with slow heating from 65^{o}C-95^{o}C with a rate of 0.5^{o}C/s. The reference gene ribosomal protein L13a (Rpl13a) data were used to normalize the amount of RNA.

3.2.6 Statistical analysis

The results were expressed as mean±standard error of mean (SEM). The statistical significant of the results was evaluated by using one-way ANOVA. The significant difference of superoxide anion generation was analyzed by two-way repeated measures ANOVA, while methylglyoxal trapping ability was determined by a two-way ANOVA. Statistical significant of the vasorelaxation response to C3R was analyzed by Student's t test. Differences between treatments were analyzed by Tukey post hoc for *in vitro* data and Duncan post hoc test for *ex vivo* and *in vivo*

data. These analyses were performed using SPSS Statistics 17.0 (SPSS Inc., Chicago, IL, USA). A *p* value of less than 0.05 was taken as the criterion of significance.

CHAPTER IV

RESULTS

4.1 The effect of cyanidin-3-rutinoside (C3R) on protein glycation mediated by monosaccharide, including ribose, fructose, glucose and galactose, and reactive dicarbonyls molecule, methylglyoxal, *in vitro.*

4.1.1 Fluorescent AGEs formation

The formation of fluorescent and non-fluorescent AGEs in four monosaccharide and methylglyoxal-mediated protein glycation was monitored during 2 weeks of incubation. As shown in figure 16, ribose showed the highest glycation mediator than fructose, galactose and glucose caused a 25.5-fold, 15.5-fold, 5.1-fold and 3.7-fold increase in the fluorescence intensity, respectively when compared with BSA for 2 weeks. The results demonstrated that the addition of C3R (0.125–1 mM) into the solution significantly reduced the formation of fluorescent AGEs in a concentration-dependent manner throughout the study period as shown in figure 17-20. At week 2 of incubation, the percentage reduction of AGEs formation by C3R (0.125–1 mM) was 2%–52% for BSA/ribose, 81%–93% for BSA/fructose, 30%–74% for BSA/glucose and 6%–79% for BSA/galactose. Similar to the effect of C3R (1 mM), a significant inhibition of fluorescent AGEs was observed in glycated BSA plus AG (1 mM). The results showed that AG inhibited the formation of fluorescent AGEs in BSA/ribose (32%), BSA/fructose (47%), BSA/glucose (25%) and BSA/galactose (21%). However, AG showed less potent than C3R at the equal concentration by 1.6-fold, 2.0-fold, 2.9-fold and 3.8-fold for BSA/ribose, BSA/fructose, BSA/glucose and BSA/galactose, respectively.

The glycating action of methylglyoxal on fluorescent AGEs formation in BSA was also determined. It was found that the addition of methylglyoxal to BSA in the BSA/methylglyoxal assay caused a 5-fold increase in the formation of fluorescent AGEs (figure 21). This methylglyoxal induced glycation of BSA was reduced when C3R was added at a level of 0.25 mM or above ($p<0.05$) and the reduction was greatest when C3R was added at 1 mM (65%) such that glycation levels were similar to BSA alone. The addition of AG was used as a positive control to inhibit the formation of fluorescent AGEs (63%) by a similar amount as 1 mM C3R.

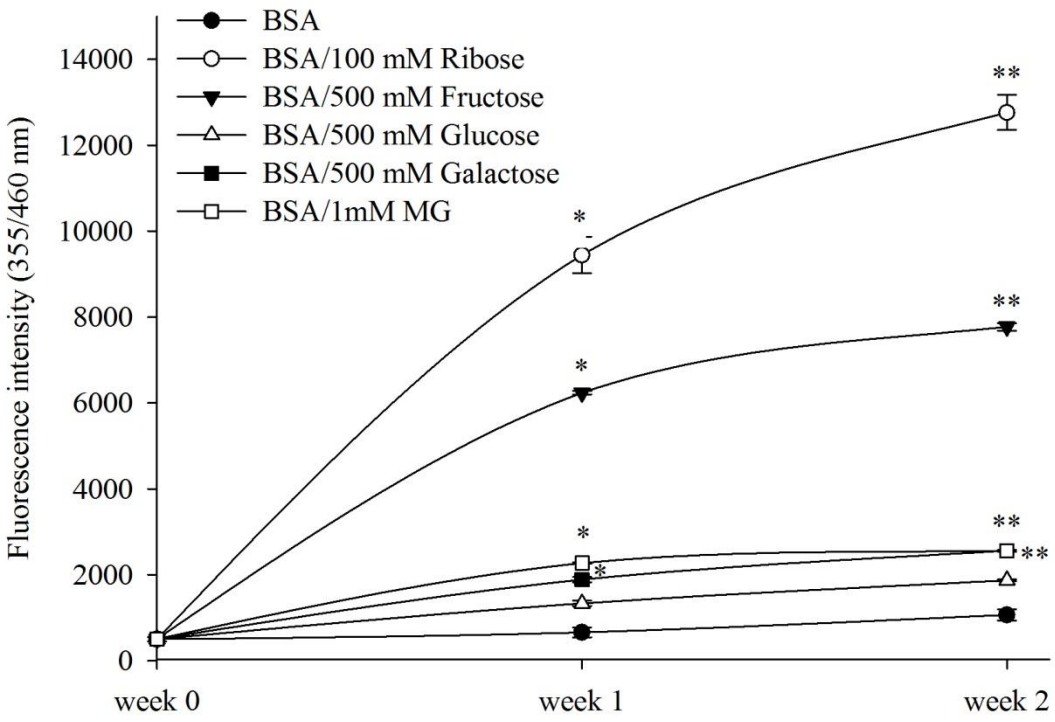

Figure 16 The effects of monosaccharides (ribose, fructose, glucose and galactose) and methylglyoxal on the formation of fluorescent AGEs in BSA.

The results are expressed as mean ± SEM (n = 3). *p<0.05 when compared to BSA at week 1 and **p<0.05 when compared to BSA at week 2.

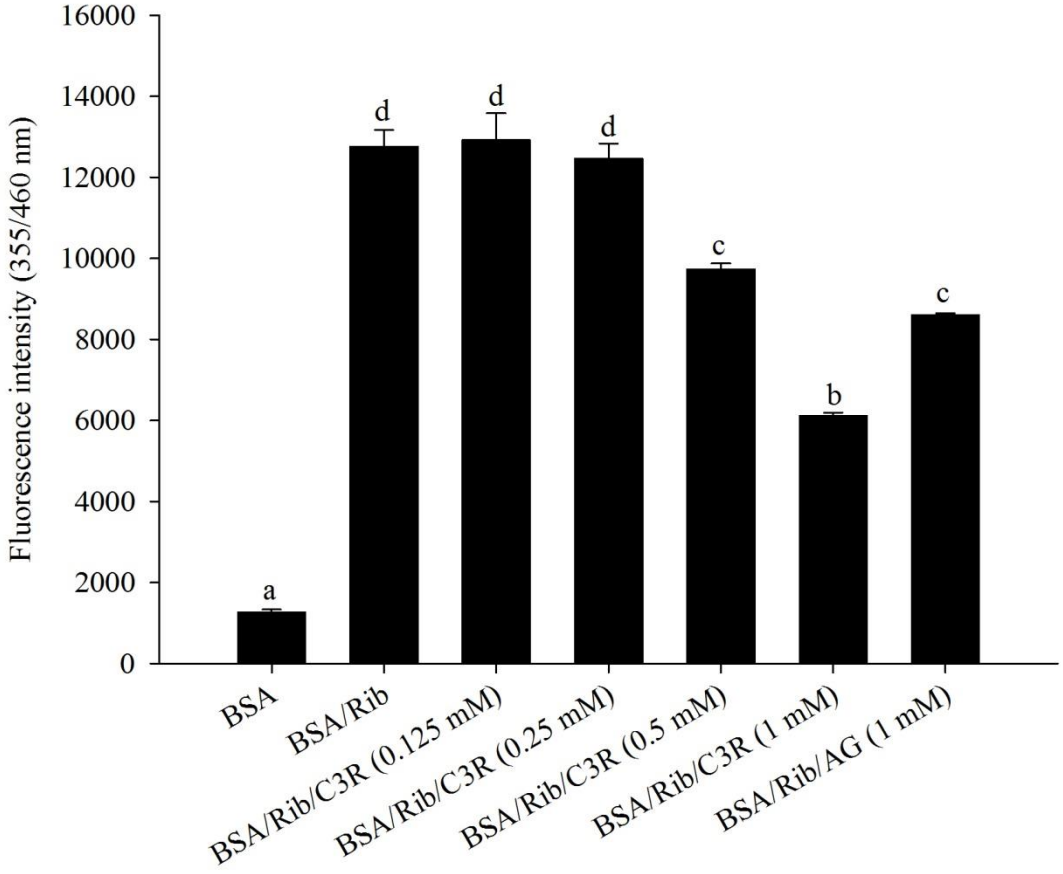

Figure 17 The effects of cyanidin-3-rutinoside (C3R) and aminoguanidine (AG) modulating the formation of fluorescent glycated protein in the BSA/ribose (Rib) assay.

The results are presented as mean ± SEM (n=3). Groups without a common letter are significant difference (p<0.05).

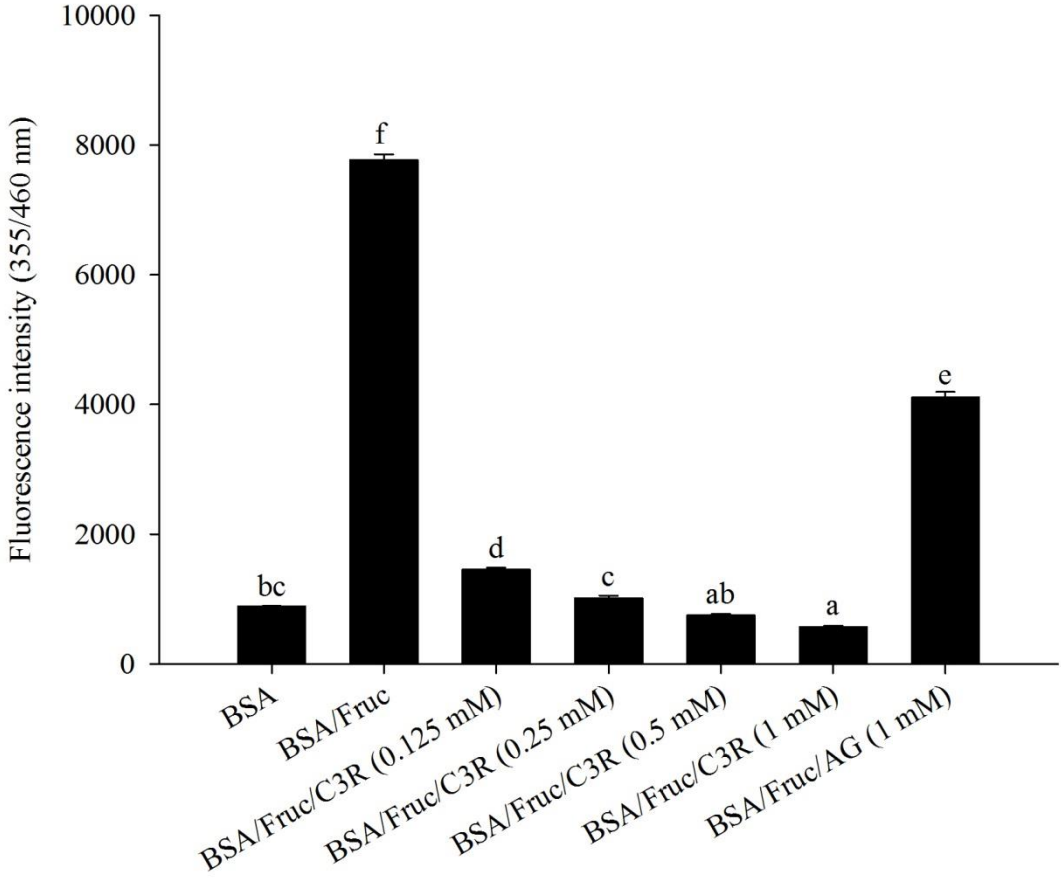

Figure 18 The effects of cyanidin-3-rutinoside (C3R) and aminoguanidine (AG) modulating the formation of fluorescent glycated protein in the BSA/fructose (Fruc) assay.

The results are presented as mean ± SEM (n=3). Groups without a common letter are significant difference (p<0.05).

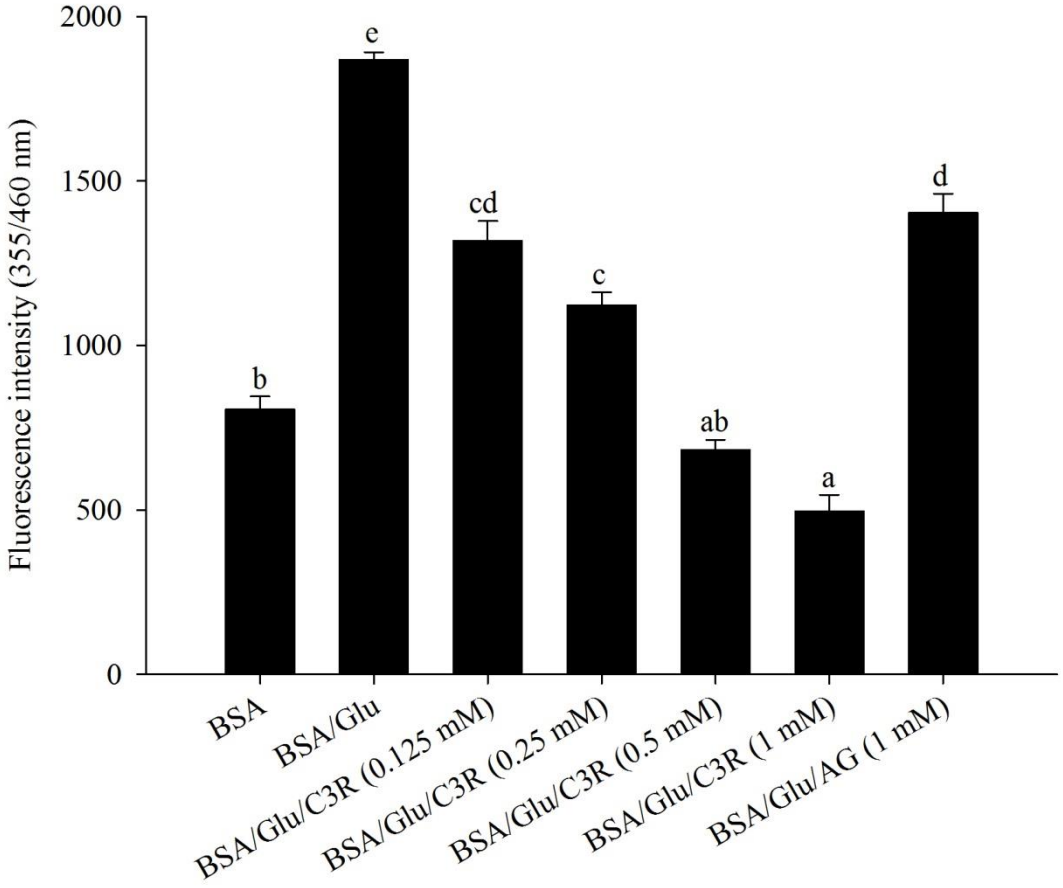

Figure 19 The effects of cyanidin-3-rutinoside (C3R) and aminoguanidine (AG) modulating the formation of fluorescent glycated protein in the BSA/glucose (Glu) assay.

The results are presented as mean ± SEM (*n*=3). Groups without a common letter are significant difference ($p<0.05$).

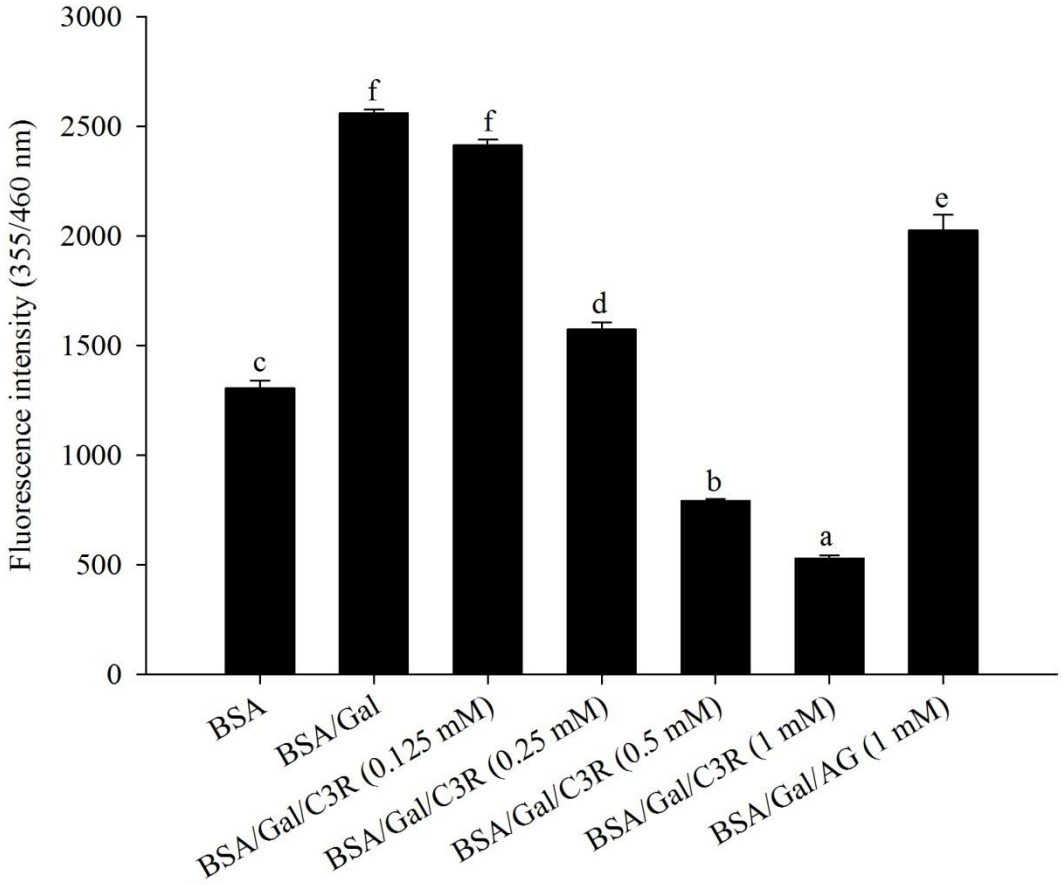

Figure 20 The effects of cyanidin-3-rutinoside (C3R) and aminoguanidine (AG) modulating the formation of fluorescent glycated protein in the BSA/Galactose (Gal) assay.

The results are presented as mean ± SEM (*n*=3). Groups without a common letter are significant difference ($p<0.05$).

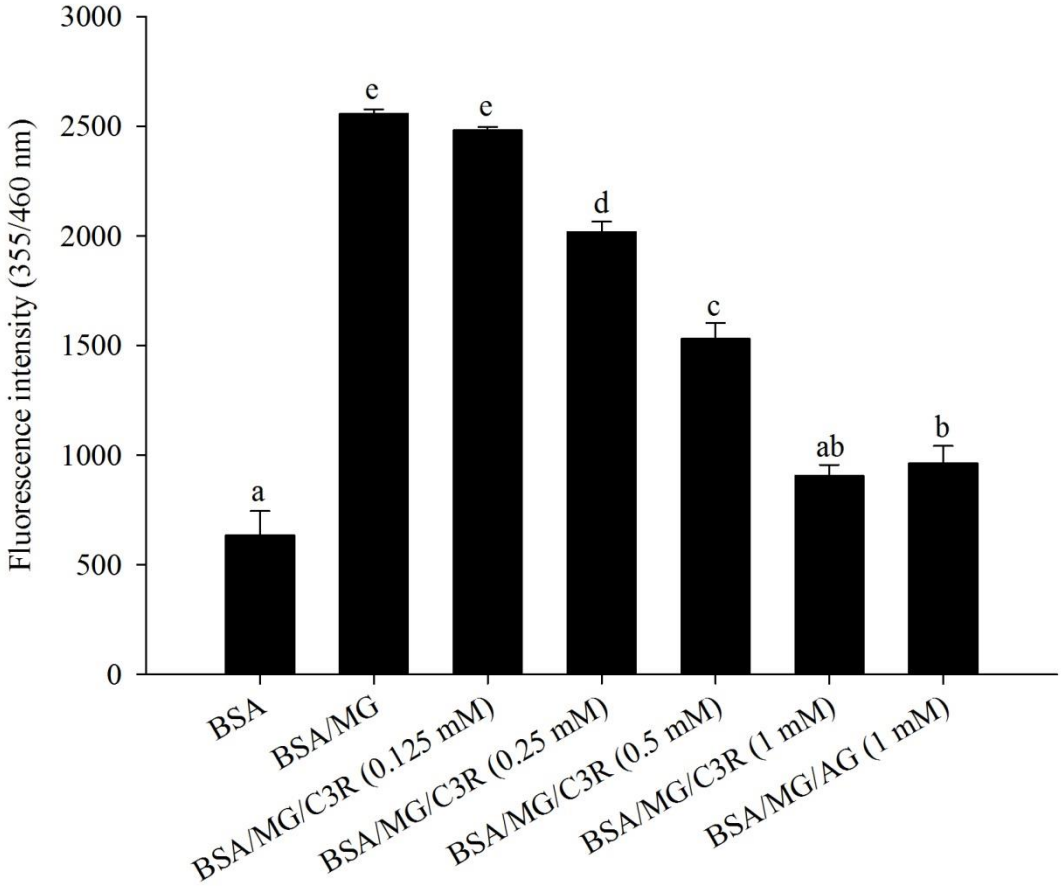

Figure 21 The effects of cyanidin-3-rutinoside (C3R) and aminoguanidine (AG) modulating the formation of fluorescent glycated protein in the BSA/Methylglyoxal (MG) assay.

The results are presented as mean ± SEM (*n*=3). Groups without a common letter are significant difference ($p<0.05$).

4.1.2 Non-fluorescent AGEs N^{ε}-(carboxymethyl) lysine (N^{ε}-CML) formation

The level of N^{ε}-CML was assessed in glycated BSA after 2 weeks of incubation. It was found that the level of N^{ε}-CML increased in the order of glucose (3-fold) < galactose (4-fold) < fructose (29-fold) < ribose (46-fold) as shown in figure 22-25. The addition of C3R (1 mM) to BSA/monosaccharide solution reduced the formation of N^{ε}-CML approximately 56% in BSA/ribose, 68% in BSA/fructose, 81% in BSA/glucose and 86% in BSA/galactose. At equal concentration with C3R (1 mM), AG had more effective reduction of N^{ε}-CML level in BSA/fructose system and showed the same potent as C3R in BSA/ribose, BSA/glucose and BSA/galactose assay. The percentage inhibition of AG was 68% for BSA/ribose, 92% for BSA/fructose and 89% for BSA/glucose and BSA/galactose.

The results showed that methylglyoxal caused a significant increase in the levels of N^{ε}-CML in BSA about 20-fold compared with BSA (Figure 26). The presence of C3R (1 mM) in the same solution resulted in a significant decrease in the level of N^{ε}-CML level (71%). However, C3R showed less potent than AG (82%) at the equal concentration. The N^{ε}-CML formation was similar to control when C3R or AG were added.

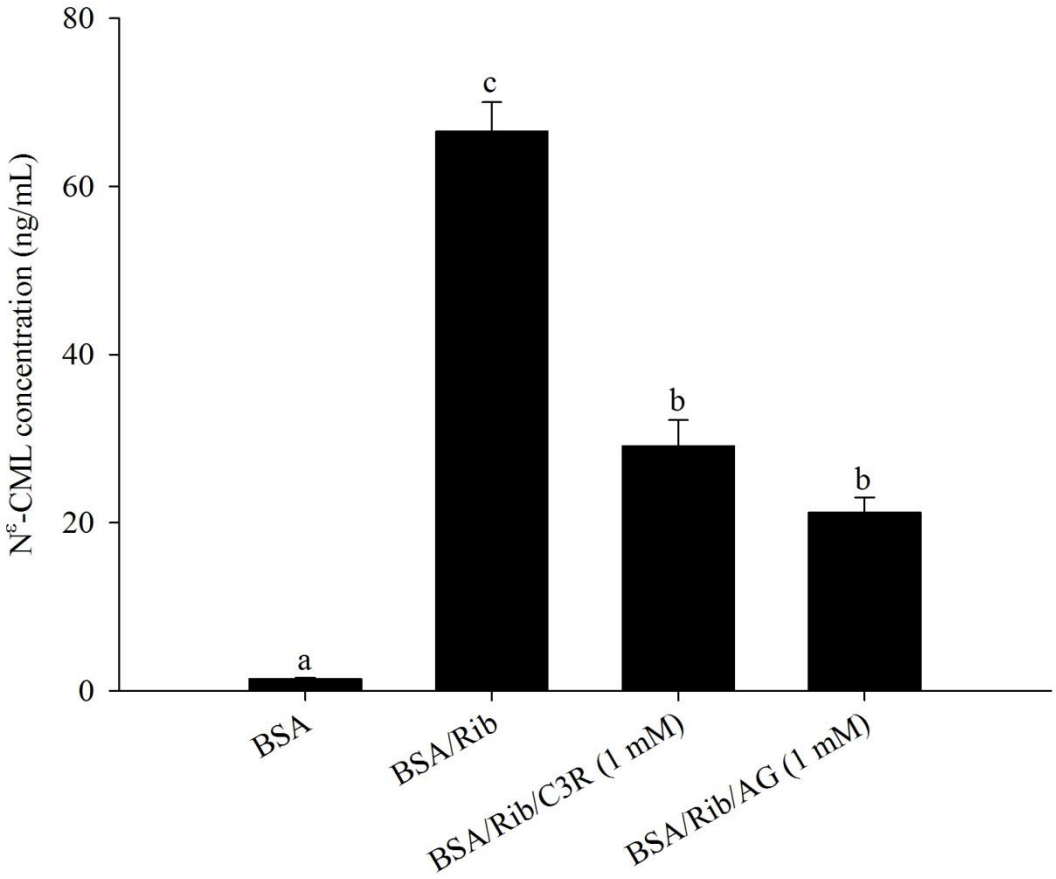

Figure 22 The effects of cyanidin-3-rutinoside (C3R) and aminoguanidine (AG) modulating the formation of non-fluorescent glycated protein N^{ε}-(carboxymethyl) lysine (N^{ε}-CML) in the BSA/Ribose (Rib) assay.

The results are presented as mean ± SEM (*n*=3). Groups without a common letter are significant difference ($p<0.05$).

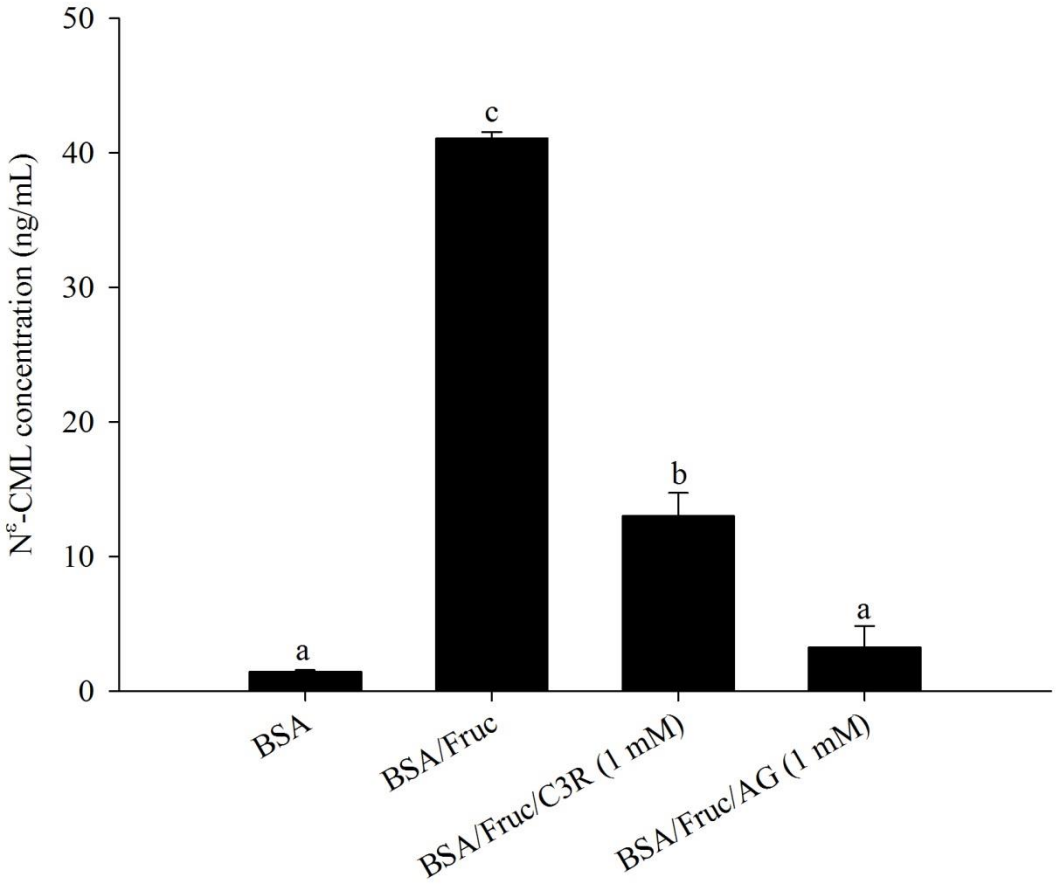

Figure 23 The effects of cyanidin-3-rutinoside (C3R) and aminoguanidine (AG) modulating the formation of non-fluorescent glycated protein N^{ε}-(carboxymethyl) lysine (N^{ε}-CML) in the BSA/Fructose (Fruc) assay.

The results are presented as mean ± SEM (*n*=3). Groups without a common letter are significant difference ($p<0.05$).

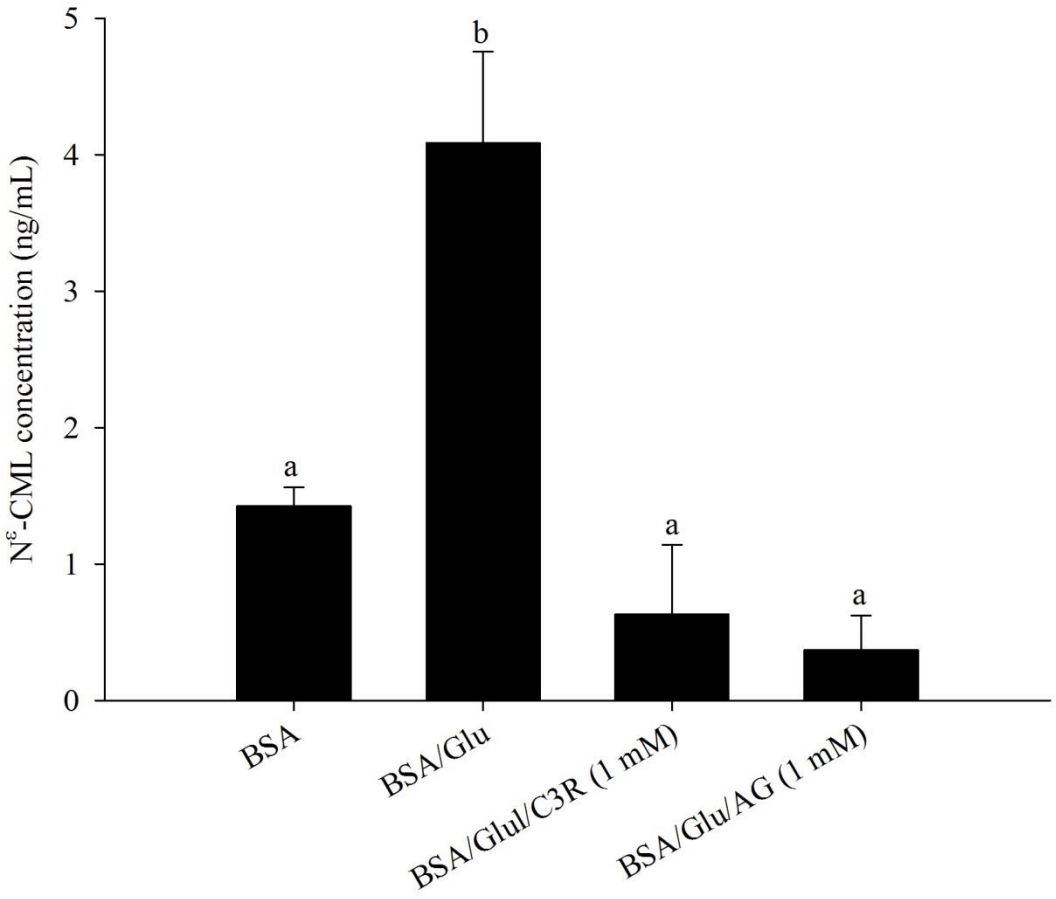

Figure 24 The effects of cyanidin-3-rutinoside (C3R) and aminoguanidine (AG) modulating the formation of non-fluorescent glycated protein N^{ε}-(carboxymethyl) lysine (N^{ε}-CML) in the BSA/Glucose (Glu) assay.

The results are presented as mean ± SEM (*n*=3). Groups without a common letter are significant difference ($p<0.05$).

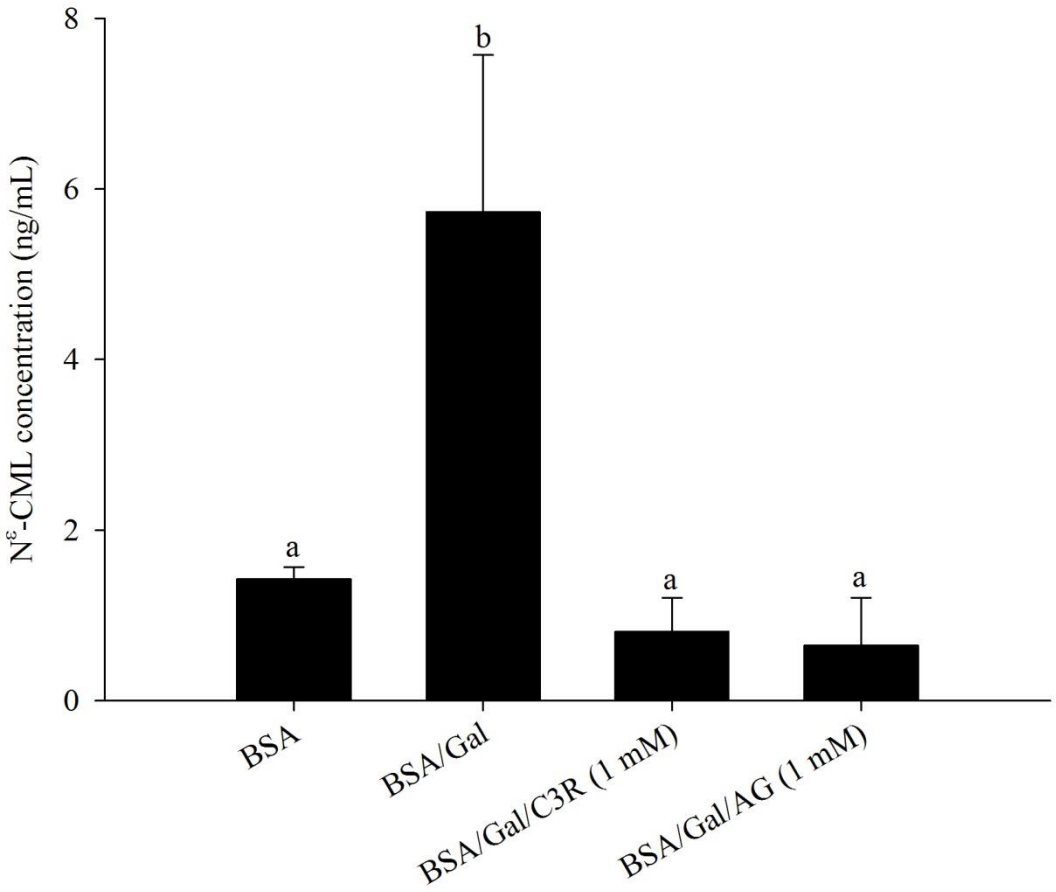

Figure 25 The effects of cyanidin-3-rutinoside (C3R) and aminoguanidine (AG) modulating the formation of non-fluorescent glycated protein N^{ε}-(carboxymethyl) lysine (N^{ε}-CML) in the BSA/Galactose (Gal) assay.

The results are presented as mean ± SEM (*n*=3). Groups without a common letter are significant difference ($p<0.05$).

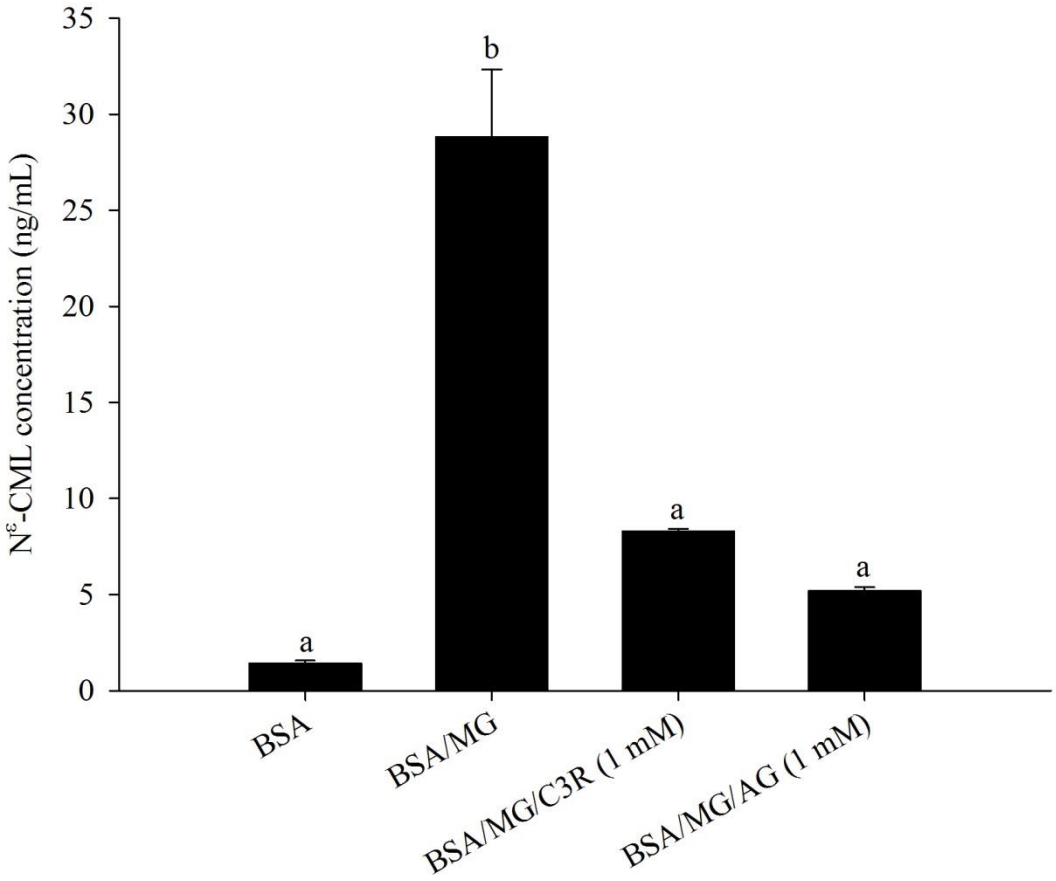

Figure 26 The effects of cyanidin-3-rutinoside (C3R) and aminoguanidine (AG) modulating the formation of non-fluorescent glycated protein N^{ε}-(carboxymethyl) lysine (N^{ε}-CML) in the BSA/Methylglyoxal (MG) assay. The results are presented as mean ± SEM (*n*=3). Groups without a common letter are significant difference ($p<0.05$).

4.1.3 Amadori products formation

The highest rate of production of fructosamine formation was observed in ribose-mediated BSA glycation by 72.1-fold, followed by a 54.9-fold in fructose, 14.3-fold in galactose and 9.5-fold in glucose when compared with BSA. As shown in figure 27-30, the addition of C3R into the solution effectively reduced the level of fructosamine in a concentration dependent manner. The results showed that C3R at concentration 0.25 or above significantly decreased the level of fructosamine in BSA/ribose (27%–43%) and BSA/fructose (15%–20%) as concentration dependent manner. However, only concentration of 1 mM C3R markedly decreased fructosamine level in BSA/glucose (37%), and BSA/galactose (32%), and the equal concentration of AG inhibited by 6% for BSA/ribose, 19% for BSA/fructose, 20% for BSA/glucose and 18% for BSA/galactose. At the end of the experimental period, C3R (1 mM) was more effective to reduce the level of fructosamine than AG by 7.0-fold, 1.1-fold, 1.9-fold and 1.8-fold in BSA/ribose, BSA/fructose, BSA/glucose and BSA/galactose system, respectively. However, the formation of Amadori product fructosamine was not detected in the BSA glycation system mediated by methylglyoxal.

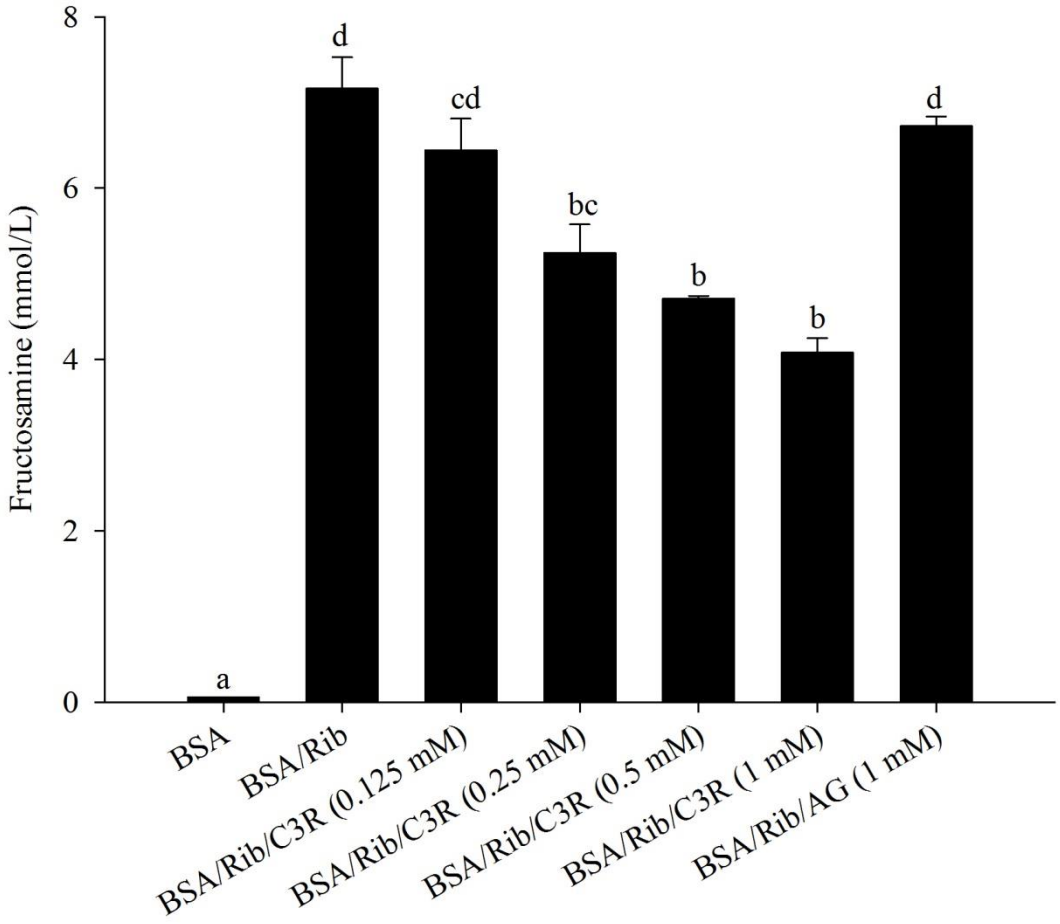

Figure 27 The effects of cyanidin-3-rutinoside (C3R) and aminoguanidine (AG) modulating the formation of fructosamine in the BSA/Ribose (Rib) assay. The results are presented as mean ± SEM (*n*=3). Groups without a common letter are significant difference ($p<0.05$).

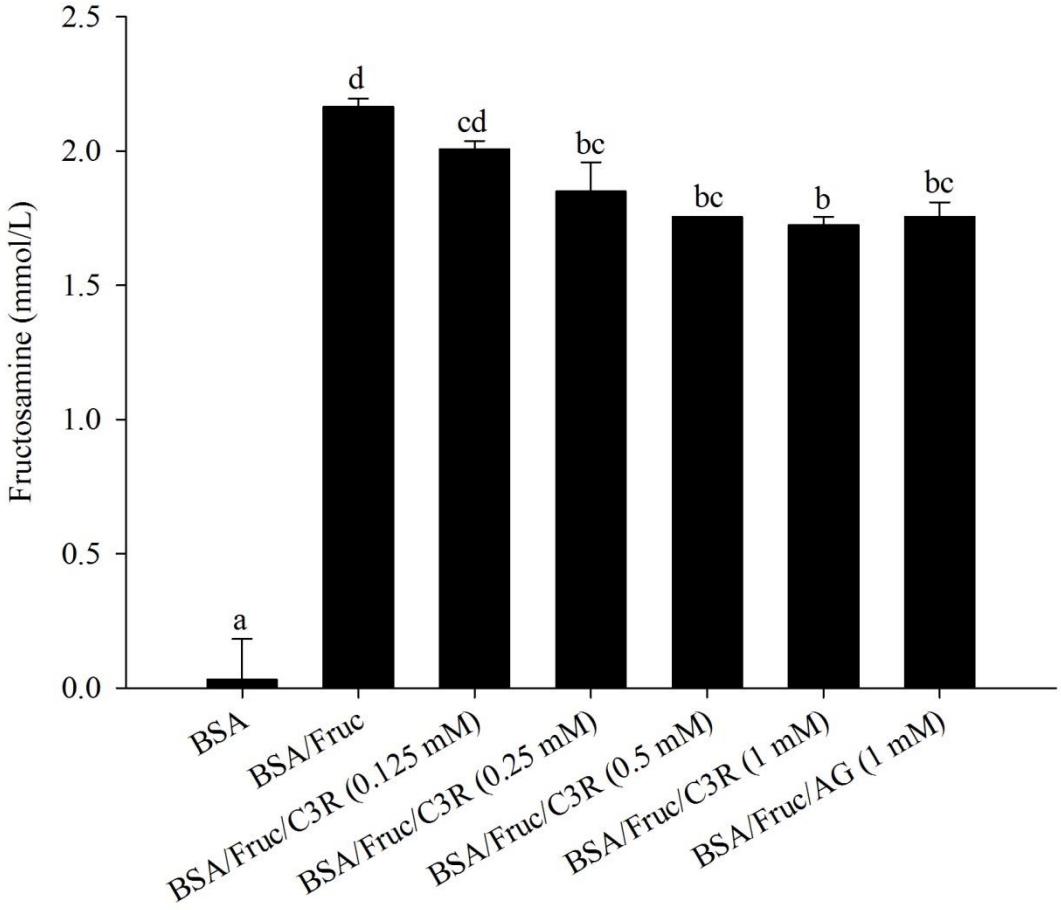

Figure 28 The effects of cyanidin-3-rutinoside (C3R) and aminoguanidine (AG) modulating the formation of fructosamine in the BSA/Fructose (Fruc) assay.

The results are presented as mean ± SEM (*n*=3). Groups without a common letter are significant difference ($p<0.05$).

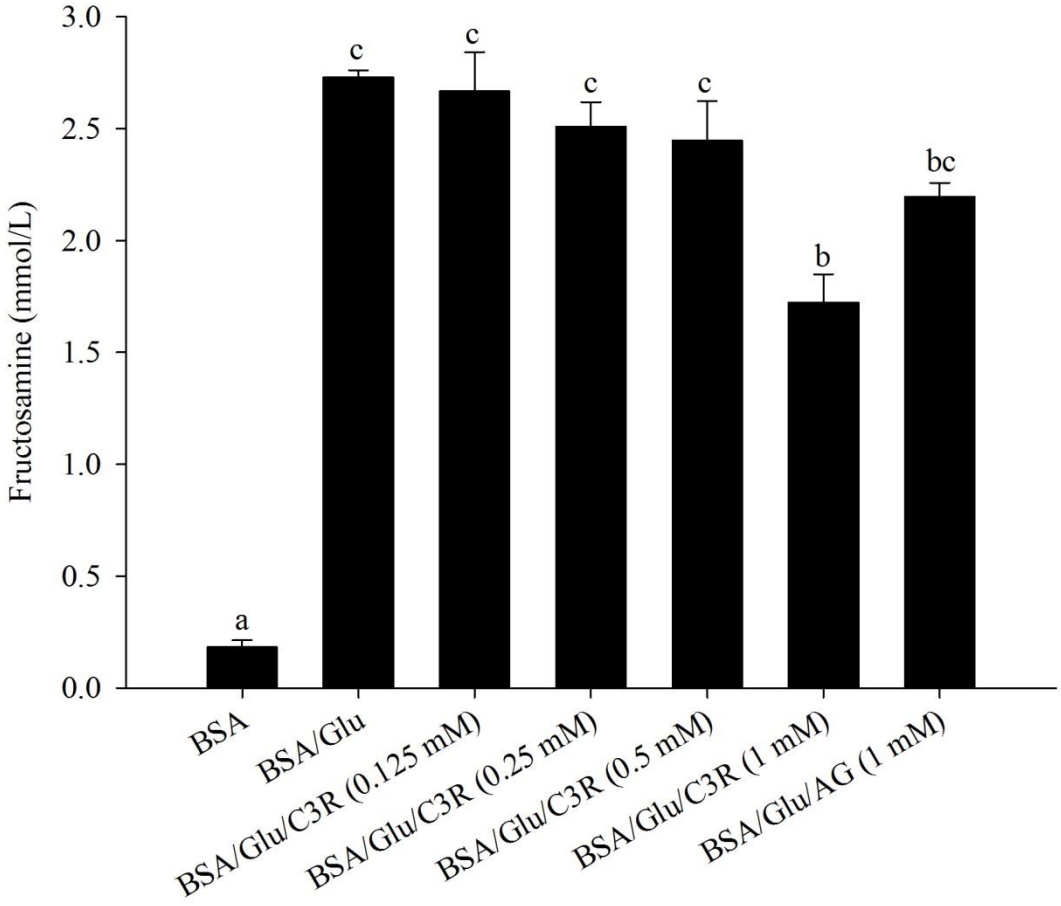

Figure 29 The effects of cyanidin-3-rutinoside (C3R) and aminoguanidine (AG) modulating the formation of fructosamine in the BSA/Glucose (Glu) assay.

The results are presented as mean ± SEM (*n*=3). Groups without a common letter are significant difference ($p<0.05$).

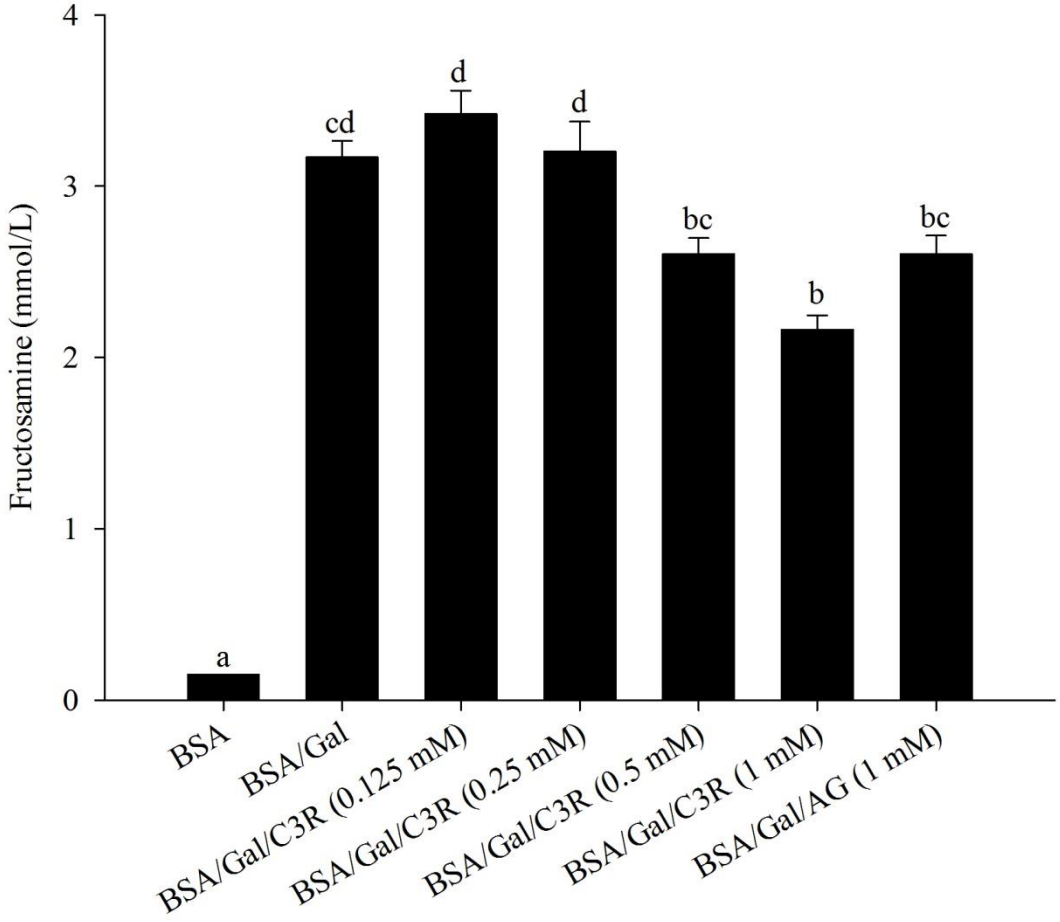

Figure 30 The effects of cyanidin-3-rutinoside (C3R) and aminoguanidine (AG) modulating the formation of fructosamine in the BSA/Galactose (Gal) assay.

The results are presented as mean ± SEM (*n*=3). Groups without a common letter are significant difference ($p<0.05$).

4.1.5 Protein oxidation

- **Protein carbonyl content**

The oxidation of protein in glycation reaction mediated by monosaccharides and methylglyoxal was determined using carbonyl content and thiol group. The following order of increased protein carbonyl content in BSA could be established: glucose (3.7-fold) < galactose (2.9-folds) < fructose (8.2-fold) < ribose (18.5-fold). After 2 weeks of incubation, the BSA/monosaccharide solution containing C3R (0.125–1 mM) reduced carbonyl content in ribose-glycated BSA (15%–25%), fructose-glycated BSA (60%-63%), glucose-glycated BSA (3%–25%), and galactose-glycated BSA (10%–23%). The addition of AG (1 mM) into the solution decreased protein carbonyl formation by 25% in BSA/ribose, 13% in BSA/fructose, 51% in BSA/glucose and 30% in BSA/galactose (figure 31-34). The level of protein carbonyl content was also investigated in BSA/methylglyoxal system. The result showed that BSA incubated with methylglyoxal increased the level of protein carbonyl content by 4.1-fold compared with BSA alone (figure 35). The presence of C3R (0.125-1 mM) in BSA/methylglyoxal solution reduced carbonyl content in range 3% to 15% whereas AG (1 mM) showed the higher potent than C3R by lowering carbonyl content for 69% when compared with BSA/methylglyoxal.

- **Protein thiol group**

The content of thiol group is a common indicator of the redox state of protein. At week 2, the depletion of protein thiol group was found in BSA/monosaccharide solution to be in the following order: galactose < glucose < fructose < ribose (figure 36-39). The results demonstrated that C3R (0.125–1 mM) prevented the depleting thiol group in ribose-glycated BSA (3%–42%), fructose-glycated BSA (12%–69%), glucose-glycated BSA (14%–87%), galactose-glycated BSA

(8%–34%), whereas AG (1 mM) had the ability to prevent the depleting thiol group approximately 63% in BSA/ribose and 47% in BSA/glucose. However, AG could not markedly prevent the loss of thiol level in BSA/fructose and BSA/galactose. In addition, the loss of protein thiol group was observed in BSA incubated with methylglyoxal by 95% after 2 week of incubation as shown in figure 40. C3R (0.125-1 mM) markedly diminished the loss of protein thiol group in BSA/methylglyoxal solution by a maximum of 33% prevention, while AG (1 mM) showed 23% prevention.

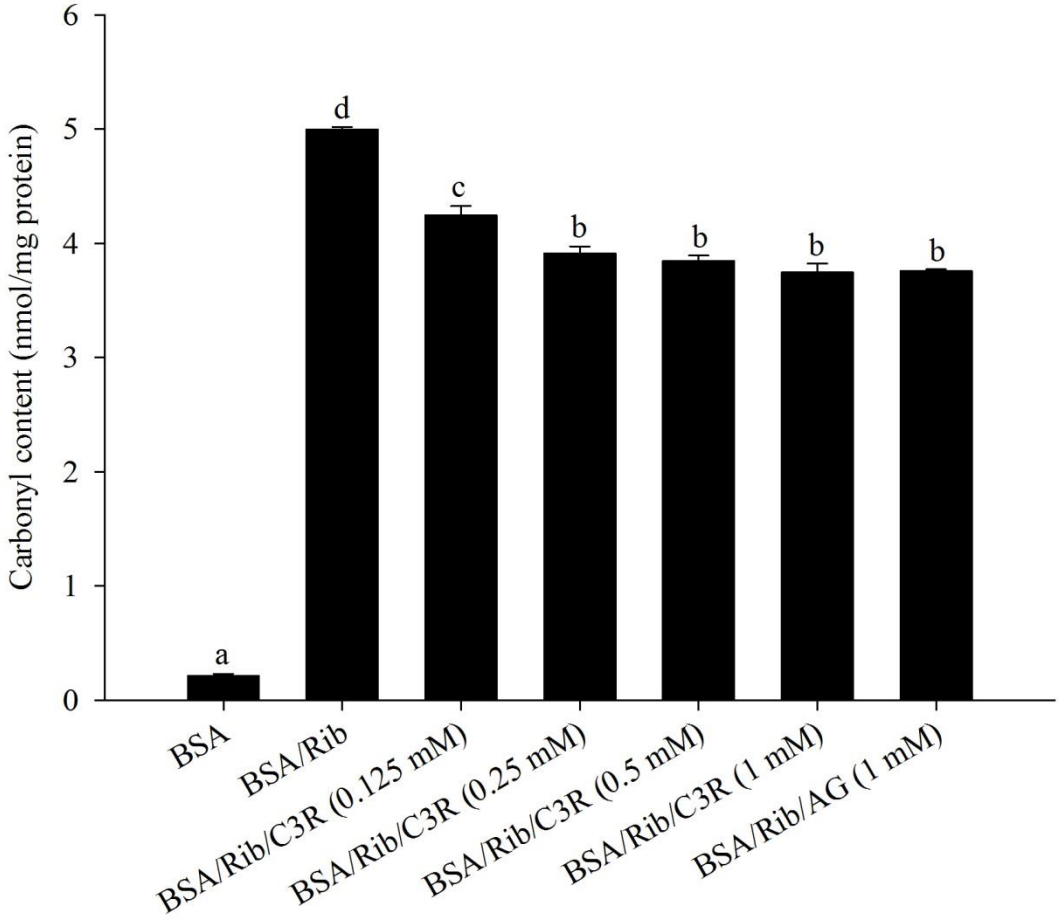

Figure 31 The effects of cyanidin-3-rutinoside (C3R) and aminoguanidine (AG) modulating the level of protein carbonyl content in the BSA/Ribose (Rib) assay.

The results are presented as mean ± SEM (*n*=3). Groups without a common letter are significant difference ($p<0.05$).

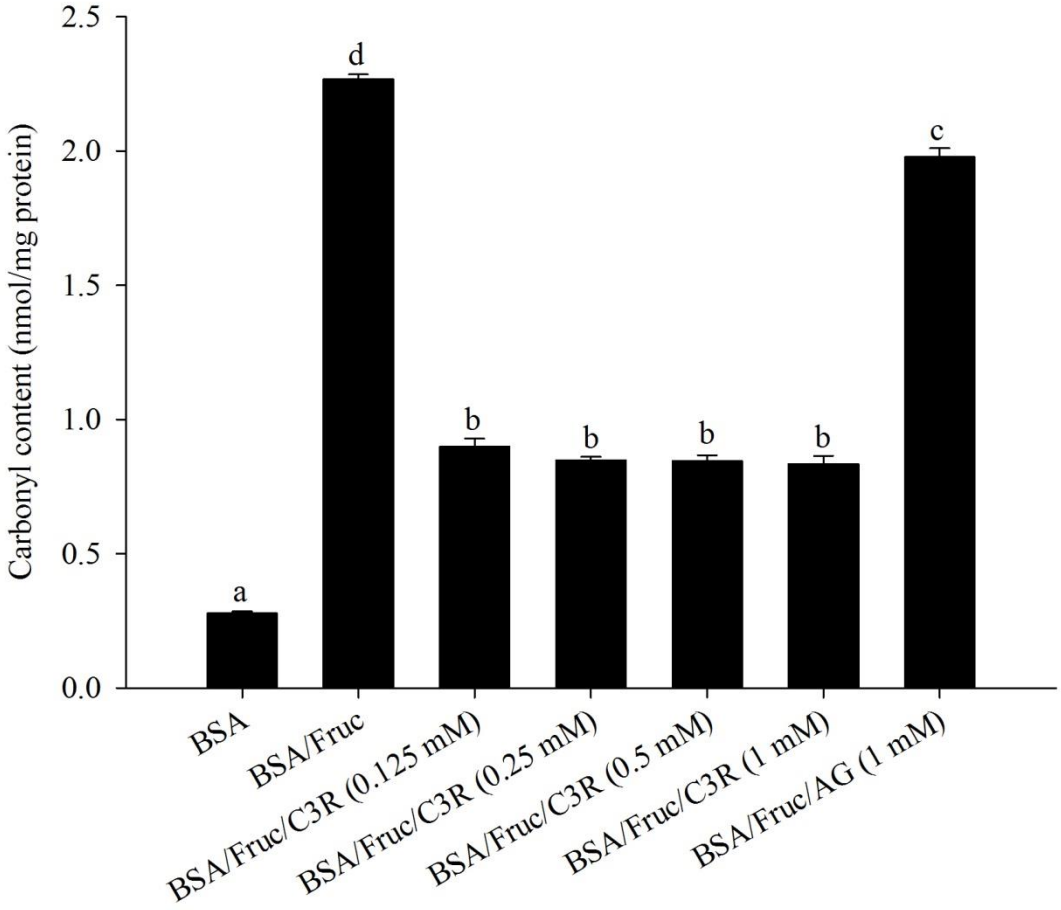

Figure 32 The effects of cyanidin-3-rutinoside (C3R) and aminoguanidine (AG) modulating the level of protein carbonyl content in the BSA/Fructose (Fruc) assay.

The results are presented as mean ± SEM (*n*=3). Groups without a common letter are significant difference ($p<0.05$).

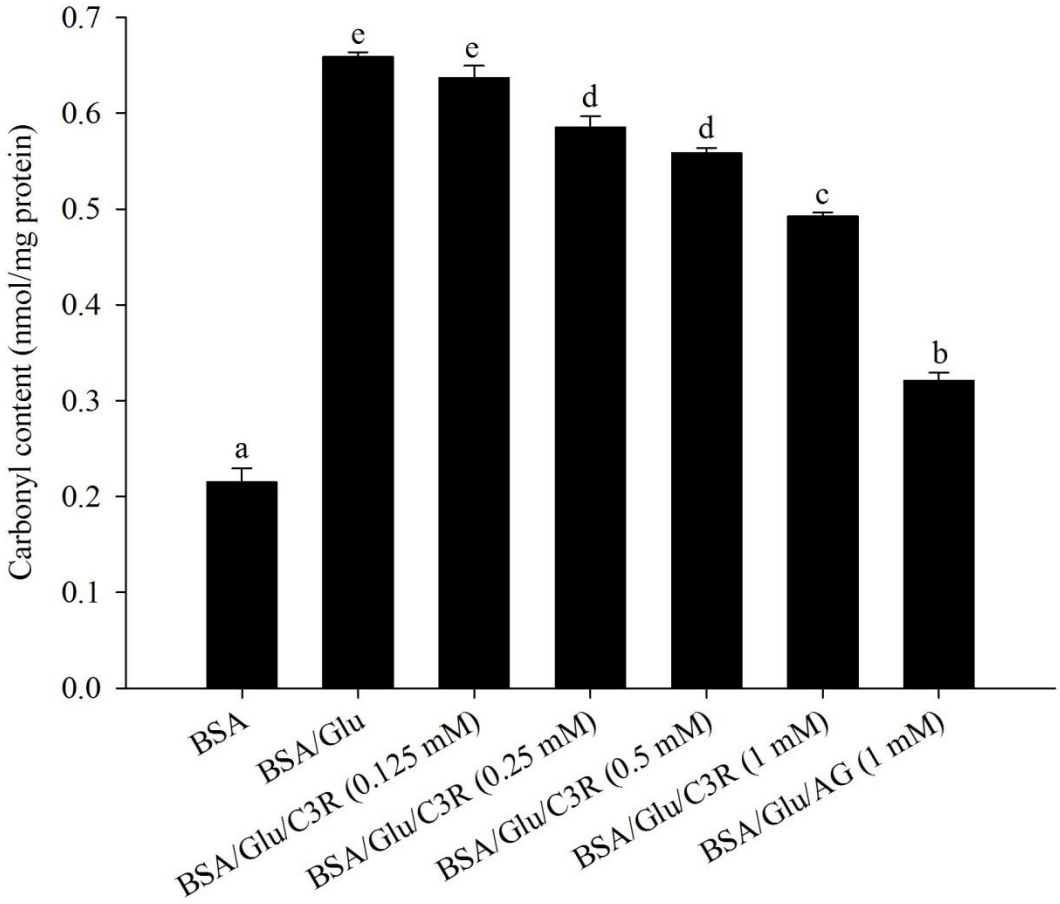

Figure 33 The effects of cyanidin-3-rutinoside (C3R) and aminoguanidine (AG) modulating the level of protein carbonyl content in the BSA/Glucose (Glu) assay.

The results are presented as mean ± SEM (*n*=3). Groups without a common letter are significant difference ($p<0.05$).

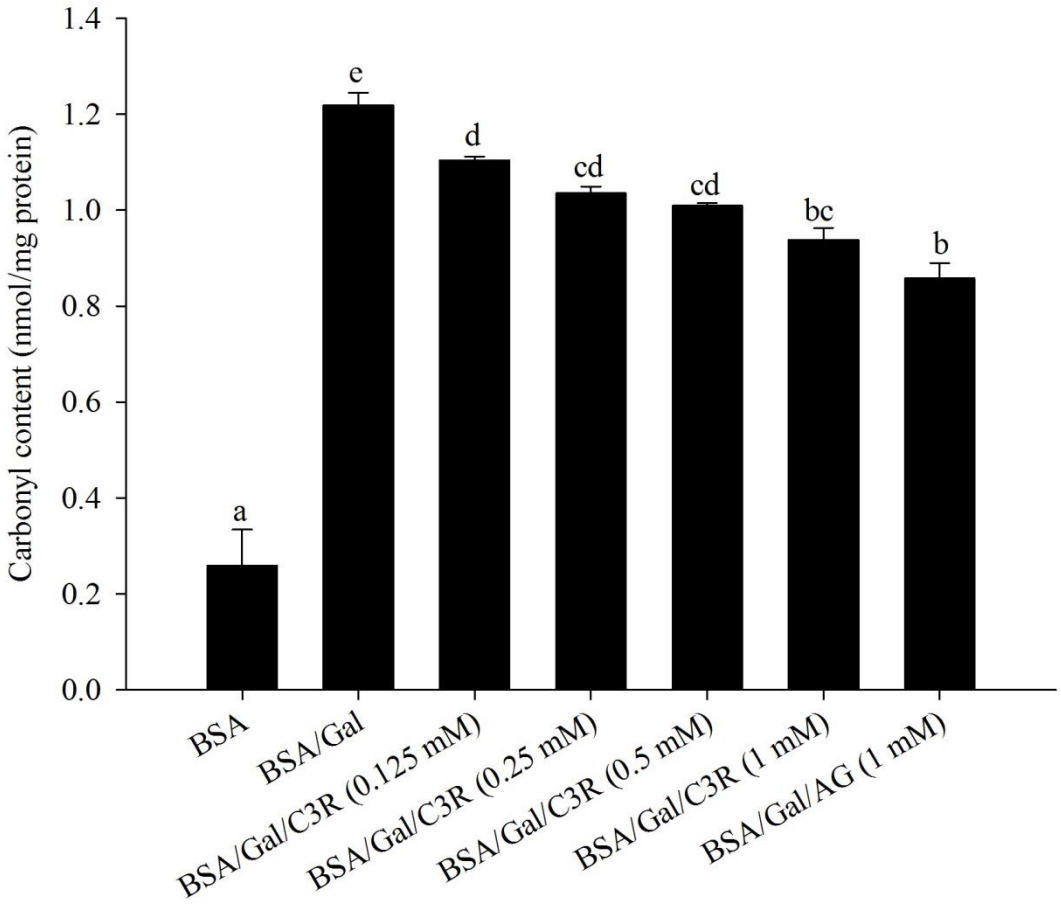

Figure 34 The effects of cyanidin-3-rutinoside (C3R) and aminoguanidine (AG) modulating the level of protein carbonyl content in the BSA/Galactose (Gal) assay.

The results are presented as mean ± SEM (*n*=3). Groups without a common letter are significant difference ($p<0.05$).

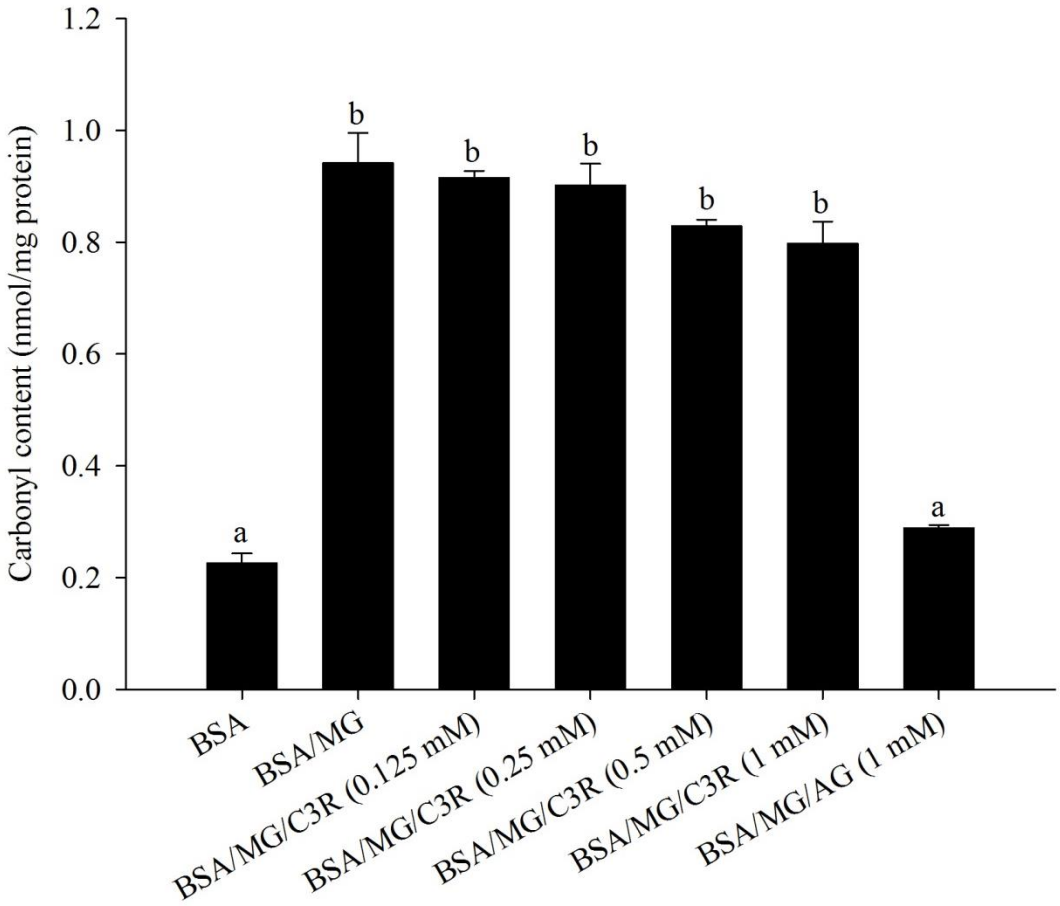

Figure 35 The effects of cyanidin-3-rutinoside (C3R) and aminoguanidine (AG) modulating the level of protein carbonyl content in the BSA/Methylglyoxal (MG) assay.

The results are presented as mean ± SEM (*n*=3). Groups without a common letter are significant difference ($p<0.05$).

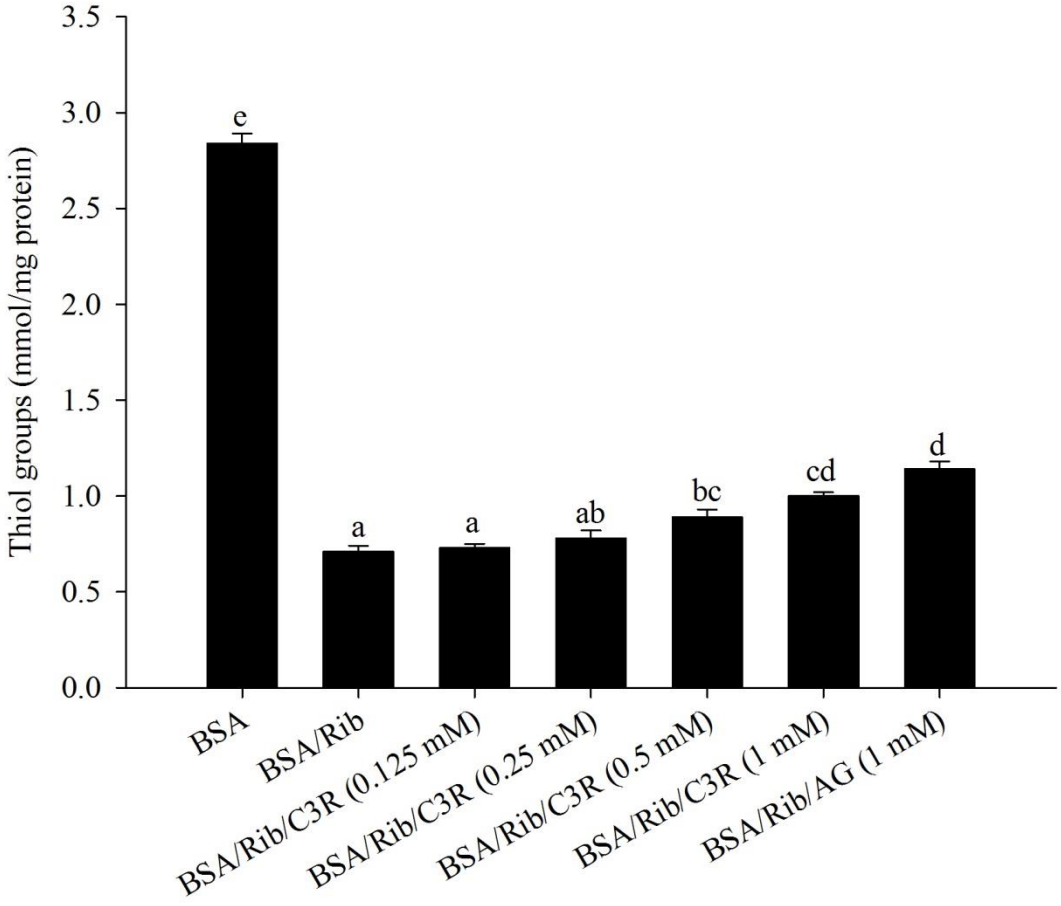

Figure 36 The effects of cyanidin-3-rutinoside (C3R) and aminoguanidine (AG) modulating the level of protein thiol group in the BSA/Ribose (Rib) assay.

The results are presented as mean ± SEM (*n*=3). Groups without a common letter are significant difference ($p<0.05$).

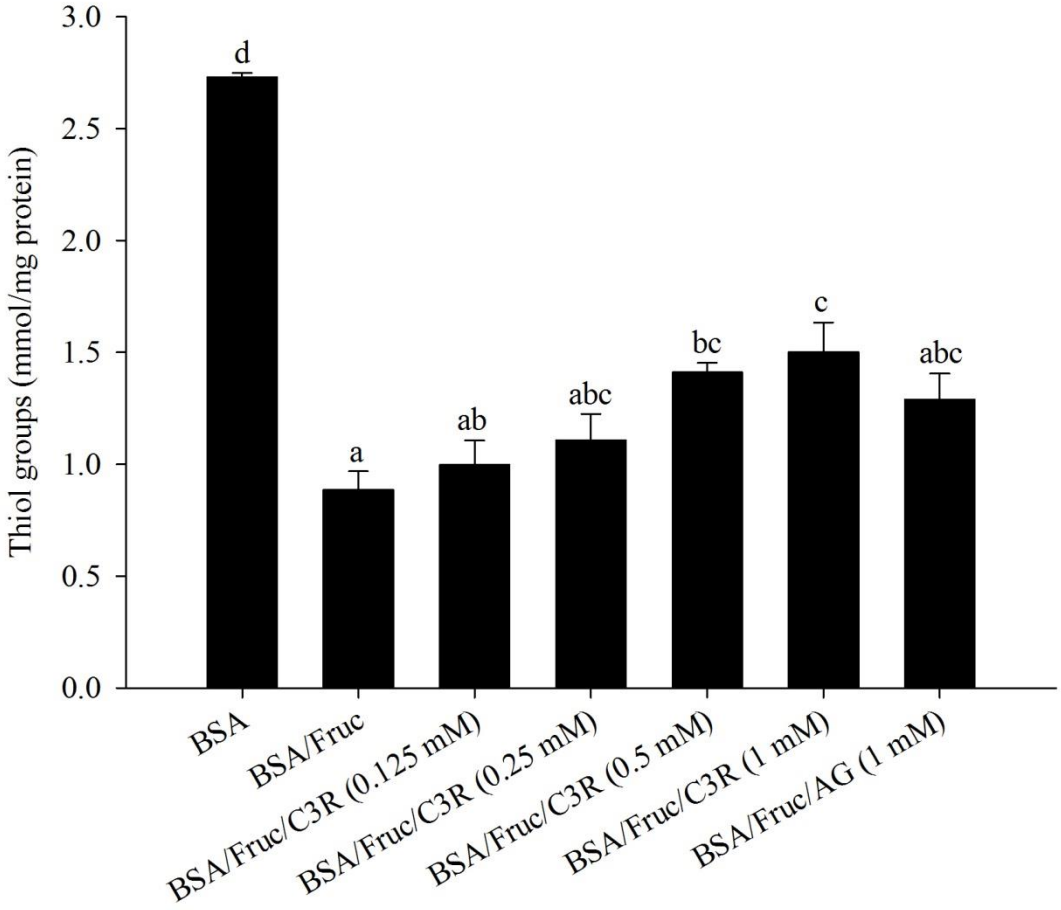

Figure 37 The effects of cyanidin-3-rutinoside (C3R) and aminoguanidine (AG) modulating the level of protein thiol group in the BSA/Fructose (Fruc) assay.

The results are presented as mean ± SEM (*n*=3). Groups without a common letter are significant difference ($p<0.05$).

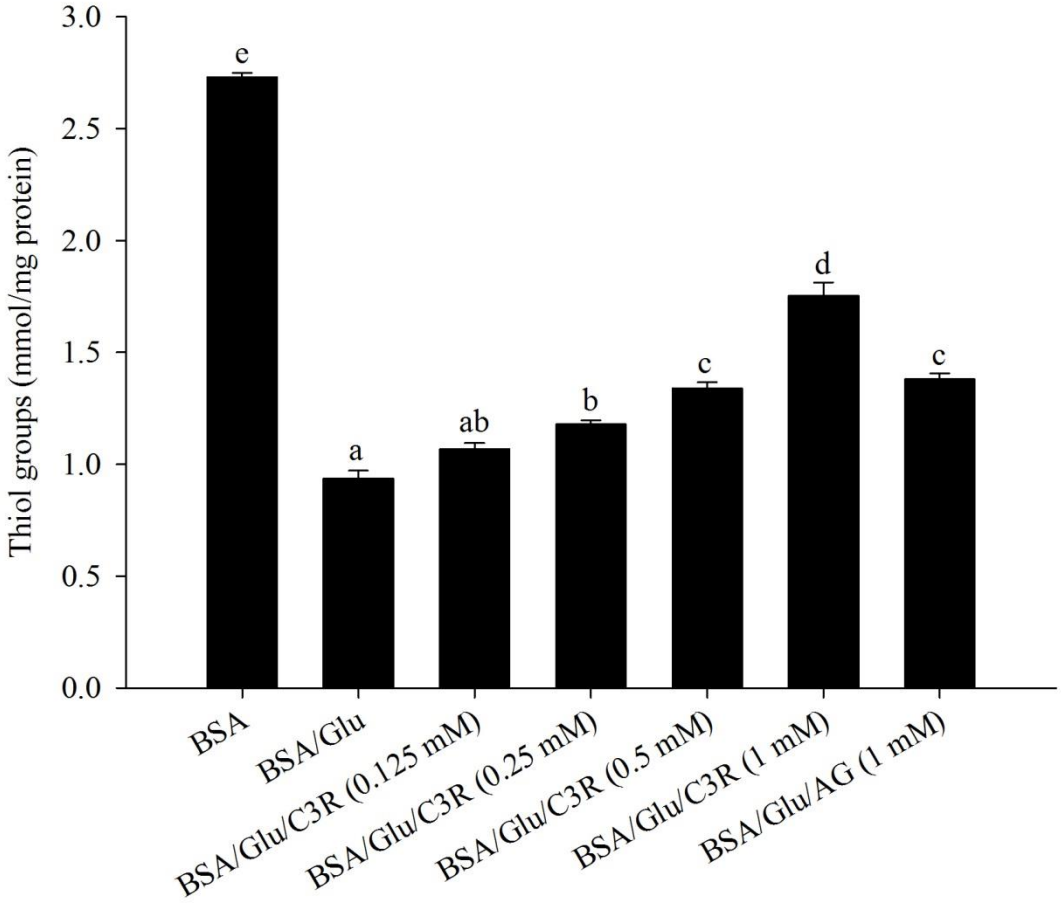

Figure 38 The effects of cyanidin-3-rutinoside (C3R) and aminoguanidine (AG) modulating the level of protein thiol group in the BSA/Glucose (Glu) assay.

The results are presented as mean ± SEM (*n*=3). Groups without a common letter are significant difference ($p<0.05$).

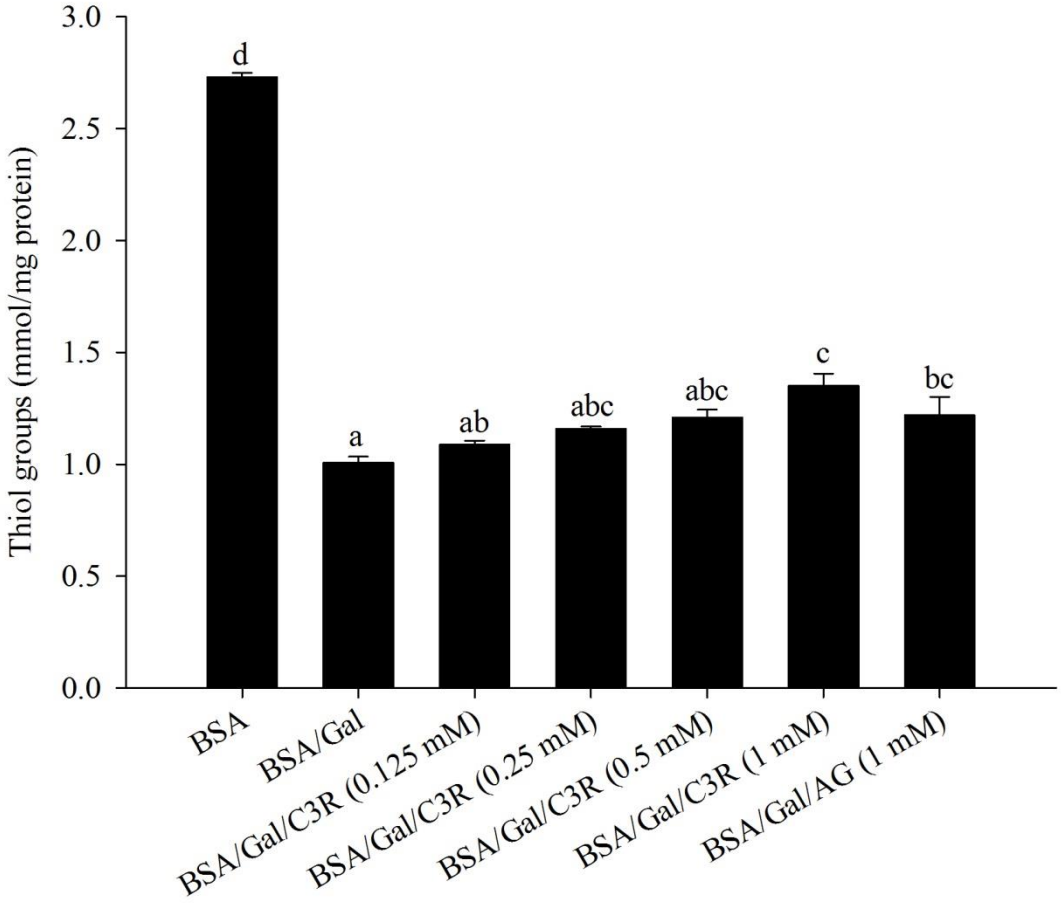

Figure 39 The effects of cyanidin-3-rutinoside (C3R) and aminoguanidine (AG) modulating the level of protein thiol group in the BSA/Galactose (Gal) assay.

The results are presented as mean ± SEM (*n*=3). Groups without a common letter are significant difference ($p<0.05$).

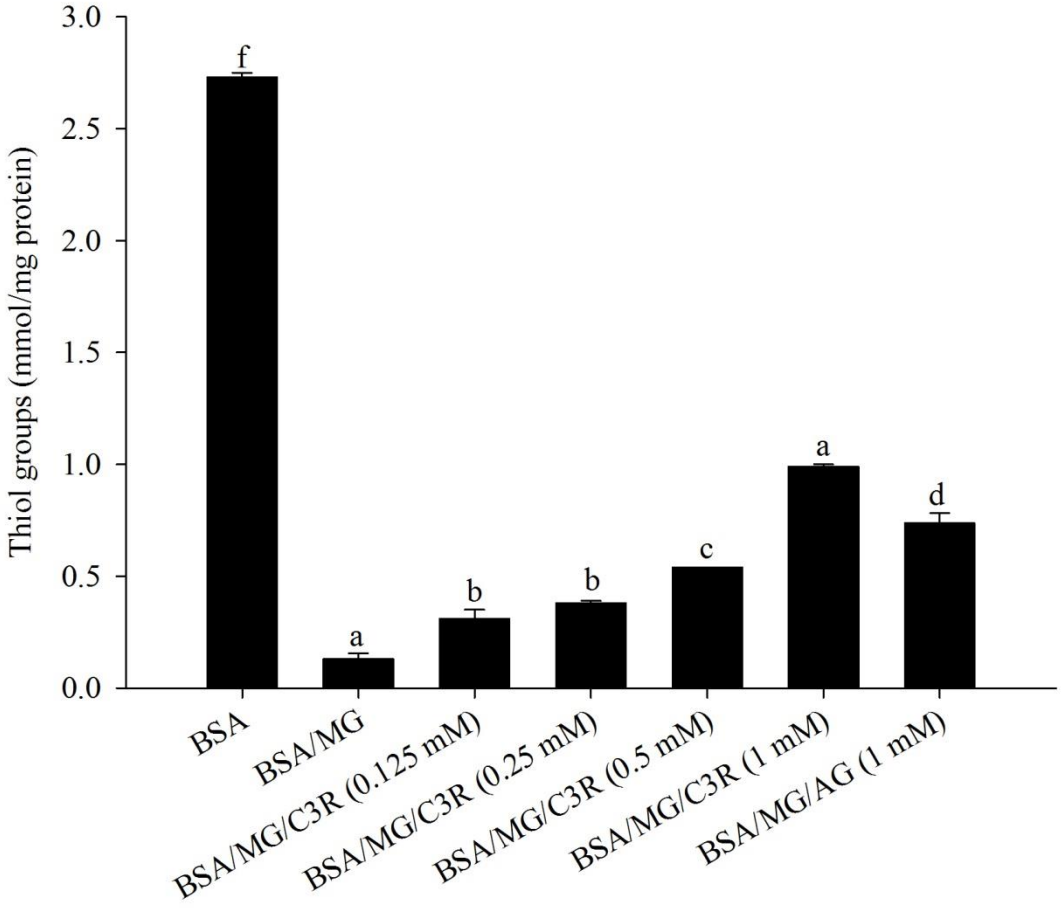

Figure 40 The effects of cyanidin-3-rutinoside (C3R) and aminoguanidine (AG) modulating the level of protein thiol group in the BSA/Methylglyoxal (MG) assay.

The results are presented as mean ± SEM (*n*=3). Groups without a common letter are significant difference ($p<0.05$).

4.1.4 Protein aggregation

The protein aggregation was measured as the level of β–amyloid cross structure as shown in figure 41-44. The highest rate production of β–amyloid cross structure was seen in ribose (1.8-fold) and followed by fructose (1.6-fold), galactose (1.3-fold), and glucose (1.3-fold) when compared with BSA without monosaccharide. At week 2, the addition of C3R (0.125-1 mM) significantly ameliorated the level of β-amyloid cross structure in ribose-glycated BSA (22%–48%), fructose-glycated BSA (52%–81%), glucose-glycated BSA (38%–66%) and galactose-glycated BSA (38%–75%). In the meantime, AG (1 mM) also reduced the formation of cross β-amyloid structure in BSA/ribose (15%), BSA/fructose (24%), BSA/glucose (3%), and BSA/galactose (11%). Nevertheless, AG showed lower efficacy than C3R by 3.3-fold, 3.4-fold, 23.7-fold and 6.6-fold for ribose-, fructose-, glucose- and galactose-induced BSA glycation, respectively.

As shown in figure 45, the level of β-amyloid cross structure was also investigated in BSA/methylglyoxal system. The result showed that the incubation of BSA with methylglyoxal increased β-amyloid cross structure level by 1.3-fold when compared with BSA alone. The addition of C3R at concentration 0.25 or above markedly decreased β-amyloid crosses structure. C3R (1 mM) inhibited β-amyloid cross structure formation by 56% whereas AG at equal concentration has only 25% inhibition.

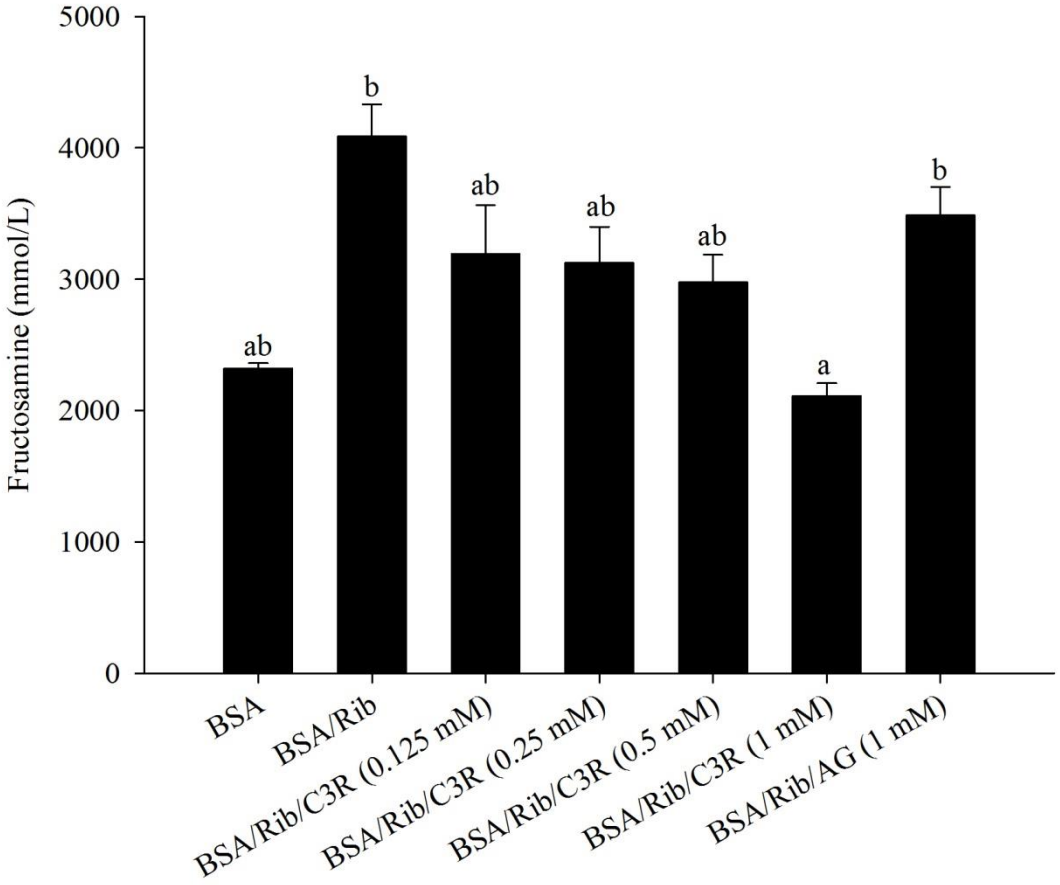

Figure 41 The effects of cyanidin-3-rutinoside (C3R) and aminoguanidine (AG) modulating the formation of β-amyloid cross structure in the BSA/Ribose (Rib) assay.

The results are presented as mean ± SEM (*n*=3). Groups without a common letter are significant difference ($p<0.05$).

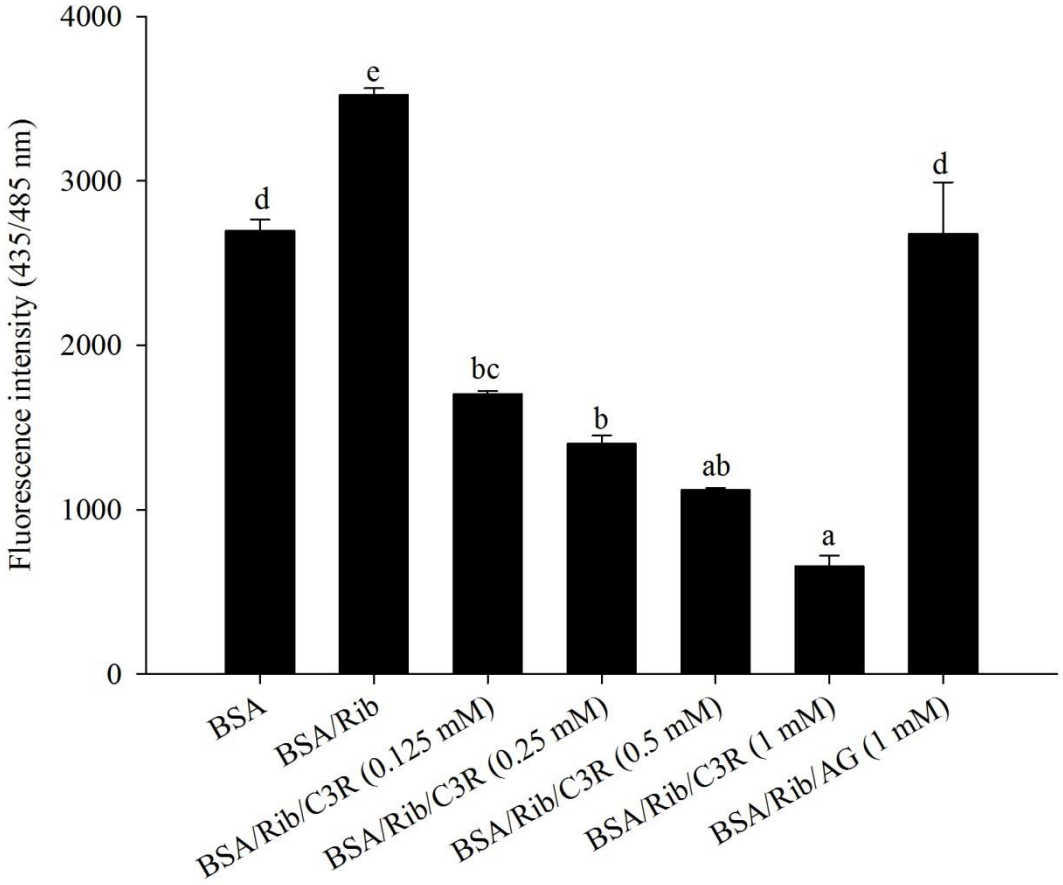

Figure 42 The effects of cyanidin-3-rutinoside (C3R) and aminoguanidine (AG) modulating the formation of β-amyloid cross structure in the BSA/Fructose (Fruc) assay.

The results are presented as mean ± SEM (*n*=3). Groups without a common letter are significant difference ($p<0.05$).

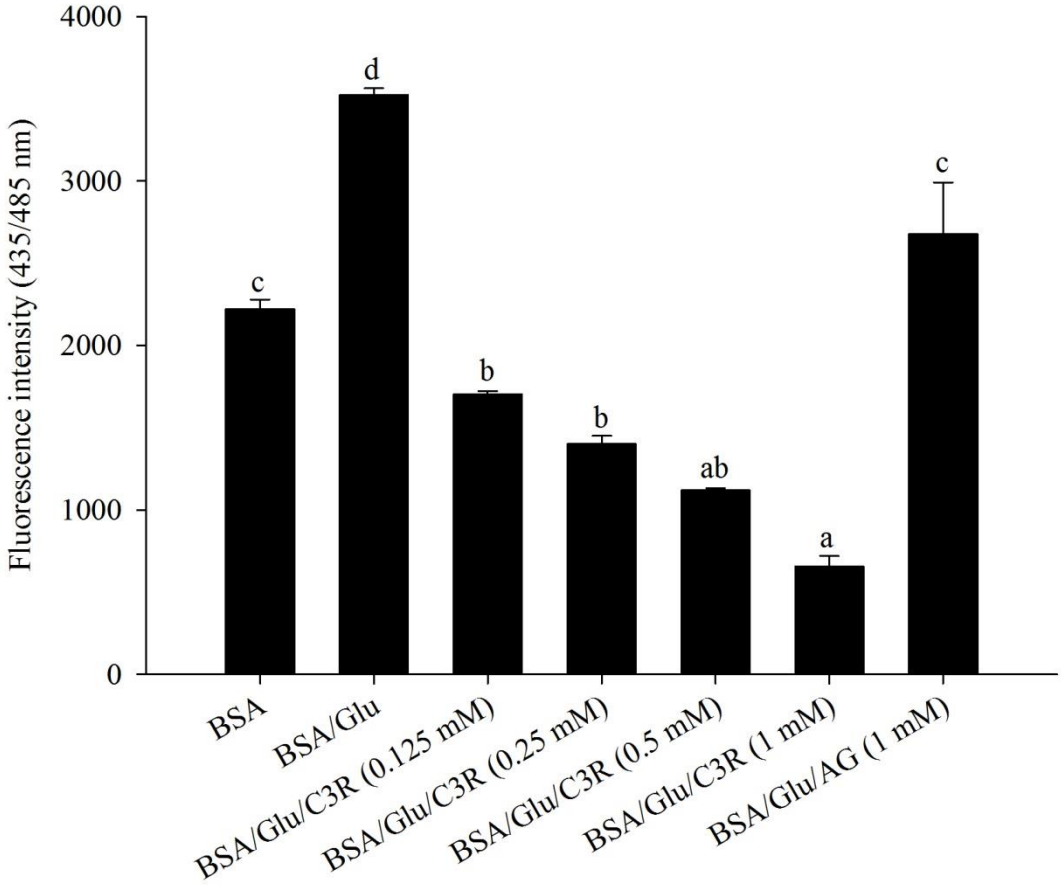

Figure 43 The effects of cyanidin-3-rutinoside (C3R) and aminoguanidine (AG) modulating the formation of β-amyloid cross structure in the BSA/Glucose (Glu) assay.

The results are presented as mean ± SEM (*n*=3). Groups without a common letter are significant difference ($p<0.05$).

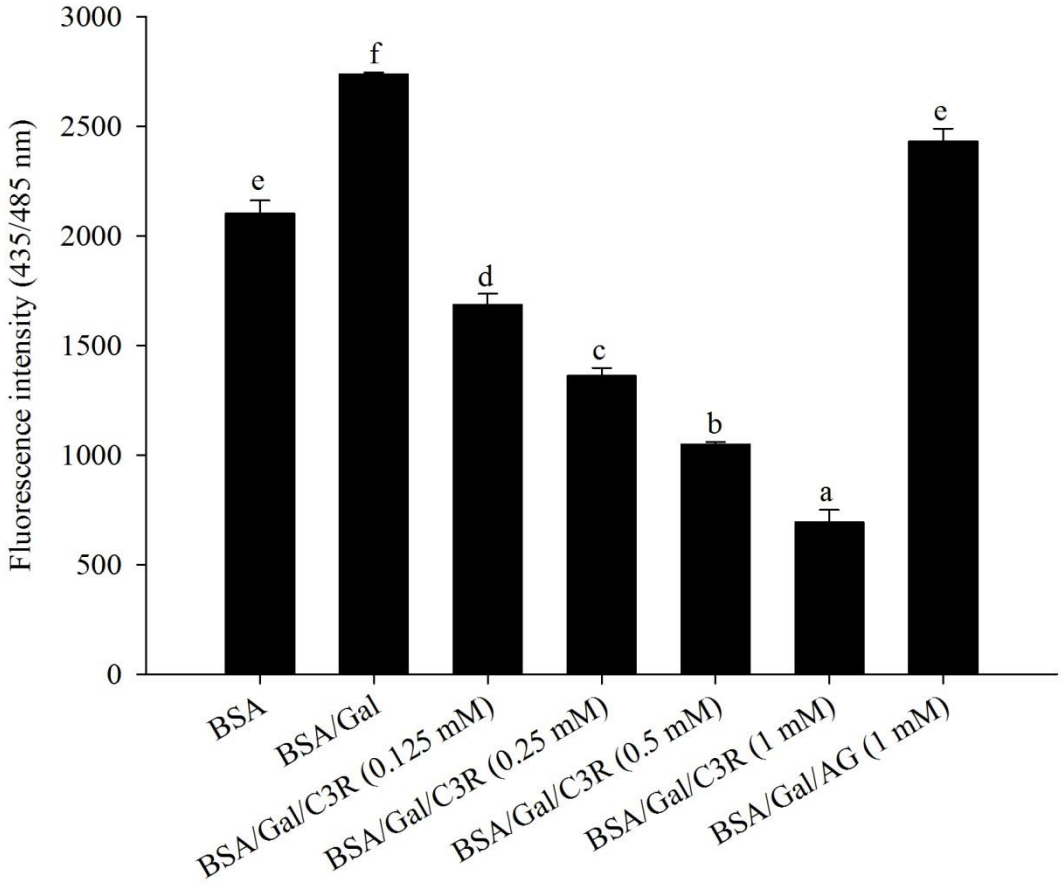

Figure 44 The effects of cyanidin-3-rutinoside (C3R) and aminoguanidine (AG) modulating the formation of β-amyloid cross structure in the BSA/Galactose (Gal) assay.

The results are presented as mean ± SEM (*n*=3). Groups without a common letter are significant difference ($p<0.05$).

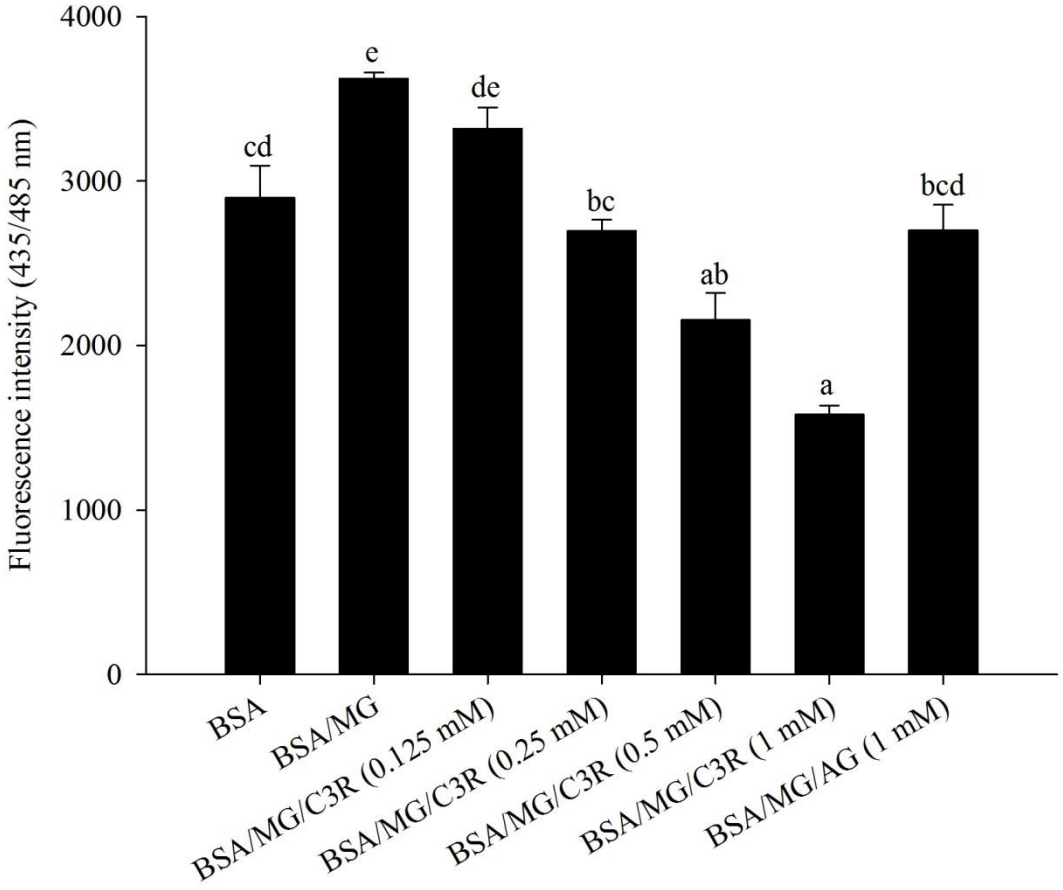

Figure 45 The effects of cyanidin-3-rutinoside (C3R) and aminoguanidine (AG) modulating the formation of β-amyloid cross structure in the BSA/Methylglyoxal (MG) assay.

The results are presented as mean ± SEM (*n*=3). Groups without a common letter are significant difference ($p<0.05$).

4.1.5 Methylglyoxal trapping ability

An evaluation of direct methylglyoxal-trapping capacity was carried out in order to investigate whether C3R could directly scavenge methylglyoxal. The percentage of methylglyoxal-trapping efficiency of C3R was consistent with the increased concentration of C3R and time of incubation ($p<0.001$). The increase in incubation time from 1 to 24 hours increased efficiency of C3R to scavenge methylglyoxal by 2-fold. In addition, the methylglyoxal trapping ability of C3R was increased as the molar ratio of C3R to methylglyoxal increased. The equal molar ratio of C3R to methylglyoxal resulted in 21% and 45% methylglyoxal-trapping capacity after 1 and 24 h of incubation as shown in figure 46. AG showed a higher trapping capacity compared to C3R as it trapped 90 and 95% of methylglyoxal when incubated with methylglyoxal (1:1 molar ratio) for 1 and 24 hours, respectively (Table 12).

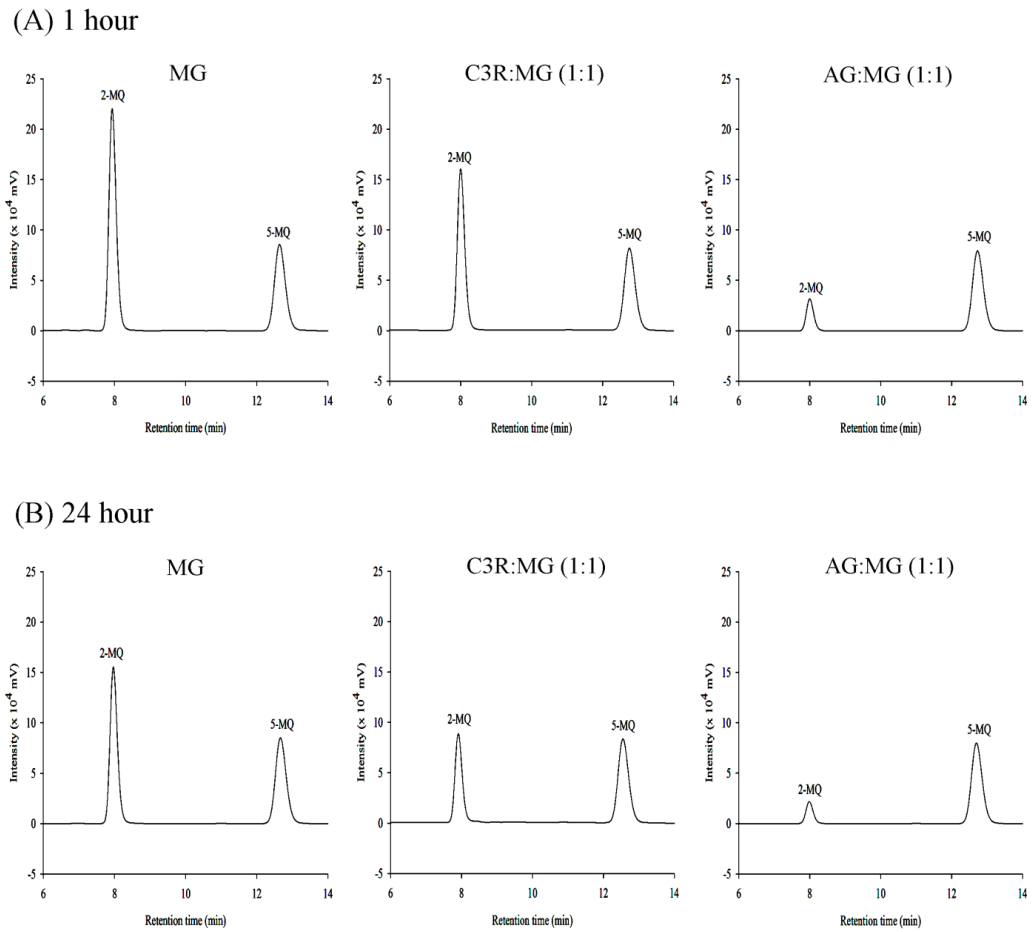

Figure 46 The HPLC chromatogram of methylglyoxal after reaction with cyanidin-3-rutinoside (C3R) and aminoguanidine (AG) at 1 hour (A) and 24 hours (B). Methylglyoxal was detected as 2-methylquinoxaline (2-MQ) after derivatization using *o*-phenylenediamine at 315 nm. 5-methylquinoxaline (5-MQ) was used as the internal standard.

Table 12 The percentage of methylglyoxal (MG)-trapping ability of cyanidin-3-rutinoside (C3R) and aminoguanidine (AG)

Time (h)	Molar ratio of C3R:MG						Molar ration of AG:MG
	0.25:1	0.5:1	1:1	2:1	4:1	16:1	1:1
1	5 ± 0.3	12 ± 1.3	21 ± 2.6	32 ± 2.0	42 ± 2.5	61 ± 1.9	90 ± 3.2
24	9 ± 1.2	21 ± 1.0	45 ± 0.7	57 ± 3.0	73 ± 3.2	89 ± 1.1	95 ± 4.6

The results are presented as mean ± SEM (*n*=3).

4.2 The effect of cyanidin-3-rutinoside (C3R) on methylglyoxal-induced oxidative DNA damage, *in vitro*.

4.2.1 DNA strand breakage

The addition of lysine, methylglyoxal, Cu^{2+} or C3R (1mM) to plasmid DNA did not cause DNA cleavage, as plasmid DNA remained in the supercoiled (SC) form (figure 47a). The addition of methylglyoxal together with lysine to plasmid DNA caused 69% strand breakage of plasmid DNA when compared to plasmid DNA alone which was indicated by increasing intensity of the open circular (OC) band (figure 47b). The lysine/methylglyoxal-induced DNA damage was markedly reduced by 26% at the highest dose of C3R (1 mM) as shown in figure 48. In the presence of Cu^{2+}, the cleavage of plasmid DNA was 6-fold higher than lysine/methylglyoxal without Cu^{2+} (figure 47c) and was markedly reduced by 12% and 18% at 0.5 and 1 mM of C3R, respectively (figure 49).

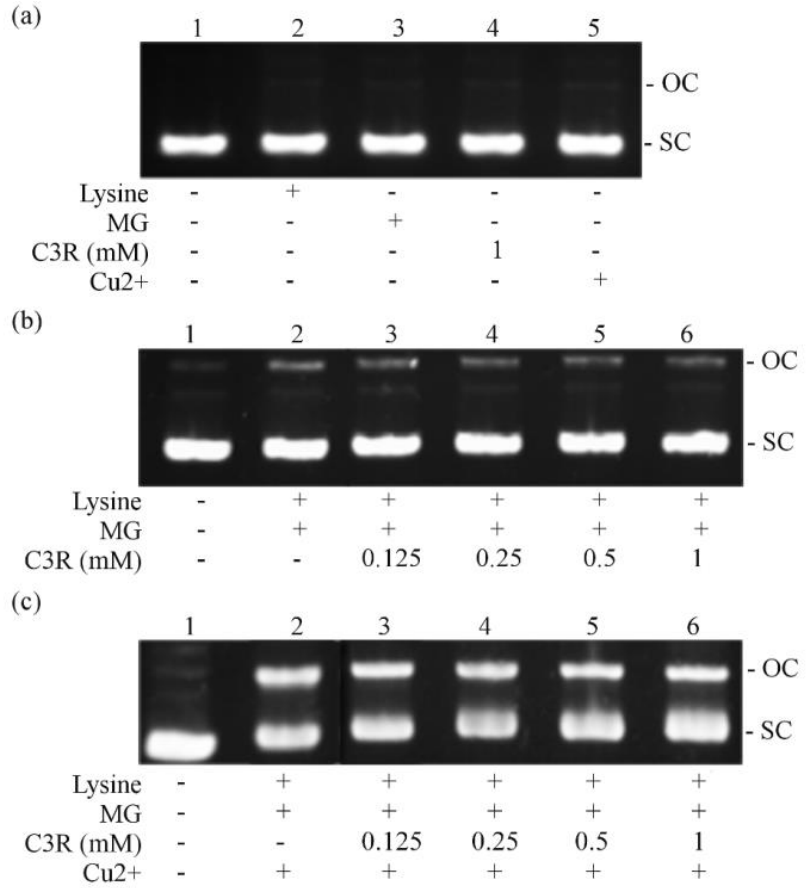

Figure 47 The effects of cyanidin-3-rutinoside (C3R) on DNA cleavage-mediated by glycation of lysine with methylglyoxal (MG) in the absence or presence of Cu^{2+}.

The major band corresponds to supercoiled form (SC), and damaged plasmid DNA is represented as opened circular form (OC). pUC19 DNA (0.25 µg) was incubated with the following: (a) Lane 1, DNA alone; Lane 2, 50 mM lysine; Lane 3, 50 mM MG; Lane 4, 300 µM $CuSO_4$; Lane 5, 1 mM C3R. (b) Lane 1, DNA alone; Lane 2, 50 mM lysine + 50 mM MG; Lane 3, 50 mM lysine + 50 mM MG + 0.125 mM C3R; Lane 4, 50 mM lysine + 50 mM MG + 0.25 mM C3R; Lane 5, 50 mM lysine + 50 mM MG + 0.5 mM C3R; Lane 6, 50 mM lysine + 50 mM MG + 1 mM C3R. (**c**) Lane 1, DNA alone; Lane 2, 50 mM lysine + 50 mM MG + 300 µM Cu^{2+}; Lane 3, 50 mM lysine + 50 mM MG + 300 µM Cu^{2+} + 0.125 mM C3R; Lane 4, 50 mM lysine + 50 mM MG + 300 µM Cu^{2+} + 0.25 mM C3R; Lane 5, 50 mM lysine + 50 mM MG + 300 µM Cu^{2+} + 0.5 mM C3R; Lane 6, 50 mM lysine + 50 mM MG + 300 µM Cu^{2+} + 1 mM C3R.

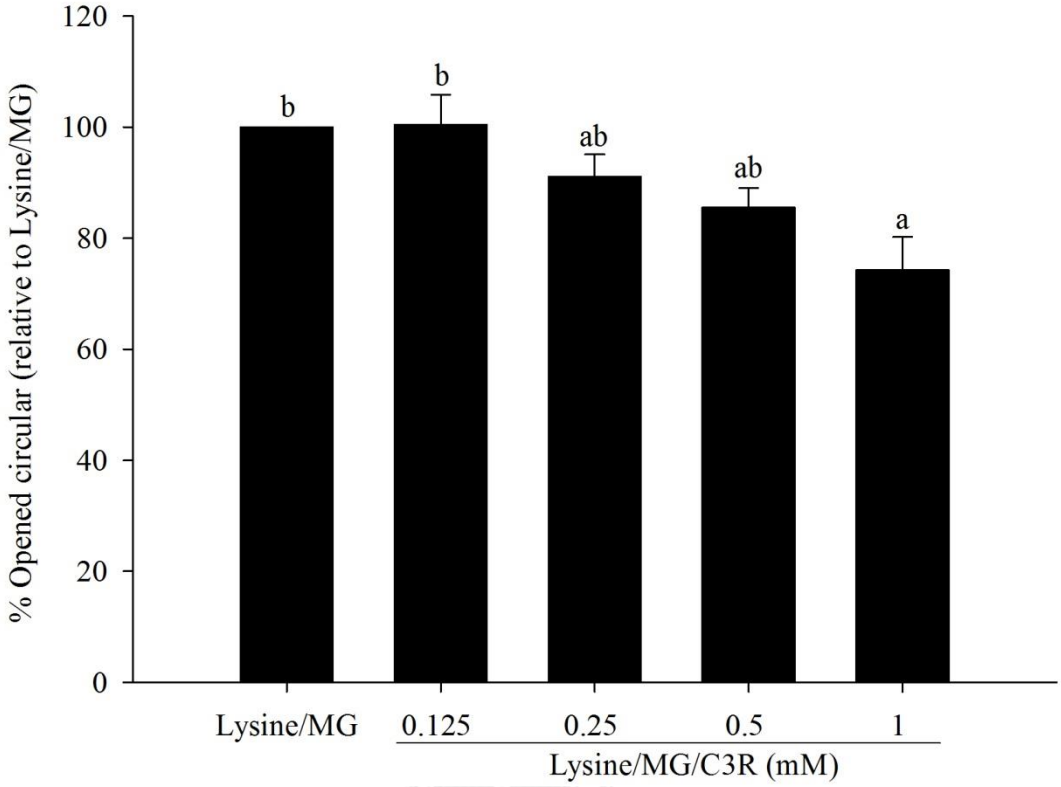

Figure 48 The effect of cyanidin-3-rutinoside (C3R) modulating % open circular (OC) form of plasmid DNA in lysine/methylglyoxal (MG)-induced DNA strand breakage in the absence of Cu^{2+}.

The results are presented as mean ± SEM (*n*=3). Groups without a common letter are significant difference ($p<0.05$).

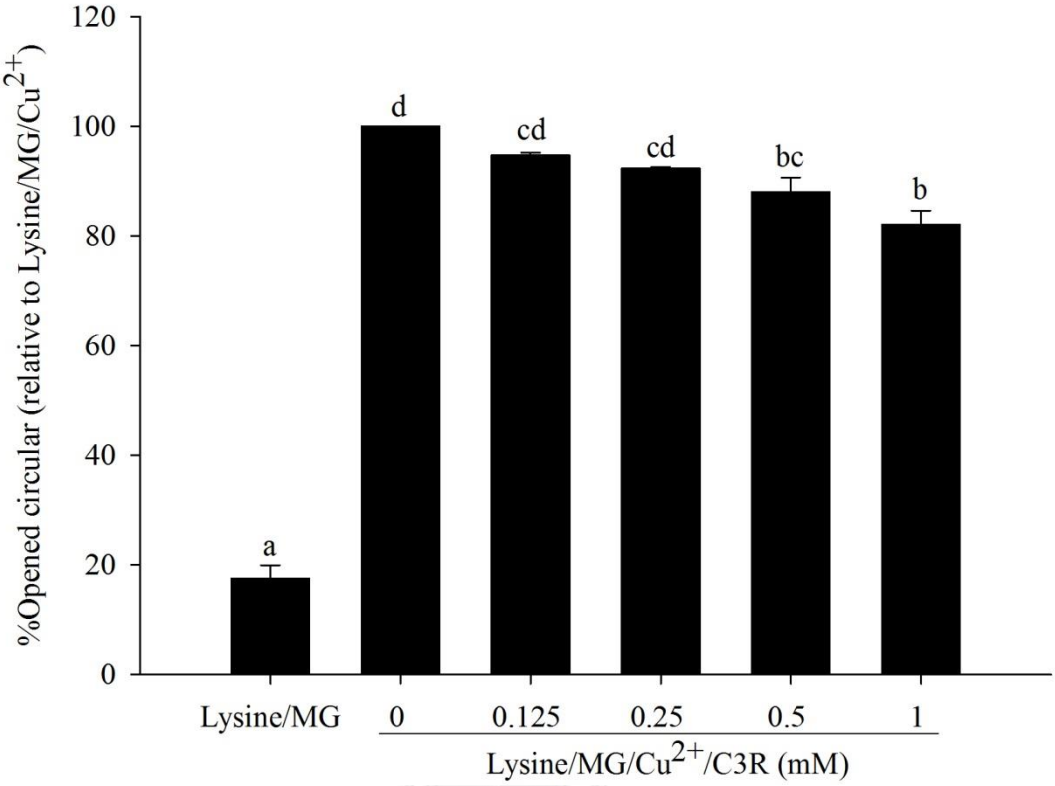

Figure 49 The effect of cyanidin-3-rutinoside (C3R) modulating % open circular (OC) form of plasmid DNA in lysine/methylglyoxal (MG)-induced DNA strand breakage in the presence of Cu^{2+}.

The results are presented as mean ± SEM (*n*=3). Groups without a common letter are significant difference ($p<0.05$).

4.2.2 Reactive oxygen species generation

The level of superoxide anion was represented by reduced cytochrome *c* level. Superoxide anion formation significant increased during the incubation period as time dependent manner in methylglyoxal alone and lysine-incubated with methylglyoxal. The reduced cytochrome *c* was increased from 0.38±0.02 in lysine to 3.09±0.09 in methylglyoxal alone and 6.82±0.36 nmol/mL lysine/methylglyoxal system ($p<0.05$). As shown in figure 50, the elevation of superoxide anion production caused by methylglyoxal or methylglyxal–incubated with lysine was prevented by all concentrations of C3R (0.125-1 mM). The addition of C3R at all concentration maintained the level of superoxide anion at the same level after 10 min until the end of experimental period at 50 min.

The lysine/methylglyoxal generated hydroxyl radicals as measured by TBARS at the level 16.30±0.28 μM after 3 hours of incubation. The addition of C3R at concentration 0.5 mM or greater markedly reduced hydroxyl radicals formation (figure 51). The highest concentration of C3R (1 mM) resulted in a 16% inhibition of hydroxyl radical generation.

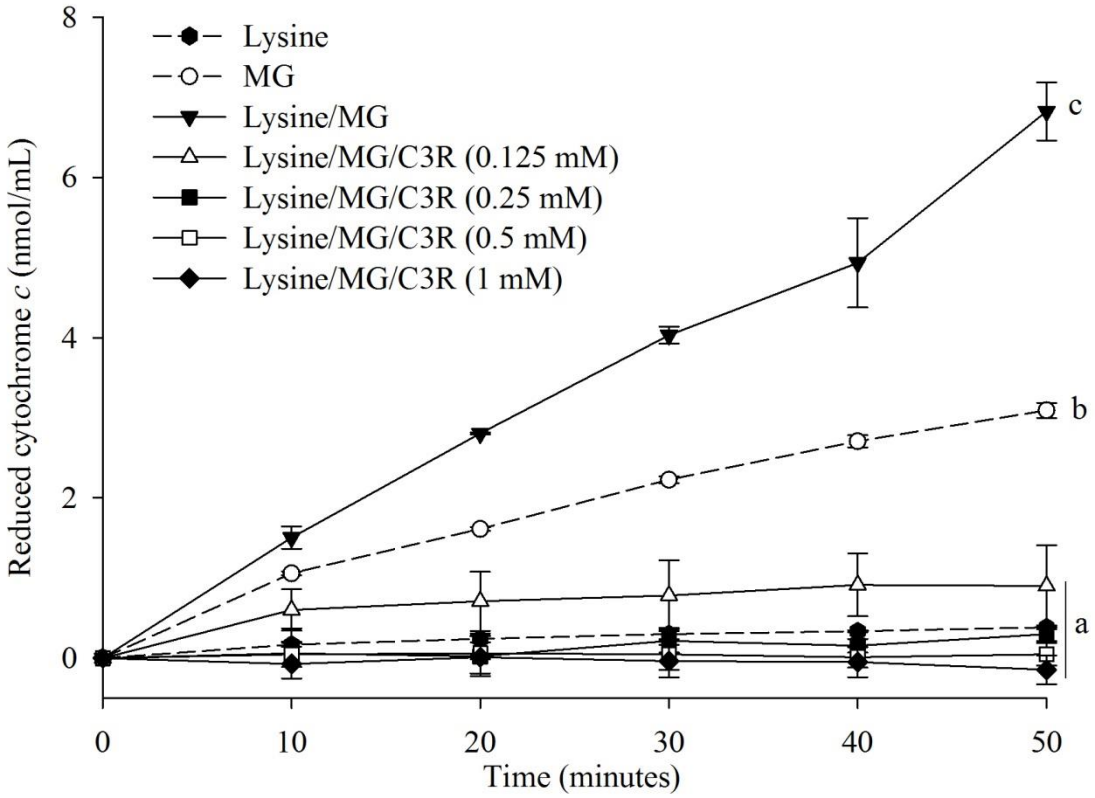

Figure 50 The effects of cyanidin-3-rutinoside (C3R) modulating the production of superoxide anion in lysine/methylglyoxal (MG)-induced glycation.

The results are presented as mean ± SEM (*n*=3). Groups without a common letter are significant difference ($p<0.05$).

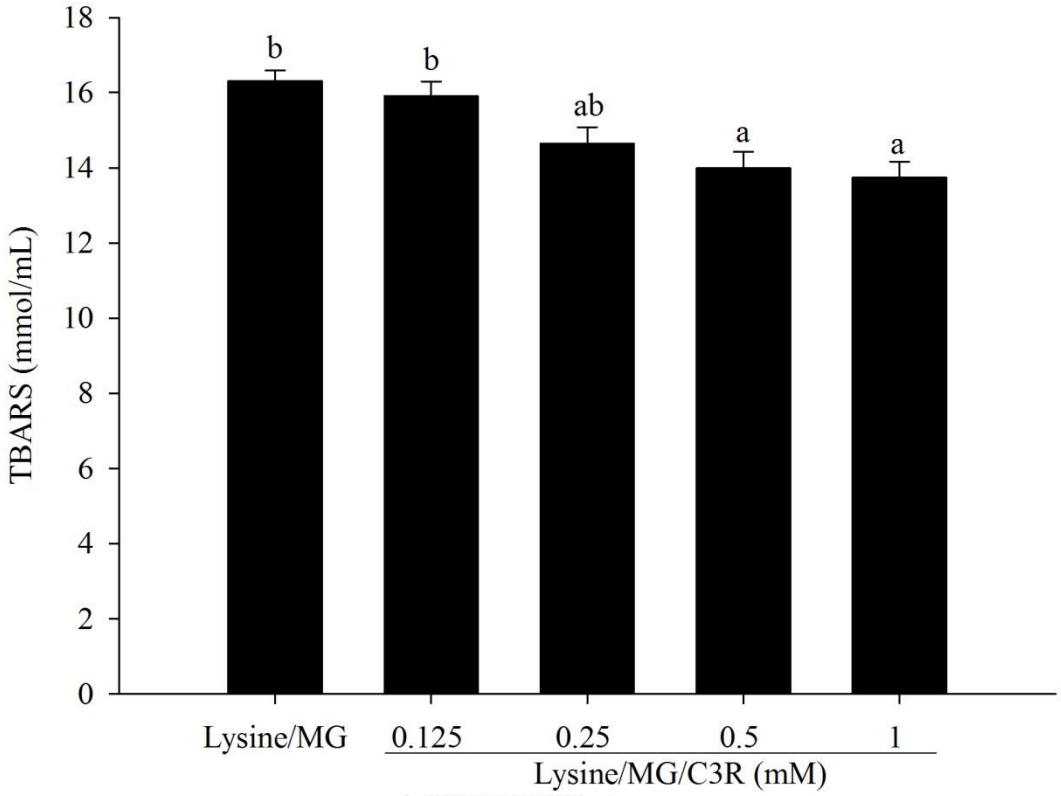

Figure 51 The effects of cyanidin-3-rutinoside (C3R) modulating the production of hydroxyl radicals in lysine/methylglyoxal (MG)-induced glycation.

The results are presented as mean ± SEM (*n*=3). Groups without a common letter are significant difference ($p<0.05$).

4.3 The effect of cyanidin-3-rutinoside (C3R) on methylglyoxal (MG)-mediated vascular abnormalities in isolated vascular preparation

4.3.1 Direct vascular relaxation effect of C3R in thoracic aorta

- **Vascular relaxation**

The relaxation response curve demonstrated that C3R began to dilate the vessel at 1 nM for endothelial-intact and at 0.3 μM for endothelial-denuded aorta (p<0.05). The vessel reached the maximum relaxation rate at 91.6±4.2% (EC_{50}=2.43±0.57 μM) and 90.5±4.5% (EC_{50}=2.56±0.65 μM) in the aorta with and without endothelium, respectively (Figure 52). The low concentration range of C3R (1-100 nM) showed endothelium-dependent vasodilation effect in endothelial-intact ring which was attenuated when endothelium was removed in endothelial-denuded ring. Treatment with NOLA (eNOS inhibitor) reduced vasodilation effect of C3R by increasing EC_{50} of C3R from 2.43±0.57 μM in untreated rings to 9.25±2.60 μM in NOLA-treated rings (p<0.05). The vessel relaxing mediated by C3R was attenuated at the concentration of 3 μM in NOLA-treated rings, but there are no differences for the maximum relaxation rate.

- **Endothelial nitric oxide synthase (eNOS) mRNA expression**

The C3R induced eNOS mRNA expression in isolated thoracic aorta as shown in figure 53. There were no significant differences observed in the aorta incubated with C3R at concentration 3 μM for 30 min incubation, while a higher concentration of C3R at 10 μM significantly increased eNOS mRNA expression by 1.3-fold when compared to control. The longer incubation time (30 min to 24 hours) caused a marked increase in eNOS mRNA expression by C3R (p<0.05). It was noted that C3R (3 μM) significantly caused eNOS mRNA expression as compared to control.

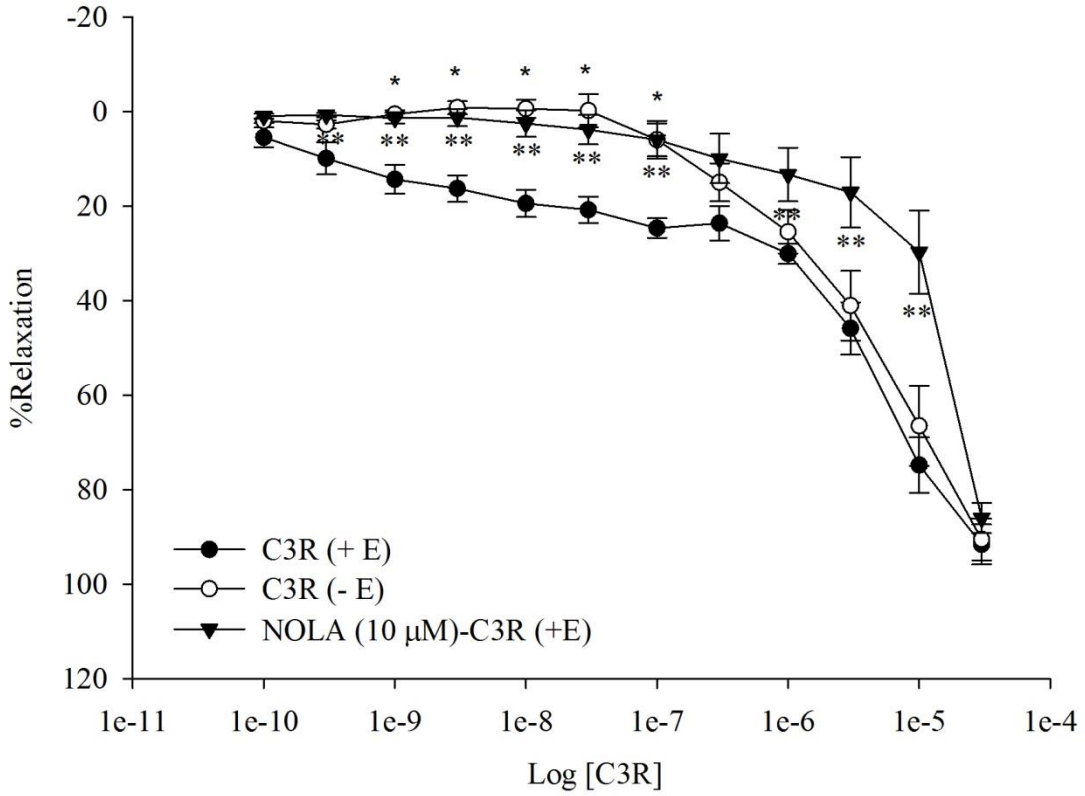

Figure 52 The cumulative concentration response curve of cyanidin-3-rutinoside (C3R) in endothelial-intact (+E) and endothelial-denuded (-E) thoracic aorta isolated from WKY rats.

The results are presented as mean ± SEM (n=6). *p<0.05 is significantly different when compared to +E.

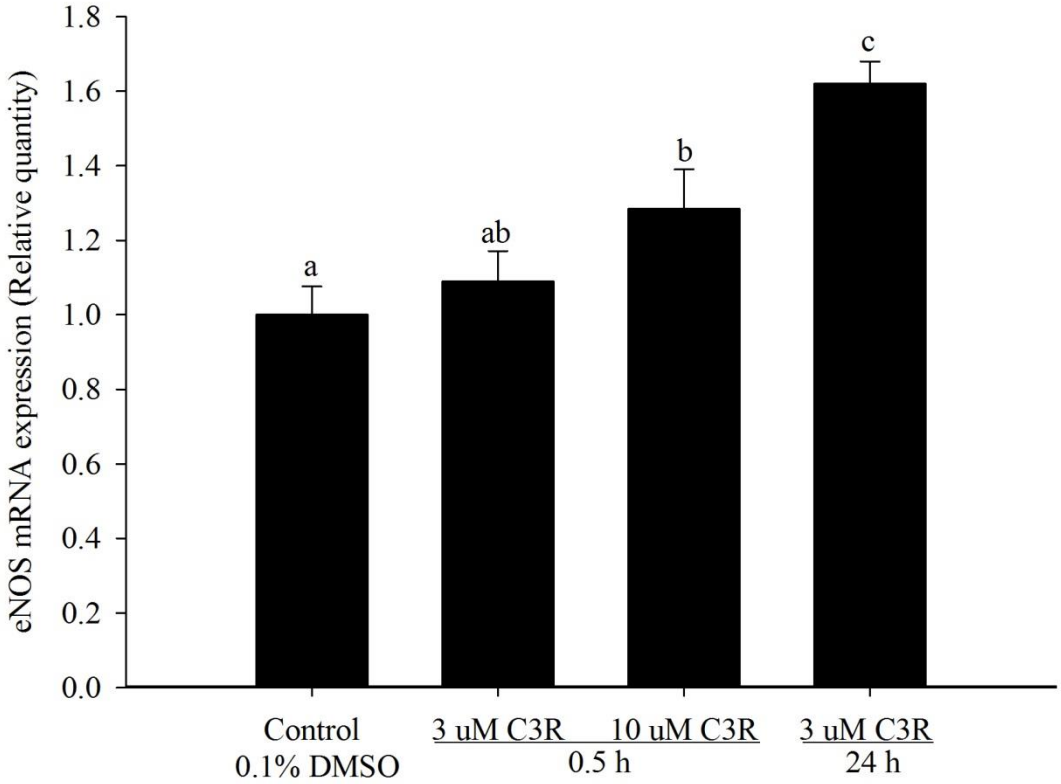

Figure 53 The effect of cyanidin-3-rutinoside (C3R) on endothelial nitric oxide synthase (eNOS) mRNA expression in isolated thoracic aorta from WKY rats after incubation for 0.5 and 24 hours.

The results are presented as mean ± SEM (*n*=6). Groups without a common letter are significant difference ($p<0.05$).

4.3.2 Direct vascular relaxation effect of C3R in mesenteric arterial bed

The vasodilation effects of C3R in the mesenteric vascular bed preparation perfused with noradrenaline EC_{50} are shown in figure 54. Whilst the maximum relaxation effect of C3R reached up to 91.6±4.2% in the aortic rings, the maximal relaxation effect in the mesenteric bed preparation was only 61.3±6.4% (EC_{50} = 25.0±1.26 μM). Incubation with endothelial nitric oxide synthase (eNOS), N^{ω}-nitro-L-arginine (NOLA), to inhibit the production of nitric oxide caused the loss of C3R activity to 32.5±6.32% (p<0.05) at concentration of 10 nM or above.

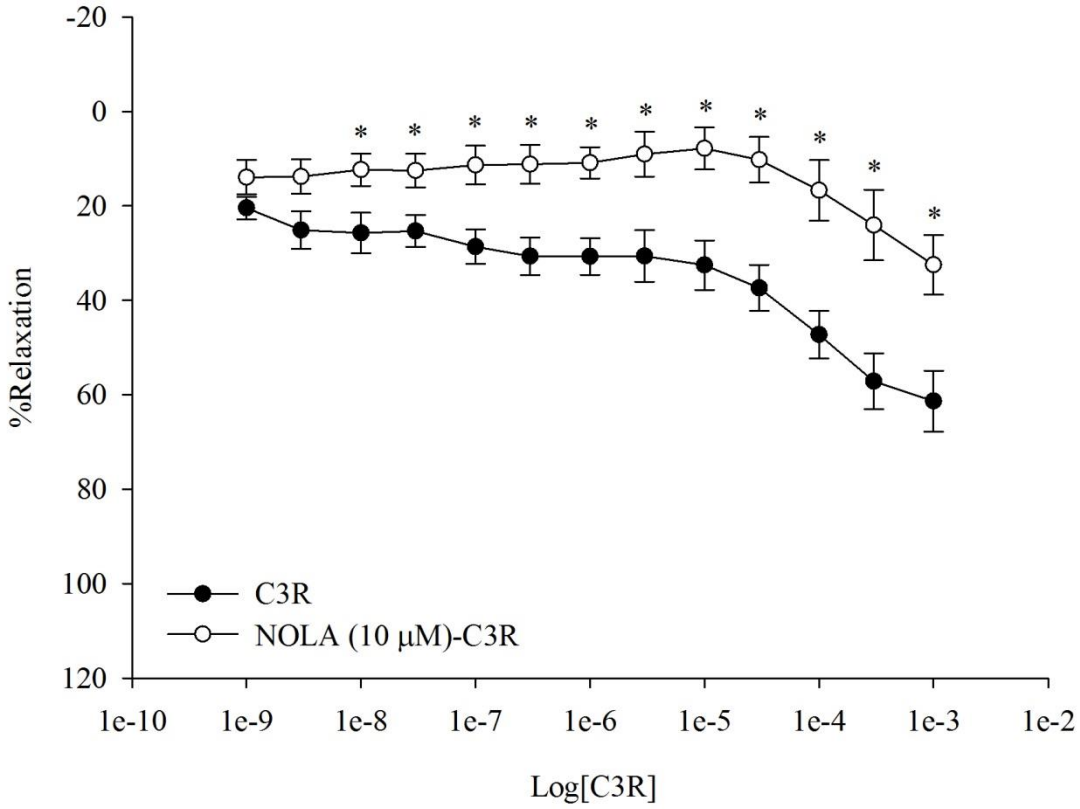

Figure 54 The cumulative concentration response curve of cyanidin-3-rutinoside (C3R) in mesenteric arterial bed isolated from WKY rats with and without endothelial nitric oxide synthase (eNOS) inhibitor, N^{ω}-nitro-L-arginine (NOLA).

The results are presented as mean ± SEM (n=6). *p<0.05 is significantly different when compared to control.

4.3.3 Vascular functions of isolated thoracic aorta after acute methylglyoxal treatment

- **Vascular contraction response to noradrenaline**

Pretreatment of aortic ring with methylglyoxal for 30 min significantly increased contraction response to noradrenaline in endothelial-intact ring when the concentration of noradrenaline at a level 60 nM or above was provided. As shown in figure 55, maximum contraction induced by noradrenaline (600 nM) increased from 100 to 125.1 ± 3.6% in methylglyoxal-treated rings ($p<0.05$) but there were no differences in the level of noradrenaline EC_{50}. Methylglyoxal (500 μM) significantly reduced vascular contraction when co-incubation with C3R (3 μM). The treatment of C3R markedly abolished the contraction response to noradrenaline at concentration 6 nM or higher and changed the noradrenaline EC_{50} from 7.91±1.02 nM in methylglyoxal to 12.01±1.54 nM in methylglyoxal/C3R. The maximum contraction in methylglyoxal/C3R treatment was similar to control. However, no significant difference of contraction response to noradrenaline was observed in endothelial-denuded rings when methylglyoxal and methylglyoxal with C3R were treated (figure 56).

- **Vascular relaxation response to acetylcholine**

The relaxation response to acetylcholine was determined in endothelial-intact rings (figure 57). Methylglyoxal (500 μM) significantly impaired acetylcholine-induced endothelium dependent relaxation by increasing EC_{50} of acetylcholine from 4.95±1.01 nM (the control) to 22.12±4.58 nM (methylglyoxal-treated rings). The concentration of acetylcholine for initial relaxation response was observed at 3 nM in the control ring while it was increased to 10 nM in methylglyoxal-treated rings. As similar to control, the presence of C3R (3 μM) markedly prevented methylglyoxal-

impaired relaxation (p<0.05). However, the maximum relaxation was not affected by all treatments.

- **Vascular relaxation response to sodium nitroprusside**

The endothelium-independent relaxation in aortic ring was determined by cumulative concentration response to sodium nitroprusside in both endothelial-intact and –denuded ring (figure 58). In endothelial-intact ring, methylglyoxal increased sodium nitroprusside-induced relaxation at concentration 0.5 nM or above by shifting the concentration response curve to the left and markedly decreasing the sodium nitroprusside EC_{50} from 1.59±0.33 nM (the control) to 0.69±0.12 nM (methylglyoxal-treated rings). The lower EC_{50} value of sodium nitroprussode represented the higher portent to induce relaxation in methylglyoxal-treated rings. The enhancing effect of methylglyoxal on sodium nitroprusside-induced relaxation was reversed as similar to control when 3 μM C3R was co-incubated (p<0.05). The maximum relaxation was observed at the concentration of 10 nM sodium nitroprusside or above for methylglyoxal-treated ring while the higher concentration of sodium nitroprusside (50 nM or greater) was used to induced maximum relaxation in the control and methylglyoxal/C3R rings. However, all treatments did not affect to alter the maximal relaxation to sodium nitroprusside.

In endothelial-denuded ring, methylglyoxal significantly increased the relaxation response to sodium nitroprusside (0.5 nM) when compared to control (figure 59). Treatment with C3R prevented the enhancing effect of methylglyoxal on vasorelaxation response to sodium nitroprusside, but the maximal relaxation and sodium nitroprusside EC_{50} were not changed by the treatments.

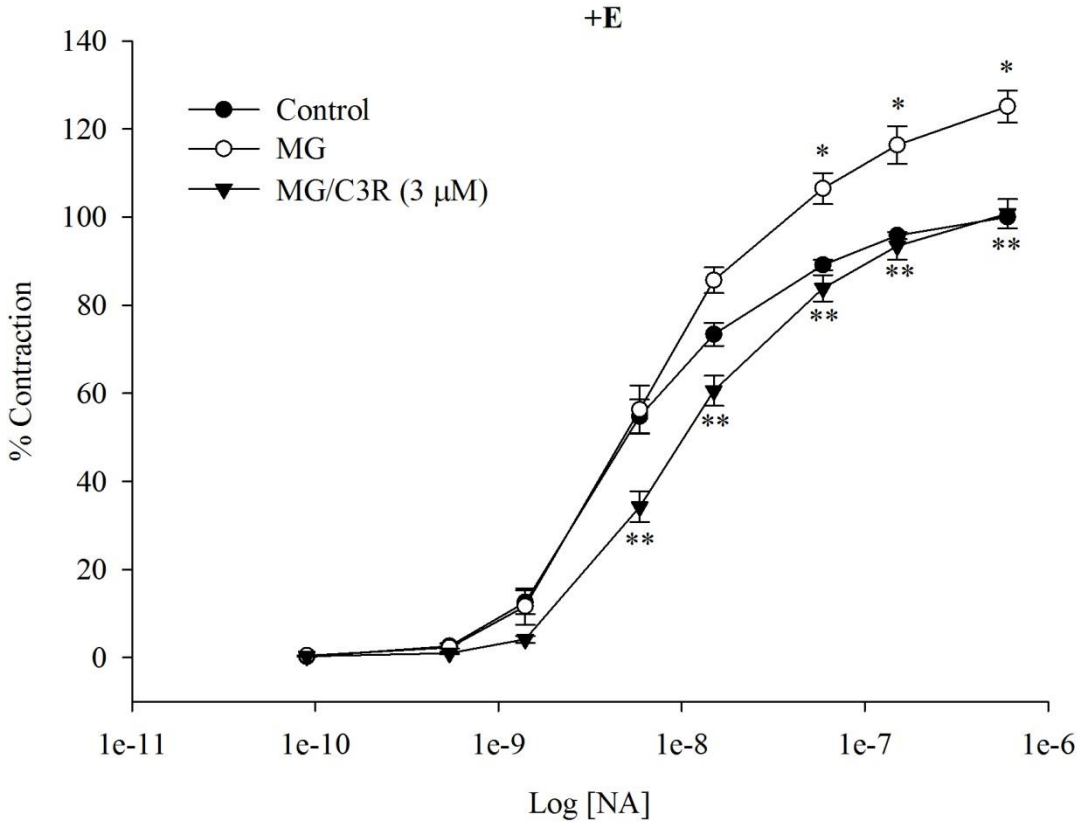

Figure 55 The effect of cyanidin-3-rutinoside (C3R) on the cumulative concentration response curve of noradrenaline (NA) in endothelial-intact (+E) thoracic aorta isolated from WKY rats after incubation with 0.1% DMSO as control, methylglyoxal (MG; 500 μM) and MG/C3R (3 μM) for 30 min.

The results are presented as mean ± SEM (*n*=6). **p*<0.05 compared to control and ***p*<0.05 compared to MG.

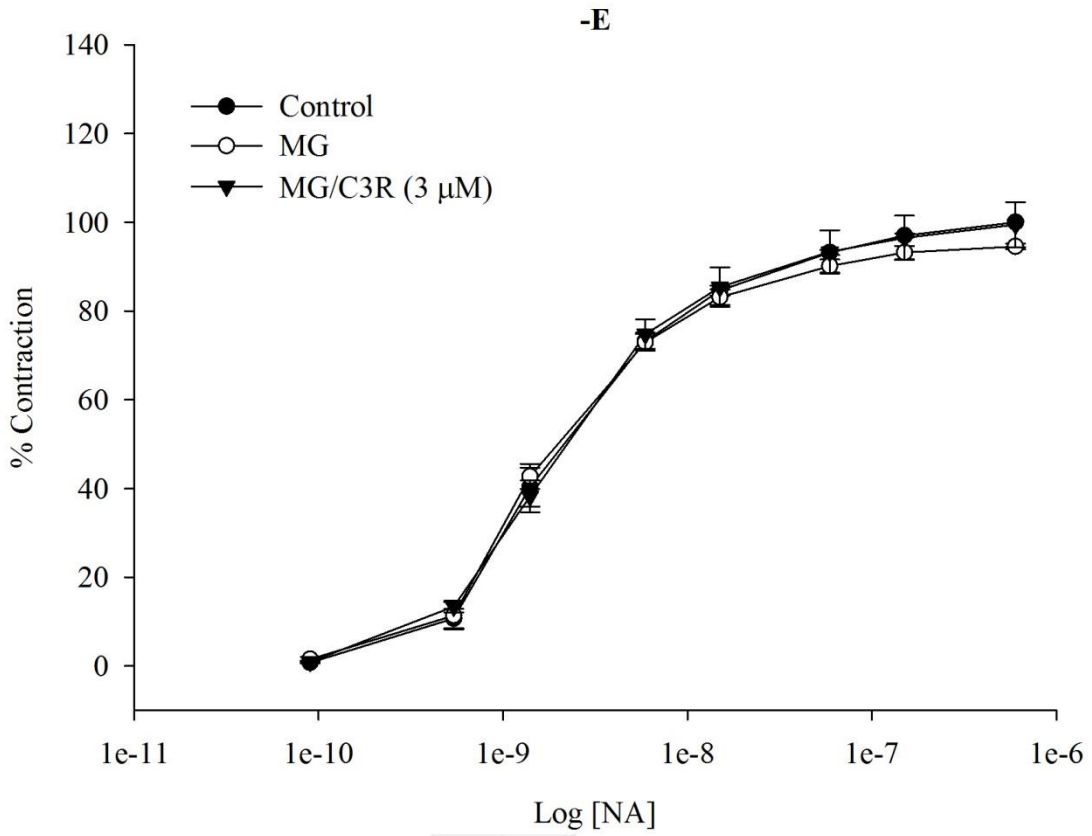

Figure 56 The effect of cyanidin-3-rutinoside (C3R) on the cumulative concentration response curve of noradrenaline (NA) in endothelial-denuded (-E) thoracic aorta isolated from WKY rats after incubation with 0.1% DMSO as control, methylglyoxal (MG; 500 μM) and MG/C3R (3 μM) for 30 min.

The results are presented as mean ± SEM (*n*=6).

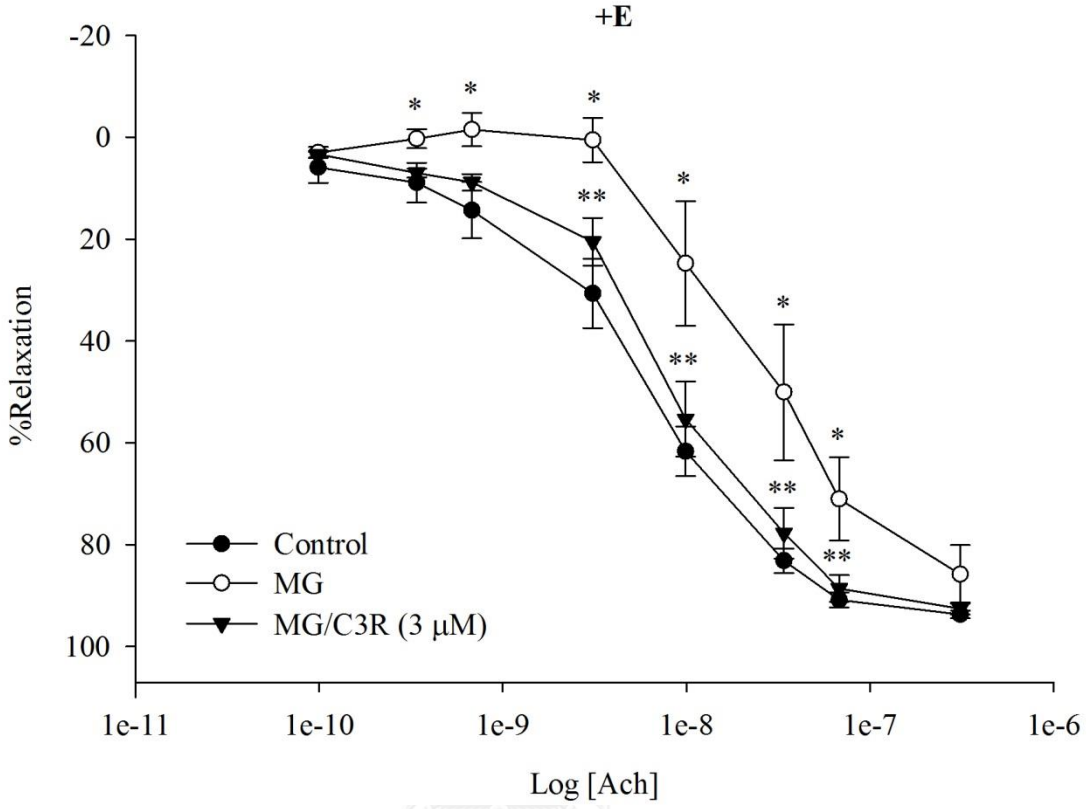

Figure 57 The effect of cyanidin-3-rutinoside (C3R) on the cumulative concentration response curve of acetylcholine (Ach) in endothelial-intact (+E) thoracic aorta isolated from WKY rats after incubation with 0.1% DMSO as control, methylglyoxal (MG; 500 μM) and MG/C3R (3 μM) for 30 min.

The results are presented as mean ± SEM (n=6). *p<0.05 compared to control and **p<0.05 compared to MG.

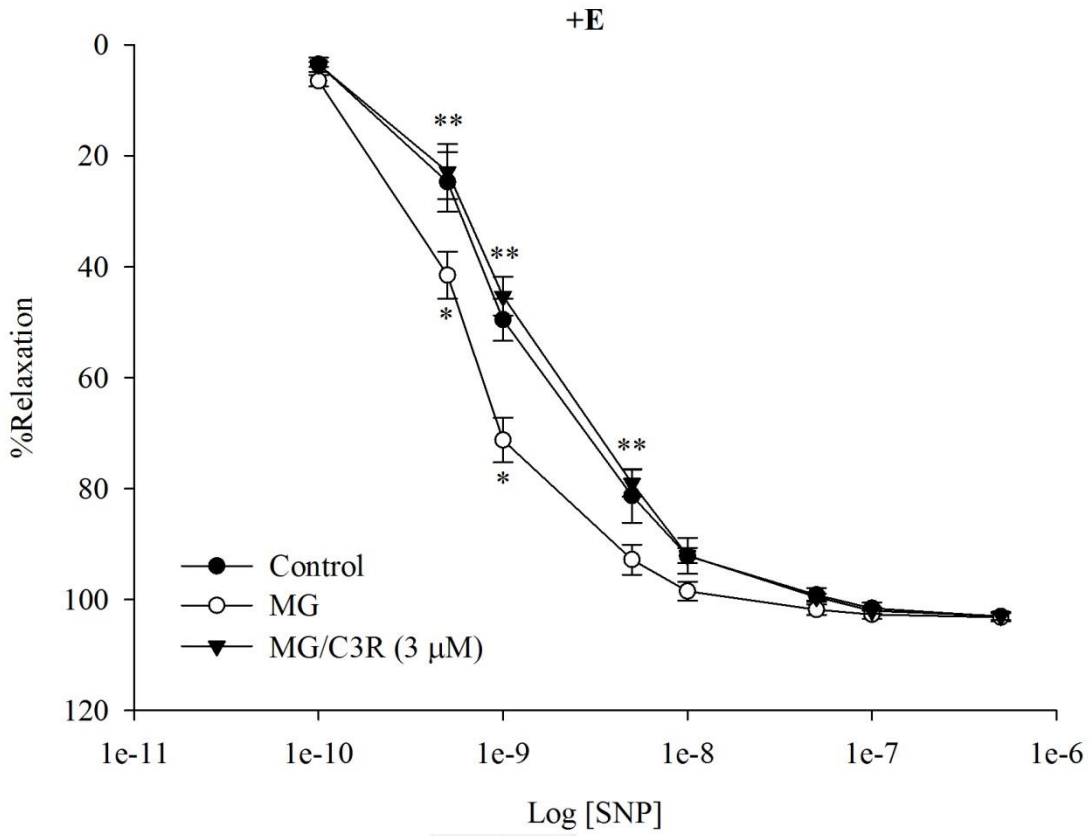

Figure 58 The effect of cyanidin-3-rutinoside (C3R) on the cumulative concentration response curve of sodium nitroprusside (SNP) in endothelial-intact (+E) thoracic aorta isolated from WKY rats after incubation with 0.1% DMSO as control, methylglyoxal (MG; 500 µM) and MG/C3R (3 µM) for 30 min.

The results are presented as mean ± SEM (n=6). *p<0.05 compared to control and **p<0.05 compared to MG.

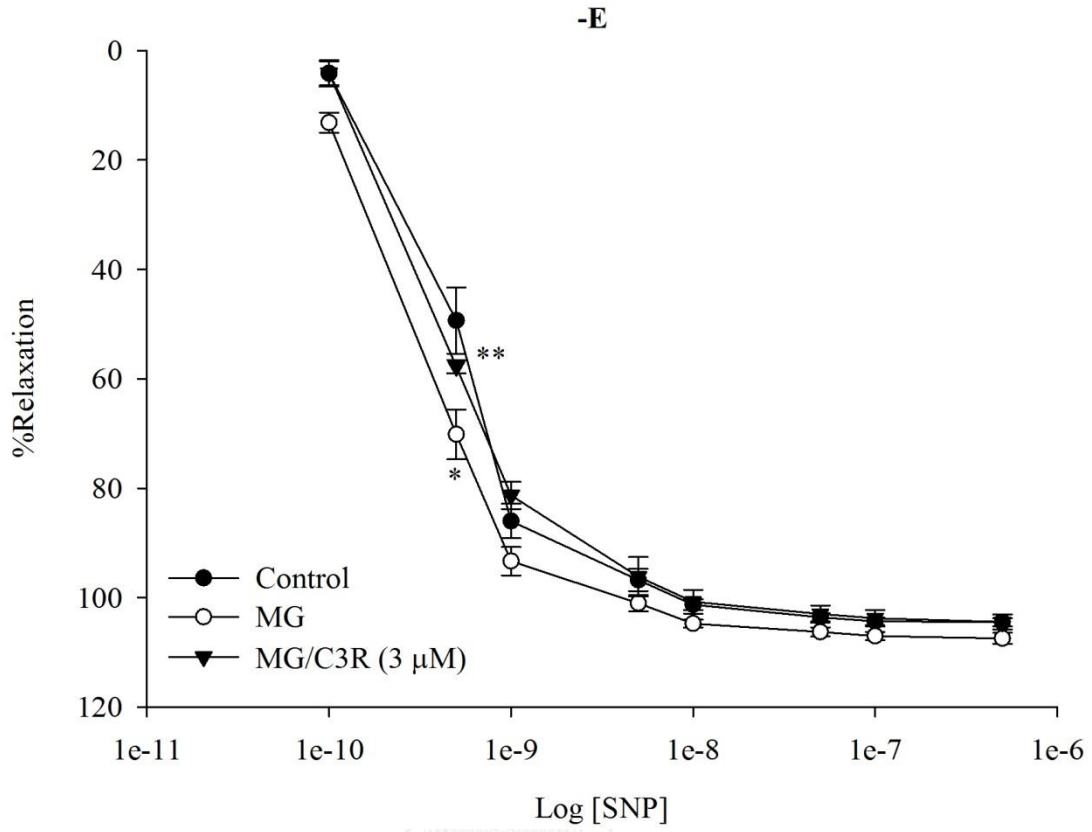

Figure 59 The effect of cyanidin-3-rutinoside (C3R) on the cumulative concentration response curve of sodium nitroprusside (SNP) in endothelial-denuded (-E) thoracic aorta isolated from WKY rats after incubation with 0.1% DMSO as control, methylglyoxal (MG; 500 µM) and MG/C3R (3 µM) for 30 min.

The results are presented as mean ± SEM (*n*=6). **p*<0.05 compared to control and ***p*<0.05 compared to MG.

4.3.4 Vascular functions of mesenteric arterial bed after acute perfusion of methylglyoxal

- **Vascular contraction response to noradrenaline**

After 30 min of perfusion of methylglyoxal to mesenteric vascular bed, there was significant reduction of noradrenaline-induced vasoconstriction at the concentration of 30 μM noradrenaline or above (figure 60). In addition, maximum contraction in response to noradrenaline was decreased from 100 to 85.3±5.6% but there was no difference change in the EC_{50} of noradrenaline. When C3R (3 μM) was added into the perfusate together with methylglyoxal, the impairment of vascular contraction was restored at noradrenaline concentration 30 μM or higher (p<0.05). C3R caused the change of maximum contraction to 119.5±2.0% but it was not altered the EC_{50} of noradrenaline.

- **Vascular relaxation response to acetylcholine**

The effects of methylglyoxal and together with C3R on the relaxation response to acetylcholine isolated mesenteric arterial bed are shown in figure 61. The endothelium dependent relaxation response to acetylcholine (20 nM or above) was significantly decreased when methylglyoxal was treated. The maximum relaxation in response to 2 μM acetylcholine was attenuated from 89.2 ± 2.1% to 79.8 ± 2.3% (p<0.05). The presence of C3R markedly prevented methylglyoxal-impaired the relaxation to acetylcholine at concentration 10 nM or greater. The increasing maximum response by C3R was 86.5 ± 1.2% when C3R was incubated with methylglyoxal without the change in the EC_{50} of acetylcholine (p<0.05).

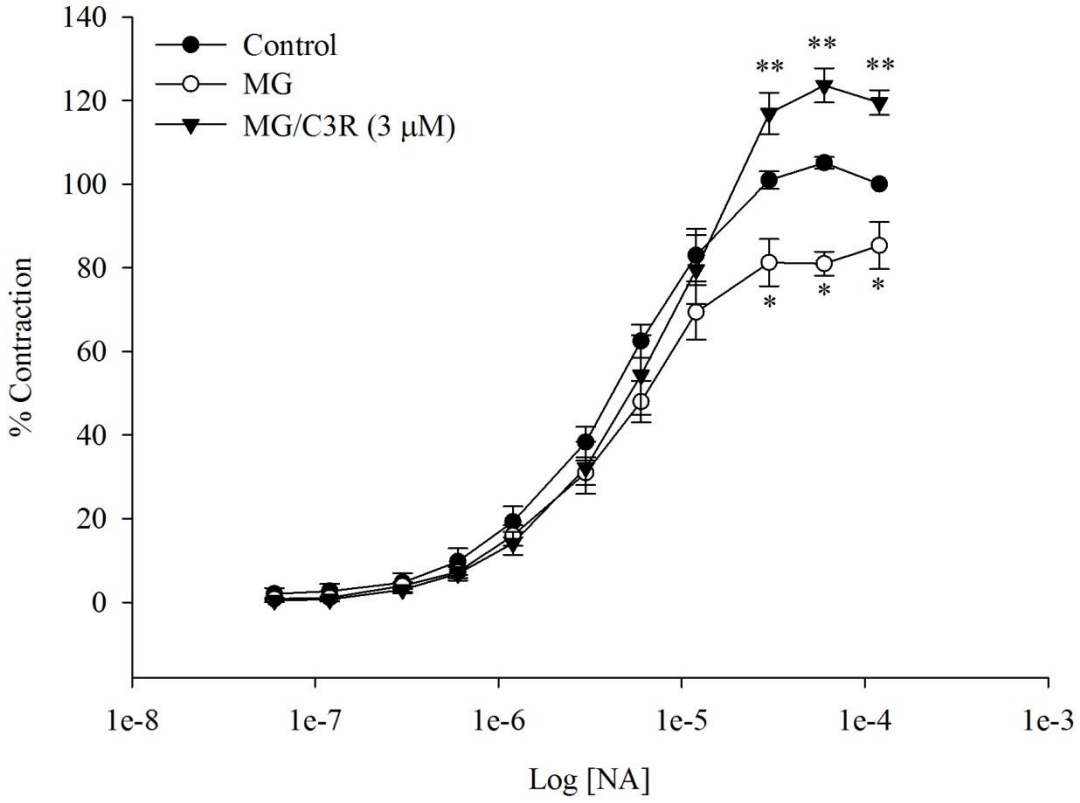

Figure 60 The effect of cyanidin-3-rutinoside (C3R) on the cumulative concentration response curve of noradrenaline (NA) in mesenteric arterial bed isolated from WKY rats after perfused with 0.1% DMSO as control, methylglyoxal (MG; 500 μM) and MG/C3R (3 μM) for 30 min.

The results are presented as mean ± SEM (n=6). *p<0.05 compared to control and **p<0.05 compared to MG.

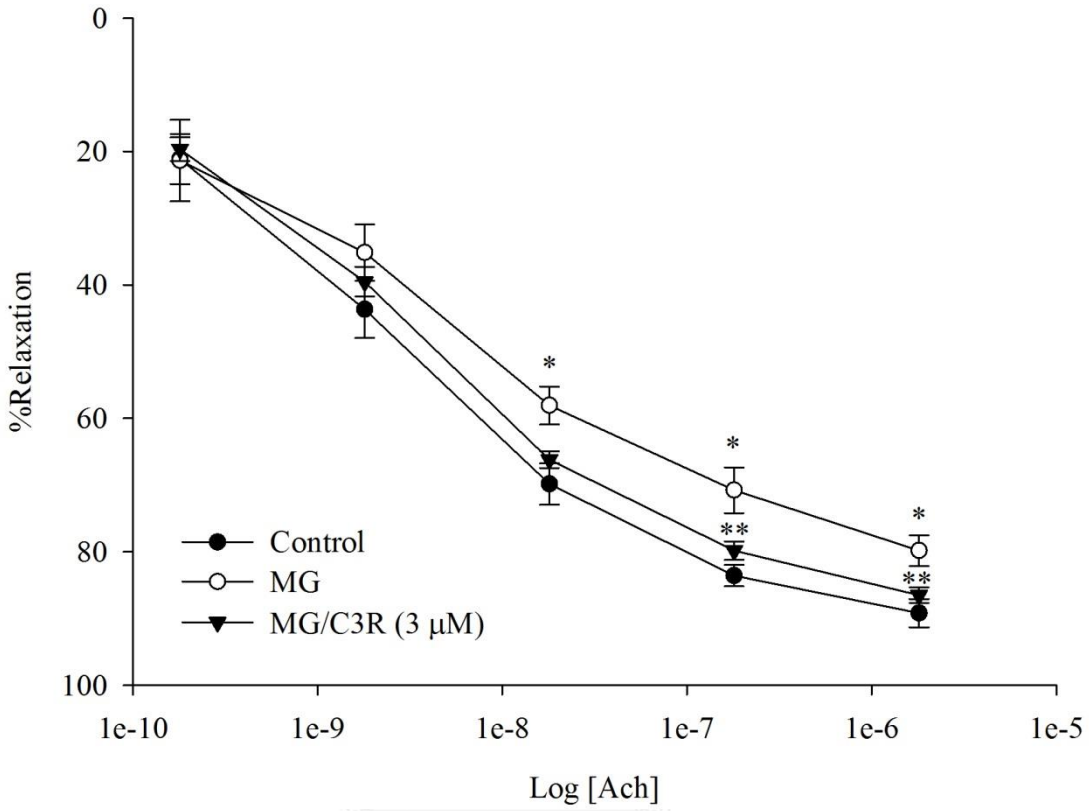

Figure 61 The effect of cyanidin-3-rutinoside (C3R) on the cumulative concentration response curve of acetylcholine (Ach) in mesenteric arterial bed isolated from WKY rats after perfused with 0.1% DMSO as control, methylglyoxal (MG; 500 µM) and MG/C3R (3 µM) for 30 min.

The results are presented as mean ± SEM (n=6). *p<0.05 compared to control and **p<0.05 compared to MG.

4.4 The effect of cyanidin-3-rutinoside (C3R) on alleviating vascular abnormalities in methylglyoxal-treated rats.

4.4.1 Biochemical parameters

No significant differences were observed in the body weight between control and methylglyoxal groups (table 13). The 9% weight loss was observed in the rats treated with methylglyoxal/C3R (30 and 100 mg/kg/day) at the end of treatment when compared to control groups. The level of BUN and creatinine were not changed in methylglyoxal group but it increased in methylglyoxal/C3R groups when compared to control group ($p<0.05$). However, the level of parameter for the kidney function test of all groups was still in the normal range. In addition to kidney function, the treatments both methylglyoxal and methylglyoxal with C3R was not caused damage to liver function as represented by liver enzymes test. No significant differences were observed in the level of AST and ALT all treatment groups.

Table 13 Body weight, kidney and liver function parameters in methylglyoxal (MG)-treated rats at the end of the study periods (8 weeks)

Parameters	Control	MG	MG/C3R (30 mg/kg/day)	MG/C3R (100 mg/kg/day)
Body weight (g)	415.5 ± 8.3^{b}	396.0 ± 7.2^{a}	377.7 ± 8.3^{a}	375.9 ± 8.0^{a}
BUN (mmol/L)	7.23 ± 0.15^{ab}	6.93 ± 0.20^{a}	7.30 ± 0.23^{ab}	7.64 ± 0.27^{b}
Creatinine(mmol/L)	35.00 ± 1.22^{ab}	33.37 ± 1.04^{a}	37.51 ± 0.92^{bc}	38.83 ± 1.36^{c}
ALT (U/L)	32.09 ± 0.83^{a}	31.32 ± 1.41^{a}	33.29 ± 2.28^{a}	28.27 ± 1.39^{a}
AST (U/L)	85.89 ± 3.94^{a}	79.12 ± 2.66^{a}	88.67 ± 4.47^{a}	80.53 ± 3.04^{a}
Glucose (mg/dL)	141.31 ± 5.58^{a}	151.85 ± 3.18^{ab}	146.29 ± 7.56^{a}	165.09 ± 4.43^{a}

C3R: Cyanidin-3-Rutinoside; BUN: Blood Urea Nitrogen; ALT: Alanine Aminotransferase; AST: Aspartate Aminotransferase. The results are presented as mean ± SEM (n=6). Groups without a common letter are significant difference (p<0.05).

4.4.2 The concentration of methylglyoxal in plasma and tissues

As shown in table 14, the treatment of methylglyoxal (60-120 mg/kg/day) for 8 weeks caused 1.2-fold increase in plasma methylglyoxal concentration (the control group= 10.02±0.17 μM and methylglyoxal groups = 11.66±0.18 μM). The elevation of plasma methylglyoxal concentration was decreased in methylglyoxal-treated rats when C3R was treated at concentration 30 and 100 mg/kg/day. The plasma methylglyoxal concentrations of C3R groups were 9.72±0.41 and 9.79 ±0.28 μM, respectively. They were similar concentration range to control group. However, there were no significant differences observed in the concentration of methylglyoxal in the kidney and the liver between the different groups.

Table 14 The level of methylglyoxal concentration in plasma, kidney and liver in rats-treated methylglyoxal (MG) at the end of the study periods (8 weeks)

Parameters	Control	MG	MG/C3R (30 mg/kg/day)	MG/C3R (100 mg/kg/day)
Plasma MG (μM)	10.02 ± 0.17[a]	11.66 ± 0.18[b]	9.76 ± 0.41[a]	9.79 ± 0.28[a]
Kidney MG (μmol/mg protein)	171.06 ± 9.56[a]	194.77 ± 10.16[a]	188.47 ± 13.09[a]	177.17 ± 9.54[a]
Liver MG (μmol/mg protein)	186.73 ± 16.57[a]	170.13 ± 6.65[a]	195.69 ± 8.68[a]	186.98 ± 13.71[a]

C3R: Cyanidin-3-Rutinoside. The results are presented as mean ± SEM (n=6). Groups without a common letter are significant difference (p<0.05).

4.4.3 Glyoxalase I (GLO1) mRNA expression in aorta

The mRNA expression of GLO1 in aortic tissues is shown in figure 62. Methylglyoxal did not alter the mRNA expression of GLO1 in methylglyoxal group when compared with the control group. In addition, the rats treated with methylglyoxal plus C3R (100 mg/kg/day) trended to increase GLO1 mRNA expression compared to methylglyoxal group.

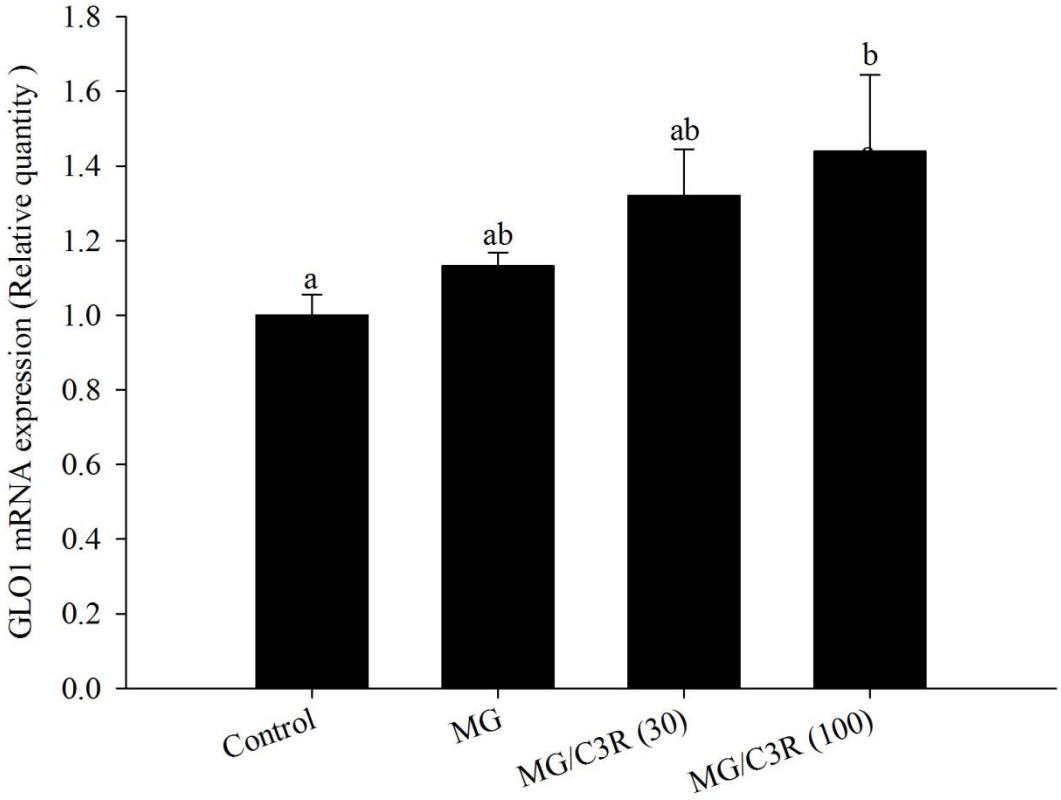

Figure 62 Glyoxalase I (GLO1) mRNA expression of aorta in methylglyoxal (MG)-treated WKY rats.

Groups of 12 weeks old male WKY rats were treated for 8 weeks with MG (60-120 mg/day) in vehicle. Cyanidin-3-rutinoside (C3R; 30 and 100 mg/kg/day) were used as supplementation. The results are presented as mean ± SEM (n=6). Groups without a common letter are significant difference (p<0.05).

4.4.4 N^{ε}-(carboxymethyl)lysine (N^{ε}-CML) level in thoracic aorta

The accumulation of N^{ε}-CML in aortic tissue is shown in figure 63. After 8 weeks of methyglyoxal treatment (60-120 mg/kg/day), N^{ε}-CML level significantly increased in aortic tissue of methylglyoxal-treated rats by 1.7-fold when compared to control. Methylglyoxal supplemented with C3R significantly reduced N^{ε}-CML accumulation in vessel as concentration dependent manner. The reduction of N^{ε}-CML level in methylglyoxal plus C3R at 30 and 100 mg/kg/day was demonstrated by 59% and 69%, respectively.

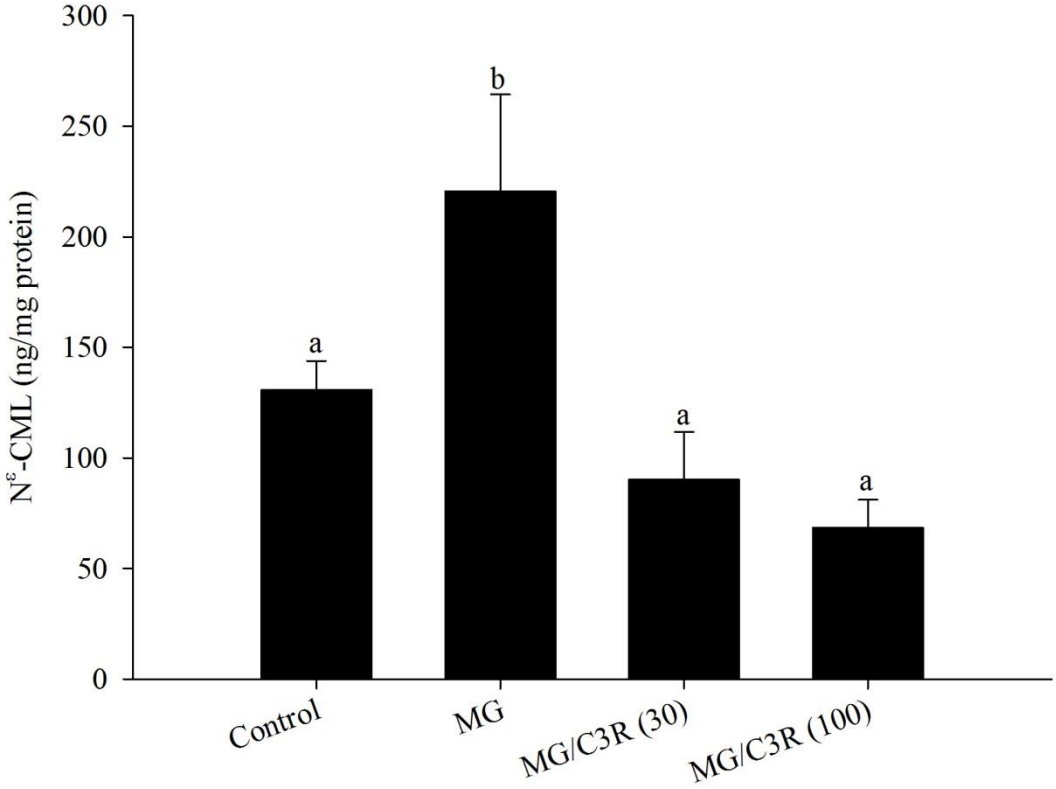

Figure 63 The level of N^{ε}-(carboxymethyl)lysine (N^{ε}-CML) in of aorta in methylglyoxal (MG)-treated WKY rats.

Groups of 12 weeks old male WKY rats were treated for 8 weeks with MG (60-120 mg/day) in vehicle. Cyanidin-3-rutinoside (C3R; 30 and 100 mg/kg/day) were used as supplementation. The results are presented as mean ± SEM (*n*=6). Groups without a common letter are significant difference ($p<0.05$).

4.4.5 Vascular functions of isolated thoracic aorta

- **Vascular contraction response to noradrenaline**

The aortic ring preparation from methylglyoxal-treated rats significantly decreased contraction response to noradrenaline in endothelial-intact ring when the concentration of noradrenaline at a level 1.5 nM or above was provided. As shown in figure 64, maximum contraction induced by noradrenaline (600 nM) was decreased from 100 to 94.3±2.1% in methylglyoxal group whereas the level of noradrenaline EC_{50} was increased from 6.64±0.54 nM in control group to 9.64±1.25 nM in methylglyoxal group ($p<0.05$). Treatment of methylglyoxal impaired contraction was significantly prevented when co-treatment with C3R (30 and 100 mg/kg/day). C3R prevented the inhibitory effect of methylglyoxal on contraction response to noradrenaline at concentration 6 nM or higher and changed the noradrenaline EC_{50} from 9.64±1.25 nM in methylglyoxal group to 5.97±0.71 nM in methylglyoxal/C3R (30 mg/kg/day) and 6.23±0.73 nM in methylglyoxal/C3R (100 mg/kg/day) The noradrenaline EC_{50} and maximum contraction in methylglyoxal/C3R treatment were similar to control group. However, no significant difference of contraction response to noradrenaline was observed in endothelial-denuded rings isolated from methylglyoxal-treated rats when compared to control group (figure 65).

- **Vascular relaxation response to acetylcholine**

The relaxation response to acetylcholine was determined in endothelial-intact rings isolated from all treatment groups (figure 66). Methylglyoxal-treated rats significantly impaired of acetylcholine-induced endothelium-dependent relaxation when the concentration of actylcholine at concentration 68 nM or higher was provided. The maximum relaxation was decreased from 94.3±1.2% (control group) to 87.4±1.7% (methylglyoxa-treated rats). As similar to control, methylglyoxal

supplemented with C3R (30 and 100 mg/kg/day) markedly improved the relaxation response to acetylcholine at concentration 68 nM or above. The maximum contraction in methylglyoxal/C3R treatment was similar to control group. The acetylcholine EC_{50} was no difference in all treatment groups.

- **Vascular relaxation response to sodium nitroprusside**

The endothelium-independent relaxation in aortic rings isolated from feeding rats was determined by cumulative concentration response to sodium nitroprusside (figure 67). Methylglyoxal-treated rats increased sensitivity to sodium nitroprusside-induced relaxation at concentration 5 nM or above in endothelial-intact rings. The concentration response curve was shifted to the left and markedly decreasing sodium nitroprusside EC_{50} from 3.07±0.56 nM (control group) to 1.92±0.28 nM (methylglyoxal-treated rats). However, no significant difference of relaxation response to sodium nitroprusside was observed between methylglyoxal group and methylglyoxal/C3R groups (30 and 100 mg/kg/day).

In endothelial-denuded ring, methylglyoxal group significantly increased the relaxation response to sodium nitroprusside at concentration 0.5 nM or above when compared to control group (figure 68). The sodium nitroprusside EC_{50} was reduced from 2.01±0.18 nM in control group to 1.09±0.33 nM methylglyoxal group ($p<0.05$). Treatment of C3R at 30 mg/kg/day significantly prevented the enhancing effect of methylglyoxal on vascular relaxation response to sodium nitroprusside at concentration 0.5-50 nM. The maximal relaxation of all rings was not affected by the treatments.

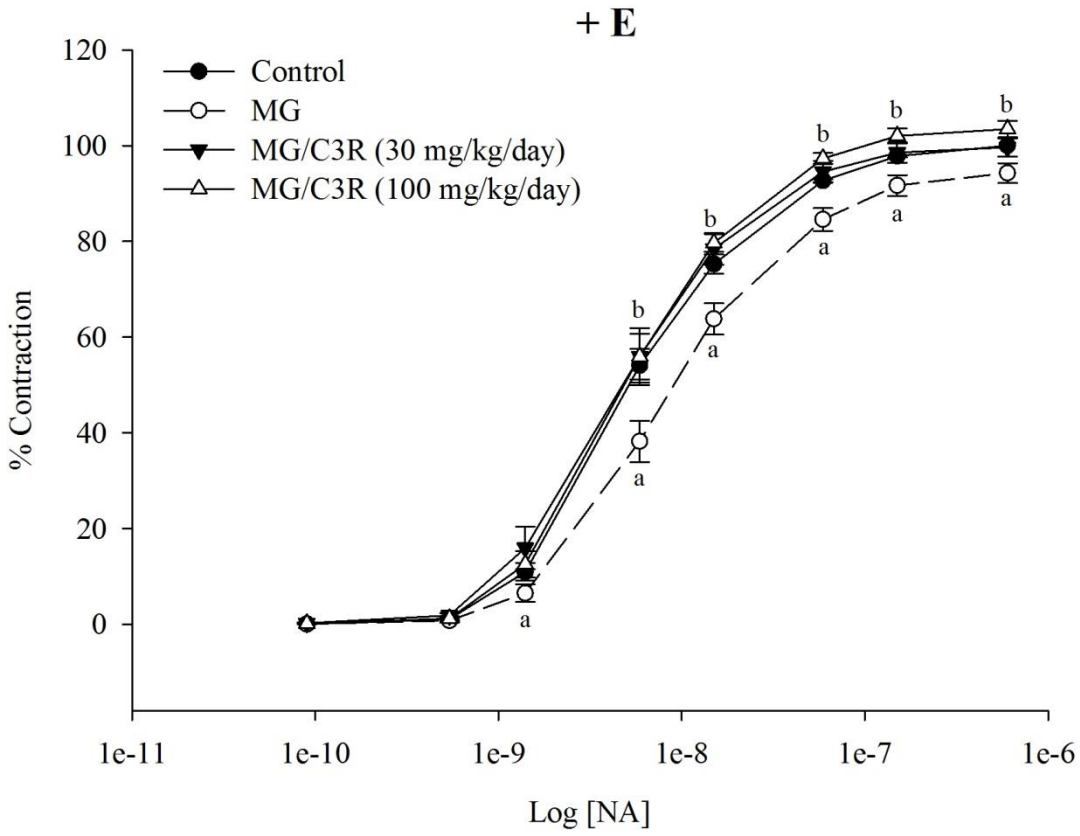

Figure 64 The cumulative concentration response curve of noradrenaline (NA) in endothelial-intact (+E) thoracic aorta isolated from methylglyoxal (MG)-treated WKY rats.

Groups of 12 weeks old male WKY rats were treated for 8 weeks with MG (60-120 mg/day) in vehicle. Cyanidin-3-rutinoside (C3R; 30 and 100 mg/kg/day) were used as supplementation. The results are presented as mean ± SEM (*n*=6). Groups without a common letter are significant difference ($p<0.05$).

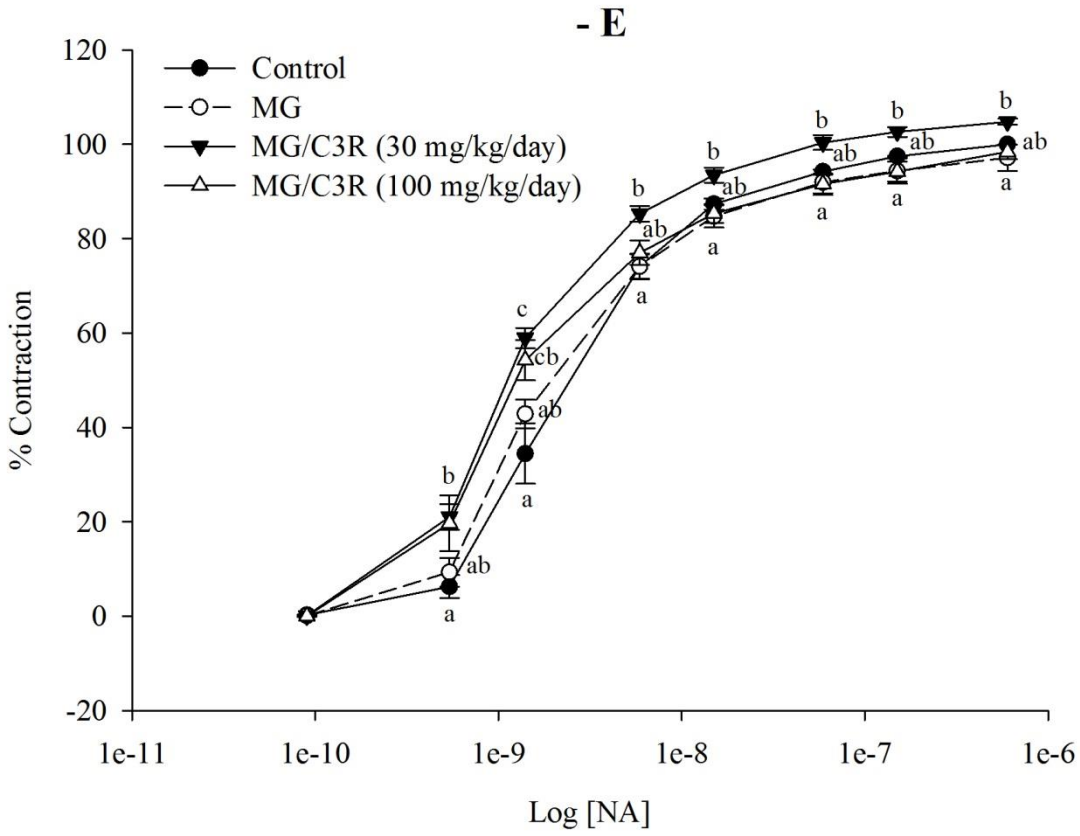

Figure 65 The cumulative concentration response curve of noradrenaline (NA) in endothelial-denuded (-E) thoracic aorta isolated from methylglyoxal (MG)-treated WKY rats.

Groups of 12 weeks old male WKY rats were treated for 8 weeks with MG (60-120 mg/day) in vehicle. Cyanidin-3-rutinoside (C3R; 30 and 100 mg/kg/day) were used as supplementation. The results are presented as mean ± SEM (n=6). Groups without a common letter are significant difference (p<0.05).

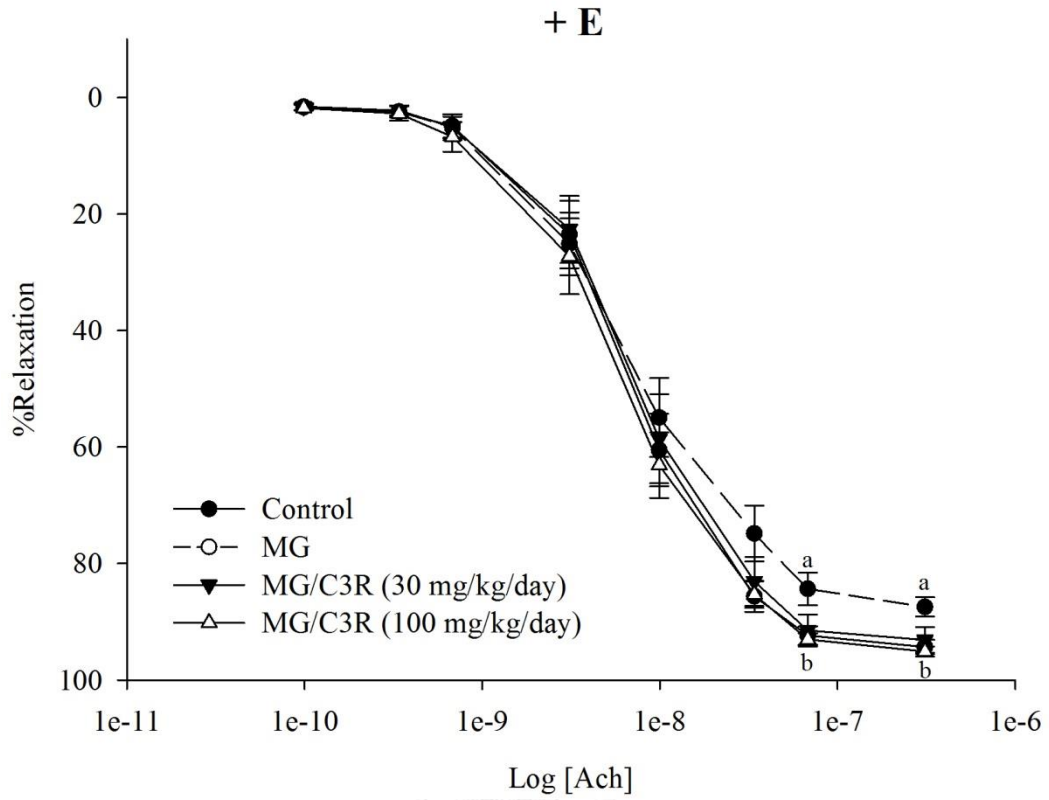

Figure 66 The cumulative concentration response curve of acetylcholine (Ach) in endothelial-intact (+E) thoracic aorta isolated from methylglyoxal (MG)-treated WKY rats.

Groups of 12 weeks old male WKY rats were treated for 8 weeks with MG (60-120 mg/day) in vehicle. Cyanidin-3-rutinoside (C3R; 30 and 100 mg/kg/day) were used as supplementation. The results are presented as mean ± SEM (n=6). Groups without a common letter are significant difference (p<0.05).

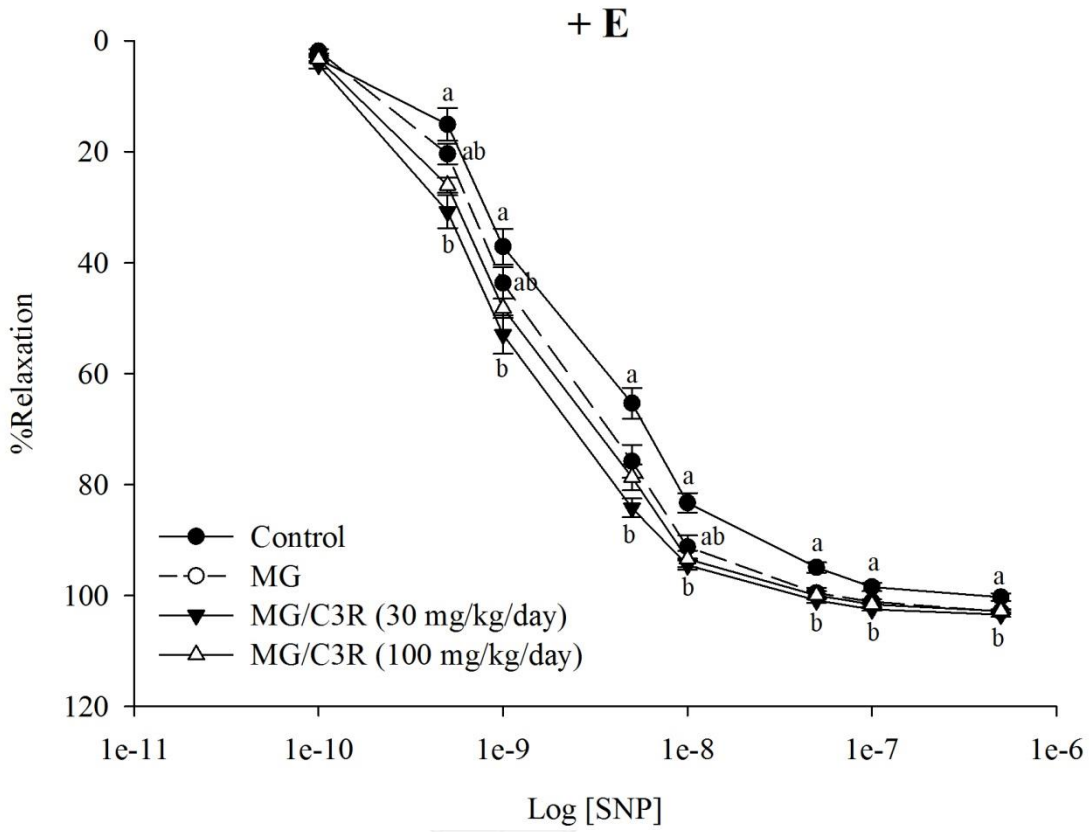

Figure 67 The cumulative concentration response curve of sodium nitroprusside (SNP) in endothelial-intact (+E) thoracic aorta isolated from methylglyoxal (MG)-treated WKY rats.

Groups of 12 weeks old male WKY rats were treated for 8 weeks with MG (60-120 mg/day) in vehicle. Cyanidin-3-rutinoside (C3R; 30 and 100 mg/kg/day) were used as supplementation. The results are presented as mean ± SEM (n=6). Groups without a common letter are significant difference (p<0.05).

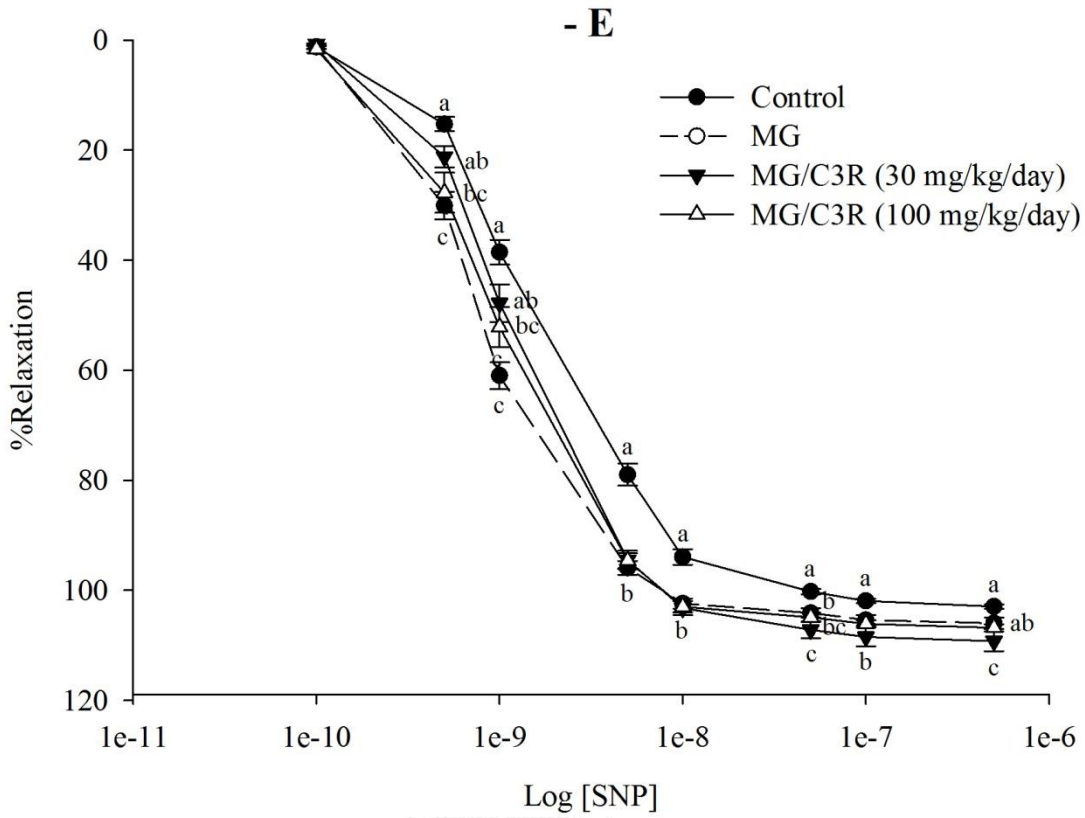

Figure 68 The cumulative concentration response curve of sodium nitroprusside (SNP) in endothelial-denuded (-E) thoracic aorta isolated from methylglyoxal (MG)-treated WKY rats.

Groups of 12 weeks old male WKY rats were treated for 8 weeks with MG (60-120 mg/day) in vehicle. Cyanidin-3-rutinoside (C3R; 30 and 100 mg/kg/day) were used as supplementation. The results are presented as mean ± SEM (n=6). Groups without a common letter are significant difference (p<0.05).

4.4.6 Vascular functions of isolated mesenteric arterial bed

- **Vascular contraction response to noradrenaline**

The mesenteric arterial bed preparation isolated from methylglyoxal-treated rats significantly decreased noradrenaline-induced contraction at concentration 15-60 μM (figure 69) but there were no differences in the maximum contraction and the level of noradrenaline EC_{50}. The impairment of vascular contraction was restored when methylglyoxal plus C3R (30 and 100 mg/kg/day) was treated. The treatment of C3R markedly increased the contraction response to noradrenaline concentration 1.5 μM or greater ($p<0.05$) and changed the noradrenaline EC_{50} from 9.10±1.48 μM in methylglyoxal group to 2.31±0.07 μM and 3.28±0.77 μM in methylglyoxal/C3R at concentration 30 and 100 mg/kg/day, respectively.

- **Vascular relaxation response to acetylcholine**

The effects of methylglyoxal-treated rat and together with C3R supplementation on relaxation response to acetylcholine in isolated mesenteric arterial bed are shown in figure 70. The endothelium-relaxation response to acetylcholine (0.2 μM or above) was significantly decreased in methylglyoxal-treated rats when compared to control group. The maximum relaxation response at 2 μM acetylcholine was reduced from 80.9±5.2% to 69.8±3.7% ($p<0.05$). Methylglyoxal plus C3R (30 and 100 mg/kg/day) markedly prevented methylglyoxal-impaired the relaxation to acetylcholine at concentration 0.2 μM or greater. The increasing maximum response by C3R (30 and 100 mg/kg/day) was 86.9±3.1% and 86.7±1.7% when treated together with methylglyoxal without the change in the EC_{50} of acetylcholine (figure 4.54).

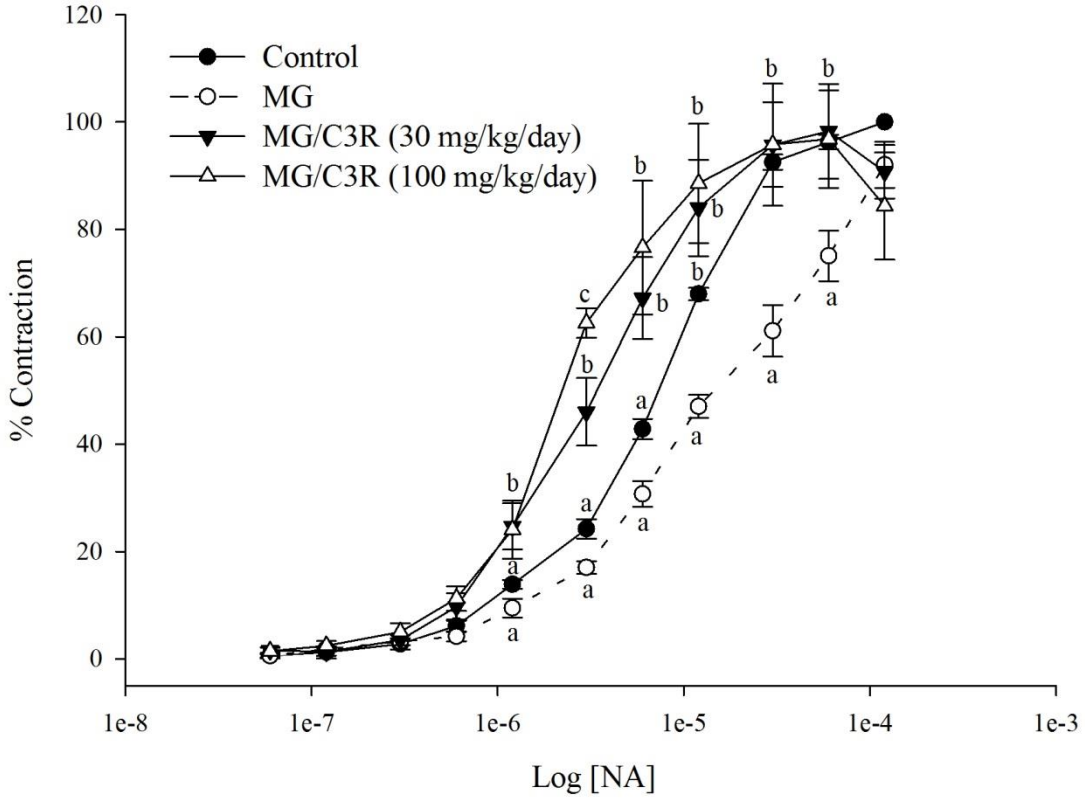

Figure 69 The cumulative concentration response curve of noradrenaline (NA) in mesenteric arterial bed isolated from methylglyoxal (MG)-treated WKY rats.

Groups of 12 weeks old male WKY rats were treated for 8 weeks with MG (60-120 mg/day) in vehicle. Cyanidin-3-rutinoside (C3R; 30 and 100 mg/kg/day) were used as supplementation. The results are presented as mean ± SEM (n=6). Groups without a common letter are significant difference (p<0.05).

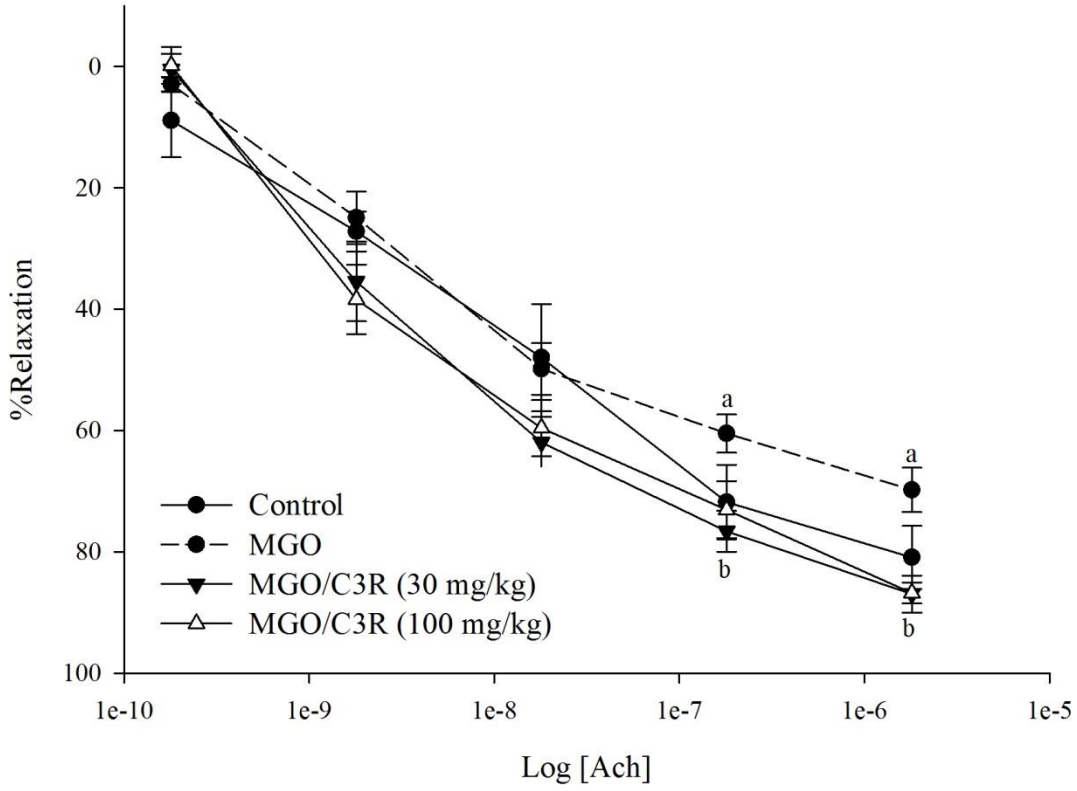

Figure 70 The cumulative concentration response curve of acetylcholine (Ach) in mesenteric arterial bed isolated from methylglyoxal (MG)-treated WKY rats.

Groups of 12 weeks old male WKY rats were treated for 8 weeks with MG (60-120 mg/day) in vehicle. Cyanidin-3-rutinoside (C3R; 30 and 100 mg/kg/day) were used as supplementation. The results are presented as mean ± SEM (n=6). Groups without a common letter are significant difference (p<0.05).

4.4.6 Endothelial nitric oxide synthase (eNOS) mRNA expression in aorta

The mRNA expression level of eNOS in aortic tissue from all treatment groups is shown in figure 71. The treatment of methylglyoxal (60-120 mg/kg/day) for 8 weeks caused a decrease in the relative level of eNOS gene expression by 30% when compared to control group. C3R supplementation in methylglyoxal-treated rats (100 mg/kg/day) significantly ameliorated the changes in the mRNA level of eNOS which was similar to control. The enhancing of the relative eNOS mRNA expression in methylglyoxal plus C3R at 30 and 100 mg/kg/day was observed by 13% and 34%, respectively relative to methylglyoxal group.

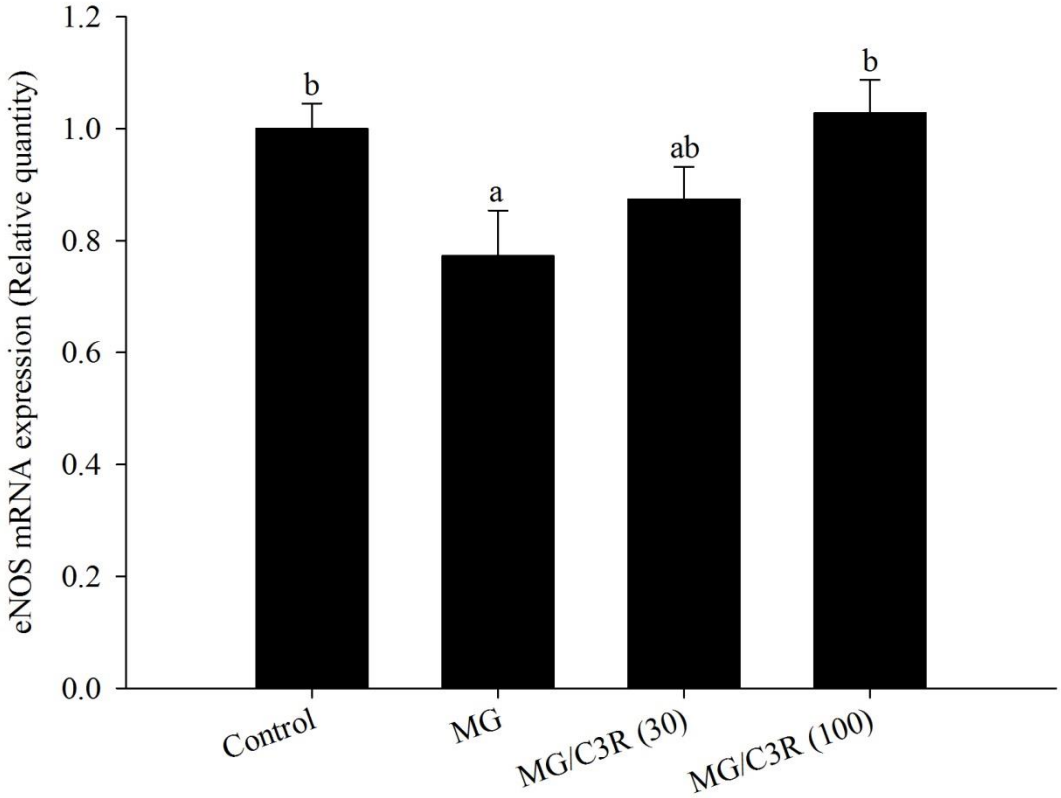

Figure 71 Endothelial nitric oxide synthase (eNOS) mRNA expression of aorta in methylglyoxal (MG)-treated WKY rats.

Groups of 12 weeks old male WKY rats were treated for 8 weeks with MG (60-120 mg/day) in vehicle. Cyanidin-3-rutinoside (C3R; 30 and 100 mg/kg/day) were used as supplementation. The results are presented as mean ± SEM (n=6). Groups without a common letter are significant difference (p<0.05).

CHAPTER V

DISCUSSION

5.1 The effect of C3R on protein glycation in BSA mediated by monosaccharides, including ribose, fructose, glucose and galactose, and reactive dicarbonyl compound, methylglyoxal *in vitro*

The development of macrovascular and microvascular diabetic complications is associated with the formation and accumulation of advanced glycation end products (AGEs) (Jakus and Rietbrock, 2004, Goldin et al., 2006). Chronic consumption of dietary monosaccharides has been associated with accelerating the aging process via the formation of non-enzymatic glycation between the carbonyl group of reducing sugars (glucose, fructose, ribose, and galactose) and the amino group of protein, leading to generate AGEs, commonly described as protein glycation (Ulrich and Cerami, 2001). The present study demonstrated that aldopentose (ribose) was the most effective inducer of protein glycation among other monosaccharides (fructose, galactose and glucose) after 2 weeks of incubation. Our findings are consistent with previous reports suggesting that aldose sugars have higher reactivity than ketose sugars to induce glycated BSA and glycated hemoglobin (Bunn and Higgins, 1981, Syrovy, 1994). This can be explained by the chemical structure of ribose which exists as a more open structure than others. This leads to a puckered conformation, resulting in an unstable structure which easily reacts with the amino group of protein (Wei et al., 2009, Wei et al., 2012).

In addition to reducing sugars, reactive dicarbonyl compounds such as methylglyoxal that generates endogenously via carbohydrate, protein and lipid metabolism and also produces from the amadori product rearrangement, schiff base

oxidation and glyoxidation, can reacts with free amino group of protein to generate AGEs at the late stage of glycation process (Wu et al., 2011). It has been reported that methylglyoxal induced protein glycation with the greater rate than the parent compounds, reducing sugar (Westwood and Thornalley, 1995). The current showed that 1 mM methylglyoxal causes an increased in fluorescent AGEs formation and N-$^{\varepsilon}$-CML at the same rate with galactose at concentration 0.5 M but less than level of AGEs formation induced by 0.1 M ribose and 0.5 M fructose.

Schiff base is generated during the early stage of protein glycation, and spontaneously rearranges to form Amadori product such as Heys rearrangement products or fructoselysine when fructose or glucose are inducer, respectively. The degradation of Amadori product by oxidative and non-oxidative fragmentation causes the formation of AGEs at the late stage of glycation process (Hinton and Ames, 2006). On the other hand, the reaction between diacarbonyl compounds and amino group of protein also produces AGEs without Amadori product formation. The recent findings indicated that ribose induced the greatest level of fructosamine and followed by galactose, glucose and fructose. Studies have shown the higher potent of fructose to induce AGEs formation when compared to glucose in glycated BSA model (Meeprom et al., 2013, Sompong *et al.*, 2013). Therefore, fructose was much more prone to produce Amadori product than glucose. However, in the present study, the level of fructosamine in fructose-glycated BSA is lower than glucose-glycated BSA. This result was consistent with previous studies (Ahmed and Furth, 1992, Sompong et al., 2013) that has explained by the limitation of fructosamine determination assay to detect the different of aldehydic Amadori production from aldose sugar and ketonic Amadori production from ketose sugar. Nitroblue tetrazolium (NBT), a choromogenic compound, commonly used to determine fructosamine, but it has disadvantage to partially react with aldehydic Amadori

product (Ahmed and Furth, 1992). This might be explained the lower level of fructosamine in glycated BSA-mediated by fructose than glucose.

Protein oxidation causes the alteration of protein structure and its biological properties. It results from ROS overproduction during protein glycation process. The auto-oxidation reaction of glucose, catalyzed by transition metal ion, causes the formation of hydrogen peroxide and reactive carbonyl compounds. The carbonyl compounds sequentially attacks with lysine and arginine residues to produce AGEs (Wolff and Dean, 1987). The oxidative protein degradation is mediated by highly reactive hydroxyl radicals that generate via Fenton reaction. Superoxide anions are also continuously generated via oxidation of early glycation products such as 1,2- and 2,3-enolization of the Schiff's base (Smith and Thornalley, 1992). A thiol group of amino acid (Cys and Met) plays a role in the oxidative defense of protein which is the key target molecules for free radical-mediated modification of protein (Aćimović et al., 2009). The direct oxidation of amino acid (Lysine, Arginine, Threonine) or secondary reaction of amino acid residues (Cysteine and Histidine) with reactive carbonyl compounds leads to generate protein carbonyl derivatives (Berlett and Stadtman, 1997, Lee et al., 1998). Therefore, protein thiol group and protein carbonyl content have been used as a marker of ROS mediated protein oxidation associating with ageing and oxidative stress. The present study indicated that BSA-incubated with monosaccharides and methylglyoxal increased the level of protein carbonyl content whereas decreased the level of protein thiol goups after 2 week of incubation period.

Protein glycation directly induces protein aggregation and alters the conformation and stability of protein. Protein aggregation further forms insoluble amyloid fibrils comprising β-amyloid cross structure (Bouma et al., 2003). The accumulations of β-amyloid cross structure in specific organs or tissues may

contribute to amyloidosis which plays a role in the pathological progression. For instance, the islet amyloid polypeptide deteriorated the islet function in type 2 diabetes (Clark *et al.*, 1996). Moreover, the accumulation of amyloid plaques represents a major breakthrough in neurodegenerative diseases (Vidal and Ghetti, 2011). The present study demonstrated that the incubation of BSA with monosaccharides and methlyglyoxal significantly increased the level of β-amyloid cross structure after 2 week of incubation.

Scientists have attempted to search for anti-glycation agents from phytochemical compounds in order to inhibit the glycation process (Wu et al., 2011, Adisakwattana et al., 2012). For example, cinnamic acid and its derivatives, naturally occurring phenolic acids, have been shown to inhibit the generation of AGEs in models of glycated BSA (Adisakwattana et al., 2012). Other phytochemical compounds such as curcumin and silymarin have been recognized as powerful antioxidants. They have been found to inhibit AGEs formation in in vitro and diabetic animal models (Sajithlal *et al.*, 1998, Wu *et al.*, 2011, Hu *et al.*, 2012). In this regard, the proposed mechanisms of their actions may be related to scavenge free-radicals and reactive dicarbonyl intermediates during the glycation process (Sajithlal et al., 1998, Wu et al., 2011, Hu et al., 2012). Recent data indicate that anthocyanin-enriched red grape skin extract demonstrates the ability to reduce the formation of AGEs and glycation-induced protein oxidation in BSA model (Jariyapamornkoon et al., 2013). In the present study, we firstly investigated the effect of C3R on different types of monosaccharide induced protein glycation. The results clearly indicated that C3R effectively inhibits the formation of fluorescent and non-fluorescent AGEs N^{ε}-CML correlated with the reduction of fructosamine in BSA. The underlying mechanisms of flavonoids have been recently proposed to act as Amadori product inhibitors, AGE inhibitors, reactive dicarbonyl scavengers, and free-radical scavengers.

Moreover, it has been reported that anthocyanins could bind to human serum albumin (HSA) with high affinity at physiological pH (Cahyana and Gordon, 2013). Cyanidin-3-glucoside (C3G) belongs to anthocyanins and is widely found in fruits and vegetables. Data regarding the intermolecular interactions of C3G with BSA has been obtained through fluorescence spectroscopy and molecular docking methods. The observations indicate that C3G spontaneously binds and insert into the hydrophobic cavity in Site II (subdomain IIIA) of BSA, recognized as the same binding site of aminoguanidine (Joglekar *et al.*, 2013, Shi *et al.*, 2013). The interactions of C3G are mainly involved in hydrophobic, polar, and charge residues in BSA with Van der Waals and hydrogen bonding interactions. After the binding of C3G, BSA retains the secondary α-helical structure of BSA (Shi et al., 2013). Joglekar *et al*. reported that monosaccharide-induced protein glycation reduced the proportion of α-helical structure of BSA, with a parallel increase in the β-sheet structure. These structural alterations were reversed in the presence of antiglycating agents (Joglekar et al., 2013). Although the chemical structure of C3R and C3G are very similar, differences exist in the type of sugar at the β-glycosidic linkage. The interaction of albumin might be explained for the mechanisms of C3R to inhibit protein glycation. Therefore, it could be hypothesized that the binding of C3R might bind at the same site specificity of subdomain IIIA in BSA and help stabilize protein structure leading to prevent the proportional changes between α-helical and β-sheet structure during the glycation process. Further studies are needed to substantiate this hypothesis.

This study also shows for the first time that C3R effectively inhibited dicarbonyl intermediate methylglyoxal-derived AGEs formation at a propagation stage of the glycation process. C3R finally suppressed the formation of fluorescent AGEs and non-fluorescent AGEs N^{ε}-CML in advanced stage of glycation process. These findings extend previous part which showed that C3R inhibited ribose-, fructose-,

glucose- and galactose-induced AGEs formation during the initial stage of glycation (Thilavech *et al.*, 2015). Furthermore, berry and grape extracts containing anthocyanin also inhibited the formation of AGEs in an in vitro model involving fructose, methylglyoxal and BSA (Wang *et al.*, 2011). It is likely that these protein glycation protective effects of the fruit extracts may be largely due to C3R content as it is the predominant anthocyanin component (Jakobek *et al.*, 2007, Hassimotto et al., 2008). These findings, taken together, suggest that C3R potentially impairs initiation and intermediate stages of protein glycation and supports the need for efficacy and bioavailability studies of C3R in animals and humans.

Anti-oxidative agents have shown the ability to inhibit protein glycation and oxidative damage (Jariyapamornkoon et al., 2013). Many studies have reported strong positive correlation between antioxidant activity of flavonoids and the abilities to inhibit protein glycation and oxidation (Harris *et al.*, 2011, Ramkissoon *et al.*, 2013). Anthocyanin-rich extract containing high concentration of C3R also exhibits potent antioxidant activity (Tulio et al., 2008, Li et al., 2012). According to these supporting data, the C3R mediated inhibition of protein glycation and oxidation is related to its antioxidant activity (Feng et al., 2007, Watanabe, 2007).

Anthocyanins have been shown to reduce β-amyloid aggregation (Riviere *et al.*, 2008). Concerning the chemical structure, the fibril inhibitory activity of anthocyanins is due to the chalcone which has C6-linker-C6 structure in aqueous solution. Hydrogen bond might play an important role in fibril inhibition of anthocyanin by reinforcing the hydrophobic interaction between the aromatic rings (Riviere et al., 2008). As a result, the present study demonstrated the ability of C3R to reduce the level of β-amyloid cross structure in BSA mediated by monosaccharides and methylglyoxal. It has been reported that C3R also markedly decreased the level of thioflavin T fluorescence which is a marker of amyloid aggregation and fibril

formation in amyloid peptide model (Wong *et al.*, 2013). Therefore, it can be speculated that C3R may help to decrease the risks of debilitating neurodegenerative disorders.

The current study demonstrated that C3R was able to directly trap methylglyoxal. This can be explained its action in preventing of methylglyoxal-mediated the formation of AGEs and oxidative protein damage. The percentage of methylglyoxal-trapping ability increased in a concentration dependent manner and these findings are supported by a previous study which showed that a purified C3R from blackcurrant extract trapped nearly 50% of methylglyoxal when it was incubated at a 1:1 ratio. The C3R-mono-methylglyoxal adduct was identified as product from the reaction by using liquid chromatography electrospray ionization mass spectrometer (LC-ESI-MS) (Chen *et al.*, 2014). The molecular weight difference between the adduct (667 m/z) and the original C3R (595 m/z) is 72 which is same as the molecular weight of one molecule of methylglyoxal. It has been reported the addition of methylglyoxal on anthocyanin may probably form tautomers with transformation of carbonyl group of methylglyoxal to hydroxyl group (Lv *et al.*, 2010). In the previous study, the methylglyoxal addition reaction reacted with phenolic compounds at carbon atom with negative electron charge more than -0.24. Therefore, carbon number 2, 6, 7 and 15 of C3R is the possible location for methylglyoxal addition reaction (Chen et al., 2014). Chen et al demonstrated the C3R/ methylglyoxal reaction for only 1 h (Chen et al., 2014) but the different molar ratio and incubation time between C3R and methylglyoxal was evaluated in the current study. The reaction rate between C3R and methylglyoxal at 1:1 molar ratio was nearly 2-fold higher when the incubation time was increased from 1 to 24 h. It suggests that the trapping ability of C3R is dependent on the concentration and time of incubation. In addition, flavonoids have also been shown to inhibit AGEs formation

via methylglyoxal-trapping ability (Sang *et al.*, 2007, Peng *et al.*, 2008, Wang et al., 2011, Hu et al., 2012, Li *et al.*, 2014) which may be due their chemical structure that consists of phenyl ring (A- and B-ring) and heterocyclic ring (C-ring). The major sites to conjugate with methylglyoxal are the carbon positions at 6 and 8 on the A-ring (Li et al., 2014) which is the same structure present in C3R and may explain their effectiveness in trapping methylglyoxal (Chen et al., 2014).

According to the findings of present study, the proposed inhibitory mechanisms of C3R on protein glycation in BSA model are shown in figure 5.1.

1) C3R might have the molecular interaction with BSA at animo groups, and then prevented monosacchrides and methylglyoxal-induced alteration of protein structure.

2) C3R act as antioxidant to scavenge ROS, resulting in the inhibition of dicarbonyl compounds production and the reduction of AGEs formation via Amadori product fructosamine. The antioxidant activity of C3R caused the prevention of loss of protein thiol group and the reduction of protein carbonyl content. C3R might have the fibril inhibitory activity leading to inhibition of protein aggregation.

3) C3R has the ability to trap methylgyoxal and consequently decreases to formation of AGEs in BSA/methylglyoxal model.

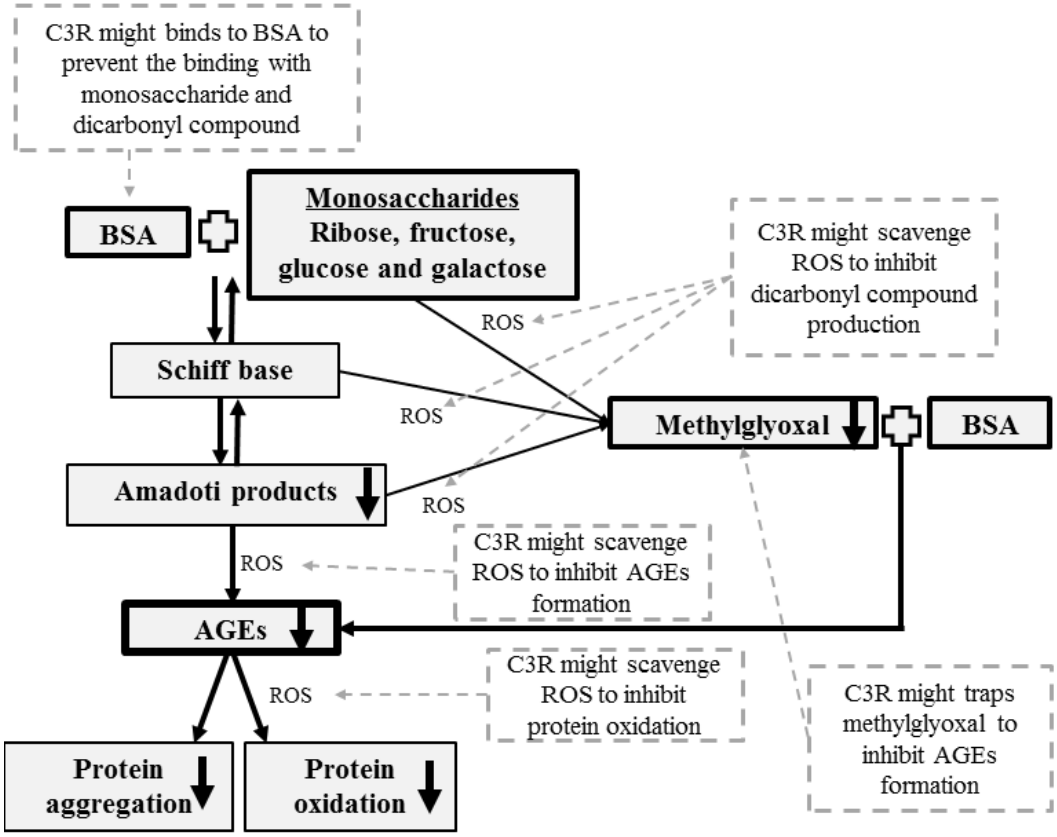

Figure 5.1 The proposed inhibitory mechanism of C3R on protein glycation mediated by monosaccharides (ribose, fructose, glucose and galactose) and methlyglyoxal in bovine serum albumin (BSA) model

5.2 The effect of C3R on methylglyoxal-induced oxidative DNA damage *in vitro*

Protein cross-linking mediated by methylglyoxal generates free radicals during this reaction including the methylglyoxal-radical anion and cross-linked radical cation (methylglyoxal-protonated cation) (Yim *et al.*, 1995). The methylglyoxal-protonated cation is a precursor of fluorescent AGEs while methylglyoxal-radical anions could donate an electron to oxygen molecule to generate a superoxide anion and hydroxyl radical resulting in oxidative damage of plasmid DNA (Kang, 2003, Wu and Yen, 2005, Suji and Sivakami, 2007). The presence of a transition metal ion such as copper or iron could stimulate the Fenton-like reaction to produce more highly reactive hydroxyl radicals that play an important role in mechanism of oxidative DNA strand breakage (Cooke *et al.*, 2003). These findings are consistent with previous studies that have demonstrated the reaction between methylglyoxal and lysine caused the oxidative DNA damage as presented by increasing OC form of plasmid DNA. In the presence of transition metal ion copper, the strand breakage of plasmid DNA was enhanced. The results confirmed that the formation of superoxide anion and hydroxyl radicals was generated from lysine and methylglyoxal by increasing cytochrome *c* reduction and TBARS.

The ability of phytochemical compounds on the prevention of methylglyoxal-induced protein glycation and DNA damage related to free radical scavenging activity has been reported (Wu and Yen, 2005, Chan and Wu, 2006, Meeprom *et al.*, 2015). Anthocyanin-rich extract containing high concentration of C3R also exhibits potent antioxidant activity (Beaulieu et al., 2010, Li et al., 2012). As shown in figure 5.2, the effectiveness of C3R in prevention of oxidative damage of DNA can be explained in part by the effect of C3R on scavenging superoxide anion and hydroxyl radicals, subsequently prevented oxidative DNA damage. the presence of lysine and methylglyoxal, C3R reduced the level of TBARS formation at concentrations of 0.25

mM or greater and maintained the reduced form of cytochrome *c* at background levels. These studies are consistent with previous reports that C3R inhibited the production of a secondary product of oxidation malonaldehyde from the degradation of 2-deoxyribose unit in DNA mediated by Fenton's reagent as well as decreased ROS production and DNA damage in hydrogen peroxide-simulated RAW 264.7 murine macrophage cell (Matsufuji *et al.*, 2006, Jung et al., 2014). As above mentioned, C3R was able to directly trap methylglyoxal and reduced the generation of ROS to induce oxidative DNA damage.

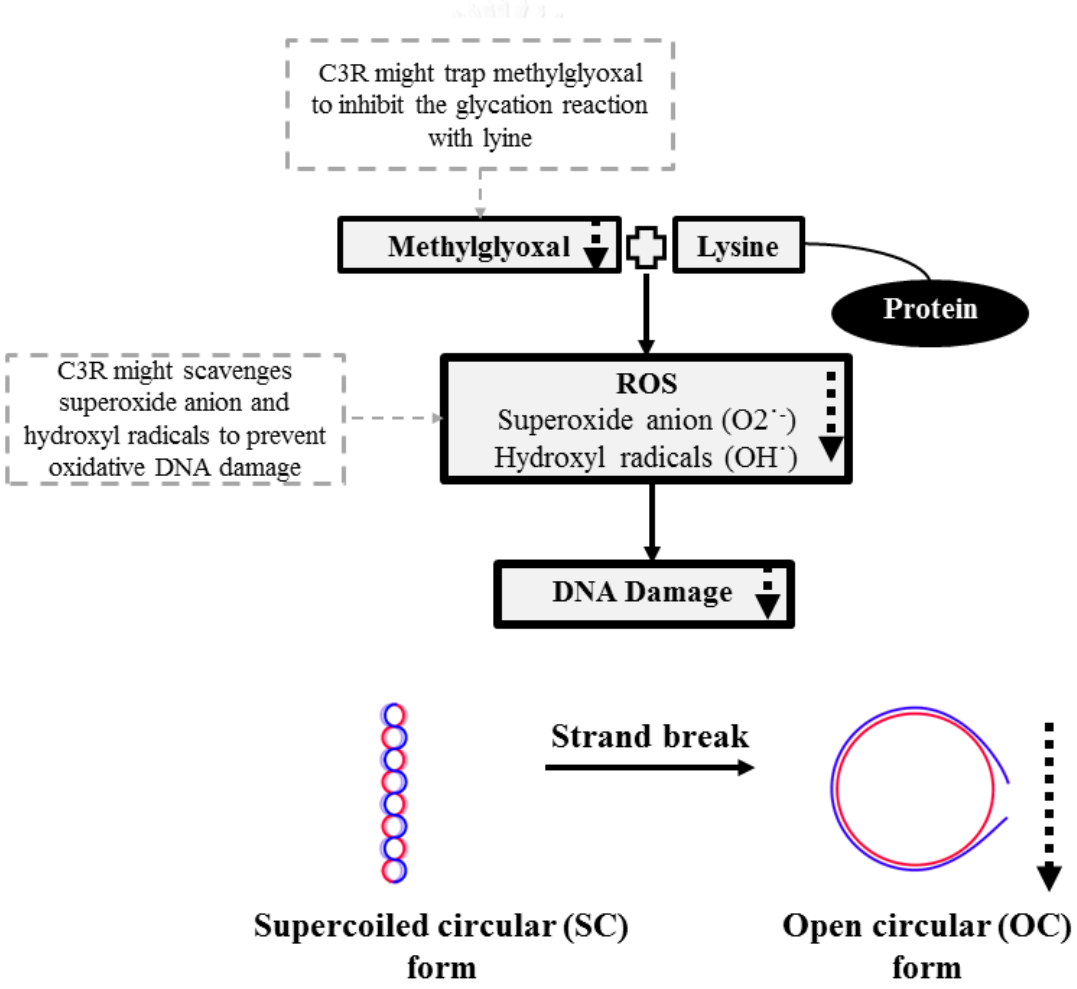

Figure 5.2 The proposed mechanism of C3R to prevent oxidative DNA damage mediated by methylgyoxal in lysine/methylglyoxal system.

5.3 The effect of C3R on methylglyoxal-mediated vascular abnormalities in isolated vascular preparation and methylglyoxal-treated rats.

It has been reported that a significant increase in blood methylglyoxal concentration are positively correlated with the level of plasma glucose and hemoglobinA_{1C} in diabetic patient (Lu *et al.*, 2011). In case cohort study with 10 years follow-up, a rise in methylglyoxal-derived AGEs formation has been associated with incident of cardiovascular events in type 2 diabetes (Hanssen *et al.*, 2015) such as diabetic nephropathy (Lu et al., 2011), neuropathy (Huang *et al.*, 2016), retinopathy (Wang *et al.*, 2014) and hypertension (Mukohda et al., 2012). In arterial walls, accumulation of methylglyoxal and methylglyoxal-derived AGEs may play a role in the development of hypertension related to vascular contractile dysfunction in spontaneous hypertensive rat (SHR) with aging (Wang et al., 2005, Mukohda et al., 2012).

The aorta is a large conductance vessel that is the critical tissue for atherosclerotic changes, while mesenteric artery is resistance artery that is responsible for local blood flow regulation (Mizutani *et al.*, 1999). Therefore, they are frequently investigated for the pathogenesis of cardiovascular diseases (Lee, 1985, Alexander, 1995, Oparil *et al.*, 2003). In the present study, acute treatment of methylglyoxal resulted in vascular abnormalities by significantly enhanced noradrenaline-induced vasoconstriction in endothelial-intact aorta, but no augmentation of contraction was observed in endothelial-denuded aorta. The findings suggest that methylglyoxal might be an endothelial-dependent vascular dysfunction mediator in aortic tissues. Methylglyoxal-mediated vasoconstriction has previously reported in the endothelium of rat carotid artery related to increase the formation of ROS such as superoxide anion and hydrogen peroxide. The overproduction of ROS increased intracellular calcium concentration, activated

thromboxane A_2 receptor and inhibited nitric oxide activity leading to vasoconstriction (Miyazawa *et al.*, 2010). In contrast to methylglyoxal-mediated vasoconstriction in aortic rings, the impairment of contraction was observed in methylglyoxal treated-mesenteric arterial bed. The opening of vascular smooth muscle calcium-activated potassium (BK_{Ca}) channel has been proposed as the mechanism of methylglyoxal-inhibit vasoconstriction (Mukohda *et al.*, 2009). In endothelial cells, methylglyoxal triggered protein expression of NADPH oxidase and nuclear factor NF-κB resulting in oxidative stress and endothelial dysfunction (Goldin et al., 2006, Miyazawa et al., 2010, Dhar *et al.*, 2012). The methylglyoxal-mediated contraction was reversed by nicotinamide adenine dinucleotide phosphate (NADPH) oxidase inhibitor apocynin and gp91ds-tat (Mukohda *et al.*, 2010). It has reported that acute methylglyoxal treatment caused vascular contractile dysfunction and disrupted autoregulation system of blood pressure. In peripheral resistance mesenteric artery, the contraction impairment may interrupt local blood flow that plays an important role in blood pressure regulation (Heagerty *et al.*, 2010). In addition, increased aortic pressure leads to elevate systolic and diastolic blood pressure (Klabunde, 2011). This alteration may affect the elevation of systematic blood pressure and renal perfusion pressure leading to the development of diabetic nephropathy (Van Buren and Toto, 2011).

In endothelial cells, binding of acetylcholine with G-protein linked receptor activates eNOS through phosphoinositide signaling pathway, eventually leading to the generation of nitric oxide. Nitric oxide rapidly diffuses into vascular smooth muscle cell and activates the enzyme guanylate cyclase which produces the secondary messenger cGMP resulting in smooth muscle relaxation (Hodgson and Marshall, 1989). The recent findings demonstrated that endothelium-dependent vascular relaxation response to acetylcholine was reduced sensitivity in

methyglyoxal-treated vessels both aortic ring and mesenteric arterial bed. The results are consistent with previous reports in vascular isolation (Brouwers *et al.*, 2010, Dhar et al., 2010). The impairment of endothelium-dependent vasorelaxation is a major characteristic of endothelial dysfunction. Under hyperglycemia condition, methylglyoxal is an important factor for endothelial dysfunction. It has been reported to decrease nitric oxide and cGMP production via the reduction of eNOS activity. Methylglyoxal also activated NADPH oxidase and NF-κB signaling cascade to produce ROS and inflammatory cytokines in endothelial cells (Dhar et al., 2010, Dhar et al., 2012, Turkseven *et al.*, 2014). Sequentially, the stability of nitric oxide was also decreased in oxidative stress condition via the reaction with superoxide anion to produce highly reactive peroxynitrite which is considered as an atherosclerotic factor (Chang *et al.*, 2005). Therefore, methylglyoxal-impaired endothelial dysfunction may associate with development of cardiovascular diseases in diabetic patient, especially hypertension and arteriosclerosis because of the accumulation of methylglyoxal in vascular tissue of SHR and arteriosclerotic plaque (Wang et al., 2005, Mukohda et al., 2012, Hanssen *et al.*, 2014).

In the present study, C3R was firstly established vasorelaxing action in isolated thoracic aorta *in vitro.* Under physiological condition, there are three important factors that regulate blood pressure including blood volume, total peripheral resistance and cardiac output. The total peripheral resistance contributed by mesenteric arterial bed is responsible for the blood flow in systematic circulation. The increased peripheral vascular resistance is the major pathology of established hypertension (Johnson, 1986, Mayet and Hughes, 2003). Moreover, the raised blood pressure also possibly results from the elevation of cardiac output linked to the changed in aortic blood flow. Our finding demonstrated that C3R-induced vascular relaxation of thoracic aorta was greater in than that of mesenteric arterial bed. At low

concentration, C3R (10 nM or above in mesenteric arterial bed and 1-100 nM in thoracic aorta) acts directly on nitric oxide-mediated vasodilation involving in the upregulation of endothelial nitric oxide synthase (eNOS) gene expression. The concentration ranges of C3R in the present study were in the nanomolar range which corresponds with their plasma concentrations following consumption of anthocyanin-rich foods in animal and human (Pojer *et al.*, 2013). For example, consumption of black currant anthocyanin drink (2.08 μmol/kg body weight of C3R) increased plasma concentration of C3R (36.1±14.2 nmol/L) after intake for 2 h in volunteers (Matsumoto et al., 2001). Therefore, an intake of C3R-endriched diet reached the effective concentration in the circulatory system which may be responsible for the vasodilation effect on thoracic aorta.

One of underlying mechanisms of vasorelaxation of anthocyanin is the up-regulation of eNOS expression that has been reported by natural anthocyanins from black currant and synthetic anthocyanin cyanidin-3-glucoside (C3G) (Xu *et al.*, 2004, Edirisinghe et al., 2011). Treatment of bovine artery endothelial cells with C3G (100 nM) increased eNOS protein expression by 6-fold, subsequently escalate nitric oxide production by 2-fold after 8 h of incubation period (Xu et al., 2004). Our present study demonstrated that C3R had ability to enhance eNOS gene expression of aortic tissue in dose- and time-dependent manners. In general, vascular endothelial cell culture is a useful and easy model for studying vascular function. Due to lacking ultrastructural support and association with cell interactions, the endothelium cells may contribute more different response in cell culture model than intact organs and create uncertainly in extrapolating data to endothelial function in vivo (Gillis *et al.*, 1989). Therefore, C3R activated eNOS mRNA expression in aortic tissues which may represent the role of C3R in the regulation of vascular function in vivo. The generation of vasodilator nitric oxide from L-arginine by eNOS plays an important role

in the maintaining cardiovascular homeostasis. The released nitric oxide from endothelial cells rapidly diffuses into smooth muscle to activate guanylyl cyclase which generates signaling molecule cGMP, responsible for smooth muscle relaxation in vasculature (Tousoulis *et al.*, 2012). However, nitric oxide has a short half-life in a few second. It reacts rapidly with superoxide anion to form peroxynitrite. The reaction was prevented by superoxide dismutase which is a superoxide anion scavenger (Fukai and Ushio-Fukai, 2011). The previous study revealed that the superoxide anion scavenging activity of red wine polyphenols contribute an increased vascular relaxation response to acetylcholine via the improvement of nitric oxide stability in normotensive rats after intragastric administration for 7 days (Diebolt *et al.*, 2001). Interestingly, C3R has been reported to be an effective superoxide anion scavenger in vitro (Chun *et al.*, 2003, Watanabe, 2007). These evidences strongly support the current study that C3R might act as a superoxide anion scavenger leading to the increased stability of nitric oxide and promote its function on vascular relaxation.

The current findings firstly revealed that treatment with C3R prevented methylglyoxal-mediated vascular abnormalities. The results showed that C3R (3 μM) attenuated methylglyoxal-induced vasoconstriction response to noradrenaline, -impaired vasorelaxation response to acetylcholine and -induced vasorelaxation response to sodium nitroprusside in rat isolated tissues. As mentioned above, C3R at concentration 3 μM caused an increase eNOS mRNA expression in aortic tissue after 24 hours. However, the eNOS mRNA upregulation was not affected by this concentration for 30 min of incubation. It is possible that C3R may play other signaling pathways by stimulating eNOS activity. It revealed that C3R (30 μM) increased eNOS activity via phosphatidylinositol-3 (PI3)/protein kinase B (Akt) signaling in human umbilical vein endothelial cell (HUVEC) after 10 min of incubation

(Edirisinghe et al., 2011). In addition to other mechanisms of action, C3R might act as a superoxide anion scavenger that ROS are generated through methylglyoxal-activated NADPH oxidase and NF-κB (Chun et al., 2003, Watanabe, 2007). The overproduction of superoxide anions rapidly reacts with nitric oxide to yield highly reactive peroxynitrite causing the degradation of nitric oxide (Diebolt et al., 2001). A decrease in available nitric oxide affects the abnormal regulation of vascular homeostasis leading to developing chronic hypertension (Rajendran *et al.*, 2013). C3R may help stabilize the available nitric oxide in the vascular system and prevent the abnormal regulation of vascular homeostasis. The present findings also found the methylglyoxal-trapping ability of C3R with the effective molar concentration ratio of 0.25:1 (C3R:MG). However, a significant effect of methylgyloxal-mediated vascular abnormalities was seen at the molar concentration ratio of 0.006:1 (C3R:MG) suggesting that C3R is not act in this manner.

In animal study, the results demonstrated that oral administration of methylglyoxal (60-120 mg/day) increased plasma concentration of methylglyoxal (11.66±0.18 μM) at week 8. It had 1.2-fold higher plasma concentration of methylglyoxal than normal rats. This was the similar range to the presence of plasma methylglyoxal concentration in diabetic rats (5 nM-15 μM) and type 2 diabetic patients (2-400 μM) (Phillips *et al.*, 1993, McLellan *et al.*, 1994, Lapolla *et al.*, 2003, Sena *et al.*, 2012, Kong *et al.*, 2014, Scheijen and Schalkwijk, 2014). In agreement with a previous study, the plasma concentration of methylglyoxal was ~1.3-fold increase in type 2 diabetic patients (Lu et al., 2011, Scheijen and Schalkwijk, 2014). In addition, the liver and kidney functions was not affected by chronic methylglyoxal treatment as represented by the normal range of liver enzymes (aspartate aminotransferase and alanine aminotransferase) and kidney function indicators (blood urea nitrogen and creatinine) after 8 week.

Under physiological condition, methylglyoxal can be detoxified by glyoxalase system as the major pathway. In the cytoplasm of all mammalian cells, methylglyoxal is converted to D-lactate using glyoxalase I and II enzymes. Glyoxalase I is the rate-limiting step enzyme for this reaction and the system requires glutathione as a cofactor (Maessen *et al.*, 2015). In arterial tissues, downregulation of glyoxalase I has been found in hyperglycemia concomitant with higher level of methylglyoxal causing an increased risk of developing cardiovascular diseases (Brouwers et al., 2010). In the current finding, no significant differences of glyoxalase I mRNA expression were observed in aortic tissues from methylglyoxal-treated rats. This results might be explained by two-pronged effect of methylglyoxal on glyoxalase I activity (Beisswenger *et al.*, 2005). With low concentration of methylglyoxal, the cells induce compensatory activation to detoxify methylglyoxal by upregulating glyoxalase I activity. The consistent data has been reported in nerve cells that methylglyoxal at low concentration (300 μM) caused glyoxalase system activation, whereas the higher concentration (750 μM) markedly inhibited and downregulated glyoxalase system (Beisswenger et al., 2005). It found that the rats treated with methylglyoxal plus C3R (100 mg/kg/day) trended to insignificantly increase glyoxalase I mRNA expression. The action of C3R may not involve in the detoxification system of GLO1 mRNA expression.

Many studies have shown that the development of hypertension strongly associated with increased the accumulation of methylglyoxal and methylglyoxal-derived AGEs (N^{ε}-CEL and N^{ε}-CML) in serum and vascular tissues of high fructose-fed rats and SHR (Wang *et al.*, 2008, Dhar *et al.*, 2013). In the present study, an increase of N^{ε}-CML accumulation was found in aortic tissue after treatment of methylglyoxal for 8 weeks. N^{ε}-CML, the most active AGEs, has been reported to increase in animal tissues with chronic methylglyoxal treatment related to the progression of several

pathologies (Guo *et al.*, 2009, Dhar *et al.*, 2011, Sena et al., 2012). In aortic tissues, the accumulation of methylglyoxal-derived AGEs has been linked to the upregulation of receptor for AGEs (RAGE) (Sena et al., 2012). When N^{ε}-CML binds with RAGE and consequently triggers multiple signaling pathways of NF-κB activation. Finally, the interaction stimulates the generation of ROS and proinflammatory cytokines resulting the damage of aortic tissues (Chavakis *et al.*, 2004, Goldin et al., 2006). Moreover, methylglyoxal-derived AGEs formation may also associated with intermolecular collagen cross-linking in arterial wall leading to diminish arterial compliance, increase vascular stiffness, and then increase diastolic dysfunction and systolic hypertension (Cooper et al. 2001). Therefore, methylglyoxal-mediated ROS production and AGEs formation might be responsible for the vascular dysfunction in aorta and mesenteric arterial bed of methylglyoxal-treated rats. The present study revealed that co-administration of methylglyoxal with C3R effectively decreased plasma methylglyoxal concentration and the accumulation of N^{ε}-CML in aortic tissue. Apart from methylglyoxal-trapping ability, the reduction of N^{ε}-CML level might be accompanied by anti-glycation activity of C3R as described previously in *in vitro* study. The inhibitory activity of C3R on the formation of AGEs supports the preventive mechanisms on methylglyoxal-induced abnormality of vascular structures and functions. The proposed mechanism also found in a previous report that administration of AGEs inhibitor, aminoguanidine, was effective in preventing formation of AGEs and cross-linking of arterial wall in diabetic rat and aging rats (Brownlee et al., 1986) (Li *et al.*, 1996).

The present study also revealed that methylglyoxal mediated the impairment of vascular reactivity that may represent early cardiovascular abnormalities in methylglyoxal-treated rats. In rat aorta and mesenteric artery, chronic methylglyoxal treatment significantly impaired contraction and relaxation response to noradrenaline

and acetylcholine, respectively. In addition, methylglyoxal enhanced sodium nitroprusside-induced relaxation in rat aorta. According to methylglyoxal-impaired relaxation response to acetylcholine, these results are linked to the downregulation of eNOS mRNA expression in aortic tissue. These results are consistent with previously report regarding to impairment of vascular reactivity in rat mesenteric artery after long-term exposure of methylglyoxal (42 μM for 3 days) (Mukohda et al., 2012, Mukohda et al., 2013). Chronic methylglyoxal treatment induced prolonged ROS production and subsequent apoptotic morphological change in the arterial wall of rat mesenteric artery (Mukohda et al., 2012, Mukohda et al., 2013). Many studies have shown that anthocyanins are potent natural compounds to promote endothelial functions and maintain vascular homeostasis by increasing nitric oxide production and bioavailability (Wallace, 2011, Speciale *et al.*, 2014). In diabetic animal model with apolipoprotein E-deficient, anthocyanin cyanidin-3-glucoside supplementation improved endothelial function and prevented accelerated atherogenesis in streptozotocin–induced diabetic rats (Zhang *et al.*, 2013). The epidemiological studies suggested that high intake of anthocyanin enriched fruits has been associated with a reduced risk of cardiovascular diseases including hypertension and myocardial infarction (Jennings *et al.*, 2012, Cassidy *et al.*, 2013). In type 2 diabetic patients, 160 mg of anthocyanin supplementation decreased systolic blood pressure after 24 weeks compared with placebo (Li *et al.*, 2015). In dietary sources, C3R predominantly comprises 20%–70% of total anthocyanin in fruits (Watanabe, 2007, Hassimotto et al., 2008, Li et al., 2012). Administration of C3R (30, 100 and 300 mg/kg body weight) has shown anti-hyperglycemia activity by reducing postprandial glucose in normal rats. The inhibitory activity of C3R on intestinal α-glucosidase and pancreatic α–amylase has been proposed as the underlying antidiabetic mechanisms (Akkarachiyasit et al., 2010, Adisakwattana et al., 2011, Akkarachiyasit et al., 2011). According to a previous study, the doses of C3R (30 and 100 mg/kg/day) was

selected for co-administration with methylglyoxal in long-term feeding study. The proposed preventive mechanisms of dietary C3R on cardiovascular abnormalities-mediated by methylglyoxal in isolated vascular preparation and methylglyoxal-treated rat are shown in figure 5.3.

1) C3R might directly trap to methylglyoxal resulting in the reduction of plasma methylglyoxal and methylglyoxal-derived AGEs N^{ε}-CML accumulation in aortic tissues.

2) C3R might act as anti-glycation agent to inhibit the formation of AGEs and protein cross-linking in arterial wall resulting in the preservation vascular function.

3) C3R might act as antioxidant to scavenge ROS, resulting in the inhibition of methylglyoxal-mediated vascular smooth muscle damage and endothelial dysfunction via NADPH oxidase activation. Moreover, C3R also improves the stability of nitric oxide and then promotes its function on vascular relaxation.

4) C3R might have the ability to improve endothelial function by upregulating eNOS mRNA expression leading to escalate nitric oxide production.

However, the extrapolation of health effects has been concerned because of low bioavailability of anthocyanins (Gao *et al.*, 2012). For example, in a human study, the oral ingestion of black currant containing C3R (1.24 mg/kg body weight) caused an increase the level of plasma C3R level (36.1±1.43 nM) with maximum at 2 hours postintake. The absorption rate is supposed to be very low (less than 1%) (Matsumoto et al., 2001). Therefore, further clinical studies are needed to clarify whether dietary C3R improves cardiovascular health in human.

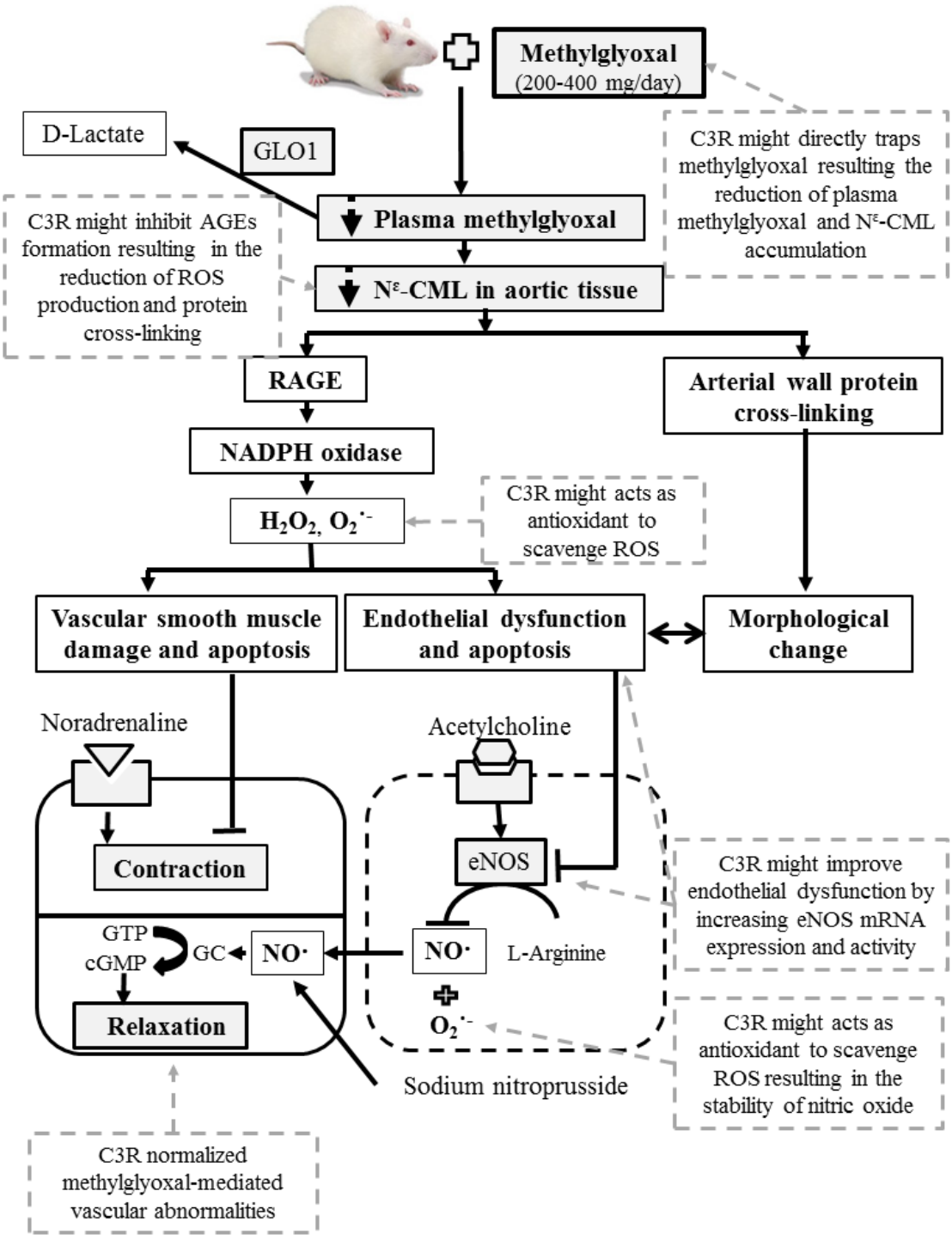

Figure 5.4 The proposed mechanism of C3R to alleviating cardiovascular abnormalities in isolated vascular preparation and methylglyoxal-treated rats.

CHAPTER VI

CONCLUSION

Firstly, C3R could inhibit against monosaccharides (ribose, fructose, glucose and galactose) and methylglyoxal-induced protein glycation in bovine serum albumin. It reduces the formation of β-amyloid cross structure and prevents oxidative protein damage by decreasing protein carbonyl content and depleting thiol group in bovine serum albumin.

In plasmid DNA model, C3R prevents lysine/methylglyoxal-induced oxidative DNA damage. The inhibitory effect of C3R is attributed in part to its ability to scavenge superoxide anion and hydroxyl radicals generated during protein glycation process. In addition, C3R directly traps reactive dicarbonyl methylglyoxal.

In isolated vascular preparation model, C3R prevented methylglyoxal-mediated vascular abnormalities in rat isolated thoracic aorta and mesenteric arterial bed by normalizing vascular functions in vasoconstriction response to noradrenaline and vasorelaxation response to nitric oxide production through acetylcholine and nitric oxide donor sodium nitroprusside.

In methylglyoxal-treated rats, dietary intake of C3R prevents the pathogenesis of cardiovascular abnormalities by decreasing plasma methylglyoxal concentration and accumulation of AGEs in aortic tissues. Moreover, C3R improves endothelial dysfunction by increasing endothelial nitric oxide synthase mRNA (eNOS) expression in aortic tissues.

Based on these findings, C3R could be a potential compound to prevent or ameliorate methylglyoxal-derived AGEs mediated vascular complications.

REFERENCES

Aćimović, J. M., B. D. Stanimirović and L. M. Mandić (2009). "The role of the thiol group in protein modification with methylglyoxal." Journal of the Serbian Chemical Society **74**(8-9): 867-883.

Adisakwattana, S., N. Ngamrojanavanich, K. Kalampakorn, W. Tiravanit, S. Roengsumran and S. Yibchok-Anun (2004). "Inhibitory activity of cyanidin-3-rutinoside on alpha-glucosidase." J Enzyme Inhib Med Chem **19**(4): 313-316.

Adisakwattana, S., W. Sompong, A. Meeprom, S. Ngamukote and S. Yibchok-Anun (2012). "Cinnamic acid and its derivatives inhibit fructose-mediated protein glycation." Int J Mol Sci **13**(2): 1778-1789.

Adisakwattana, S., S. Yibchok-Anun, P. Charoenlertkul and N. Wongsasiripat (2011). "Cyanidin-3-rutinoside alleviates postprandial hyperglycemia and its synergism with acarbose by inhibition of intestinal alpha-glucosidase." J Clin Biochem Nutr **49**(1): 36-41.

Ahmed, N. (2005). "Advanced glycation endproducts--role in pathology of diabetic complications." Diabetes Res Clin Pract **67**(1): 3-21.

Ahmed, N. and A. J. Furth (1992). "Failure of common glycation assays to detect glycation by fructose." Clin Chem **38**(7): 1301-1303.

Akkarachiyasit, S., P. Charoenlertkul, S. Yibchok-Anun and S. Adisakwattana (2010). "Inhibitory activities of cyanidin and its glycosides and synergistic effect with acarbose against intestinal alpha-glucosidase and pancreatic alpha-amylase." Int J Mol Sci **11**(9): 3387-3396.

Akkarachiyasit, S., S. Yibchok-Anun, S. Wacharasindhu and S. Adisakwattana (2011). "In vitro inhibitory effects of cyandin-3-rutinoside on pancreatic alpha-amylase and its combined effect with acarbose." Molecules **16**(3): 2075-2083.

Al-Awwadi, N. A., C. Araiz, A. Bornet, S. Delbosc, J. P. Cristol, N. Linck, et al. (2005). "Extracts enriched in different polyphenolic families normalize increased cardiac NADPH oxidase expression while having differential effects on insulin resistance, hypertension, and cardiac hypertrophy in high-fructose-fed rats." J Agric Food Chem **53**(1): 151-157.

Alexander, R. W. (1995). "Theodore Cooper Memorial Lecture. Hypertension and the pathogenesis of atherosclerosis. Oxidative stress and the mediation of arterial inflammatory response: a new perspective." Hypertension **25**(2): 155-161.

American Diabetes, A. (2007). "Diagnosis and classification of diabetes mellitus." Diabetes Care **30 Suppl 1**: S42-47.

Ansari, N. A. and D. Dash (2013). "Amadori glycated proteins: role in production of autoantibodies in diabetes mellitus and effect of inhibitors on non-enzymatic glycation." Aging Dis **4**(1): 50-56.

Anuradha, C. V. and S. D. Balakrishnan (1999). "Taurine attenuates hypertension and improves insulin sensitivity in the fructose-fed rat, an animal model of insulin resistance." Can J Physiol Pharmacol **77**(10): 749-754.

Ardestani, A. and R. Yazdanparast (2007). "Inhibitory effects of ethyl acetate extract of Teucrium polium on in vitro protein glycoxidation." Food Chem Toxicol **45**(12): 2402-2411.

Armbruster, D. A. (1987). "Fructosamine: structure, analysis, and clinical usefulness." Clin Chem **33**(12): 2153-2163.

Association, A. D. (2003). "Gestational diabetes mellitus." Diabetes care **26**: S103.

Babacanoglu, C., N. Yildirim, G. Sadi, M. B. Pektas and F. Akar (2013). "Resveratrol prevents high-fructose corn syrup-induced vascular insulin resistance and dysfunction in rats." Food Chem Toxicol **60**: 160-167.

Balu, M., P. Sangeetha, G. Murali and C. Panneerselvam (2005). "Age-related oxidative protein damages in central nervous system of rats: modulatory role of grape seed extract." Int J Dev Neurosci **23**(6): 501-507.

Basta, G., A. M. Schmidt and R. De Caterina (2004). "Advanced glycation end products and vascular inflammation: implications for accelerated atherosclerosis in diabetes." Cardiovasc Res **63**(4): 582-592.

Beaulieu, L. P., C. S. Harris, A. Saleem, A. Cuerrier, P. S. Haddad, L. C. Martineau, et al. (2010). "Inhibitory effect of the Cree traditional medicine wiishichimanaanh (Vaccinium vitis-idaea) on advanced glycation endproduct formation: identification of active principles." Phytother Res **24**(5): 741-747.

Beisswenger, P. and D. Ruggiero-Lopez (2003). "Metformin inhibition of glycation processes." Diabetes Metab **29**(4 Pt 2): 6S95-103.

Beisswenger, P. J., K. S. Drummond, R. G. Nelson, S. K. Howell, B. S. Szwergold and M. Mauer (2005). "Susceptibility to Diabetic Nephropathy Is Related to Dicarbonyl and Oxidative Stress." Diabetes **54**(11): 3274-3281.

Beisswenger, P. J., S. K. Howell, R. M. O'Dell, M. E. Wood, A. D. Touchette and B. S. Szwergold (2001). "alpha-Dicarbonyls increase in the postprandial period and reflect the degree of hyperglycemia." Diabetes Care **24**(4): 726-732.

Bener, A., N. M. Saleh and A. Al-Hamaq (2011). "Prevalence of gestational diabetes and associated maternal and neonatal complications in a fast-developing community: global comparisons." Int J Womens Health **3**: 367-373.

Berlett, B. S. and E. R. Stadtman (1997). "Protein oxidation in aging, disease, and oxidative stress." J Biol Chem **272**(33): 20313-20316.

Bierhaus, A., M. A. Hofmann, R. Ziegler and P. P. Nawroth (1998). "AGEs and their interaction with AGE-receptors in vascular disease and diabetes mellitus. I. The AGE concept." Cardiovasc Res **37**(3): 586-600.

Bolton, W. K., D. C. Cattran, M. E. Williams, S. G. Adler, G. B. Appel, K. Cartwright, et al. (2004). "Randomized trial of an inhibitor of formation of advanced glycation end products in diabetic nephropathy." Am J Nephrol **24**(1): 32-40.

Bouma, B., L. M. Kroon-Batenburg, Y. P. Wu, B. Brunjes, G. Posthuma, O. Kranenburg, et al. (2003). "Glycation induces formation of amyloid cross-beta structure in albumin." J Biol Chem **278**(43): 41810-41819.

Bowen-Forbes, C. S., Y. Zhang and M. G. Nair (2010). "Anthocyanin content, antioxidant, anti-inflammatory and anticancer properties of blackberry and raspberry fruits." Journal of Food Composition and Analysis **23**(6): 554-560.

Brouwers, O., P. M. Niessen, G. Haenen, T. Miyata, M. Brownlee, C. D. Stehouwer, et al. (2010). "Hyperglycaemia-induced impairment of endothelium-dependent vasorelaxation in rat mesenteric arteries is mediated by intracellular methylglyoxal levels in a pathway dependent on oxidative stress." Diabetologia **53**(5): 989-1000.

Brownlee, M. (2005). "The pathobiology of diabetic complications: a unifying mechanism." Diabetes **54**(6): 1615-1625.

Brownlee, M., H. Vlassara, A. Kooney, P. Ulrich and A. Cerami (1986). "Aminoguanidine prevents diabetes-induced arterial wall protein cross-linking." Science **232**(4758): 1629-1632.

Bunn, H. F. and P. J. Higgins (1981). "Reaction of monosaccharides with proteins: possible evolutionary significance." Science **213**(4504): 222-224.

Cahyana, Y. and M. H. Gordon (2013). "Interaction of anthocyanins with human serum albumin: influence of pH and chemical structure on binding." Food Chem **141**(3): 2278-2285.

Cassidy, A., K. J. Mukamal, L. Liu, M. Franz, A. H. Eliassen and E. B. Rimm (2013). "High anthocyanin intake is associated with a reduced risk of myocardial infarction in young and middle-aged women." Circulation **127**(2): 188-196.

Chan, W. H. and H. J. Wu (2006). "Protective effects of curcumin on methylglyoxal-induced oxidative DNA damage and cell injury in human mononuclear cells." Acta Pharmacol Sin **27**(9): 1192-1198.

Chang, T., R. Wang and L. Wu (2005). "Methylglyoxal-induced nitric oxide and peroxynitrite production in vascular smooth muscle cells." Free Radic Biol Med **38**(2): 286-293.

Chavakis, T., A. Bierhaus and P. P. Nawroth (2004). "RAGE (receptor for advanced glycation end products): a central player in the inflammatory response." Microbes Infect **6**(13): 1219-1225.

Chen, X.-Y., I. M. Huang, L. S. Hwang, C.-T. Ho, S. Li and C.-Y. Lo (2014). "Anthocyanins in blackcurrant effectively prevent the formation of advanced glycation end products by trapping methylglyoxal." Journal of Functional Foods **8**(0): 259-268.

Chun, O. K., D. O. Kim and C. Y. Lee (2003). "Superoxide radical scavenging activity of the major polyphenols in fresh plums." J Agric Food Chem **51**(27): 8067-8072.

Clark, A., S. B. Charge, M. K. Badman, D. A. MacArthur and E. J. de Koning (1996). "Islet amyloid polypeptide: actions and role in the pathogenesis of diabetes." Biochem Soc Trans **24**(2): 594-599.

Clarke, R. E., A. L. Dordevic, S. M. Tan, L. Ryan and M. T. Coughlan (2016). "Dietary Advanced Glycation End Products and Risk Factors for Chronic Disease: A Systematic Review of Randomised Controlled Trials." Nutrients **8**(3).

Cooke, M. S., M. D. Evans, M. Dizdaroglu and J. Lunec (2003). "Oxidative DNA damage: mechanisms, mutation, and disease." FASEB J **17**(10): 1195-1214.

Cotham, W. E., T. O. Metz, P. L. Ferguson, J. W. Brock, D. J. Hinton, S. R. Thorpe, et al. (2004). "Proteomic analysis of arginine adducts on glyoxal-modified ribonuclease." Mol Cell Proteomics **3**(12): 1145-1153.

Coughlan, M. T., J. M. Forbes and M. E. Cooper (2007). "Role of the AGE crosslink breaker, alagebrium, as a renoprotective agent in diabetes." Kidney Int Suppl(106): S54-60.

Crisostomo, J., P. Matafome, D. Santos-Silva, L. Rodrigues, C. M. Sena, P. Pereira, et al. (2013). "Methylglyoxal chronic administration promotes diabetes-like cardiac ischaemia disease in Wistar normal rats." Nutr Metab Cardiovasc Dis.

da Silva Morrone, M., A. M. de Assis, R. F. da Rocha, J. Gasparotto, A. C. Gazola, G. M. Costa, et al. (2013). "Passiflora manicata (Juss.) aqueous leaf extract protects against reactive oxygen species and protein glycation in vitro and ex vivo models." Food Chem Toxicol **60**: 45-51.

Dalle-Donne, I., R. Rossi, D. Giustarini, A. Milzani and R. Colombo (2003). "Protein carbonyl groups as biomarkers of oxidative stress." Clin Chim Acta **329**(1-2): 23-38.

de Pascual-Teresa, S., D. A. Moreno and C. Garcia-Viguera (2010). "Flavanols and anthocyanins in cardiovascular health: a review of current evidence." Int J Mol Sci **11**(4): 1679-1703.

Degenhardt, T. P., S. R. Thorpe and J. W. Baynes (1998). "Chemical modification of proteins by methylglyoxal." Cell Mol Biol (Noisy-le-grand) **44**(7): 1139-1145.

Deng, G. F., X. R. Xu, Y. Zhang, D. Li, R. Y. Gan and H. B. Li (2013). "Phenolic compounds and bioactivities of pigmented rice." Crit Rev Food Sci Nutr **53**(3): 296-306.

Dhar, A., I. Dhar, K. M. Desai and L. Wu (2010). "Methylglyoxal scavengers attenuate endothelial dysfunction induced by methylglyoxal and high concentrations of glucose." Br J Pharmacol **161**(8): 1843-1856.

Dhar, A., I. Dhar, B. Jiang, K. M. Desai and L. Wu (2011). "Chronic methylglyoxal infusion by minipump causes pancreatic beta-cell dysfunction and induces type 2 diabetes in Sprague-Dawley rats." Diabetes **60**(3): 899-908.

Dhar, I. and K. Desai (2012). Aging: Drugs to Eliminate Methylglyoxal, a Reactive Glucose Metabolite, and Advanced Glycation Endproducts, INTECH Open Access Publisher.

Dhar, I., A. Dhar, L. Wu and K. Desai (2012). "Arginine attenuates methylglyoxal- and high glucose-induced endothelial dysfunction and oxidative stress by an endothelial nitric-oxide synthase-independent mechanism." J Pharmacol Exp Ther **342**(1): 196-204.

Dhar, I., A. Dhar, L. Wu and K. M. Desai (2013). "Increased methylglyoxal formation with upregulation of Renin Angiotensin system in fructose fed sprague dawley rats." PLoS One **8**(9): e74212.

Diaconeasa, Z., L. Leopold, D. Rugina, H. Ayvaz and C. Socaciu (2015). "Antiproliferative and antioxidant properties of anthocyanin rich extracts from blueberry and blackcurrant juice." Int J Mol Sci **16**(2): 2352-2365.

Diebolt, M., B. Bucher and R. Andriantsitohaina (2001). "Wine polyphenols decrease blood pressure, improve NO vasodilatation, and induce gene expression." Hypertension **38**(2): 159-165.

Dyer, D. G., J. A. Dunn, S. R. Thorpe, K. E. Bailie, T. J. Lyons, D. R. McCance, et al. (1993). "Accumulation of Maillard reaction products in skin collagen in diabetes and aging." J Clin Invest **91**(6): 2463-2469.

Edirisinghe, I., K. Banaszewski, J. Cappozzo, D. McCarthy and B. M. Burton-Freeman (2011). "Effect of black currant anthocyanins on the activation of endothelial nitric oxide synthase (eNOS) in vitro in human endothelial cells." J Agric Food Chem **59**(16): 8616-8624.

Elhabiri, M., P. Figueiredo, A. Fougerousse and R. Brouillard (1995). "A convenient method for conversion of flavonols into anthocyanins." Tetrahedron letters **36**(26): 4611-4614.

Ellman, G. L. (1959). "Tissue sulfhydryl groups." Arch Biochem Biophys **82**(1): 70-77.

Feng, R., H. M. Ni, S. Y. Wang, I. L. Tourkova, M. R. Shurin, H. Harada, et al. (2007). "Cyanidin-3-rutinoside, a natural polyphenol antioxidant, selectively kills leukemic cells by induction of oxidative stress." J Biol Chem **282**(18): 13468-13476.

Freedman, B. I., J.-P. Wuerth, K. Cartwright, R. P. Bain, S. Dippe, K. Hershon, et al. (1999). "Design and baseline characteristics for the aminoguanidine clinical trial in overt Type 2 diabetic nephropathy (ACTION II)." Controlled clinical trials **20**(5): 493-510.

Freedman, B. I., J. P. Wuerth, K. Cartwright, R. P. Bain, S. Dippe, K. Hershon, et al. (1999). "Design and baseline characteristics for the aminoguanidine clinical trial in overt type 2 diabetic nephropathy (ACTION II)." Control Clin Trials **20**(5): 493-510.

Fukai, T. and M. Ushio-Fukai (2011). "Superoxide dismutases: role in redox signaling, vascular function, and diseases." Antioxid Redox Signal **15**(6): 1583-1606.

Galvano, F., L. La Fauci, P. Vitaglione, V. Fogliano, L. Vanella and C. Felgines (2007). "Bioavailability, antioxidant and biological properties of the natural free-radical scavengers cyanidin and related glycosides." Ann Ist Super Sanita **43**(4): 382-393.

Gao, S., S. Basu, Z. Yang, A. Deb and M. Hu (2012). "Bioavailability challenges associated with development of saponins as therapeutic and chemopreventive agents." Curr Drug Targets **13**(14): 1885-1899.

Gensberger, S., S. Mittelmaier, M. A. Glomb and M. Pischetsrieder (2012). "Identification and quantification of six major alpha-dicarbonyl process contaminants in high-fructose corn syrup." Anal Bioanal Chem **403**(10): 2923-2931.

Giacco, F. and M. Brownlee (2010). "Oxidative stress and diabetic complications." Circ Res **107**(9): 1058-1070.

Gillis, C. N., M. P. Merker and W. W. Carley (1989). Vascular Endothelial Surface Proteins in the Perfused Rabbit Lung. Vascular Endothelium: Receptors and Transduction Mechanisms. J. D. Catravas, C. N. Gillis and U. S. Ryan. Boston, MA, Springer US**:** 43-54.

Glomb, M. A. and V. M. Monnier (1995). "Mechanism of protein modification by glyoxal and glycolaldehyde, reactive intermediates of the Maillard reaction." J Biol Chem **270**(17): 10017-10026.

Goldin, A., J. A. Beckman, A. M. Schmidt and M. A. Creager (2006). "Advanced glycation end products: sparking the development of diabetic vascular injury." Circulation **114**(6): 597-605.

Gouvêa, A. C. M. S., M. C. P. d. Araujo, D. F. Schulz, S. Pacheco, R. L. d. O. Godoy and L. M. C. Cabral (2012). "Anthocyanins standards (cyanidin-3-O-glucoside and cyanidin-3-O-rutinoside) isolation from freeze-dried açaí (Euterpe oleraceae Mart.) by HPLC." Food Science and Technology (Campinas) **32**: 43-46.

Guo, Q., T. Mori, Y. Jiang, C. Hu, Y. Osaki, Y. Yoneki, et al. (2009). "Methylglyoxal contributes to the development of insulin resistance and salt sensitivity in Sprague-Dawley rats." J Hypertens **27**(8): 1664-1671.

Hanamura, T., T. Hagiwara and H. Kawagishi (2005). "Structural and functional characterization of polyphenols isolated from acerola (Malpighia emarginata DC.) fruit." Biosci Biotechnol Biochem **69**(2): 280-286.

Hanssen, N. M., J. W. Beulens, S. van Dieren, J. L. Scheijen, A. D. van der, A. M. Spijkerman, et al. (2015). "Plasma advanced glycation end products are associated with incident cardiovascular events in individuals with type 2 diabetes: a case-cohort study with a median follow-up of 10 years (EPIC-NL)." Diabetes **64**(1): 257-265.

Hanssen, N. M., C. D. Stehouwer and C. G. Schalkwijk (2014). "Methylglyoxal and glyoxalase I in atherosclerosis." Biochem Soc Trans **42**(2): 443-449.

Harman, D. (2009). "Origin and evolution of the free radical theory of aging: a brief personal history, 1954-2009." Biogerontology **10**(6): 773-781.

Harris, C. S., L. P. Beaulieu, M. H. Fraser, K. L. McIntyre, P. L. Owen, L. C. Martineau, et al. (2011). "Inhibition of advanced glycation end product formation by medicinal plant extracts correlates with phenolic metabolites and antioxidant activity." Planta Med **77**(2): 196-204.

Hassimotto, N. M., M. I. Genovese and F. M. Lajolo (2008). "Absorption and metabolism of cyanidin-3-glucoside and cyanidin-3-rutinoside extracted from wild mulberry (Morus nigra L.) in rats." Nutr Res **28**(3): 198-207.

He, H. and Y. H. Lu (2013). "Comparison of inhibitory activities and mechanisms of five mulberry plant bioactive components against alpha-glucosidase." J Agric Food Chem **61**(34): 8110-8119.

Heagerty, A. M., E. H. Heerkens and A. S. Izzard (2010). "Small artery structure and function in hypertension." J Cell Mol Med **14**(5): 1037-1043.

Hinton, D. J. and J. M. Ames (2006). "Site specificity of glycation and carboxymethylation of bovine serum albumin by fructose." Amino Acids **30**(4): 425-434.

Hodgson, J. M. and J. J. Marshall (1989). "Direct vasoconstriction and endothelium-dependent vasodilation. Mechanisms of acetylcholine effects on coronary flow and arterial diameter in patients with nonstenotic coronary arteries." Circulation **79**(5): 1043-1051.

Hou, F. F., J. Boyce, G. M. Chertow, J. Kay and W. F. Owen, Jr. (1998). "Aminoguanidine inhibits advanced glycation end products formation on beta2-microglobulin." J Am Soc Nephrol **9**(2): 277-283.

Hu, T. Y., C. L. Liu, C. C. Chyau and M. L. Hu (2012). "Trapping of methylglyoxal by curcumin in cell-free systems and in human umbilical vein endothelial cells." J Agric Food Chem **60**(33): 8190-8196.

Huang, Q., Y. Chen, N. Gong and Y. X. Wang (2016). "Methylglyoxal mediates streptozotocin-induced diabetic neuropathic pain via activation of the peripheral TRPA1 and Nav1.8 channels." Metabolism **65**(4): 463-474.

Huang, Y. J., V. S. Fang, C. C. Juan, Y. C. Chou, C. F. Kwok and L. T. Ho (1997). "Amelioration of insulin resistance and hypertension in a fructose-fed rat model with fish oil supplementation." Metabolism **46**(11): 1252-1258.

Ihm, S. H., H. J. Yoo, S. W. Park and J. Ihm (1999). "Effect of aminoguanidine on lipid peroxidation in streptozotocin-induced diabetic rats." Metabolism **48**(9): 1141-1145.

Jakobek, L., M. Šeruga, M. Medvidović-Kosanović and I. N. Jovanović (2007). "Anthocyanin content and antioxidant activity of various red fruit juices." Deutsche Lebensmittel-Rundshau **103**(2): 58-64.

Jakus, V. and N. Rietbrock (2004). "Advanced glycation end-products and the progress of diabetic vascular complications." Physiol Res **53**(2): 131-142.

Jariyapamornkoon, N., S. Yibchok-Anun and S. Adisakwattana (2013). "Inhibition of advanced glycation end products by red grape skin extract and its antioxidant activity." BMC Complement Altern Med **13**: 171.

Jennings, A., A. A. Welch, S. J. Fairweather-Tait, C. Kay, A. M. Minihane, P. Chowienczyk, et al. (2012). "Higher anthocyanin intake is associated with lower arterial stiffness and central blood pressure in women." Am J Clin Nutr **96**(4): 781-788.

Joglekar, M. M., S. N. Panaskar, A. D. Chougale, M. J. Kulkarni and A. U. Arvindekar (2013). "A novel mechanism for antiglycative action of limonene through stabilization of protein conformation." Mol Biosyst **9**(10): 2463-2472.

Johnson, P. C. (1986). "Brief Review: Autoregulation of blood flow." Circ Res **59**: 483-495.

Johnson, R. N., P. A. Metcalf and J. R. Baker (1983). "Fructosamine: a new approach to the estimation of serum glycosylprotein. An index of diabetic control." Clin Chim Acta **127**(1): 87-95.

Jung, H., H.-K. Kwak and K. Hwang (2014). "Antioxidant and antiinflammatory activities of cyanidin-3-glucoside and cyanidin-3-rutinoside in hydrogen peroxide and lipopolysaccharide-treated RAW264.7 cells." Food Science and Biotechnology **23**(6): 2053-2062.

Jung, H., H.-K. Kwak and K. T. Hwang (2014). "Antioxidant and antiinflammatory activities of cyanidin-3-glucoside and cyanidin-3-rutinoside in hydrogen peroxide and lipopolysaccharide-treated RAW264.7 cells." Food Science and Biotechnology **23**(6): 2053-2062.

Juraschek, S. P., M. W. Steffes and E. Selvin (2012). "Associations of alternative markers of glycemia with hemoglobin A(1c) and fasting glucose." Clin Chem **58**(12): 1648-1655.

Kalapos, M. P. (1999). "Methylglyoxal in living organisms: chemistry, biochemistry, toxicology and biological implications." Toxicol Lett **110**(3): 145-175.

Kang, J. H. (2003). "Oxidative damage of DNA induced by methylglyoxal in vitro." Toxicol Lett **145**(2): 181-187.

Kang, Y. S., Y. G. Park, B. K. Kim, S. Y. Han, Y. H. Jee, K. H. Han, et al. (2006). "Angiotensin II stimulates the synthesis of vascular endothelial growth factor through the p38 mitogen activated protein kinase pathway in cultured mouse podocytes." J Mol Endocrinol **36**(2): 377-388.

Kanwar, M. and R. A. Kowluru (2009). "Role of glyceraldehyde 3-phosphate dehydrogenase in the development and progression of diabetic retinopathy." Diabetes **58**(1): 227-234.

Kazachkov, M., K. Chen, S. Babiy and P. H. Yu (2007). "Evidence for in vivo scavenging by aminoguanidine of formaldehyde produced via semicarbazide-sensitive amine oxidase-mediated deamination." J Pharmacol Exp Ther **322**(3): 1201-1207.

Khazaei, M. R., M. Bakhti and M. Habibi-Rezaei (2010). "Nicotine reduces the cytotoxic effect of glycated proteins on microglial cells." Neurochem Res **35**(4): 548-558.

Kilhovd, B. K., T. J. Berg, K. I. Birkeland, P. Thorsby and K. F. Hanssen (1999). "Serum levels of advanced glycation end products are increased in patients with type 2 diabetes and coronary heart disease." Diabetes Care **22**(9): 1543-1548.

Kitabchi, A. E., G. E. Umpierrez, J. M. Miles and J. N. Fisher (2009). "Hyperglycemic crises in adult patients with diabetes." Diabetes Care **32**(7): 1335-1343.

Klabunde, R. (2011). Cardiovascular physiology concepts, Lippincott Williams & Wilkins.

Kohei, K. (2010). "Pathophysiology of type 2 diabetes and its treatment policy." JMAJ **53**(1): 41-46.

Kong, X., M. Z. Ma, K. Huang, L. Qin, H. M. Zhang, Z. Yang, et al. (2014). "Increased plasma levels of the methylglyoxal in patients with newly diagnosed type 2 diabetes 2." J Diabetes **6**(6): 535-540.

Kusunoki, H., S. Miyata, T. Ohara, B. F. Liu, A. Uriuhara, H. Kojima, et al. (2003). "Relation between serum 3-deoxyglucosone and development of diabetic microangiopathy." Diabetes Care **26**(6): 1889-1894.

Lapolla, A., R. Flamini, A. Dalla Vedova, A. Senesi, R. Reitano, D. Fedele, et al. (2003). "Glyoxal and methylglyoxal levels in diabetic patients: quantitative determination by a new GC/MS method." Clin Chem Lab Med **41**(9): 1166-1173.

Lee, C., M. B. Yim, P. B. Chock, H. S. Yim and S. O. Kang (1998). "Oxidation-reduction properties of methylglyoxal-modified protein in relation to free radical generation." J Biol Chem **273**(39): 25272-25278.

Lee, R. M. (1985). "Vascular changes at the prehypertensive phase in the mesenteric arteries from spontaneously hypertensive rats." Blood Vessels **22**(3): 105-126.

Leslie, R. D. and R. M. Cohen (2009). "Biologic variability in plasma glucose, hemoglobin A1c, and advanced glycation end products associated with diabetes complications." J Diabetes Sci Technol **3**(4): 635-643.

Levine, R. L., D. Garland, C. N. Oliver, A. Amici, I. Climent, A. G. Lenz, et al. (1990). "Determination of carbonyl content in oxidatively modified proteins." Methods Enzymol **186**: 464-478.

Li, D., Y. Zhang, Y. Liu, R. Sun and M. Xia (2015). "Purified anthocyanin supplementation reduces dyslipidemia, enhances antioxidant capacity, and prevents insulin resistance in diabetic patients." J Nutr **145**(4): 742-748.

Li, W., H. Liang, M. W. Zhang, R. F. Zhang, Y. Y. Deng, Z. C. Wei, et al. (2012). "Phenolic profiles and antioxidant activity of litchi (Litchi Chinensis Sonn.) fruit pericarp from different commercially available cultivars." Molecules **17**(12): 14954-14967.

Li, X., T. Zheng, S. Sang and L. Lv (2014). "Quercetin inhibits advanced glycation end product formation by trapping methylglyoxal and glyoxal." J Agric Food Chem **62**(50): 12152-12158.

Li, Y., W. Xu, Z. Liao, B. Yao, X. Chen, Z. Huang, et al. (2004). "Induction of long-term glycemic control in newly diagnosed type 2 diabetic patients is associated with improvement of beta-cell function." Diabetes Care **27**(11): 2597-2602.

Li, Y. M., M. Steffes, T. Donnelly, C. Liu, H. Fuh, J. Basgen, et al. (1996). "Prevention of cardiovascular and renal pathology of aging by the advanced glycation inhibitor aminoguanidine." Proc Natl Acad Sci U S A **93**(9): 3902-3907.

Liu, H., H. Liu, W. Wang, C. Khoo, J. Taylor and L. Gu (2011). "Cranberry phytochemicals inhibit glycation of human hemoglobin and serum albumin by scavenging reactive carbonyls." Food Funct **2**(8): 475-482.

Lo, T. W., M. E. Westwood, A. C. McLellan, T. Selwood and P. J. Thornalley (1994). "Binding and modification of proteins by methylglyoxal under physiological conditions. A kinetic and mechanistic study with N alpha-acetylarginine, N alpha-acetylcysteine, and N alpha-acetyllysine, and bovine serum albumin." J Biol Chem **269**(51): 32299-32305.

Longhurst, P. A., R. E. Stitzel and R. J. Head (1986). "Perfusion of the intact and partially isolated rat mesenteric vascular bed: application to vessels from hypertensive and normotensive rats." Blood Vessels **23**(6): 288-296.

Lu, J., J. Ji, H. Meng, D. Wang, B. Jiang, L. Liu, et al. (2013). "The protective effect and underlying mechanism of metformin on neointima formation in fructose-induced insulin resistant rats." Cardiovasc Diabetol **12**: 58.

Lu, J., E. Randell, Y. Han, K. Adeli, J. Krahn and Q. H. Meng (2011). "Increased plasma methylglyoxal level, inflammation, and vascular endothelial dysfunction in diabetic nephropathy." Clin Biochem **44**(4): 307-311.

Luevano-Contreras, C. and K. Chapman-Novakofski (2010). "Dietary advanced glycation end products and aging." Nutrients **2**(12): 1247-1265.

Lv, L., X. Shao, L. Wang, D. Huang, C. T. Ho and S. Sang (2010). "Stilbene glucoside from Polygonum multiflorum Thunb.: a novel natural inhibitor of advanced glycation end product formation by trapping of methylglyoxal." J Agric Food Chem **58**(4): 2239-2245.

Maessen, D. E., C. D. Stehouwer and C. G. Schalkwijk (2015). "The role of methylglyoxal and the glyoxalase system in diabetes and other age-related diseases." Clin Sci (Lond) **128**(12): 839-861.

Marceau, E. and V. A. Yaylayan (2009). "Profiling of alpha-dicarbonyl content of commercial honeys from different botanical origins: identification of 3,4-dideoxyglucoson-3-ene (3,4-DGE) and related compounds." J Agric Food Chem **57**(22): 10837-10844.

Matafome, P., C. Sena and R. Seica (2012). "Methylglyoxal, obesity, and diabetes." Endocrine.

Matafome, P., C. Sena and R. Seica (2013). "Methylglyoxal, obesity, and diabetes." Endocrine **43**(3): 472-484.

Matsufuji, H., H. Ochi and T. Shibamoto (2006). "Formation and inhibition of genotoxic malonaldehyde from DNA oxidation controlled with EDTA." Food Chem Toxicol **44**(2): 236-241.

Matsumoto, H., H. Inaba, M. Kishi, S. Tominaga, M. Hirayama and T. Tsuda (2001). "Orally administered delphinidin 3-rutinoside and cyanidin 3-rutinoside are directly

absorbed in rats and humans and appear in the blood as the intact forms." J Agric Food Chem **49**(3): 1546-1551.

Mayet, J. and A. Hughes (2003). "Cardiac and vascular pathophysiology in hypertension." Heart **89**(9): 1104-1109.

McCance, D. R., D. G. Dyer, J. A. Dunn, K. E. Bailie, S. R. Thorpe, J. W. Baynes, et al. (1993). "Maillard reaction products and their relation to complications in insulin-dependent diabetes mellitus." J Clin Invest **91**(6): 2470-2478.

McLellan, A. C., P. J. Thornalley, J. Benn and P. H. Sonksen (1994). "Glyoxalase system in clinical diabetes mellitus and correlation with diabetic complications." Clin Sci (Lond) **87**(1): 21-29.

Meeprom, A., W. Sompong, C. B. Chan and S. Adisakwattana (2013). "Isoferulic acid, a new anti-glycation agent, inhibits fructose- and glucose-mediated protein glycation in vitro." Molecules **18**(6): 6439-6454.

Meeprom, A., W. Sompong, T. Suantawee, T. Thilavech, C. B. Chan and S. Adisakwattana (2015). "Isoferulic acid prevents methylglyoxal-induced protein glycation and DNA damage by free radical scavenging activity." BMC Complement Altern Med **15**(1): 346.

Metascreen Writing, C., R. Bonadonna, D. Cucinotta, D. Fedele, G. Riccardi and A. Tiengo (2006). "The metabolic syndrome is a risk indicator of microvascular and macrovascular complications in diabetes: results from Metascreen, a multicenter diabetes clinic-based survey." Diabetes Care **29**(12): 2701-2707.

Millar, D., G. Taylor, P. Thornalley, C. Holmes and A. Dawnay (2002). Comparison of in vitro protein modification with advanced glycation endproduct (AGE) precursors methylglyoxal, glyoxal, 3-deoxyglucosone and glucose using mass spectrometry. International Congress Series, Elsevier.

Mitch, W. E., J. L. Bailey, X. Wang, C. Jurkovitz, D. Newby and S. R. Price (1999). "Evaluation of signals activating ubiquitin-proteasome proteolysis in a model of muscle wasting." Am J Physiol **276**(5 Pt 1): C1132-1138.

Miyazawa, N., M. Abe, T. Souma, M. Tanemoto, T. Abe, M. Nakayama, et al. (2010). "Methylglyoxal augments intracellular oxidative stress in human aortic endothelial cells." Free Radic Res **44**(1): 101-107.

Mizutani, K., K. Ikeda, Y. Kawai and Y. Yamori (1999). "Biomechanical properties and chemical composition of the aorta in genetic hypertensive rats." J Hypertens **17**(4): 481-487.

Mukohda, M., T. Morita, M. Okada, Y. Hara and H. Yamawaki (2012). "Long-term methylglyoxal treatment impairs smooth muscle contractility in organ-cultured rat mesenteric artery." Pharmacol Res **65**(1): 91-99.

Mukohda, M., T. Morita, M. Okada, Y. Hara and H. Yamawaki (2013). "Long-term methylglyoxal treatment causes endothelial dysfunction of rat isolated mesenteric artery." J Vet Med Sci **75**(2): 151-157.

Mukohda, M., M. Okada, Y. Hara and H. Yamawaki (2012). "Exploring mechanisms of diabetes-related macrovascular complications: role of methylglyoxal, a metabolite of glucose on regulation of vascular contractility." J Pharmacol Sci **118**(3): 303-310.

Mukohda, M., M. Okada, Y. Hara and H. Yamawaki (2012). "Methylglyoxal accumulation in arterial walls causes vascular contractile dysfunction in spontaneously hypertensive rats." J Pharmacol Sci **120**(1): 26-35.

Mukohda, M., H. Yamawaki, H. Nomura, M. Okada and Y. Hara (2009). "Methylglyoxal inhibits smooth muscle contraction in isolated blood vessels." J Pharmacol Sci **109**(2): 305-310.

Mukohda, M., H. Yamawaki, M. Okada and Y. Hara (2010). "Methylglyoxal augments angiotensin II-induced contraction in rat isolated carotid artery." J Pharmacol Sci **114**(4): 390-398.

Nagai, R., M. Jinno, M. Ichihashi, H. Koyama, Y. Yamamoto and Y. Yonei (2012). "Advanced glycation end products and their receptors as risk factors for aging." Anti-Aging Medicine **9**(4): 108-113.

Nagai, R., D. B. Murray, T. O. Metz and J. W. Baynes (2012). "Chelation: a fundamental mechanism of action of AGE inhibitors, AGE breakers, and other inhibitors of diabetes complications." Diabetes **61**(3): 549-559.

Nakamura, Y., H. Matsumoto and K. Todoki (2002). "Endothelium-dependent vasorelaxation induced by black currant concentrate in rat thoracic aorta." Jpn J Pharmacol **89**(1): 29-35.

Nijveldt, R. J., E. van Nood, D. E. van Hoorn, P. G. Boelens, K. van Norren and P. A. van Leeuwen (2001). "Flavonoids: a review of probable mechanisms of action and potential applications." Am J Clin Nutr **74**(4): 418-425.

O'Keefe, J. H., M. D. Carter and C. J. Lavie (2009). "Primary and secondary prevention of cardiovascular diseases: a practical evidence-based approach." Mayo Clin Proc **84**(8): 741-757.

Oparil, S., M. A. Zaman and D. A. Calhoun (2003). "Pathogenesis of hypertension." Ann Intern Med **139**(9): 761-776.

Ortiz, J., M. R. Marin-Arroyo, M. J. Noriega-Dominguez, M. Navarro and I. Arozarena (2013). "Color, phenolics, and antioxidant activity of blackberry (Rubus glaucus Benth.), blueberry (Vaccinium floribundum Kunth.), and apple wines from Ecuador." J Food Sci **78**(7): C985-993.

Park, Y. S., Y. H. Koh, M. Takahashi, Y. Miyamoto, K. Suzuki, N. Dohmae, et al. (2003). "Identification of the binding site of methylglyoxal on glutathione peroxidase: methylglyoxal inhibits glutathione peroxidase activity via binding to glutathione binding sites Arg 184 and 185." Free Radic Res **37**(2): 205-211.

Peng, X., K. W. Cheng, J. Ma, B. Chen, C. T. Ho, C. Lo, et al. (2008). "Cinnamon bark proanthocyanidins as reactive carbonyl scavengers to prevent the formation of advanced glycation endproducts." J Agric Food Chem **56**(6): 1907-1911.

Peng, X., Z. Zheng, K.-W. Cheng, F. Shan, G.-X. Ren, F. Chen, et al. (2008). "Inhibitory effect of mung bean extract and its constituents vitexin and isovitexin on the formation of advanced glycation endproducts." Food Chemistry **106**(2): 475-481.

Phillips, S. A., D. Mirrlees and P. J. Thornalley (1993). "Modification of the glyoxalase system in streptozotocin-induced diabetic rats: effect of the aldose reductase inhibitor Statil." Biochemical pharmacology **46**(5): 805-811.

Phillips, S. A. and P. J. Thornalley (1993). "The formation of methylglyoxal from triose phosphates. Investigation using a specific assay for methylglyoxal." Eur J Biochem **212**(1): 101-105.

Pojer, E., F. Mattivi, D. Johnson and C. S. Stockley (2013). "The Case for Anthocyanin Consumption to Promote Human Health: A Review." Comprehensive Reviews in Food Science and Food Safety **12**(5): 483-508.

Puddu, A., D. Storace, P. Odetti and G. L. Viviani (2010). "Advanced glycation end-products affect transcription factors regulating insulin gene expression." Biochem Biophys Res Commun **395**(1): 122-125.

Qian, P., S. Cheng, J. Guo and Y. Niu (2000). "[Effects of vitamin E and vitamin C on nonenzymatic glycation and peroxidation in experimental diabetic rats]." Wei Sheng Yan Jiu **29**(4): 226-228.

Rabbani, N., L. Godfrey, M. Xue, F. Shaheen, M. Geoffrion, R. Milne, et al. (2011). "Glycation of LDL by methylglyoxal increases arterial atherogenicity: a possible contributor to increased risk of cardiovascular disease in diabetes." Diabetes **60**(7): 1973-1980.

Rajendran, P., T. Rengarajan, J. Thangavel, Y. Nishigaki, D. Sakthisekaran, G. Sethi, et al. (2013). "The vascular endothelium and human diseases." Int J Biol Sci **9**(10): 1057-1069.

Ramasamy, R., S. F. Yan and A. M. Schmidt (2006). "Methylglyoxal comes of AGE." Cell **124**(2): 258-260.

Ramkissoon, J. S., M. F. Mahomoodally, N. Ahmed and A. H. Subratty (2013). "Antioxidant and anti-glycation activities correlates with phenolic composition of tropical medicinal herbs." Asian Pac J Trop Med **6**(7): 561-569.

Riboulet-Chavey, A., A. Pierron, I. Durand, J. Murdaca, J. Giudicelli and E. Van Obberghen (2006). "Methylglyoxal impairs the insulin signaling pathways independently of the formation of intracellular reactive oxygen species." Diabetes **55**(5): 1289-1299.

Richard, J. P. (1991). "Kinetic parameters for the elimination reaction catalyzed by triosephosphate isomerase and an estimation of the reaction's physiological significance." Biochemistry **30**(18): 4581-4585.

Riviere, C., T. Richard, X. Vitrac, J. M. Merillon, J. Valls and J. P. Monti (2008). "New polyphenols active on beta-amyloid aggregation." Bioorg Med Chem Lett **18**(2): 828-831.

Rosolova, H., B. Petrlova, J. Simon, P. Sifalda, I. Sipova and F. Sefrna (2008). "[Macrovascular and microvascular complications in type 2 diabetes patients]." Vnitr Lek **54**(3): 229-237.

Runnie, I., M. N. Salleh, S. Mohamed, R. J. Head and M. Y. Abeywardena (2004). "Vasorelaxation induced by common edible tropical plant extracts in isolated rat aorta and mesenteric vascular bed." J Ethnopharmacol **92**(2-3): 311-316.

Sagripanti, J. L. and K. H. Kraemer (1989). "Site-specific oxidative DNA damage at polyguanosines produced by copper plus hydrogen peroxide." J Biol Chem **264**(3): 1729-1734.

Sajithlal, G. B., P. Chithra and G. Chandrakasan (1998). "Effect of curcumin on the advanced glycation and cross-linking of collagen in diabetic rats." Biochem Pharmacol **56**(12): 1607-1614.

Sang, S., X. Shao, N. Bai, C. Y. Lo, C. S. Yang and C. T. Ho (2007). "Tea polyphenol (-)-epigallocatechin-3-gallate: a new trapping agent of reactive dicarbonyl species." Chem Res Toxicol **20**(12): 1862-1870.

Saric, A., S. Sobocanec, T. Balog, B. Kusic, V. Sverko, V. Dragovic-Uzelac, et al. (2009). "Improved antioxidant and anti-inflammatory potential in mice consuming sour cherry juice (Prunus Cerasus cv. Maraska)." Plant Foods Hum Nutr **64**(4): 231-237.

Scheen, A. J. (2003). "Pathophysiology of type 2 diabetes." Acta Clin Belg **58**(6): 335-341.

Scheijen, J. L. and C. G. Schalkwijk (2014). "Quantification of glyoxal, methylglyoxal and 3-deoxyglucosone in blood and plasma by ultra performance liquid chromatography tandem mass spectrometry: evaluation of blood specimen." Clin Chem Lab Med **52**(1): 85-91.

Seeram, N. P., R. A. Momin, M. G. Nair and L. D. Bourquin (2001). "Cyclooxygenase inhibitory and antioxidant cyanidin glycosides in cherries and berries." Phytomedicine **8**(5): 362-369.

Semchyshyn, H. M. and V. I. Lushchak (2012). "Interplay between oxidative and carbonyl stresses: molecular mechanisms, biological effects and therapeutic strategies of protection." Oxidative Stress—Molecular Mechanisms and Biological Effects: 15-46.

Sena, C. M., P. Matafome, J. Crisostomo, L. Rodrigues, R. Fernandes, P. Pereira, et al. (2012). "Methylglyoxal promotes oxidative stress and endothelial dysfunction." Pharmacol Res **65**(5): 497-506.

Seneviratne, C., G. W. Dombi, W. Liu and J. A. Dain (2011). "The in vitro glycation of human serum albumin in the presence of Zn(II)." J Inorg Biochem **105**(12): 1548-1554.

Shamsi, F. A., A. Partal, C. Sady, M. A. Glomb and R. H. Nagaraj (1998). "Immunological evidence for methylglyoxal-derived modifications in vivo. Determination of antigenic epitopes." J Biol Chem **273**(12): 6928-6936.

Shi, J. H., J. Wang, Y. Y. Zhu and J. Chen (2013). "Characterization of intermolecular interaction between cyanidin-3-glucoside and bovine serum albumin: Spectroscopic and molecular docking methods." Luminescence.

Singh, P., R. H. Jayaramaiah, S. B. Agawane, G. Vannuruswamy, A. M. Korwar, A. Anand, et al. (2016). "Potential Dual Role of Eugenol in Inhibiting Advanced Glycation End Products in Diabetes: Proteomic and Mechanistic Insights." Sci Rep **6**: 18798.

Singh, R., A. Barden, T. Mori and L. Beilin (2001). "Advanced glycation end-products: a review." Diabetologia **44**(2): 129-146.

Singh, V. P., A. Bali, N. Singh and A. S. Jaggi (2014). "Advanced glycation end products and diabetic complications." Korean J Physiol Pharmacol **18**(1): 1-14.

Smith, P. R. and P. J. Thornalley (1992). "Mechanism of the degradation of non-enzymatically glycated proteins under physiological conditions." Eur J Biochem **210**(3): 729-739.

Sompong, W., A. Meeprom, H. Cheng and S. Adisakwattana (2013). "A comparative study of ferulic acid on different monosaccharide-mediated protein glycation and oxidative damage in bovine serum albumin." Molecules **18**(11): 13886-13903.

Soulis-Liparota, T., M. Cooper, D. Papazoglou, B. Clarke and G. Jerums (1991). "Retardation by aminoguanidine of development of albuminuria, mesangial expansion, and tissue fluorescence in streptozocin-induced diabetic rat." Diabetes **40**(10): 1328-1334.

Speciale, A., F. Cimino, A. Saija, R. Canali and F. Virgili (2014). "Bioavailability and molecular activities of anthocyanins as modulators of endothelial function." Genes Nutr **9**(4): 404.

Sri Harsha, P. S., C. Gardana, P. Simonetti, G. Spigno and V. Lavelli (2013). "Characterization of phenolics, in vitro reducing capacity and anti-glycation activity of

red grape skins recovered from winemaking by-products." Bioresour Technol **140**: 263-268.

Stevens, A. (1998). "The contribution of glycation to cataract formation in diabetes." J Am Optom Assoc **69**(8): 519-530.

Stitt, A. W. (2001). "Advanced glycation: an important pathological event in diabetic and age related ocular disease." Br J Ophthalmol **85**(6): 746-753.

Su, Y., S. M. Qadri, L. Wu and L. Liu (2013). "Methylglyoxal modulates endothelial nitric oxide synthase-associated functions in EA.hy926 endothelial cells." Cardiovasc Diabetol **12**: 134.

Suji, G. and S. Sivakami (2007). "DNA damage during glycation of lysine by methylglyoxal: assessment of vitamins in preventing damage." Amino Acids **33**(4): 615-621.

Swamy, M. S. and E. C. Abraham (1989). "Inhibition of lens crystallin glycation and high molecular weight aggregate formation by aspirin in vitro and in vivo." Invest Ophthalmol Vis Sci **30**(6): 1120-1126.

Syrovy, I. (1994). "Glycation of albumin: reaction with glucose, fructose, galactose, ribose or glyceraldehyde measured using four methods." J Biochem Biophys Methods **28**(2): 115-121.

Thilavech, T., S. Ngamukote, M. Abeywardena and S. Adisakwattana (2015). "Protective effects of cyanidin-3-rutinoside against monosaccharides-induced protein glycation and oxidation." Int J Biol Macromol **75**: 515-520.

Thornalley, P. J. (2003). "Use of aminoguanidine (Pimagedine) to prevent the formation of advanced glycation endproducts." Arch Biochem Biophys **419**(1): 31-40.

Thornalley, P. J., A. Yurek-George and O. K. Argirov (2000). "Kinetics and mechanism of the reaction of aminoguanidine with the alpha-oxoaldehydes glyoxal, methylglyoxal, and 3-deoxyglucosone under physiological conditions." Biochem Pharmacol **60**(1): 55-65.

Tousoulis, D., A. M. Kampoli, C. Tentolouris, N. Papageorgiou and C. Stefanadis (2012). "The role of nitric oxide on endothelial function." Curr Vasc Pharmacol **10**(1): 4-18.

Tran, L. T., V. G. Yuen and J. H. McNeill (2009). "The fructose-fed rat: a review on the mechanisms of fructose-induced insulin resistance and hypertension." Mol Cell Biochem **332**(1-2): 145-159.

Tulio, A. Z., Jr., R. N. Reese, F. J. Wyzgoski, P. L. Rinaldi, R. Fu, J. C. Scheerens, et al. (2008). "Cyanidin 3-rutinoside and cyanidin 3-xylosylrutinoside as primary phenolic antioxidants in black raspberry." J Agric Food Chem **56**(6): 1880-1888.

Tupe, R. S. and V. V. Agte (2010). "Role of zinc along with ascorbic acid and folic acid during long-term in vitro albumin glycation." Br J Nutr **103**(3): 370-377.

Turk, Z., I. Misur, N. Turk and B. Benko (1999). "Rat tissue collagen modified by advanced glycation: correlation with duration of diabetes and glycemic control." Clin Chem Lab Med **37**(8): 813-820.

Turkseven, S., E. Ertuna, G. Yetik-Anacak and M. Yasa (2014). "Methylglyoxal causes endothelial dysfunction: the role of endothelial nitric oxide synthase and AMP-activated protein kinase alpha." J Basic Clin Physiol Pharmacol **25**(1): 109-115.

Ulrich, P. and A. Cerami (2001). "Protein glycation, diabetes, and aging." Recent Prog Horm Res **56**: 1-21.

Uribarri, J., S. Woodruff, S. Goodman, W. Cai, X. Chen, R. Pyzik, et al. (2010). "Advanced glycation end products in foods and a practical guide to their reduction in the diet." J Am Diet Assoc **110**(6): 911-916 e912.

Van Buren, P. N. and R. Toto (2011). "Hypertension in diabetic nephropathy: epidemiology, mechanisms, and management." Adv Chronic Kidney Dis **18**(1): 28-41.

Vander Jagt, D. L. (2008). "Methylglyoxal, diabetes mellitus and diabetic complications." Drug Metabol Drug Interact **23**(1-2): 93-124.

Vander Jagt, D. L. and L. A. Hunsaker (2003). "Methylglyoxal metabolism and diabetic complications: roles of aldose reductase, glyoxalase-I, betaine aldehyde dehydrogenase and 2-oxoaldehyde dehydrogenase." Chem Biol Interact **143-144**: 341-351.

Vidal, R. and B. Ghetti (2011). "Characterization of amyloid deposits in neurodegenerative diseases." Methods Mol Biol **793**: 241-258.

Wada, R. and S. Yagihashi (2005). "Role of advanced glycation end products and their receptors in development of diabetic neuropathy." Ann N Y Acad Sci **1043**: 598-604.

Wallace, T. C. (2011). "Anthocyanins in cardiovascular disease." Adv Nutr **2**(1): 1-7.

Wang, H., Q. H. Meng, J. R. Gordon, H. Khandwala and L. Wu (2007). "Proinflammatory and proapoptotic effects of methylglyoxal on neutrophils from patients with type 2 diabetes mellitus." Clin Biochem **40**(16-17): 1232-1239.

Wang, H., H. Yang and K. J. Tracey (2004). "Extracellular role of HMGB1 in inflammation and sepsis." J Intern Med **255**(3): 320-331.

Wang, J., J. Lin, A. Schlotterer, L. Wu, T. Fleming, S. Busch, et al. (2014). "CD74 indicates microglial activation in experimental diabetic retinopathy and exogenous methylglyoxal mimics the response in normoglycemic retina." Acta Diabetol **51**(5): 813-821.

Wang, W., Y. Yagiz, T. J. Buran, C. d. N. Nunes and L. Gu (2011). "Phytochemicals from berries and grapes inhibited the formation of advanced glycation end-products by scavenging reactive carbonyls." Food Research International **44**(9): 2666-2673.

Wang, X., K. Desai, T. Chang and L. Wu (2005). "Vascular methylglyoxal metabolism and the development of hypertension." J Hypertens **23**(8): 1565-1573.

Wang, X., X. Jia, T. Chang, K. Desai and L. Wu (2008). "Attenuation of hypertension development by scavenging methylglyoxal in fructose-treated rats." J Hypertens **26**(4): 765-772.

Watanabe, M. (2007). "An anthocyanin compound in buckwheat sprouts and its contribution to antioxidant capacity." Biosci Biotechnol Biochem **71**(2): 579-582.

Wei, Y., L. Chen, J. Chen, L. Ge and R. Q. He (2009). "Rapid glycation with D-ribose induces globular amyloid-like aggregations of BSA with high cytotoxicity to SH-SY5Y cells." BMC Cell Biol **10**: 10.

Wei, Y., C. S. Han, J. Zhou, Y. Liu, L. Chen and R. Q. He (2012). "D-ribose in glycation and protein aggregation." Biochim Biophys Acta **1820**(4): 488-494.

Westwood, M. E. and P. J. Thornalley (1995). "Molecular characteristics of methylglyoxal-modified bovine and human serum albumins. Comparison with glucose-derived advanced glycation endproduct-modified serum albumins." J Protein Chem **14**(5): 359-372.

Wolff, S. P. and R. T. Dean (1987). "Glucose autoxidation and protein modification. The potential role of 'autoxidative glycosylation' in diabetes." Biochem J **245**(1): 243-250.

Wong, D. Y., I. F. Musgrave, B. S. Harvey and S. D. Smid (2013). "Acai (Euterpe oleraceae Mart.) berry extract exerts neuroprotective effects against beta-amyloid exposure in vitro." Neurosci Lett **556**: 221-226.

Wu, C. H., S. M. Huang, J. A. Lin and G. C. Yen (2011). "Inhibition of advanced glycation endproduct formation by foodstuffs." Food Funct **2**(5): 224-234.

Wu, C. H., S. M. Huang and G. C. Yen (2011). "Silymarin: a novel antioxidant with antiglycation and antiinflammatory properties in vitro and in vivo." Antioxid Redox Signal **14**(3): 353-366.

Wu, C. H. and G. C. Yen (2005). "Inhibitory effect of naturally occurring flavonoids on the formation of advanced glycation endproducts." J Agric Food Chem **53**(8): 3167-3173.

Wu, L. and B. H. Juurlink (2002). "Increased methylglyoxal and oxidative stress in hypertensive rat vascular smooth muscle cells." Hypertension **39**(3): 809-814.

Xu, J. W., K. Ikeda and Y. Yamori (2004). "Upregulation of endothelial nitric oxide synthase by cyanidin-3-glucoside, a typical anthocyanin pigment." Hypertension **44**(2): 217-222.

Xue, M., N. Rabbani and P. J. Thornalley (2011). "Glyoxalase in ageing." Semin Cell Dev Biol **22**(3): 293-301.

Yao, D. and M. Brownlee (2010). "Hyperglycemia-induced reactive oxygen species increase expression of the receptor for advanced glycation end products (RAGE) and RAGE ligands." Diabetes **59**(1): 249-255.

Yim, H. S., S. O. Kang, Y. C. Hah, P. B. Chock and M. B. Yim (1995). "Free radicals generated during the glycation reaction of amino acids by methylglyoxal. A model study of protein-cross-linked free radicals." J Biol Chem **270**(47): 28228-28233.

Zafra-Stone, S., T. Yasmin, M. Bagchi, A. Chatterjee, J. A. Vinson and D. Bagchi (2007). "Berry anthocyanins as novel antioxidants in human health and disease prevention." Mol Nutr Food Res **51**(6): 675-683.

Zhang, Y., X. Wang, Y. Wang, Y. Liu and M. Xia (2013). "Supplementation of cyanidin-3-O-beta-glucoside promotes endothelial repair and prevents enhanced atherogenesis in diabetic apolipoprotein E-deficient mice." J Nutr **143**(8): 1248-1253.

APPENDIX

VITA

Thavaree Thilavech was born in February 22nd, 1989 in Ranong, Thailand. After graduating high school grade 12 in 2007 from Pichairattanakarn School, she attended Chulalongkorn University for undergraduate degree in major Nutrition and dietetics and minor Molecular Biology at the department of Nutrition and dietetics, Faculty of Allied Health Sciences. She graduated with her Bachelors of Science with first class honor in 2011. After that she really interested to finding the new knowledge and experiences in graduate degree. Thus, she entered to Ph.D program in Biomedical Sciences, Graduate School Chulongkorn University. Her research focused on antiglycation and cardioprotective properties of cyanidin-3-rutinoside in vitro and in vivo. and her thesis advisor was Accoc. Prof. Sirichai Adisakwattana, Ph.D.